IntechOpen

Carbon Capture, Utilization and Sequestration

Edited by Ramesh K. Agarwal

CARBON CAPTURE, UTILIZATION AND SEQUESTRATION

Edited by **Ramesh K. Agarwal**

Carbon Capture, Utilization and Sequestration
http://dx.doi.org/10.5772/intechopen.73109
Edited by Ramesh K. Agarwal

Contributors

Luqman Abidoye, Abdelaziz Nasr El-Hoshoudy, Saad Desouky, Ahmed Chinade Abdullahi, Chamhuri Siwar, Anizan Isahak, Shaharuddin Mohamad, Shenen Chen, Yangguang Liu, Vinod Krishna Sethi, Partha Sarthi Dutta, Gianluca Valenti, Davide Bonalumi, Reza Barati, Sherifa Cudjoe, Prem Bikkina, Imran Shaik, David K A Barnes, Zia Ur Rahman Farooqi, Muhammad Sabir, Nukshab Zeeshan

Notice

First published in London, United Kingdom, 2018 by IntechOpen
eBook (PDF) Published by IntechOpen, 2019
IntechOpen is the global imprint of INTECHOPEN LIMITED, registered in England and Wales, registration number: 11086078, The Shard, 25th floor, 32 London Bridge Street
London, SE19SG – United Kingdom
Printed in Croatia

British Library Cataloguing-in-Publication Data
A catalogue record for this book is available from the British Library

Additional hard and PDF copies can be obtained from orders@intechopen.com

Carbon Capture, Utilization and Sequestration
Edited by Ramesh K. Agarwal

p. cm.

Print ISBN 978-1-78923-764-1

Online ISBN 978-1-78923-765-8

eBook (PDF) ISBN 978-1-83881-716-9

Meet the editor

Professor Ramesh K. Agarwal is the William Palm Professor of Engineering at Washington University in St. Louis, USA. From 1994 to 2001, he was the Sam Bloomfield Distinguished Professor and Executive Director of the National Institute for Aviation Research at Wichita State University in Kansas. From 1978 to 1994, he worked in various scientific and managerial positions at McDonnell Douglas Research Laboratories in St. Louis; he became the Program Director and McDonnell Douglas Fellow in 1990. Dr. Agarwal received a PhD in Aeronautical Sciences from Stanford University in 1975, an MS in Aeronautical Engineering from the University of Minnesota in 1969, and a BS in Mechanical Engineering from the Indian Institute of Technology, Kharagpur, India, in 1968. Professor Agarwal has worked in computational fluid dynamics and its applications to problems in aerospace and mechanical engineering, and in energy and the environment.

Contents

Preface

This book is a compilation of review and research articles in the broad field of carbon capture, utilization and storage (CCUS). The book is divided in two sections. Three chapters in the first section provide a state-of-the-art review of various carbon sinks for CO_2 sequestration such as soil and oceans. Two chapters discuss the carbon sequestration achieved by storage in kerogen nanopores and CO_2 miscible flooding, respectively. The other two chapters discuss the generation of energy efficient solvents for postcombustion CO_2 capture and chemical absorption of CO_2 by aqueous solution of ammonia. Chapters in the second section focus on monitoring and tracking of CO_2 migration in various types of storage sites, as well as important physical parameters relevant to sequestration. Thus, the book covers a wide variety of topics related to CCUS. It is hoped that it can serve as a useful source of reference to both researchers and students interested in learning about various aspects of CCUS technology.

Ramesh K. Agarwal
Washington University
St. Louis, USA

Section 1

Carbon Capture and Sequestration

Chapter 1

Carbon Sequestration in Soils: The Opportunities and Challenges

Ahmed Chinade Abdullahi, Chamhuri Siwar,
Mohamad Isma'il Shaharudin and Isahak Anizan

Additional information is available at the end of the chapter

http://dx.doi.org/10.5772/intechopen.79347

Abstract

Recently, the contributions of the soil in various ecosystems have become more prominent with the recognition of its role as a carbon sink and the potential of that in reducing the concentration of carbon dioxide (CO_2), which is a vital greenhouse gas, from the atmosphere. Conversely, the soil capacity to increase the concentration of CO_2 in the atmosphere through mineralization of organic matter is also a source of concern. Mineralization of only 10% of the soil organic carbon pool globally is believed to be equivalent to about 30 years of anthropogenic emissions. This underscores the need to preventing carbon loss (emission) from the soil resource. Globally, the soil contains a large carbon pool estimated at approximately 1500Gt of organic carbon in the first one meter of the soil profile. This is much higher than the 560 Gt of carbon (C) found in the biotic pool and twice more than atmospheric CO_2. By holding this huge carbon stock, the soil is preventing carbon dioxide build up in the atmosphere which will confound the problem of climate change. There are a lot of strategies used in sequestering carbon in different soils, however, many challenges are being encountered in making them cost effective and widely acceptable.

Keywords: soil carbon sequestration, climate change, carbon dioxide, ecosystem services

1. Introduction

The role of soil the ecosystem is increasingly being recognized with the realization that it has the capacity of reducing the concentration of carbon dioxide (CO_2) in the atmosphere (through sequestration of organic carbon in the soil) and also by releasing this CO_2 back into

the atmosphere (through mineralization of soil organic matter). It has been reported that mineralization of only 10% of the soil organic carbon pool globally can be equivalent to about 30 years of anthropogenic emissions [1].

This underscores the need to preventing carbon loss (emission) from the soil resource. Globally, the soil contains a large carbon pool estimated at approximately 1500 Gt of organic carbon in the first 1 m of the soil profile [2–4]. This is much higher than the 560 Gt of carbon (C) found in the biotic pool [5] and twice more than atmospheric CO_2 [6]. By holding this huge carbon stock, the soil is preventing carbon dioxide build up in the atmosphere which will compound the problem of climate change.

There is huge opportunity of sequestering atmospheric carbon in the soil for a long period of time because already 24% of global soils and 50% of agricultural soils are degraded globally [7]. Because most of agricultural soils are already degraded, they are estimated to have the potential of sequestering up to 1.2 billion tonnes of carbon per year [8].

Carbon sequestration in soils can be a short term solution of reducing CO_2 concentration in the atmosphere until when more effective strategies are found [4].

Despite the huge carbon deposit in soil ecosystem globally, research efforts in sequestration has been primarily focused on geological and vegetation carbon capture and storage while giving less attention on the role of soil as a viable carbon sink [9].

This chapter will trace the origin of carbon sequestration idea as a potential climate mitigation measure as well as review the conceptual basis and mechanism of carbon capture and sequestration in soils. The benefits and challenges facing carbon sequestration in soils are also discussed extensively. Finally, some proven management practices and strategies used in enhancing the soil carbon stock under forest and agricultural ecosystems are outlined. The chapter concludes by emphasizing the need for the scientific community to resolve most the challenges making widespread adoption of this initiative difficult.

2. Genesis of the carbon sequestration idea in terrestrial systems

The idea that the concentration of CO_2 in the atmosphere can be minimized by sequestering it in terrestrial ecosystems, including the soil was first proposed by Dyson in 1977 [10]. He realized that the danger of rising CO_2 concentration in the atmosphere outweighs the benefits and that increased CO_2 into the atmosphere is inevitable in the light of continued dependence on fossil fuels. Therefore, a strategy was needed for reducing CO_2 emission without 'drastic shutdown of industrial civilization'. He proposed that the excess CO_2 could be absorbed by trees in a large scale plantation as a potential strategy for halting the continuous CO_2 build up in the atmosphere. This is in light of evidence that the photosynthetic turnover is 20 times larger than the annual increase in atmospheric CO_2 [10]. He therefore concluded that by planting of fast growing trees on a massive scale on marginal land or growing and harvesting swamp-plants and converting them into humus or peat the concentration of CO_2 in the atmosphere could be minimized. This could be a short gap measure to hold the atmospheric CO_2

level down until alternatives to fossil fuels are found. Much later in 1989, Sedjo and Solomon also wondered whether CO_2 can be offset by increasing the size of forest areas globally [11].

3. Evidence that carbon is sequestered in the soil and terrestrial ecosystems

The soil is reputed to contain the largest terrestrial carbon pool estimated at approximately 2344 Gt (1 gigaton = 1 billion tonnes) of organic carbon in the first 3 m, 1500 Gt in the first 1 m and 615 Gt stored in the top 20 cm of the soil profile [2–4]. By holding this huge carbon stock, the soil is preventing or delaying carbon dioxide build up in the atmosphere which will compound the problem of climate change. Considering the fact that only 9 Gt of C is added to the atmosphere yearly through anthropogenic activities from fossil fuels and ecosystem degradation [4], the soil can be counted on as an effective carbon sink that renders vital climate regulation services.

Conversely, the soil also emits CO_2 back to the atmosphere due to SOM decomposition estimated at 150 Gt which leaves a vacuum that could be filled if the lost C can be recaptured back and stored in the soil [12].

The amount of carbon emitted annually into the atmosphere is estimated at 8.7 Gt C while only 3.8 Gt/year is found in the atmosphere at a given time [4]. This leaves an unaccounted balance of 4.9 Gt C/year that is believed to have been sequestered on terrestrial systems (oceans, forests, soils, etc.). The realization that the terrestrial systems (including soil) have the capacity to sequester this difference (4.9 Gt C/year) has generated interest in the potential of these systems to sequester and store carbon in long-lived pools thereby preventing its accumulation in the atmosphere [3, 4, 13–15]. Just like the way the soil sequesters and stores, organic carbon, thereby reducing the amount in the atmosphere, it can equally release carbon (through CO_2) into the atmosphere and raise the concentration of carbon dioxide [12].

Over the last few decades, the soil has lost considerable quantity of carbon as a result of anthropogenic activities such as deforestation and agricultural activities. Managed ecosystems such as agriculture are believed to have already lost 30–55% of their original soil organic carbon stock since conversion [7]. The lost productivity of agricultural and degraded lands together offers an opportunity for recovering 50–60% of the original carbon content through adoption of carbon sequestration strategies [13]. This situation creates an opportunity for the replenishment of the lost carbon stock through adoption of deliberate strategies and policies of carbon sequestration. This may likely reduce the amount of CO_2 in the atmosphere.

3.1. Mechanisms of carbon capture and sequestration

Soil carbon is originally derived from the CO_2 assimilated by plants through photosynthesis and converted to simple sugars and eventually returned to the soil as soil organic matter. Photosynthesis is the process where plants produces organic compounds such as carbohydrate by using solar energy to convert CO_2 and water into organic compounds such as

carbohydrates. These organic compounds are then used in making the plants structural components (also known as biomass) and generating the energy needed for metabolic activities. The maximum amount of carbon that can be produced, otherwise known as gross primary productivity (GPP), depends on the plant's ability to produce these compounds through photosynthesis. The biomass produced through photosynthesis is utilized by the plants themselves in generating the energy needed for metabolic activities in a process called respiration. The difference between the GPP and respiration is called the net primary productivity (NPP). NPP is generally believed to be 45% of the GPP [16].

NPP is determined by the potion of solar radiation captured by the plants and used for the photosynthesis (also known as photosynthetically active radiation (PAR), the leaf area index, the light use efficiency (the ratio of primary productivity to absorbed PAR) of the vegetation and autotrophic respiration [12]. The higher the NPP the more carbon is transferred to stable pools in the soils [17].

4. Carbon sequestration

Carbon sequestration is the process of transferring carbon dioxide (CO_2) from the atmosphere into stable terrestrial carbon (C) pools.

The process can be driven naturally or anthropogenically. The anthropogenically driven sequestration ensures that there is no net gain in the atmospheric C pool because the CO_2 sequestered comes from the atmosphere. There are basically two types of sequestration: abiotic and biotic. The abiotic techniques involve injection of CO_2 into deep oceans, geological strata, old coal mines and oil wells. The biotic component on the other hand, involves managing higher plants and micro-organisms to remove more CO_2 from the atmosphere and fixing this C instable soil pools. Biotic sequestration is further subdivided into oceanic and terrestrial sequestration. Oceanic sequestration involves C capture by photosynthetic activities of organisms such as phytoplankton, which converts the C into particulate organic material and deposits such on the ocean floor. This type of sequestration is reported to fix about 45 Pg C/year [18].

Terrestrial sequestration involves the transfer of CO_2 from the atmosphere into the biotic and pedologic C pools. This is accomplished by the transfer or sequestration of CO_2 through photosynthesis and storage in live and dead organic matter. The major terrestrial C sinks include: forests, soils and wetlands.

4.1. Carbon sequestration in soil ecosystem

Soil carbon sequestration is defined by Olson et al. [19] as:

> *the process of transferring carbon dioxide from the atmosphere into the soil of a land unit through plants, plant residues, and other organic solids, which are stored or retained in the unit as part of the soil organic matter (humus)* [19].

According to the Soil Science Society of America, it is the storage of carbon in a stable solid form in the soil as a result of direct and indirect fixation of atmospheric CO_2 [20]. The direct fixation involves natural conversion of CO_2 into soil inorganic compounds such as calcium and magnesium carbonates while the indirect sequestration takes place when plants produce biomass through the process of photosynthesis. This biomass is eventually transferred into the soil and indirectly sequestered as soil organic carbon after decomposition. Subsequently, some of this plant biomass is indirectly sequestered as soil organic carbon (SOC) during decomposition processes. The amount of carbon sequestered in the soil reflects the long term balance between carbon uptake and release mechanisms. Many agronomic, forestry and conservation practices, including best management practices lead to a beneficial net gain in carbon fixation in soil. The carbon sequestered under direct fixation is also referred to as soil inorganic carbon (SIC) while C fixed indirectly is called soil organic carbon (SOC) [5].

Carbon can also be sequestered in soil through the accumulation of humus onto the surface layers (usually 0.5–1 m depth) of soil or anthropogenically through land use change or adoption of right management practices (RMPs) in agricultural, pastoral or forest ecosystems [5]. Soils in managed ecosystems tend to have a lower SOC pool than those in natural ecosystems due to oxidation or mineralization, leaching and erosion [5]. Globally, soils are reported to the have the capacity of sequestering 0.4–0.8 Pg [21].

The sequestration of carbon in soils depends on a number of factors depending on whether it is abiotic or biotic. Abiotic soil C sequestration depends on clay content, mineralogy, structural stability, landscape position, soil moisture and temperature regimes [22]. Biotic soil C sequestration on the other hand depends on management practice, climate and activities of soil organisms [23, 24].

4.2. Carbon stock in forest soils

Carbon is stored in forest ecosystems mainly in biomass and soil and to a lesser extent in coarse woody debris [25]. The carbon stock in forest soils play a large role in global carbon cycle due to the large expanse of forest ecosystems estimated at 4.1 billion hectares globally [26]. It has been estimated that, globally, the forest ecosystem contains about 1240 Pg C [27]. Out of this amount, the plants (vegetation) contain about 536 Pg C while the soil is believed to contain up to 704 Pg C. This is a very significant amount.

The forest ecosystems contain more than 70% of global soil organic carbon (SOC) and forest soils are believed to hold about 43% of the carbon in the forest ecosystem to 1 m depth [2].

However, unfortunately this high carbon content inherent in natural forest soils is easily depleted by decrease in the amount of biomass (above and below ground) returned to the soil, changes in soil moisture and temperature regimes and degree of decomposability of soil organic matter (due to difference in C:N ratio and lignin content) [14]. Anthropogenic activities such as conversion of forests to agricultural land also deplete the soil organic carbon (SOC) stock by 20–25% [28]. Deforestation is reported to emit about 1.6–1.7 Pg C/year (about 20% of anthropogenic emission [29].

4.3. Carbon stock in agricultural soils

According to the IPCC agricultural soils have the potential of sequestering up to 1.2 billion tonnes of carbon per year. However, it has been estimated that already about 50% of agricultural soils have been degraded globally, a situation that creates an opportunity for sequestering atmospheric carbon in the soil for a long period of time [8].

The potential of sequestering carbon in agricultural land is huge as over one third of the world's arable land is in agriculture [30]. Agricultural land could sequester at least 10% of the current annual emissions of 8–10 Gt/year [31].

5. The role of soil carbon in different ecosystems

The carbon in soil plays significant roles in different ecosystems. Some of these include:

5.1. Mitigation of climate change

The continuous increase in the concentration of carbon dioxide (CO_2) and other GHGs in the atmosphere largely due to anthropogenic sources is believed to be responsible for climatic changes and related consequences being experienced across the globe [21, 23].

This situation has generated interest in developing strategies for reducing GHGs build up in the atmosphere.

Out of the approximately 8.7 Gt C/year being emitted into the atmosphere, from anthropogenic sources, only 3.8 Gt C/year remains [5, 32]. The unaccounted difference of 4.9 Gt C/year is believed to be sequestered in terrestrial (oceans, forests, soils, etc.) bodies which is referred to as the 'missing sink' [32, 33]. This realization has generated interest on the potential of terrestrial sector (including soil) to sequester carbon in long-lived pools thereby reducing the amount that is present in the atmosphere [3, 4, 13, 14].

5.2. Sustainable land management

Apart from reducing the concentration of greenhouse gases (GHGs) in the atmosphere, soil carbon sequestration also complements efforts geared at improving land (forest or agricultural land) productivity. This is because all strategies that sequester carbon in soil also improve soil quality and land productivity by increasing the organic matter content of the soil. Organic matter improves soil's structural stability, water-holding capacity, nutrients availability and provide favorable environment for soil organisms [13].

Carbon sequestration activities offer an opportunity for regaining lost productivity especially under agricultural systems. It has been reported that managed ecosystems such as agriculture have lost 30–55% of their original soil organic carbon stock since conversion [7]. The lost productivity of agricultural and degraded lands together offers an opportunity for recovering 50–60% of the original carbon content through adoption of carbon sequestration strategies [13].

5.3. Ancillary benefits

Apart from climate change mitigation and improving forest land productivity, carbon sequestration in soils (of different ecosystems) also have several ancillary benefits. Some of these include: improvement in water holding capacity and infiltration, provision of substrate for soil organisms, serving as a source and reservoir of important plant nutrients, improvement of soil structural stability among others [13]. According to [34] the environmental benefits associated with soil carbon sequestration is 40–70% higher than the productivity benefits. Based on these reasons, therefore, any policy, strategy or practice that increase soil carbon sequestration also generates these benefits.

5.4. Carbon inventories

The obligation on countries, that are parties to the UNFCC, to deposit their independent nationally determined contributions (INDCs) requires a comprehensive estimation and valuation all carbon sink and sources in the terrestrial and other sectors. These estimation and valuation of carbon in the LULUCF sector will be incomplete if the contribution of soil carbon is excluded due to its large percentage (36–46%). Carbon inventory is a process of estimating changes in the stocks (emission and removals) of carbon in soil and biomass periodically for various reasons [35].

6. Challenges of carbon sequestration in soils

Although there are a lot of opportunities in leveraging carbon stock and sequestration potential in the soil of different ecosystems, there are numerous challenges making this difficult in reality. Some of these challenges include:

a. *Measurement and verification*: the stock of carbon in soils is difficult, time-consuming and expensive to measure. Changes within the range of 10% are very difficult to detect due to sampling errors, small-scale variability and uncertainties with measures and analysis [36]. The annual incremental stock of carbon in soil is very small usually within 0.25–1.0 t/ha [37]. It is even more difficult to account for little gains or losses in soil carbon at various scales due to methodological difficulties such as monitoring, verification, sampling and depth [38]. Even if these small changes (gains or losses) are detected, it is not easy to link such changes to management or land use practice in a given context. The capacity of the soil to sequester and retain carbon is also finite as it reaches a steady state after sometime.

b. *Carbon pools*: sequestered carbon exists in the soil in different pools with varying degree of residence time in the ecosystem. These pools include:

  i. Passive, recalcitrant or refractory pool: organic carbon held in this pool has a very long residence time ranging from decades to thousands of years.

  ii. Active, labile or fast pool: carbon held in this pool stays in the soil for much shorter period due to fast decomposition. The residence time normally ranges from 1 day to a year.

iii. Slow, stable or humus pool: carbon held in this pool has long turnover time due to slow rate of decomposition. The residence time typically ranges from 1 year to a decade.

d. *Permanence*: another challenge of carbon sequestration in soil is non-permanence of the sequestered carbon as it can be released back to the atmosphere as easily as it is gained as a result of decomposition or mineralization. It is for this reason that sequestered carbon is considered a short-term option for removing carbon from the atmosphere. The rate of carbon loss depends on several climatic, land use and management factors.

e. *Separation*: it is very difficult to isolate and differentiate the portion of carbon sequestered in the soil as result of management activities or land use and that which occurred naturally. The principle of separation requires that the carbon sequestered or GHGs emission prevented as a result of management intervention be distinguished from that which would have occurred due to natural causes. Methods are therefore needed that can differentiate naturally sequestered carbon from that captured due to human management [39].

7. Strategies of increasing carbon stock in soils

There are proven practices and strategies that lead to increase in soil carbon stock in different terrestrial ecosystems. Most of these strategies increases the carbon stock in biomass through photosynthesis and indirectly builds up below ground and soil carbon through increased deposition of organic matter. According to Post and Kwon in 2000, organic carbon level of soil can be improved by increasing the amount of organic matter input, changing the decomposability of organic matter, placing organic matter in deep layer and enhancing better physical protection of the soil aggregates or formation of organo-mineral complexes [14].

In the forest ecosystem, the following have been widely reported.

- Afforestation
- Reforestation
- Natural regeneration
- Enrichment planting
- Reduced impact logging (RIL)
- Increasing the carbon stock of existing forests using several silvilcultural techniques among others [40–43].

In the agricultural ecosystem, some strategies that enhance carbon capture and storage in the soil include:

- Manuring and fertilizing
- Conservation tillage (minimum, zero/no-till)

- Crop residue management
- Cover cropping
- Application of farmyard manure
- Application of inorganic fertilizers
- Rotational grazing
- Perennial cropping systems
- Etc.

8. Conclusion

There has been increasing interest on carbon capture and storage in the soils of different ecosystems as a climate mitigation measure. However, enhancing the carbon stock of soils also have ancillary benefits such as improving soil health and productivity, water retention, fertility enhancement among others. Although, theoretically this idea sounds appealing, however it is difficult to operationalize it in practice due to a number of challenges. Some of these include difficulties in measurement of soil carbon stock, permanence, carbon pools with different carbon residence times, separation, the tendency of the soil to reach saturation level when the maximum attainable carbon that could be captured is reached. Advances have been made in tackling most of these challenges, however, deliberate actions to enhance carbon capture and sequestration in the soil ecosystem is yet to get wide acceptance by practitioners and policy makers alike. This chapter is written in an attempt to create more awareness on the potential of soils in capturing and storing atmospheric CO_2 in long lived pools thereby mitigating climate change in the process. Researchers should also work assiduously in finding solutions to the challenges making widespread adoption of this initiative difficult.

Author details

Ahmed Chinade Abdullahi[2]*, Chamhuri Siwar[1], Mohamad Isma'il Shaharudin[1] and Isahak Anizan[3]

*Address all correspondence to: caabdullahi@atbu.edu.ng

1 Institute of Environment and Development, National University of Malaysia, Bangi, Selangor, Malaysia

2 Department of Environmental Management Technology, Abubakar Tafawa Balewa University Bauchi, Nigeria

3 Faculty of Science and Technology, National University of Malaysia (UKM), Bangi, Selangor, Malaysia

References

[1] Kirschbaum MUF. Will changes in soil organic carbon act as a positive or negative feedback on global warming? Biogeochemistry. 2000;**48**:21-51

[2] Jobbágy EG, Jackson RB. The vertical distribution of soil organic carbon and its relation to climate and vegetation. Ecological Applications. 2000;**10**(2):423-436

[3] Guo LB, Gifford RM. Soil carbon stocks and land use change: A meta analysis. Global Change Biology. 2002;**8**:345-360

[4] Stockmann U, Adams M, Crawford JW, Field DJ, Henakaarchchia N, Jenkins M, Minasnya B, McBratneya AB, de Courcelles VD, Singha K, Wheeler I, Abbott L, Angers DA, Baldock J, Birde M, Brookes PC, Chenug C, Jastrow JD, Lal R, Lehmann J, O'Donnell AG, Parton W, Whitehead D, Zimmermann M. The knowns, known unknowns and unknowns of sequestration of soil organic carbon. Agriculture, Ecosystems and Environment. 2013;**164**(2013):80-90

[5] Lal R. Carbon sequestration. Philosophical transactions of the Royal Society of London. Series B, Biological Sciences. 2008;**362**:815-830

[6] IPCC. Summary for Policymakers. In: Stocker TF, Qin D, Plattner G-K, Tignor M, Allen SK, Boschung J, Nauels A, Xia Y, Bex V, Midgley PM, editors. Climate Change 2013: The Physical Science Basis. Contribution of Working Group I to the Fifth Assessment Report of the Intergovernmental Panel on Climate Change. Cambridge, United Kingdom and New York, NY, USA: Cambridge University Press; 2013

[7] Batjes NH. Reader for the soil carbon benefits module. In: Proceedings of the ISRIC Spring School; April 22-26, 2013; Wageningen University Campus, The Netherlands. 2013. pp. 1-16

[8] IPCC. Summary for policymakers. In: Edenhofer O, Pichs-Madruga R, Sokona Y, Arahani E, Kadner S, Seboth K, Adler A, Baum I, Brunner S, Eickemeier P, Kriemann B, Savolainen J, Schlomer S, van Stechow C, Zwickel T, Minx JC, editors. Climate Change 2014, Mitigation of Climate Change. Contribution of Working Group III to the Fifth Assessment Report of the Intergovernmental Panel on Climate Change. Cambridge, United Kingdom and New York, NY, USA: Cambridge University Press; 2014

[9] Kane D. Carbon Sequestration Potential on Agricultural Lands: A Review of Current Science and Available Practices. Working Paper. National Sustainable Farming Coalition. 2015. Retrieved from: http://sustainableagriculture.net/wp-content/uploads/2015/12/Soil_C_review_Kane_Dec_4-final-v4.pdf [Accessed 19th April 2018]

[10] Dyson FJ. Can we control the carbon dioxide in the atmosphere? Energy. 1977;**2**(3):287-291. Available at: http://linkinghub.elsevier.com/retrieve/pii/0360544277900330 [Accessed: 10th April, 2018]

[11] Sedjo RA, Solomon AM. Climate and forests. In: Rosenberg NJ et al., editors. Greenhouse Warming: Abatement and Adaptation. Washington, DC: Resources for the Future; 1989. pp. 105-119

[12] Sanderman J, Farquharson R, Baldock J. Soil Carbon Sequestration Potential: A Review of Australian Agriculture. CSIRO Publication; 2010. Available: https://www.mla.com.au/globalassets/mla-corporate/blocks/research-and-development/csiro-soil-c-review.pdf [Accessed: 20th April 2018]

[13] Lal R. Soil carbon sequestration to mitigate climate change. Geoderma. 2004;**123**:1-22

[14] Post WM, Kwon KC. Soil carbon sequestration and land-use change: Processes and potential. Global Change Biology. 2000;**6**:317-327

[15] Smith P. Land use change and soil organic carbon dynamics. Nutrient Cycling in Agroecosystems. 2008;**81**:169-178

[16] Gifford RM. Plant respiration in productivity models: Conceptualisation, representation and issues for global terrestrial carbon-cycle research. Functional Plant Biology. 2003;**30**:171-186

[17] Sitch S, Huntingford C, Gedney N, Levy PE, Lomas M. Evaluation of the terrestrial carbon cycle, future plant geography and climate-carbon cycle feedbacks using five Dynamic Global Vegetation Models (DGVMs). Global Change Biology. 2008;**14**:2015-2039

[18] Falkowski PG, Scholes RJ, Boyle E, Canadell J, Canfield D, Elser J, Gruber N. The global carbon cycle: A test of our knowledge of earth as a system. Science. 2000;**290**:291-296. DOI: 10.1126/science.290.5490.291

[19] Olson KR. Soil organic carbon sequestration, storage, retention and loss in U.S. croplands: Issues paper for protocol development. Geoderma. 2014;**195-196**:201-206

[20] Burras CL, Kimble JM, Lal R, Mausbach MJ, Uehara G, Cheng HH, Kissel DE, Luxmoore RJ, Rice CW, Wilding LP. Carbon Sequestration: Position of the Soil Science Society of America. Agronomy Publications. Paper 59. 2001

[21] IPCC. Climate Change 2001: The Scientific Basis. Contribution of Working Group I to the Third Assessment Report of the Intergovernmental Panel on Climate Change. Cambridge, UK: Cambridge University Press; 2001. p. 881. ISBN-13: 9780521807678

[22] Jimenez JJ, Lal R, Leblanc HA, Russo RO. Soil organic carbon pool under native tree plantations in the Caribbean lowlands of cost Rica. Forest Ecology and Management. 2007;**241**:134-144. DOI: 10.1016/j.foreco.2007.01.022

[23] Lal R, Follett R, Stewart BA, Kimble JM. Soil carbon sequestration to mitigate climate change and advance food security. Soil Science. 2007;**172**(12):943-956

[24] Abdullahi AC, Siwar C, Shaharuddin MI, Anizan I. Leveraging the potentials of soil carbon sequestration in sustaining forest ecosystems in Malaysia. The Malaysian Forester. 2014;**77**(2):91-100

[25] Ngo KM, Turner BL, Muller-Landau H, Davies SJ, Larjavaara M, Nik Hassan NF, Lum S. Carbon stocks in primary and secondary tropical forests in Singapore. Forest Ecology Management. 2013;**296**:81-89

[26] Dixon RK, Wisniewski J. Global forest systems: An uncertain response to atmospheric pollutants and global climate change. Water, Air, and Soil Pollution. 1995;**85**:101-110

[27] Dixon RK, Brown S, Houghton RA, Solomon AM, Trexler MC, Wisniewski J. Carbon pools and flux of global forest ecosystems. Science. 1994;**263**:185-190

[28] Lal R. Forest soils and carbon sequestration. Forest Ecology and Management. 2005;**220**(1-3):242-258

[29] Watson RT, Noble IR, Bolin B, Ravindranath NH, Verardo DJ, Dokken DJ. Land Use, Land-Use Change and Forestry. Cambridge, UK: Cambridge University Press; 2000. p. 375. ISBN-13: 9780521800839

[30] World Bank. Agricultural land (% of land area). 2015. Available from: http://data.worldbank.org/indicator/AG.LND.AGRI.ZS/countries?display=graph [Accessed 21 April 2018]

[31] Hansen JP, Kharecha M, Sato V, Masson-Delmotte F, Ackerman DJ, et al. Assessing "Dangerous Climate Change": Required reduction of carbon emissions to protect young people, future generations and nature (JA Añel, Ed.). PLoS One. 2013;**8**(12):e81648

[32] Denman KL, Brasseur G, Chidthaisong A, Ciais P, Cox PM, Dickinson RE, Hauglustaine D, Heinze C, Holland E, Jacob D, Lohmann U, Ramachandran S, da Silva Dias PL, Wofsy SC, Zhang X. Couplings between changes in the climate system and biogeochemistry. In: Solomon S, Qin D, Manning M, Chen Z, Marquis M, Averyt KB, Tignor M, Miller HL, editors. Climate Change. 2007. The Physical Science Basis. Contribution of Working Group I to the Fourth Assessment Report of the Intergovernmental Panel on Climate Change. Cambridge, New York: Cambridge University Press; 2007

[33] Battle M, Bender ML, Tans PP, White JWC, Ellis JT, Conway T, Francey R. Global carbon sinks and their variability inferred from atmospheric O_2 and δ13 C. Science. 2000;**287**: 2467-2470

[34] Fung I. Variable carbon sinks. Science. 2000;**290**:1313-3131

[35] Pacala S, Socolow R. Stabilization wedges: Solving the climate problem for the next 50 years with current technologies. Science. 2004;**305**:968-972

[36] Sparling GP, Wheeler D, Vesely ET, Schipper LA. What is soil organic matter worth? Journal of Environmental Quality. 2006;**35**:548-557

[37] Ravindranath NH, Ostwald M. Generic methods for inventory of carbon pools. In: Carbon Inventory Methods: Handbook for Greenhouse Gas Inventory, Carbon Mitigation and Roundwood Production Projects. Netherlands: Springer; 2008. pp. 99-111

[38] Trumbore SE, Torn MS. Soils and the global carbon cycle. In: Holland EA, editor. Soils and Global Change. Belgium: NATO Advanced Study Institute; 2003

[39] Swift RS. Sequestration of carbon by soil. Soil Science. 2001;**166**(11):858-871

[40] Walcott J, Bruce S, Sims J. Soil Carbon for Carbon Sequestration and Trading: A Review of Issues for Agriculture and Forestry. Canberra: Bureau of Rural Sciences, Department of Agriculture, Fisheries and Forestry; 2009

[41] Batjes NH. Management options for reducing CO_2 concentrations in the atmosphere by increasing carbon sequestration in the soil. In: NRP Report No. 410-200-031, Dutch National Research Programme on Global Air Pollution and Climate Change and Technical Paper 30. Wageningen, The Netherlands: International Soil Reference and Information Centre; 1999. http://www.isric.org/isric/webdocs/docs/NRP410200031.pdf

[42] Boer R. Economic assessment of mitigation options for enhancing and maintaining carbon sink capacity in Indonesia. Mitigation and Adaptation Strategies for Global Change. 2001;**6**:257-290

[43] Jandl R, Vesterdal L, Olsson M, Bens O, Badeck F, Rock J. Carbon sequestration and forest management. CAB Reviews: Perspectives in Agriculture, Veterinary Science, Nutrition and Natural Resources. 2007;**2**(17):1-16

Chapter 2

Enhancing Carbon Sequestration Using Organic Amendments and Agricultural Practices

Zia Ur Rahman Farooqi, Muhammad Sabir, Nukshab Zeeshan, Khurram Naveed and Muhammad Mahroz Hussain

Additional information is available at the end of the chapter

http://dx.doi.org/10.5772/intechopen.79336

Abstract

Carbon sequestration (CS) is an important strategy for the mitigation of climate change (CC) as well as for improving the soil fertility of agricultural soils. Carbon sequestration in crop lands and rangelands requires a certain amount of organic matter (OM) presence in the soil called soil organic matter (SOM). Organic amendments like animal and poultry manures, the incorporation of different crop residues, different types of compost, sugarcane bagasse, peat soils, different wood chips, biochar and good agricultural practices like cover crops, nutrient management, mulching, zero and no-tillage techniques, soil biota management and mulching are effectively used for this purpose. These enhance the SOM and improve the soil's physical and chemical properties which help to sequester more C in soil which ultimately contributes towards CS and CC mitigation.

Keywords: carbon sequestration, amendments, biochar, agricultural practices, tillage

1. Introduction

There is an increase in atmospheric C concentration by 31% which is 270 ± 30 Pg since industrial uprising due to the change in land use patterns. Depletion of SOM has contributed up to 78 ± 12 Pg in the atmosphere. Agricultural soils have lost two-thirds of the original SOC with a cumulative loss of 30–40 Mg C ha^{-1}. Atmospheric C removal and storing it in the soils is one of the best options. From soils, agricultural soils are thought to be a major sink and can sequester more and more quantities of C if we adopt agroforestry. It has received widespread credit due

to its advantages of helping in agricultural sustainability CC mitigation [1]. The CS potential of agroforestry systems is estimated between 12 and 228 Mg ha^{-1}. So, based on the Earth's total suitable area for crop production, which is 585–1215 × 10^6 ha, a total of 1.1–2.2 Pg C can be sequestered in the agricultural soils in the next 50 years [2]. Overall, the agriculture sector has a great potential for CS in the soil as well as in crop plants. Changes in agricultural practice and managements can also result in enhanced CS in them. It is presumed that if we change the management practice, it will result in decreased crop yields but the net C flux can be greater

Sr. No.	Term	Definition	Reference
1	Carbon sequestration	It is the processes by which C is removed from the atmosphere and stored in the sinks like ocean, forest and crops, soils and geologic formations.	[11]
2	Agroforestry	It is a combination of two words, agriculture and forestry in which perennial trees and shrubs are grown in combination with agricultural crops.	[12]
3	Mulching	It is a detached vegetation covering wheat straw, compost or may be plastic sheets which are spread around plants to secure them from excessive evaporation, cold stress and promoting SOM contents in soil.	[13]
4	Crop residues	Detached vegetative parts of crop plants that are intentionally left to decay in agricultural fields after crop harvesting.	[14]
5	Crop rotation	It is the systematic planting of different crops in a specific order for several years in the same agricultural field.	[15]
6	Nutrient management	It is the combination of strategies which links soil, crop and weather factors and irrigation for ideal nutrient use efficiency to crops.	[16]
7	Zero tillage	A tillage system in which soil disturbances through ploughing is not being done.	[17]
8	Conservation tillage	If we leave crop residues of previous crop on fields to improve SOM, reducing soil erosion and runoff.	[18]
9	Biochar	It is carbonized biomass obtained from sustainable sources and sequestered in soils and can also be obtained by pyrolysis synthetically.	[19]
10	Cover crops	Crop which is grown for the benefit of the soil rather than the crop yield.	[20]
11	Compost	Material which largely consists of decayed organic matter and is used for fertilizing and conditioning of agricultural soil.	[21]
12	Cropping intensity	It is the fraction of the cultivated area that is harvested.	[22]
13	Bagasse	It is a dry pulp like material which is left when we extract juice from sugar cane.	[23]
14	Animal manure	Animals excreta collected from livestock farms and barnyards used to enrich the soil.	[24]
15	Peat moss	It is also called bog moss or sphagnum moss, a plant very rich in organic matter and used to enhance SOM.	[25]

Table 1. Some terms used in the chapter and their definitions.

under the new system. It will only happen when crop demand remains the same and additional lands are brought into production. Conversely, if increasing crop yields lead to land abandonment, the overall C savings from changes in management will be greater than when soil CS alone is considered [3]. Application of organic amendments and N fertilizer incurs C emissions to the atmosphere, which must be deducted by increasing SOM. Application of manures is important for maintaining agricultural soil health [4, 5].

When agricultural waste lands are vegetated, C is increased in them and can accumulate SOM in them. This accumulation reverses C losses from soils when these lands are converted to perennial vegetation. Maximum rates of CS during the early stage of perennial trees is $100gCm^{-2}yr^{-1}$ while average rates are like forests and grasslands, that is, 33.8 and $33.2gCm^{-2}y^{-1}$, respectively [6]. Carbon sequestration (CS) potential by agroforestry is estimated up to 9, 21, 50, and 63 Mg C ha^{-1} in semiarid, sub-humid, humid and temperate regions, respectively. For small land holdings, CS potential ranges from 1.5 to 3.5 Mg C ha^{-1} $yr.^{-1}$. Another advantage of agroforestry is soil property enhancement which also enhances the CS in plants and soils. Agroforestry systems are important C sinks but intensively managed agroforestry practice in combination with annual crops is like conventional agriculture which does not contribute in CS [7]. Agricultural practices like CT is effective in in enhancing CS [8]. The global potential of CS through agroforestry and CT is around 0.9 ± 0.3 Pg C $year^{-1}$ offsetting 25–75% of the annual C emissions. It is a truly win-win strategy which restores degraded soils, enhances biomass production, purifies surface and ground waters and reduces C from the atmospheric [9, 10] (**Table 1**).

2. Agriculture practices which involve CS

Agricultural practices help in sequestering C in soils such as zero or reduced tillage, crop residue incorporation in fields, nutrient management, preventing OM loss, supplying nutrients and maintaining soil microbes, soil erosion control, vegetation or revegetation, cover cropping, green manuring, crop rotations, agro-forestry, soil rehabilitation, reclamation and use of salt-affected soils for forest plantations and crop production.

2.1. Zero tillage and conservation agriculture

Zero tillage is the type of conservation agriculture which does not disturb the soil comprising minimum soil disturbance, crop residues, cover crops and their diversification; this is also promoted for reducing soil disturbance and improving SOM and its sustainability as well as it also mitigates the CC through CS up to 0.16–0.49 Mg C ha^{-1} yr^{-1}. Increase in SOC concentration from CA induces improvement in the soil's physical and chemical attributes which ultimately contribute to increase the sustainability and CC mitigation through CS [26]. In Brazil, the government is trying to increase the agricultural area under zero tillage from 32 to 40 million ha by 2020 to mitigate C emissions. It was calculated that average annual CS is 1.61–1.48 Mg C ha^{-1} yr^{-1} in Brazil for the 8 years from 2003 to 2011. So, converting 8 million ha of cropland to zero tillage can sequester an estimated soil C storage of about 8 Tg C yr^{-1} in 10–15 years [27].

In Haryana, India, conventional and zero tillage techniques were tested for the efficiency of CS; results showed that nearly USD 97.5 ha^{-1} can be earned extra by adopting zero tillage as zero tillage reduces the tillage implement costs, labor and fuel costs by spending USD 76 ha^{-1} and 97.5 USD earnings show that shifting from conventional to zero tillage reduces cost and additionally, sequester C emission by 1.5 Mg C ha^{-1} $season^{-1}$ [28, 29]. Zero tillage generates considerable benefits up to US D 97 ha^{-1}; it also increases the crop yield by 5–7%, saving costs up to USD 52 ha^{-1} [30–32].

2.2. Conservation tillage

Soil organic matter (SOM) is considered as C pool as well as its source while it decomposes. It decomposes when conventional tillage (CoT) is done. To check the effectiveness of conservation tillage in SOM retention, three scenarios of conservation tillage in model were used, that is, 27%; the current usages are 57 and 76%. The SOM content for major field crops up to 30 cm was 5304–8654 Tg C with 1710–2831 Tg C at 0–8 cm depth and 1383–2240 Tg C at 8–15 cm depth [33]. Changes in the SOC are greatly influenced by long-term tillage practices. For example, soil from 0 to 60 cm after 25 years of CT showed 5% higher soil bulk density for conservation tillage as compared to CoT practices. Analysis also showed that CS and storage was significantly higher in CT soil than CoT. So, it was concluded that CT practices increased SOM and CS as compared to CoT [34, 35]. It is a fact that interest in C storage in soils has gained a lot of interest in the last few years, especially C with its potential to help alleviate or offset some of the negative effects of the increase in greenhouse gases in the atmosphere. Several questions still exist about what management practices can optimize CS in the soil. Primary method is to conserve SOM by not ploughing. As in a study involving different tillage practices like CT, ZT, NT and CoT, it showed that CS throughout the profile was significantly affected by tillage practices. Conservation, ZT and NT showed that there is the greatest potential of CS while applying ZT, NT and CoT [36]. Conservation tillage is highly recommended in crop lands as a means of enhancing CS in these soils. Carbon sequestration can be increased by 3.15 ± 2.42 t ha^{-1} by adopting CT [37].

2.3. Nutrient management

Agricultural soils can be a sink for atmospheric C concentrations by CS. It is accomplished by the formation of SOM or humus which is limited by the availability of nutrients such as nitrogen (N). Optimization of N can be a good mean for CS. Practices that enhance N in soil are no or reduced tillage and increased crop intensity. Nitrogen additions are important for increasing biomass yield and hence crop residues' decomposition in soil which increases SOM concentration. Practices like CT and increased cropping intensity and crop rotations yield more quantity of crop residues, increasing N availability and CS. Croplands have the potential of sequestering C from 8 to 298 Tg C $yr.^{-1}$ [38]. Soil organic matter and N are directly influenced by tillage, residue return and N fertilization management practices [39], and that is why, intensive use of N fertilizers is employed to achieve higher economic value of high-grain yields and is generally perceived to bring about CS and by increasing the inputs of crop residues [40]. To determine the effects of N, tillage and crop rotation on SOM, long-term

tillage and rotation studies were conducted. Conventional techniques and ZT were applied and C and N were determined from soils at depths of 0–2.5, 2.5–7.5, 7.5–15 and 15–30 cm. It was revealed that compared with CT, NT had greater organic C, N and SOM. Increases in SOM were directly related to the tillage practice and N fertilizer application [41].

2.4. Cropping system and intensity

Soils represent a C pool of approximately 1500 Gt. Any modification or change of land use or land management can induce variations in soil C stocks [42]. Intense cropping systems always cause depletion of SOM but applying crop residues, balanced fertilization with NPK and use of organic amendments can increase CS levels to 5–10Mgha^{-1}yr.$^{-1}$. As these amendments also contain 10.7–18% C in them, they also help in CS [43].

In agricultural systems, there is a need for the optimization of C and N by cropping intensity and system to sequester C in the form of SOM which, in addition, gives stable soil structure, more yield and economic benefits [44]. Here, one challenge is to analyze the mechanism, capacity and longevity of C stabilization in agricultural lands by cropping intensity and systems. It is estimated that across 10 cropping systems, annual soil CS rates range up to 0.56 Mg C ha^{-1} yr.$^{-1}$ [45]. Continuous and intense crop production accumulates 10–17% more SOM and N [46]. Increases in CS in soil can be attained by improved soil fertility, extensive cropping systems with shifting cultivation cropped fallows and cover crops [47]. Tillage, land cover, nutrients and cropping system management can contribute in CS up to 30–105 million metric tons of C (MMTC) yr.$^{-1}$. Cropping intensity and rotations have the potential to sequester 14–29 MMTC yr.$^{-1}$. By adopting these strategies, biomass production is increased and so, the C usage in the plants is increased and more C is sequestered in the plant and soil. If nutrient inputs combined the above strategies, this CS amount can be doubled [48]. Increase in SOM can be seen under long-term maize-wheat-cowpea cropping system up to 1.83 Tg C yr.$^{-1}$ [49].

2.5. Mulching

Carbon concentration and SOM is increased by adding mulch, and crop residues are widely applied in the form of mulch for CS and crop protection against cold stress. Mulch can increase CS in agricultural soils up to 8–16 Mg ha^{-1} yr.$^{-1}$ and additionally, the soil's physical and chemical properties are also improved. Total SOM by using mulch increased from 1.26 to 1.50% [50]. Mulch also plays a key role in supplying nutrients, playing a role in the C and N cycle and the sink of C. It can significantly increase SOM and CS in the topsoil layer of 0–5 cm. This variation in the CS is attributed to the mulch rates. As more is the mulch and time after applying mulch, more will be the CS rate. For example, there will be 41% more CS after 4 years of mulching and 52% more CS after 11 years of mulching [51, 52].

2.6. Residues and nutrient management

Crop residues and nutrients especially N help in sequestering C in soils up to 21.3%–32.5% and simultaneously improve soil quality and plant growth [53]. Total SOM stocks are improved

by crop residues which suggests the substitution of SOM by fresh SOC derived from crop residues from 3.5 to 5.5 Mg C ha^{-1} [54]. The use of crop residue as a source of CS and keeping the soil in good quality helps in nutrient management and conservation. In the USA, a total of 367 × 10^6 Mg $year^{-1}$ crop residues from 9 cereal crops, 450 × 10^6 Mg $year^{-1}$ for 14 cereals and legumes and 488 × 10^6 Mg $year^{-1}$ for 21 crops are produced. The amount of total crop residue production in the world is 2802 × 10^6 Mg $year^{-1}$ from cereal crops and 3758 × 10^6 Mg $year^{-1}$ from 27 food crops which can sequester 40–60% of total agricultural C emissions through their incorporation in the fields [55].

2.7. Soil biota management

Biological CS is accomplished by microbial activities. Mechanisms of CS by microbes need to be developed based on experiments and field investigations to predict the CS potential and C cycling under potential global change scenarios [56, 57]. Microbes improve the physical, chemical and biological soil properties in RT or NT areas. The evaluation of the soil microbial and biochemical environment greatly in these areas aids predictions of C availability in soil and plants to quantify CS. Where microbial communities are higher, C and N were 1.32–1.82 [58, 59]. Carbon sequestration was recorded higher up to 49.9 g C kg^{-1} in soils which were rich in soil microbes like fungi and soil bacteria [60].

2.8. Cover crops

The use of cover crops for the maintenance and restoration of SOM and soil productivity is a popular option [61]. Planting cover crops is a promising option to sequester C in cropping systems by the implementation of recommended management practices. The highest CS rate up to 5.3 t C ha^{-1} $yr.^{-1}$ is observed by cover cropping of olive orchards, vineyards and almond orchards. Soil CS rate tends to be the highest during the first years after the change of the management and progressively attains equilibrium. Soil CS rates in cover cropping are much higher than that of fields with low or no cover cropping which suggests that the adoption of cover cropping is a sustainable and efficient measure to mitigate CC [62].

2.9. Soil fertility management

Rice-fallow-rice is one of the dominant cropping systems which has received attention to improve SOM by using organic amendments. Understanding the contributions of organic amendments in CS is important for the estimation of CS, their nutrient supply potential and their role in it. In different organic amendments, poultry manure is found to be more efficient in increasing C and other nutrients in soils and microbial activities which contribute to CS in the rice-rice cropping system [63, 64]. Raw adzuki bean (*Vigna angularis* (Willd.) Ohwi and Ohashi) and wheat (*Triticum aestivum* L.) straw residues can supply C into fields by 499 ± 119 kg C ha^{-1} [65]. The Mekong Delta, Vietnam, produces 21 Mt. of rough rice (*Oryza sativa* L.) and an estimated 24 Mt. of rice straw annually. The spread of these crop residues in this area can increase CS and SOM, significantly reducing GHG emissions [66]. Crop residue decomposition acceleration can enhance the SOM [67].

3. Organic amendments

3.1. Animal manure

Animal manure is the source of C and the addition of animal manure to different crop fields has impacts on C contents [68]. Different researchers conducted the experiments in Germany to check the soil's C levels. The experiment showed that the annual application rate of 200 Mg ha^{-1} $yr.^{-1}$ of manure to the crop field shows a high level of SOM with respect to adjacent fields [69]. Powlson reported that the mean annual SOC sequestration rates of three long-term (>49) years of manure applications ranged from 10 to 22 kg C ha^{-1} $yr.^{-1}$ t^{-1} of dry solids, while SOC sequestration rates with shorter-term experiments (8–25 years of farmyard manure, cattle slurry and boiler litter) were from 30 to 200 kg C ha^{-1} $yr.^{-1}$ t^{-1} of dry solids [70]. The experiment was conducted to improve the soil quality and crop productivity. Improved soil properties refer to better C management. Animal manure also increases the salt concentration of the soil. The long-term application of manure increases the SOM significantly [71]. In another study, the farm yard manure was applied to the rice-wheat cropping system with NPK fertilizers and results showed significantly an increase in C sequestration in farm yard manure-applied plots than NPK-applied plots [72]. The same experiment was conducted on the maize-wheat cropping system, but in this experiment, the farm yard manure is applied with green manure and indicates that green manure sequesters more C [73]. It was also observed that the high application of N has the potential to sequester C almost at the rate of 1.0–1.4 Mg ha^{-1} $yr.^{-1}$ [74].

3.2. Crop residues

The researchers investigated that the annual production of crop residues is about 3.4×10^9 tones worldwide. If 15% of the total residue is applied to the soil, it will increase the C contents of soil. The crop residues are the remains of the agricultural crops. The intensive agriculture system increases the crop residue production significantly. This may increase the SOM and soil aggregation and hence C storage [75]. The degradation of crop residue depends upon its composition. For example, it is difficult for microorganisms to start the degradation of the substances which contain a high content of lignin. There three mechanisms, which are classified by different researchers based on the stabilization of SOM, include chemical, biochemical and physical stabilization [76]. Agricultural practices such as the addition of crop residues increase the SOM as well as nutrients contents in the soil by integrated nutrient management [77]. Most studies focus on the fact that the change of crop residue traits has positive effects of the soil CS in organic farming system [78].

3.3. Composting

Composting is the systematic and controlled breakdown of different types of organic matter including animal manure, woody material and other organic waste. The C content is available in the form of plant uptake in the composting. When the compost matures, 50% of C is available in the form of humic substances [79] and is thought to be more stable practically [80]. In the

long-term application of compost, about 8 years or 5 years, a mean 60 kg C ha^{-1} $yr.^{-1}$ t^{-1} of dry solids were monitored [81]. The compost applied in different plots and the soil organic C stock increased significantly compared with the initial stock [82]. It is a win-win condition to increase C storage in the soil as well as plant growth and yield by chemical fertilization. The compost application at the rate of 10 Mg ha^{-1} $yr.^{-1}$ results in higher CS. This clear cut indicates that composting not only increases the net primary production but also the C content of the soil [83].

3.4. Bagasse

The application of different types of biomass in soil is the best technique to enhance CS in the agricultural sites. The application of bagasse as a biomass in the field showed that bagasse has the potential to sequester C at about 1200–1800 t C $year^{-1}$ [84]. The application of biochar produced from bagasse is a very authentic organic amendment to soil for retaining its water content [85]. Another study suggested that Bagasse can be converted into B and applied in the soil and it has the potential to sequester C. The porous and high surface area is efficient for the sequestration of C from the atmosphere. Bagasse (B) produced at 600°C showed the most adsorption of C (73.55 mg g^{-1} at 25°C) [86]. The use of bagasse ash is investigated in an experiment. Different ashes like bagasse and rice husk ash were investigated on wheat soil and the soil organic C content and enzymatic activity were monitored. Bagasse ash increases the soil organic contents at the rate of 525 kg ha^{-1} y^{-1} while rice husk ash has no increase of SOM. Bagasse ash increases the soil dehydrogenase and cellulose activity. Long-term investigations are needed to check the effect of ash effects on the soil's physical, chemical and biological properties [87].

3.5. Wood chips

The world is under threat due to drastic effects of CC, energy access and availability of food. Wood is mostly used as a fuel to cook food and considered as a renewable energy source. Bamboo plantation can sequester C and fix it by producing high biomass. This biomass can be used to generate chips and pellets and as the alternative of fuel; as a result, it can sequester approximately 1.78 kg of C [88]. Another research was conducted and wood chips and straw were applied in the soil and the results showed that nitrogen mineralization and nitrification rates were higher significantly in the soil-applied wood chips. The bad thing is that when we applied wood chips in the soil, nitrogen deficiency occurs and then an additional supplement of nitrogen is required [89]. Carbon contents of early woods are higher than late woods [90]. It is produced from wood-based biomass at a low pyrolysis temperature (400°C) suitable for enhancing the cation exchange capacity, whereas B produced from wood-based biomass at a high pyrolysis temperature (800°C) can enhance nitrate adsorption [85].

3.6. Biochar

Biochar (B) is usually obtained by the breakdown of crop residues, wood chips, at a low temperature range (350–600°C) in the atmosphere having very little or no oxygen. If the condition remained optimum during the process of B formation including temperature and oxygen, then almost >50% of the C is retained by the B with respect to original biomass [91]. It is resistive to

microbial attack and hence when applied to the soil will remain stable for thousands of years and thus reduce the release of terrestrial C to the atmosphere in the form of CO_2 [92]. It has long-term benefits including increase in soil pH [93], increases in crop yield, maintaining the cation exchange capacity, nutrient retention and water-holding capacity. Biochar also reduces the emissions of others greenhouse gases like methane and nitrous oxides [94]. Increased concentration of nitrogen oxides in the atmosphere affects the plant growth by necrosis, slow photosynthetic rate and increased sensitivity of the plants. Gases usually affect the plants by entering them through the stomata of plants [95]. The B has been classified into two classes on the basis of degradation. Class 1 has the potential to store C in soil to about 21.3% and class 2 has potential of about 32.5%. The presence of alkali metals in the B reduces their stability. The B can store 0.55 Pg CO_2 $yr.^{-1}$ in soils over long time use [96]. The findings suggest that the application of B to soil is profitable amendments if the B price is low enough [97]. The response of B at different pH levels was investigated and found that acidic medium emits more carbon dioxide than the alkaline medium. The enhancement of copiotrophic bacteria like gemmatimonadetes and bacteroidetes and the decrease of oligotrophic bacteria increase the C emission in the acidic medium of soil [98]. Biochar-based C management networks have the potential to mitigate CC but the quality of B should be appropriate [99] (**Table 2**).

The studies in China indicate that cultivated and forest soils have the CS potential around 38.5–77 Mt., respectively [107, 108]. The research shows that due to the increase of temperature from South to North, there is also a decrease of soil organic carbon (SOC) [109].

In Belgium in different studies, the C stock was found to be around 319 Mt. and this is due to the increase in mean elevation from Northeast coast to Southeast, and as a result, it leads to a decrease in temperature and an increase in precipitation. Carbon stock is higher in Southeast than Northeast. The C contents in topsoil were found to be 48 t C ha^{-1} in Luvisols while 113 t C ha^{-1} in Cambisols soil types [110].

Strategy	Area	CS rate (t C ha^{-1})	Observational time	Reference
Organic manure	China	0.62	14–40 y	[100]
Organic matter plus in-organic fertilizer	China	0.62–0.69	03–25 y	[101]
Animal manure	Belgium	0.45	20 y	[102]
Fertilizer plus crop residues	Indonesia	0.52 ± 0.16	40 y	[103]
Inorganic fertilizers	South Korea	0.32 ± 0.29	8 y	[103]
Different crop residues	Nigeria	0.24	18 y	[104]
Crop stubbles	Australia	0.19 ± 0.08	—	[105]
Inorganic fertilizer	South Korea	0.32 ± 0.29	8 y	[103]
Crop residue	Nigeria	0.24	18 y	[104]
Crop stubbles retention	Australia	0.19 ± 0.08	4–40	[105, 106]

Table 2. Different strategies and their carbon sequestration potential.

It was found by Indonesian scientists that total SOM was higher if the high clay and silt content was found in soil. The other factors like low pH, rainfall and higher altitude were found responsible for higher soil organic content. The organic content of peatland soil was estimated to be about 33.7 Gt of the 20.9 M ha area of peat soils [111].

Agricultural land of South Korea is about 174 Mt. (1 m depth) for the storage of carbon. Soil organic carbon stocks in grass and agricultural lands were as large as 88 and 68 t C ha^{-1}, respectively [112].

A study in Nigeria also revealed that 20-60 t ha^{-1} is found in top 0.3 m soil layer and a total of 118 Mg C ha^{-1} can be found in the top 1 m. Humid forest zone contains more C than any other zone [113], and the C stock of Australian topsoils was found to be around 25 Gt because of great land mass as well as low temperature [114].

4. Conclusions

Greenhouse effect was the natural phenomena, but humans are responsible for the escalation of it leading to the global warming and climate change (CC). Due to climate change, the natural environment is facing different types of unexpected and high-intensity weather events. Climate change mitigation or the solution of all the above problems lies in the reduction of the C concentrations in the atmosphere. There are many sinks for CS including forests, soil, oceans and crop plants. Soil CS and crop production is a better, economical and reliable option because it captures C as well as grows plants which provide food to us. C sequestration in crop lands and rangelands requires certain amounts of organic matter (OM) presence in the soil called soil organic matter (SOM). Organic amendments like animal and poultry manures, the incorporation of different crop residues, different types of compost, sugarcane bagasse, peat soils, different wood chips, B and good agricultural practices like cover crops, nutrient management, mulching, zero and no-tillage techniques, soil biota management and mulching are effectively used for this purpose. These enhance the soil organic matter and improve the soil's physical and chemical properties that help to sequester more C in the soil, which ultimately contributes towards CS and CC mitigation.

Abbreviations

B	biochar
C	carbon
SOM	soil organic matter
CS	carbon sequestration
CT	conservation tillage

ZT	zero tillage
CoT	conventional tillage
N	nitrogen
SOC	soil organic carbon
CA	conservation agriculture

Author details

Zia Ur Rahman Farooqi, Muhammad Sabir*, Nukshab Zeeshan, Khurram Naveed and Muhammad Mahroz Hussain

*Address all correspondence to: cmsuaf@gmail.com

Institute of Soil and Environmental Sciences, University of Agriculture, Faisalabad, Pakistan

References

[1] Lal R. Soil carbon sequestration to mitigate climate change. Geoderma. 2004;**123**:1-22

[2] Albrecht A, Kandji ST. Carbon sequestration in tropical agroforestry systems. Agriculture, Ecosystems & Environment. 2003;**99**:15-27

[3] West TO, Marland G. Net carbon flux from agriculture: Carbon emissions, carbon sequestration, crop yield, and land-use change. Biogeochemistry. 2003;**63**:73-83

[4] Schlesinger WH. Carbon sequestration in soils. Science. 1999;**284**:2095

[5] Baker JM, Ochsner TE, Venterea RT, Griffis TJ. Tillage and soil carbon sequestration—What do we really know? Agriculture, Ecosystems & Environment. 2007;**118**:1-5

[6] Post WM, Kwon KC. Soil carbon sequestration and land-use change: Processes and potential. Global Change Biology. 2000;**6**:317-327

[7] Montagnini F, Nair PKR. Carbon sequestration: An underexploited environmental benefit of agroforestry systems. In: Nair PKR, Rao MR, Buck LE, editors. New Vistas in Agroforestry: A Compendium for 1st World Congress of Agroforestry. Dordrecht: Springer Netherlands; 2004. pp. 281-295

[8] West TO, Marland G. A synthesis of carbon sequestration, carbon emissions, and net carbon flux in agriculture: Comparing tillage practices in the United States. Agriculture, Ecosystems & Environment. 2002;**91**:217-232

[9] Lal R. World crop residues production and implications of its use as a biofuel. Environment International. 2005;**31**:575-584

[10] Silver WL, Ostertag R, Lugo AE. The potential for carbon sequestration through reforestation of abandoned tropical agricultural and pasture lands. Restoration Ecology. 2000;**8**:394-407

[11] Lal R. Soil carbon sequestration impacts on global climate change and food security. Science. 2004;**304**:1623-1627

[12] King K. The history of agroforestry. Agroforestry. USA: KLGWER Academic Publishers; 1987. pp. 1-11

[13] Mulumba LN, Lal R. Mulching effects on selected soil physical properties. Soil and Tillage Research. 2008;**98**:106-111

[14] Bannari A, Pacheco A, Staenz K, McNairn H, Omari K. Estimating and mapping crop residues cover on agricultural lands using hyperspectral and IKONOS data. Remote Sensing of Environment. 2006;**104**:447-459

[15] Liebman M, Dyck E. Crop rotation and intercropping strategies for weed management. Ecological Applications. 1993;**3**:92-122

[16] Havlin JL, Kissel DE, Maddux LD, Claassen MM, Long JH. Crop rotation and tillage effects on soil organic carbon and nitrogen. Soil Science Society of America Journal. 1990;**54**:448-452

[17] Govaerts B, Sayre KD, Deckers J. Stable high yields with zero tillage and permanent bed planting? Field Crops Research. 2005;**94**:33-42

[18] Holland J. The environmental consequences of adopting conservation tillage in Europe: Reviewing the evidence. Agriculture, Ecosystems & Environment. 2004;**103**:1-25

[19] Lehmann J, Joseph S. Biochar for Environmental Management: Science, Technology and Implementation. USA: Routledge; 2015

[20] Snapp S et al. Evaluating cover crops for benefits, costs and performance within cropping system niches. Agronomy Journal. 2005;**97**:322-332

[21] Haug R. The Practical Handbook of Compost Engineering. USA: Routledge; 2018

[22] Peterson G, Halvorson A, Havlin J, Jones O, Lyon D, Tanaka D. Reduced tillage and increasing cropping intensity in the Great Plains conserves soil C. Soil and Tillage Research. 1998;**47**:207-218

[23] Mohan D, Singh KP. Single-and multi-component adsorption of cadmium and zinc using activated carbon derived from bagasse—An agricultural waste. Water Research. 2002;**36**:2304-2318

[24] Kumar K, Gupta S, Baidoo S, Chander Y, Rosen C. Antibiotic uptake by plants from soil fertilized with animal manure. Journal of Environmental Quality. 2005;**34**:2082-2085

[25] Crum H, Planisek S. A Focus on Peatlands and Peat Mosses. USA: University of Michigan Press; 1992

[26] Powlson DS, Stirling CM, Thierfelder C, White RP, Jat ML. Does conservation agriculture deliver climate change mitigation through soil carbon sequestration in tropical agro-ecosystems? Agriculture, Ecosystems & Environment. 2016;**220**:164-174

[27] Corbeels M, Marchão RL, Neto MS, Ferreira EG, Madari BE, Scopel E, Brito OR. Evidence of limited carbon sequestration in soils under no-tillage systems in the Cerrado of Brazil. Scientific Reports. 2016;**6**:21450

[28] Aryal JP, Sapkota TB, Jat ML, Bishnoi DK. On-farm economic and environmental impact of zero-tillage wheat: A case of North-west India. Experimental Agriculture. 2014;**51**:1-16

[29] Erenstein O, Farooq U, Malik RK, Sharif M. On-farm impacts of zero tillage wheat in South Asia's rice–wheat systems. Field Crops Research. 2008;**105**:240-252

[30] Erenstein O, Laxmi V. Zero tillage impacts in India's rice–wheat systems: A review. Soil and Tillage Research. 2008;**100**:1-14

[31] Erenstein O. Adoption and Impacts of Zero Tillage as a Resource Conserving Technology in the Irrigated Plains of South Asia. Vol. 19. CIMMYT; 2007

[32] Landers JN, Sant' Anna De c Barros G, Rocha MT, Manfrinato WA, Weiss J. Environmental impacts of zero tillage in Brazil—A first approximation. In: García-Torres L, Benites J, Martínez-Vilela A, Holgado-Cabrera A, editors. Conservation Agriculture: Environment, Farmers Experiences, Innovations, Socio-economy, Policy. Netherlands, Dordrecht: Springer; 2003. pp 341-350

[33] Kern JS, Johnson MG. Conservation tillage impacts on national soil and atmospheric carbon levels. Soil Science Society of America Journal. 1993;**57**:200-210

[34] Deen W, Kataki PK. Carbon sequestration in a long-term conventional versus conservation tillage experiment. Soil and Tillage Research. 2003;**74**:143-150

[35] Sheehy J, Regina K, Alakukku L, Six J. Impact of no-till and reduced tillage on aggregation and aggregate-associated carbon in Northern European agroecosystems. Soil and Tillage Research. 2015;**150**:107-113

[36] Varvel GE, Wilhelm WW. No-tillage increases soil profile carbon and nitrogen under long-term rainfed cropping systems. Soil and Tillage Research. 2011;**114**:28-36

[37] Luo Z, Wang E, Sun OJ. Can no-tillage stimulate carbon sequestration in agricultural soils? A meta-analysis of paired experiments. Agriculture, Ecosystems & Environment. 2010;**139**:224-231

[38] Christopher SF, Lal R. Nitrogen management affects carbon sequestration in North American cropland soils. Critical Reviews in Plant Sciences. 2007;**26**:45-64

[39] Dolan MS, Clapp CE, Allmaras RR, Baker JM, Molina JAE. Soil organic carbon and nitrogen in a Minnesota soil as related to tillage, residue and nitrogen management. Soil and Tillage Research. 2006;**89**:221-231

[40] Khan SA, Mulvaney RL, Ellsworth TR, Boast CW. The myth of nitrogen fertilization for soil carbon sequestration. Journal of Environmental Quality. 2007;**36**:1821-1832. All

[41] Havlin JL, Beaton JD, Tisdale SL, Nelson WL. Soil Fertility and Fertilizers: An Introduction to Nutrient Management, vol. 515. Upper Saddle River, NJ: Pearson Prentice Hall; 2005

[42] Bernoux M et al. Cropping systems, carbon sequestration and erosion in Brazil, a review. Agronomy for Sustainable Development. 2006;**26**:1-8

[43] Mandal B et al. The potential of cropping systems and soil amendments for carbon sequestration in soils under long-term experiments in subtropical India. Global Change Biology. 2007;**13**:357-369

[44] Drinkwater LE, Wagoner P, Sarrantonio M. Legume-based cropping systems have reduced carbon and nitrogen losses. Nature. 1998;**396**:262

[45] Kong AYY, Six J, Bryant DC, Denison RF, van Kessel C. The relationship between carbon input, aggregation, and soil organic carbon stabilization in sustainable cropping systems. Soil Science Society of America Journal. 2005;**69**:1078-1085

[46] Sherrod LA, Peterson GA, Westfall DG, Ahuja LR. Cropping intensity enhances soil organic carbon and nitrogen in a no-till agroecosystem. Soil Science Society of America Journal. 2003;**67**:1533-1543

[47] Hutchinson JJ, Campbell CA, Desjardins RL. Some perspectives on carbon sequestration in agriculture. Agricultural and Forest Meteorology. 2007;**142**:288-302

[48] Follett RF. Soil management concepts and carbon sequestration in cropland soils. Soil and Tillage Research. 2001;**61**:77-92

[49] Purakayastha TJ, Rudrappa L, Singh D, Swarup A, Bhadraray S. Long-term impact of fertilizers on soil organic carbon pools and sequestration rates in maize–wheat–cowpea cropping system. Geoderma. 2008;**144**:370-378

[50] Kahlon MS, Lal R, Ann-Varughese M. Twenty two years of tillage and mulching impacts on soil physical characteristics and carbon sequestration in Central Ohio. Soil and Tillage Research. 2013;**126**:151-158

[51] Saroa GS, Lal R. Soil restorative effects of mulching on aggregation and carbon sequestration in a Miamian soil in central Ohio. Land Degradation & Development. 2003;**14**:481-493

[52] Duiker SW, Lal R. Crop residue and tillage effects on carbon sequestration in a Luvisol in central Ohio. Soil and Tillage Research. 1999;**52**:73-81

[53] Windeatt JH, Ross AB, Williams PT, Forster PM, Nahil MA, Singh S. Characteristics of Bs from crop residues: Potential for C sequestration and soil amendment. Journal of Environmental Management. 2014;**146**:189-197

[54] Van De Vreken P, Gobin A, Baken S, Van Holm L, Verhasselt A, Smolders E, Merckx R. Crop residue management and oxalate-extractable iron and aluminium explain

long-term soil organic carbon sequestration and dynamics. European Journal of Soil Science. 2016;**67**:332-340

[55] Lal R. Residue management conservation tillage and soil restoration for mitigating greenhouse effect by CO_2-enrichment. Soil and Tillage Research. 1997;**43**:81-107

[56] Jiao N et al. Mechanisms of microbial carbon sequestration in the ocean—Future research directions. Biogeosciences. 2014;**11**:5285-5306

[57] Wang CJ, Pan GX, Tian YG, Li LQ, Zhang XH, Han XJ. Changes in cropland topsoil organic C with different fertilizations under long-term agro-ecosystem experiments across mainland China. Science China. Life Sciences. 2010;**53**:858-867

[58] Doran JW. Soil microbial and biochemical changes associated with reduced tillage. Soil Science Society of America Journal. 1980;**44**:765-771

[59] Six J, Frey S, Thiet R, Batten K. Bacterial and fungal contributions to carbon sequestration in agroecosystems. Soil Science Society of America Journal. 2006;**70**:555-569

[60] Bailey VL, Smith JL, Bolton H. Fungal-to-bacterial ratios in soils investigated for enhanced C sequestration. Soil Biology and Biochemistry. 2002;**34**:997-1007

[61] Olson K, Ebelhar SA, Lang JM. Long-term effects of cover crops on crop yields, soil organic carbon stocks and sequestration. Open Journal of Soil Science. 2014;**4**:284

[62] Vicente-Vicente JL, García-Ruiz R, Francaviglia R, Aguilera E, Smith P. Soil carbon sequestration rates under Mediterranean woody crops using recommended management practices: A meta-analysis. Agriculture, Ecosystems & Environment. 2016;**235**:204-214

[63] Rahman F, Rahman MM, Rahman GKMM, Saleque MA, Hossain ATMS, Miah MG. Effect of organic and inorganic fertilizers and rice straw on carbon sequestration and soil fertility under a rice–rice cropping pattern. Carbon Management. 2016;**7**:41-53

[64] Cheng W et al. Changes in the soil C and N contents, C decomposition and N mineralization potentials in a rice paddy after long-term application of inorganic fertilizers and organic matter. Soil Science and Plant Nutrition. 2016;**62**:212-219

[65] Koga N, Hayashi K, Shimoda S. Differences in CO_2 and N_2O emission rates following crop residue incorporation with or without field burning: A case study of adzuki bean residue and wheat straw. Soil Science and Plant Nutrition. 2016;**62**:52-56

[66] Arai H, Hosen Y, Pham Hong VN, Thi NT, Huu CN, Inubushi K. Greenhouse gas emissions from rice straw burning and straw-mushroom cultivation in a triple rice cropping system in the Mekong Delta. Soil Science and Plant Nutrition. 2015;**61**:719-735

[67] Nakajima M et al. Modeling aerobic decomposition of rice straw during the off-rice season in an Andisol paddy soil in a cold temperate region of Japan: Effects of soil temperature and moisture. Soil Science and Plant Nutrition. 2016;**62**:90-98

[68] Stewart CE, Paustian K, Conant RT, Plante AF, Six J. Soil C sequestration: Concept, evidence and evaluation. Biogeochemistry. 2007;**86**:19-31

[69] Blair N, Faulkner RD, Till AR, Korschens M, Schulz E. Long-term management impacts on soil C, N and physical fertility-Part II: Bad Lauchstadt static and extreme FYM experiments. Soil and Tillage Research. 2006;**91**:39-47

[70] Powlson DS, Whitmore AP, Goulding WT. Soil C sequestration to mitigate climate change: A critical re-examination to identify the true and the false. European Journal of Soil Science. 2011;**62**:42-55

[71] Guo ZC, Zhang ZB, Zhou H, Rahman MT, Wang DZ, Guo XS, Li LJ, Peng XH. Long-term animal manure application promoted biological binding agents but not soil aggregation in a Vertisol. Soil and Tillage Research. 2018;**180**:232-237

[72] Naresh RK, Gupta RK, Minhas PS, Rathore RS, Ashish and D, Purushottam. Climate change and challenges of water and food security for smallholder farmers of Uttar Pradesh and mitigation through C sequestration in agricultural lands: An overview. International Journal of Chemical Studies. 2017

[73] Kukal SS, Rasool R, Benbi DK. Soil organic C sequestration in relation to organic and inorganic fertilization in rice-wheat and maize-wheat systems. Soil and Tillage Research. 2009;**102**:87-92

[74] Liebig MA, Varvel GE, Doran JW, Wienhold BJ. Crop sequence and nitrogen fertilization effects on soil properties in the western Corn Belt. Soil Science Society of America Journal. 2002;**66**:596-601

[75] Novelli LE, Caviglia OP, Piñeiro G. Increased cropping intensity improves crop residue inputs to the soil and aggregate-associated soil organic C stocks. Soil and Tillage Research. 2017;**165**:128-136

[76] Christensen BT. Physical fractionation of soil and structural and functional complexity in organic matter turnover. European Journal of Soil Science. 2001;**52**(3):345-353

[77] Fang Y, Nazaries L, Singh BK, Singh PB. Microbial mechanisms of C priming effects revealed during the interaction of crop residue and nutrient inputs in contrasting soils. Global Change Biology. 2018;**24**(7):2775-2790

[78] Pablo GP, Andreas G, Helene BJ, Lijbert B, Filipe C, Helena C, Jean-Christophe C, Gerlinde DD, Tina DH, Arnaud F, Katarina H, Sandra L, Nicolas L, Martina L, Paul M, Martínez-García LB, da Silva PM, Adrian M, Eduardo N, Filipa R, Sarah S, José PS, Rubén M. Crop traits drive soil C sequestration under organic farming. Journal of Applied Ecology. 2018;**00**:1-10

[79] Inbar Y, Chen Y, Hadar Y. Humic substances formed during the composting of organic matter. Soil Science Society of America Journal. 1990;**54**:1316-1323

[80] Post WM, Kwon KC. Soil C sequestration and land-use change: processes and potential. Global Change Biology. 2000;**6**:317-327

[81] Wallace P. Compost use in agriculture consolidated report phase 2. Grant Scape and the Applied Research Forum. London: Routledge, Taylor and Francis Group; 2007

[82] Farina R, Testani E, Campanelli G, Leteo F, Napoli R, Canali S, Tittarelli F. Potential C sequestration in a Mediterranean organic vegetable cropping system. A model approach for evaluating the effects of compost and agro-ecological service crops (ASCs). Agricultural Systems. 2018;**162**:239-248

[83] Baldi E, Cavani L, Margon A, Quartieri M, Sorrenti G, Marzadori C, Toselli M. Effect of compost application on the dynamics of C in a nectarine orchard ecosystem. Science of the Total Environment. 2018;**637-638**:918-925

[84] Kameyama K, Shinogi Y, Miyamoto T, Agarie K. Estimation of net C sequestration potential with farmland application of bagasse charcoal: Life cycle inventory analysis through a pilot sugarcane bagasse carbonisation plant. Soil Research. 2010;**48**:586-592

[85] Kameyama K, Iwata Y, Miyamoto T. B amendment of soils according to their physico-chemical properties. Japan Agricultural Research Quarterly. 2017;**51**:117-127

[86] Creamer AE, Gao B, Zhang M. C dioxide capture using B produced from sugarcane bagasse and hickory wood. Chemical Engineering Journal. 2014;**249**:174-179

[87] Benbi DK, Thind HS, Sharma S, Brar K, Toor AS. Bagasse ash application stimulates agricultural soil C sequestration without inhibiting soil enzyme activity. Communications in Soil Science and Plant Analysis. 2017;**48**:1822-1833

[88] Patel B, Gami B, Patel P. C Sequestration by Bamboo Farming on Marginal Land and Sustainable Use of Wood Waste for Bioenergy: Case Studies from Abellon Clean Energy. Singapore: Springer Singapore; 2017. pp. 451-467

[89] Margenot AJ, Griffin DE, Alves BSQ, Rippner DA, Li C, Parikh SJ. Substitution of peat moss with softwood B for soil-free marigold growth. Industrial Crops and Products. 2018;**112**:160-169

[90] Lamlom SH, Savidge RA. A reassessment of C content in wood: variation within and between 41 North American species. Biomass and Bioenergy. 2003;**25**:381-388

[91] Laird DA. The charcoal version: A win-win scenario for simultaneously producing bioenergy, permanently sequestering C, while improving soil and water quality. Agronomy Journal. 2008;**100**:178-181

[92] Lehmann J. Bio-energy in the black. Frontiers in Ecology and Environment. 2007;**5**:381-387

[93] Hecht SB. Agroforestry in the Amazon Basin: Practice, theory and limits of a promising land use. In: Hecht SB, editor. Amazonia: Agriculture and Land Use Research. Proc. Int. Conf., Cali, Colombia; 1982. pp. 331-372

[94] Rondon M, Ramirez JA, Lehmann J. Charcoal additions reduce net emissions of greenhouse gases to the atmosphere. In: Proceedings of the 3rd USDA Symposium on Greenhouse Gases and C Sequestration; March 21-24, 2005; Baltimore, USA. 2005. pp. 28

[95] Zeeshan N, Nasir MS, Nasir A, Saifullah, Farooqi ZR, Naveed K. Air contamination and its impact on plants, humans and water of Pakistan—A review. Journal of Applied Environmental and Biological Sciences. 2016;**6**(8), 32-39

[96] Windeatt JH, Ross AB, Williams PT, Forster PM, Nahil MA, Singh S. Characteristics of biochars from crop residues: Potential for carbon sequestration and soil amendment. Journal of Environmental Management. 2014;**146**:189-197

[97] Galinato SP, Yoder JK, Granatstein D. The economic value of B in crop production and C sequestration. Energy Policy. 2011;**39**:6344-6350

[98] Sheng Y, Zhu L. B alters microbial community and C sequestration potential across different soil pH. Science of The Total Environment. 2018;**622-623**:1391-1399

[99] Belmonte BA, Benjamin MFD, Tan RR. Bi-objective optimization of B-based C management networks. Journal of Cleaner Production. 2018;**188**:911-920

[100] Wang X, Feng Y, Liu J, Lee H, Li C, Li N, Ren N. Sequestration of CO_2 discharged from anode by algal cathode in microbial carbon capture cells (MCCs). Biosensors and Bioelectronics. 2010;**25**:2639-2643

[101] Jin L, Li Y, Gao Q, Liu Y, Wan Y, Qin X, Shi F. Estimate of C sequestration under cropland management in China. Scientia Agricultura Sinica. 2008;**41**:734-743. in Chinese with English summary

[102] Buysse P, Roisin C, Aubinet M. Fifty years of contrasted residue management of an agricultural crop: impacts on the soil C budget and on soil heterotrophic respiration. Agriculture, Ecosystems and Environment. 2013;**167**:52-59

[103] Minasny B, McBratney AB, Hong SY, Sulaeman Y, Kim MS, Zhang YS, Kim YH, Han KH. Continuous rice cropping has been sequestering C in soils in Java and South Korea for the past 30 years. Global Biogeochemical Cycles. 2012:26-34

[104] Raji BA, Ogunwole JO. Potential of soil C sequestration under various land use in the sub-humid and semi-arid savanna of Nigeria: Lessons from long-term experiments. International Journal of Soil Science. 2006;**1**(1):33-43

[105] Sanderman J, Farquharson R, Baldock J. Soil C sequestration potential: A review for Australian agriculture. A report prepared for the Department of Climate Change and Energy Efficiency CSIRO National Research Flagships; 2010

[106] Lam SK, Chen D, Mosier AR, Roush R. The potential for C sequestration in Australian agricultural soils is technically and economically limited. Scientific Report. 2013;**3** (Article number: 2179)

[107] Tsai CC, Chen ZS, Hseu ZY, Duh CT, Guo HY. Organic carbon storage and management strategies of the forest soils on the forest soil survey database in Taiwan. In: Chen ZS, Agus F, editors. In: Proceedings of International Workshop on Evaluation and Sustainable Management of Soil Carbon Sequestration in Asian Countries; Sep 28-29, 2010; Bogor, Indonesia. 2010. pp. 85-102

[108] Jien SH, Hseu ZY, Guo HY, Tsai CC, Chen ZS. Organic carbon storage and management strategies of the rural soils on the basis of soil information system in Taiwan. In: Chen ZS, Agus F, editors. In: Proceedings of International Workshop on Evaluation and

Sustainable Management of Soil Carbon Sequestration in Asian Countries; Sep 28-29, 2010; Bogor, Indonesia. 2010. pp. 125-137

[109] Tsui CC, Tsai CC, Chen ZS. Soil organic carbon stocks in relation to elevation gradients in volcanic ash soils of Taiwan. Geoderma. 2013;**209**:119-127

[110] National Inventory Report (NIR). Belgium's greenhouse gas inventory (1990-2014). National Inventory Report submitted under the United Nations Framework Convention on Climate Change. Brussels: VMM, VITO, AWAC, IBGE, IRCEL, ECONOTEC; 2016. 360 pp

[111] Wahyunto DA, Agus F. Distribution, properties, and carbon stock of Indonesian Peatland. In: Chen ZS, Agus F, editors. In: Proc. of Int. Workshop on Evaluation and Sustainable Management of Soil Carbon Sequestration in Asian Countries (ISRI-FFTC-NIAES, Bogor); Sept. 28-29, 2010; Bogor, Indonesia. 2010. pp. 187-204

[112] Hong SY, Minasny B, Zhang YS, Kim YH, Jung KH. Digital soil mapping using legacy soil data in Korea. In: Proceedings of the 19th World Congress of Soil Science, Soil Solutions for a Changing World; 1-6 August 2010; Brisbane, Australia. 2010

[113] Akpa SIC, Odeh IOA, Bishop TFA, Hartermink AE, Amapu IY. Total soil organic carbon and carbon sequestration potential in Nigeria. Geoderma. 2016;**271**:202-215

[114] Viscarra Rossel RA, Webster R, Bui EN, Baldock JA. Baselinemap of organic carbon in Australian soil to support national carbon accounting and monitoring under climate change. Global Change Biology. 2014;**20**:2953-2970

Chapter 3

Blue Carbon on Polar and Subpolar Seabeds

David Keith Alan Barnes

Additional information is available at the end of the chapter

http://dx.doi.org/10.5772/intechopen.78237

Abstract

When marine organisms eat and grow they capture and store carbon, termed blue carbon. Polar seas have extreme light climates and sea temperatures. Their continental shelves have amongst the most intense phytoplankton (algal) blooms. This carbon drawdown, storage and burial by biodiversity is a quantifiable 'ecosystem service'. Most of that carbon sinks to be recycled by microbes, but some enters a wider food web of zooplankton and their predators or diverse seabed life. How much carbon becomes stored long term or buried to become genuinely sequestered varies with a wide range of factors, e.g. geography, history, substratum etc. The Arctic and Antarctic are dynamic and in a phase of rapid but contrasting, complex physical change and marine organismal carbon capture and storage is altering in response. For example, an ice shelf calving a 5000 km^2 iceberg actually results in 10^6 tons of additional blue carbon per year. Polar blue carbon increases have resulted from new and longer climate-forced, phytoplankton blooms driven by sea ice losses and ice shelf collapses. Polar blue carbon gains with sea ice losses are probably the largest natural negative feedback against climate change. Here the current status, variability and future of polar blue carbon is considered.

Keywords: blue carbon, polar oceans, benthos, carbon immobilization, negative feedback

1. Introduction

Blue carbon is carbon captured and held within marine organisms. It is considered as one type of 'ecosystem service' that biodiversity provides, and thus is part of the value of biodiversity, often termed 'natural capital'. Typically blue carbon evaluations mainly consider habitats such as kelp forests, sea grass beds, salt marshes and mangrove swamps. These are global organismal powerhouses of carbon turnover and support huge biomasses of varied animal life [1]. These

environments are all characterized by rapid growth (high carbon capture) and high biomass (high carbon storage) but over relatively small, coastal areas that are dwindling with anthropogenic land use pressures. Of these environments, only kelp forests are represented in the polar and subpolar regions (**Figure** 1**a**), and even these are scarce because of regular iceberg scouring in shallow waters. Thus blue carbon ecosystem services have to date been little considered in the Arctic and Antarctic, although on land it was realized that a warming Arctic could lead to increased Taiga forest carbon capture and storage. However the magnitude of any negative feedback (mitigation) on climate change is complicated by change in permafrost gas release, reduced albedo because of altered snow cover and less than expected forest growth gains [2]. Nevertheless warming-induced Arctic vegetation expansion represents a rare, and significant, increasing source of carbon capture and thus negative feedback on climate change (this is because of Taiga forest carbon capture is increasing with regional warming, which reduces the greenhouse gas Carbon Dioxide). Antarctica has no forests and > 1% is ice free for the very limited plant biodiversity present, although this is likely to increases with snow and ice retreats.

There are very considerable, if intensely seasonal, phytoplankton (micro-algae) blooms around Arctic and Antarctic coasts and on the underside of seasonal sea ice (the ocean surfaces freeze in winter) [3]. The composition of these blooms vary in time and space but are mainly tiny algae called diatoms, which can be eaten by animals in the food web. On death the vast majority of this huge summer primary productivity sinks through the water column where it is recycled by microbes (mainly bacteria) or eventually reaches the seabed, where most is again recycled, but by seabed microbes. This is called the microbial loop and is responsible for most

Figure 1. High latitude benthic biomass and blue carbon. Macro algae at South Georgia (a), benthic fauna in the shallows of Antarctic, Adelaide Island (b) and Arctic Tromsø (b), and at deeper continental shelf depths around Kerguelen.

http://dx.doi.org/10.5772/intechopen.78237

polar blue carbon and energy cycling, but little is known about how much of this carbon is ultimately buried and thus genuinely sequestered. Even though only a small proportion of this productivity is consumed by animals, this still supports the largest abundances of animals on Earth, the copepod and euphausiid shrimps (krill). Their biomass, their feces [4] and in turn that of their predators (seabirds, seals and whales), become significant agents of carbon storage and turnover. As with primary productivity though, to be sequestered, the carbon accumulated in water column animals must sink to considerable depths and avoid microbial recycling on route or once it arrives at the seabed and be quickly buried. Recent work on the marine primary consumers (often called herbivores) amongst the zooplankton has shown that their vertical migrations, coupled with considerable lipid storage is a major factor in transferring carbon to the seabed [5]. Furthermore passing through the guts of zooplankton, such as krill, changes iron chemically to make it more bio-available, thus promoting and sustaining the very phytoplankton blooms on which they feed [6]. As a result the increased phytoplankton bloom fixes more CO2 and becomes another system feedback.

Although life in the water column in polar oceans is extremely numerous, it is not rich or diverse, compared with the seabed, and crucially is a long way in time and space for the site of ultimate carbon sequestration – the seabed. The vast majority of known polar species are benthic (seabed dwelling) as adults and many for their entire life-cycles [7]. Living on the seabed, especially as most of it is soft sediment (muds and clays), gives considerable potential for benthos to deliver carbon burial and sequestration. One of the primary factors hindering this pathway is seabed disturbance, unburying and reworking carbon in dead organisms. Storms can do this in the shallows and bioturbation (e.g. burrowing activity) across depths, but in the polar regions icebergs and diving mammals (e.g. walrus) can be major reducers of carbon sequestration. However a big factor is human disturbance of the seabed, such as harvesting by trawling. Most of the world's continental shelf seabed, including the Arctic, is territorial water of varying countries, which has valuable harvestable resources, such as food. In contrast the continental shelf around Antarctica is not owned, and the limited fishing which does occur is strongly regulated by the Committee for Conservation of Antarctic Marine Living Resources (CCAMLR). This governance, and as a result benthic harvesting impact, difference between the polar regions must have very significant influences on the magnitude of carbon buried and sequestered.

This chapter investigates blue carbon on high latitude seabeds (see **Figure 1**). Such a consideration starts by focusing on how and why it varies, between organism types, spatially, historically and with specific environmental factors. How blue carbon capture and storage is now changing in response to rapid, recent, regional physical change, such as 'global climate change' and stratospheric ozone losses. This is important given that parts of the polar regions are amongst the most rapidly and profoundly changing areas on Earth. An attempt is then made to evaluate the importance of polar blue carbon to the Earth system, with its respect to its action as a negative feedback on climate change. Lastly the likely future of polar blue carbon is considered and how this might be better monitored, for example by initiatives such as the Southern Ocean Observing System (SOOS). The polar oceans are key sinks for anthropogenic production of CO_2 and the sensitivity of their carbon cycles to physical change is poorly known and understood [9]. Blue carbon, in contrast to that stored dissolved in polar oceans storage is undoubtedly very much smaller, but increasing and with high genuine sequestration potential, and perhaps its quantification could lead to understanding some of the current unexplained variability in global model projections.

2. Environmental influences on the distribution and magnitude of benthic blue carbon around polar seabeds

Sediment cores taken by geological scientists around the polar regions have shown very considerable patchiness in the both the amount and proportion of carbonate ($CaCO_3$) in polar sediments [8]. Benthic biological work over the last century has similarly demonstrated a huge variety in the carbon stocks held in biota on the seabed [10]. The source of these is the dissolved carbon (dioxide) in water masses and huge, but intensely seasonal productivity by phytoplankton and dependent consumers, such as copepods and euphausiid crustaceans. The variability in the blue carbon component, despite being complex in both time and space, is predictable on some scales, but knowledge levels are also very patchy. The interface of the water column and the underlying sediments, the seabed, is a very dynamic environment for carbon [11]. Primary productivity, fecal pellets and dead organisms rain down to the seabed where they are mainly broken down by the 'microbial loop', thus recycling much of the carbon from near surface waters.

2.1. Carbonate in sediments

Remarkably it was not until 2012 that the first circum-southern polar data set of carbonate in sediments was compiled (from just over 200 sediments cores from Antarctica's shelf seas [8]). Low-Magnesium calcite is the dominant phase of sediment carbonate, but high-Magnesium calcite, pure calcite and aragonite are also present. The study found that the proportion of carbonate in sediments was typically low, but could be above 15% in some shallow Weddell and deep Amundsen and Bellingshausen shelf areas. The magnitude of values found was very patchy, but most of the highest values were close to the edge of shelf (termed 'shelf break'). Even at the shelf break in the same sea carbonate could vary an order of magnitude between adjacent sites, so clearly local factors are very important as well. Notably sediments in regions of high primary production (surface microalgae productivity) such as the West Antarctic Peninsula and Ross Sea were generally below 5% carbonate. The authors concluded that the evidence in their meta-analysis was that benthic animals were not significant contributors to sediment carbonate content. Their core and data spatial coverage, although sparse around East Antarctica (as most marine data sets are), seemingly represented the spectrum of most shelf environments. However the conclusions based on existing samples could be underestimating faunal contributions for several reasons. 1) Across depths, faunal biomass and production is typically highest in the shallows (top 100 m) which were not represented. 2) Across habitats, faunal biomass and production is typically highest in difficult to core situations, such as glacial moraines, sea mounts and steep surfaces. 3) Much faunal production close to shelf breaks may be bulldozed over the edge to cascade down steep continental slopes and canyons – these are heavily iceberg scoured environments (**Figure 2**). However most blue carbon, the totality of carbon captured by organisms, is not in the form of carbonate but organic carbon as tissue.

2.2. Carbon held by marine animals (blue carbon)

Carbon captured by, and stored in, benthic organisms varies (within a set amount of space) over several orders of magnitude. Standing stocks peak in the kelp forests of the subpolar shallows with many kilograms per m^2 but decreases to less than a few grams by continental

http://dx.doi.org/10.5772/intechopen.78237

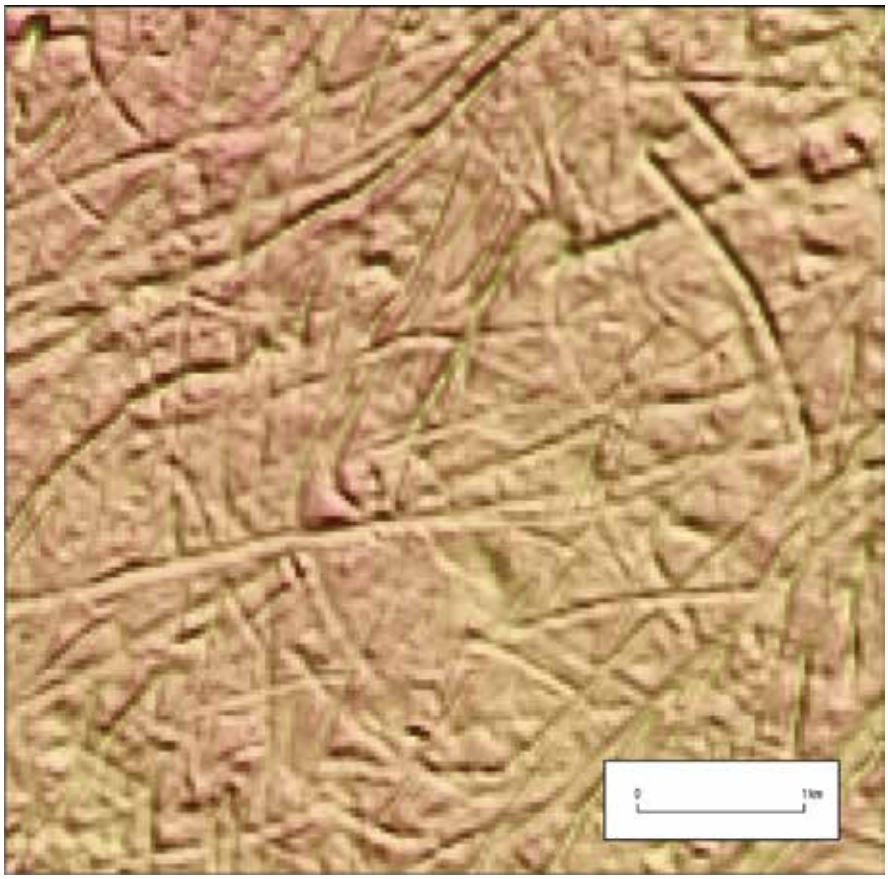

Figure 2. Iceberg scouring tracks recorded by the NERC-Conicyt ICEBERGS voyage of RRS James Clark Ross, Marguerite Bay, West Antarctic peninsula, 2017.

slope depths, on young or ice scoured surfaces, underneath Antarctic ice shelves or in other extreme environmental situations.

2.2.1. Organism identity

Some organism types are very much more important than others in terms of carbon and carbonate capture and storage. Some entire animal groups are poorly represented or absent altogether in the polar waters so clearly contribute little to carbon budgets. Typically variability in carbon contribution can be because of population and individual size (biomass), growth rates, ubiquity and the body structure and chemistry of different organisms. For example amongst the plankton the tiny foraminifera *Neogloboquadrina pachyderma* is both very abundant and ubiquitous around the Southern Ocean, and superabundant in sea ice, making it the single biggest carbonate producer [12]. A very different type and size of animal, the pelagic mollusk, pteropods (**Figure 3**) is next most important. As with foraminifers, around the Antarctica one species, *Limacina helicina*, dominates biomass [13]. Blue carbon captured and stored on the seabed by benthos is much less dominated by any one species or even any one type of animal. Sponges, echinoderms (such as sea stars and sea urchins), bryozoans (**Figure** 1**a**), polychaete worms (**Figure** 1**b**), molluscs

Figure 3. Pteropod shells are superabundant on the seabed around some Atlantic Ocean seamounts, here collected on a National Geographic Pristine Seas expedition in 2017.

(such as clams and snails), brachiopods (lampshells) are all typically important, and can each by dominant at particular sites but lots of other taxa can be important depending on the situation (environmental characteristics). Nevertheless organism identity can still qualify much information about the nature of blue carbon at a site, because of differences in the rate and timing of carbon capture, time to first reproduction and life span, chemical form of carbon stored (e.g. skeletal aragonite vs. calcite) vulnerability and other variables.

2.2.2. Substratum type and profile as a factor

The nature of the seabed often shapes and is shaped by the energy of the environment and thus has a major role in structuring which organisms live there and the quality and quality

http://dx.doi.org/10.5772/intechopen.78237

of their resources, such as food. For example very steep surfaces are nearly always bedrock and associated with high current flow whereas very gently sloping, flat seabeds are usually sediment and associated with lower flow. So-called infauna require soft sediments to burrow into or eat to extract microbes whereas hard surfaces are required by many anchored sessile organisms, such as kelp algae and encrusting animals. The spectrum from bed rock to muds and clays can all potentially hold high and low carbon standing stock biodiversity in the polar regions. Investigation of blue carbon by substratum type is often confounded by interaction with other variables, such as depth, geography, history and functional traits (e.g. feeding type). Nevertheless hard surfaces typically have high densities of rich biota, particularly those which are carbonaceous (bryozoans, brachiopods, corals, sponges and some molluscs). Stones which have been embedded in glacier ice, fall out on melting (termed drop-stones) to form blue carbon hotspots of suspension feeders on otherwise less diverse, sediment plains (**Figure** 4**a**) [14]. As a

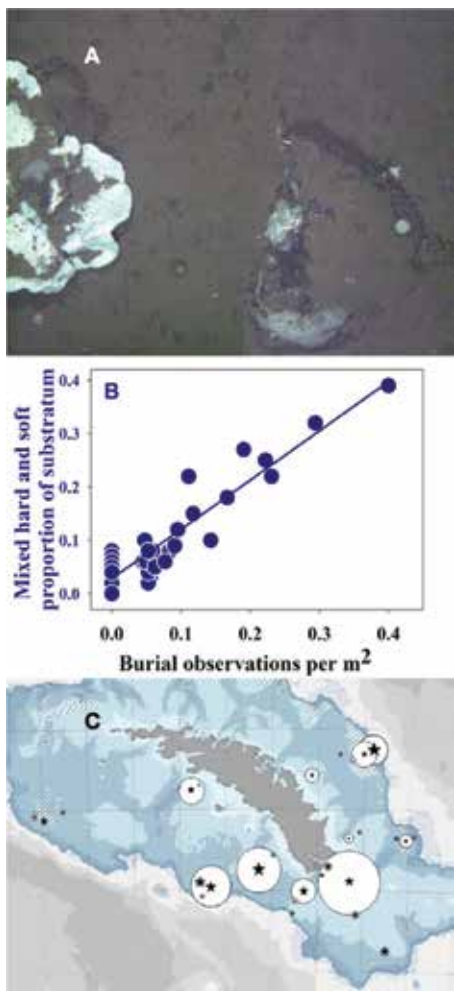

Figure 4. Blue carbon with substratum type and history. Drop-stones are blue carbon rich oases in the Arctic Barents Sea (A). Highest burial rates of zoobenthic carbon are associated with mixed substrata of boulders in sediments at South Georgia (B). Estimates of Carbon immobilization (circle size) and sequestration (star size) (C) [15].

result accumulation of blue carbon by zoobenthos is often most associated with hard surfaces such as boulder scree and glacial moraines [15]. The same work showed that hard surfaces facilitate immobilization of carbon, which is when organic carbon is held within tight matrices of skeleton, such as stony coral polyps (e.g. heavily skeletalized animals are much more likely to fossilize, thus sequestering carbon rather than it being broken down in the microbial loop). However burial conditions, which lead to sequestration are considerably stronger on sediments. Thus highest burial and sequestration rates are found at the interface of hard and soft substrata (**Figure** 4**b,c**). Such a combination is hard to investigate because it is a challenging environment to try and obtain cores from (e.g. the hard rocks break the plastic multi-cores and jam box core closing mechanisms).

2.2.3. Depth as a factor

Many physical and biological characteristics alter with depth so unsurprisingly it can correlate strongly with benthic carbon accumulation [4]. Increased depth away from the near-surface photic zone progressively separates fauna from their main food supply, phytoplankton, so it reduces growth, densities and biomass [1, 3, 10, 16]. The values of carbon accumulation, immobilization and sequestration can be an order of magnitude lower on the deep continental shelf than in the shallows (**Figure 5**). In deeper water blue carbon values are probably at least an order of magnitude lower again. Conversely to negative depth influences on blue carbon

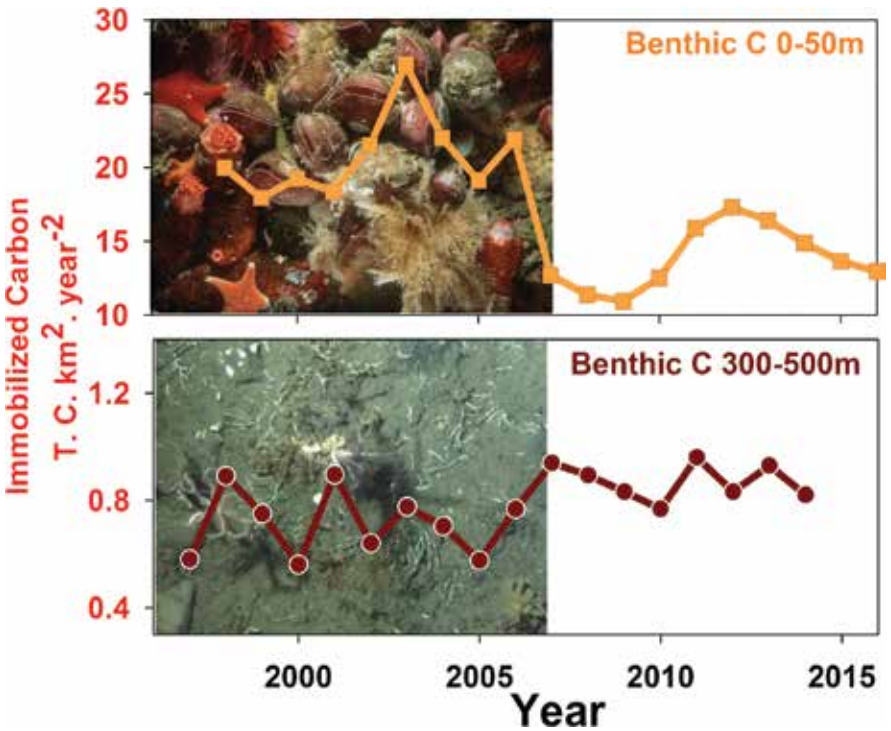

Figure 5. Zoobenthic blue carbon storage fluctuation with time and depth on the West Antarctic peninsula, modified from [4]. Note the apparent phase shift since 2006 coincident with low sea ice levels and high iceberg scouring levels.

accumulation, increased depth also reduces the probability and frequency of iceberg scouring on the seabed, thereby increasing the potential life span of benthos and burial chances. The effect of these confounding depth-correlates are complex biological responses to climate change with depth. For example, climate-forced reductions in sea ice, as is happening around the Arctic and parts of the West Antarctic, can reduce blue carbon in the shallows because of increased ice scour but increase it in deep water because of longer phytoplankton blooms [4]. Substratum type and profile, temperature and geographic factors also change with depth. An example of the latter is that benthos become more geographically separated in time and space (not just bathymetrically) from the origin point of their food because of water current velocities and directions.

2.2.4. Geography and history as factors

Most, though not all, shallows and shelf are associated with coast in the polar regions, just like elsewhere in the world. This drives an onshore-offshore gradient in polar blue carbon, but it is further exacerbated by most physical change (e.g. melt runoff, glacier retreat and ice shelf collapse) also being coast-associated. There is major temperature, sea ice duration and productivity variability associated with different regions around and between the polar seas, as is reflected in strongly contrasting biomass [10] and sediment carbonate values [8]. Within a distinct area the separation of different habitats and zoobenthic blue carbon performance can be geographically predictable factors, which also reflect regional history. A clear example of this can be seen in the continental shelf around the South Georgia archipelago. Blue carbon accumulation is highest on the glacial moraines, which are generally found close to the shelf break, the furthest extent of grounded ice in the Last Glacial Maximum [15]. However such moraines can also be found at the head of canyons and part way along some coastal fjords. The oldest sediments beyond these moraines have the highest sediment blue carbon values, whereas the sediments within these moraines (which were covered by grounded ice just 20 kya are blue carbon poor (**Figure** 4**c**). The highest blue carbon burial and estimated sequestration rates were at the interface of these moraines and sediments.

Zoobenthic blue carbon levels also reflect more recent historical and geographic factors, such as invasion of seabed following glacier retreat, ice shelf collapses and recovery from iceberg impacts. At South Georgia depressed blue carbon values have been measured nearly a decade after giant (thousands of square km in size) iceberg impact [17]. The same study showed there are distinct macrogeographic hotspots of giant iceberg grounding, but the same is true within regions, where shelf breaks are most likely to be impacted. The hotspots of smaller icebergs are more associated with retreating glaciers and longer periods of open water, such as the West Antarctic Peninsula [16, 17]. As with biodiversity succession, the seabed blue carbon within the shallowest hundred meters probably strongly reflects the duration of recovery since the last iceberg scour at any one location. The lowest continental shelf values of blue carbon are those underneath the thick floating ice shelves [18]. However collapse of these can lead to major new phytoplankton blooms and the highest blue carbon capture rates and benthic growth (blue carbon storage levels) [19]. Ice shelf collapses have been most associated with the Weddell and Bellingshausen seas, most recently the major breakout of the 6000 km^2 iceberg from Larsen C. Such events are very important in terms of blue carbon budgets and

dynamics, both in the water column [20] and the seabed [17]. As a result there is strong connectivity between temperature, ice changes and blue carbon.

2.2.5. Temperature as a factor

The polar regions, particularly the Southern Ocean, are typically the most thermally constant surface regions of our planet. Annual polar sea temperature variability is generally less than 4°C in the Southern hemisphere but more geographically variable around the Arctic. A major source of variability has been Milankovitch 41 and 101 kyr Earth orbital cycles but this has been overshadowed in the Arctic by rapid, recent, regional climate change. Temperature can theoretically influence blue carbon through influences of ocean chemistry, sea ice formation and duration and physical constraints on enzyme performance, effecting food processing, carbonate synthesis and biomass growth rates. Ashton et al. [21] recently attempted to manipulate polar seabed temperature, whilst leaving other factors unchanged. Their study at Rothera Research Station (WAP), which established a series of temperature controlled artificial substrata, found that temperature had a stronger and more complex influence on growth than expected. A 1°C increase led to a significant increase in blue carbon (but measured as growth increment) whereas responses to a 2°C increase resulted in increased variance of assemblages. The major surprise was the extent of the increased growth (approximately double), which far exceeded that predicted by calculations of a pure temperature effect. The experimental infrastructure has now been transferred to the Canadian Arctic station of Cambridge Bay to compare the response of raised temperature of northern to southern polar nearshore fauna.

2.2.6. Other factors (sedimentation and water chemistry)

Many environmental factors are likely to influence blue carbon capture and storage rates around polar seas but our knowledge and understanding of these is patchy. Amongst the best studied locations are King George Island (South Shetland Islands, Antarctic Peninsula) in the south and West Spitsbergen (Svalbard) in the North. Multinational, interdisciplinary efforts to study biotic interactions to a multitude of environmental parameters at such places are enabling scientists to examine which factors are most important, to which organism types and to which stages of the carbon pathway. In contrast to Ryder Bay, adjacent to Rothera Research Station, where ice scouring [16, 17] and temperature [21] seem to be most important to carbon storage, at Potter Cove, King George Island, sedimentation mainly dictates the composition and performance of benthos. Sahade et al.'s [22] monitoring of that cove since 1998 showed that amongst the many varying factors for benthic life close to a retreating glacier, it was sediment levels and tolerance to this which drove drastic shifts in organism type. However sedimentation is not only co-linked to other variability such as salinity and nutrients but also varies in several different aspects, such as particle density and particle size distributions.

A new multi-year, multi-project investigation of the Atlantic sector of the Arctic, 'Changing Arctic Ocean', should elucidate the nature and dynamics of hyperboreal carbon pathways. Of these the Changing Arctic Ocean Seabed (ChAOS) project lead by Leeds University, UK is monitoring oceanography, geochemistry and biology at a latitudinal series of sites along the Barents Sea trough (**Figure 6**). Results from new initiatives like these should greatly increase our ability to estimate the value and variability of Arctic blue carbon ecosystem services [5, 9] and crucially how it is likely to respond to the very considerable, recent physical changes.

http://dx.doi.org/10.5772/intechopen.78237

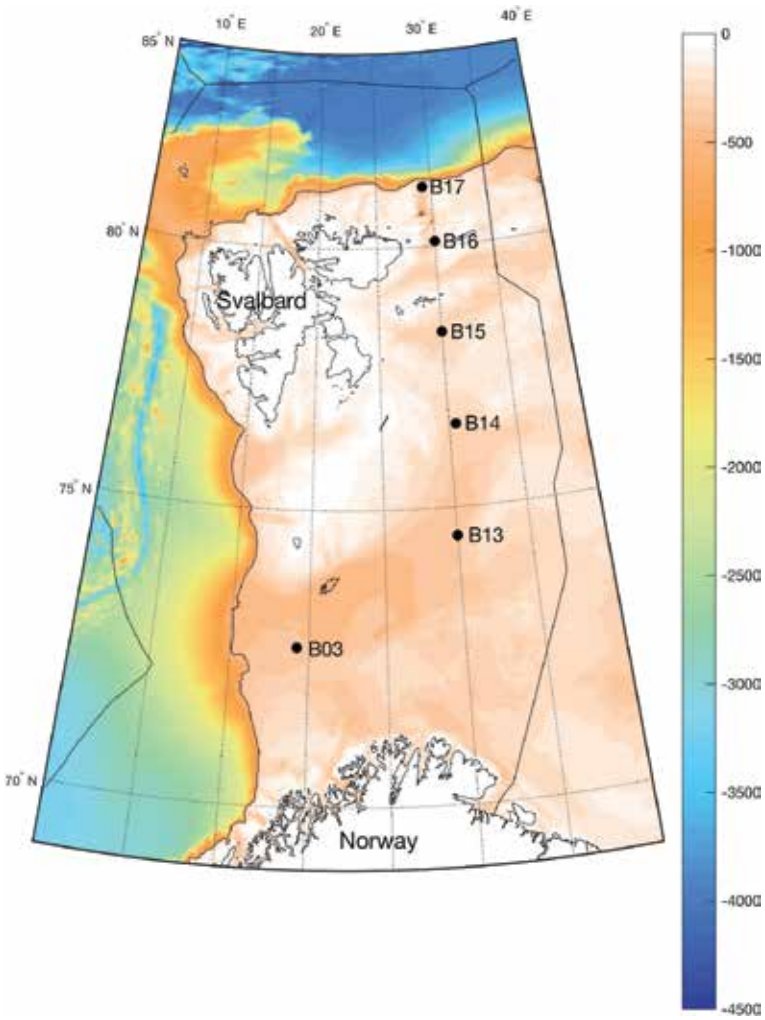

Figure 6. Continental shelf monitoring sites of the changing Arctic Ocean seabed (ChAOS) project, through the Barents Sea.

2.3. Seasonal and annual increment (growth)

Organisms incrementally capture and store carbon with distinct seasonal and annual variation (mainly caused by feeding reduction or cessation in winter). These temporal signals in carbon accumulation are externally visible in some organisms and observable in others by section (like tree rings) or through isotopic analyses. Thus one of the easiest approaches to measure carbon capture and storage on the seabed is to sequentially sample benthic growth to establish its variance. Because of the multitude of environmental factors influencing the magnitude of these (Section 2.2 above), simultaneous measurement of many local parameters needs to be made, in order to detect and understand any organismal performance trends. Growth (along with other processes, e.g. development) is typically considered to be slow in polar ectotherm organisms, in comparison with those at lower latitudes in the world [10]. However there is considerable variability in blue carbon captured in that organismal growth,

within and between regions, organisms, environments and time. Partitioning out the causes and effects of variability is key to meaningful estimates of blue carbon stocks and how they are likely to change. For example, young animals are likely to have higher specific growth rates (thus have high carbon capture but low storage values) whereas older animals would typically be larger but grow slower (and thus be associated with low carbon capture but high carbon storage values). Thus an event influencing population demographics (e.g. iceberg scour) could change carbon capture relative to storage rates, and this could alter depend on which season it occurred in.

Recent work in the Ross, Weddell and Bellingshausen seas have shown rapid growth rates, and changes in growth rates, are possible in polar organisms. Such blue carbon change has happened in response to wind-driven or ice shelf collapse promoted increased food availability [18, 19, 23] respectively, or increase in temperature [21]. With carbon sinks, sources and flux values being so important to global climate as well as projecting trends and predicting future scenarios it is clear that quantification of blue carbon has an important role in this, and the polar regions are the most poorly known. Understanding biological response to polar change has become even more important since it has become apparent that amongst the most severe physical changes have been associated with these areas.

3. Changing blue carbon capture and storage rates in polar seas

Despite the relative constancy in many oceanographic parameters over geological time, the polar regions are quite dynamic in fluctuation between ice ages, the duration and rate of change to interglacial periods and within these, the position of the marginal sea ice zone, water masses and ice shelf extent. All of these can directly alter the biomass of organisms, their carbon capture and storage rates as well as direct carbon dioxide uptake and release by oceanic storage. Section 2 has highlighted that sediment carbonate levels [8] and organism blue carbon capture and storage rates [10, 15] all vary considerably between and within regions. Measuring any change over time necessarily must have georeferenced baselines to measure against but most 'long term monitoring' programmes are relatively young. One of the most notable multidecadal data sets is that for zooplankton, focused on krill and salps. Analysis of this was one of the first to show change in polar ecosystems (krill reductions) in response to climate [24]. However these organisms are mobile and ice edge associated, which highlight both problems in measurement and interpretation – are the less krill in there survey areas because there are less overall or because they are somewhere-else? Crustacean zooplankton, such as Krill, are important to blue carbon capture and storage rates [5, 6] and may be important to sequestration rates as well [4].

We know little about blue carbon capture, storage and sequestration rates for the vast majority of the seabed, and there are a tiny number of sites which have been monitored regularly for more than a decade. Recently a series of ice shelf disintegrations along the Antarctic Peninsula and some elsewhere have been accompanied by major increases in primary [18] and secondary [19] production. These new and increased stocks of seabed blue carbon there have been estimated to constitute ~$7x10^5$ tons of carbon per year equivalent to 10,000 hectares of tropical rainforest [19]. These ice shelf collapses have formed an increasing number of giant icebergs,

which have also increased carbon capture in the water column through ocean fertilization [20]. Duprat et al. [20] estimated the increases in water column blue carbon of a number of such icebergs. Those estimates were later built upon in terms of their total blue carbon impact (trade-offs of creating new sink areas and ocean fertilization versus scouring potential) to show a 5000 km^2 iceberg contributes a net positive of 10^6 tons of carbon per year [17]. Ice shelf losses, iceberg production and arctic forest increases [2] are not the only sources of blue carbon change around the polar regions.

Sea ice extent, particularly 'fast ice' (the freezing of the sea surface, anchored to land) has been one of the most drastic physical changes in the polar regions, particularly throughout the Arctic. Sea ice changes and primary production responses have been more complex around Antarctica [25], but crucially most sea ice losses have been over productive continental shelf whereas most of the sea ice gains have been over deeper slope and abyssal ocean depths [16]. Historical expedition zoobenthic collections and modern samples of longer lived animals with relevant information in skeletons has shown that blue carbon capture rates may have doubled over the last 25 years around West Antarctica [26]. The mechanism for this seems to be that reduced extent (in time and space) of sea ice leads to longer (but not necessarily larger biomass) phytoplankton blooms, resulting in longer meal times for primary consumers resulting in more carbon storage as growth (**Figure 7**). The total blue carbon increases driven by sea ice losses [17, 26] probably greatly exceed those caused by ice shelf collapse/giant iceberg formation [17–20]. However, from what we currently know, change in polar blue carbon is a complex of increases

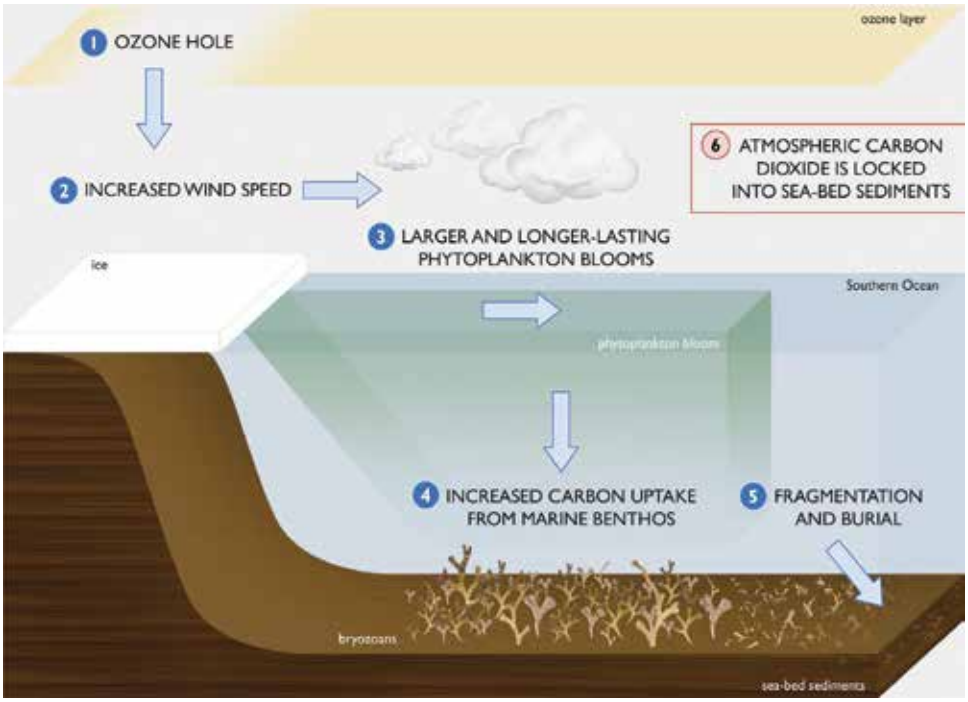

Figure 7. Schematic showing influence of ozone losses on phytoplankton carbon capture and zoobenthic carbon storage on polar seabeds.

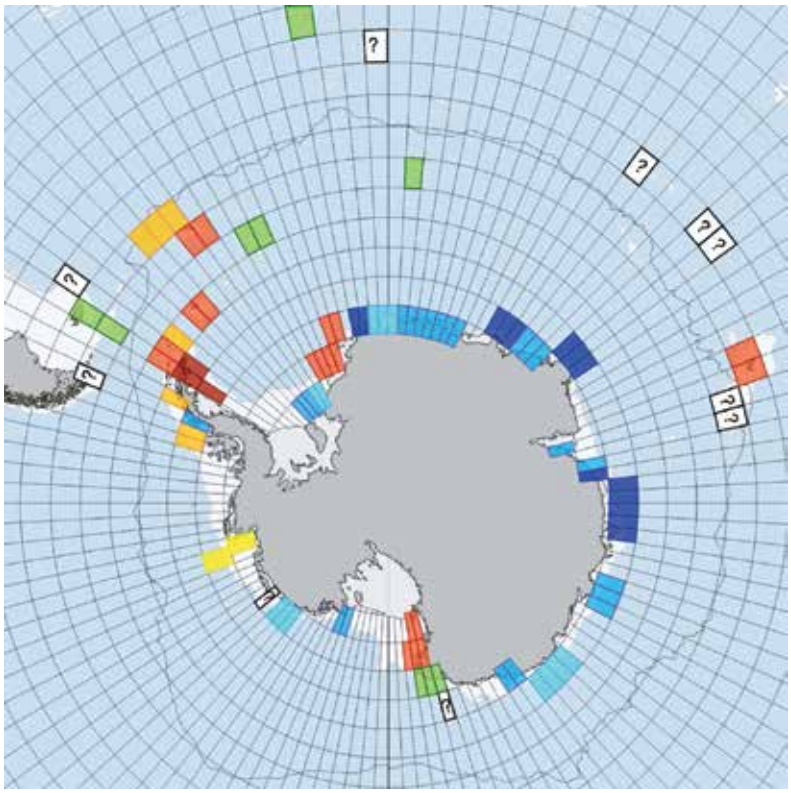

Figure 8. Trends in zoobenthic blue carbon accumulation around the Southern Ocean. The key to cell (3x3 degrees) colors are red (biggest increase) to blue (biggest decrease) [17]. Cells with question marks are samples awaiting analysis (from the Antarctic circumnavigation expedition and future British Antarctic survey scientific cruises.

and decreases (**Figure 8**). Around the Southern Ocean blue carbon increases are most associated with West Antarctic seas and decreases with the East Antarctic coasts [17] but the vast majority of all shelf carbon stocks and change is unknown. It seems likely that the biggest blue carbon changes are near coast caused by ice shelf collapse [18–20], iceberg scour [19] and glacier retreat driven sedimentation [22] but there could also be significant offshore change associated with a shifting seasonal sea ice margin [4, 24, 25]. Given the higher potential ectotherm growth performances at slightly higher sea temperatures [21] it also seems likely that the Arctic and subpolar regions are key areas to quantify blue carbon budgets for. Quantifying these becomes one of the key steps in estimating biotic feedbacks on climate change.

4. The importance of life on polar seabeds to carbon storage and feedbacks on climate change

The cold waters of polar oceans are the major marine sinks for atmospheric CO_2 but these are finite, likely diminishing and do not negatively feedback on global climate change. There is evidence to show that polar marine algal capture of CO_2 has increased with ice shelf loss

http://dx.doi.org/10.5772/intechopen.78237

[18], sea ice loss [25] and iceberg production [20]. It also seems likely that polar macroalgal production could increase spatial and temporal extent with exposure of new habitats, sea ice reduction and increased light energy reaching the shallows. These negatively feedback (mitigate) on climate change through increased capture of CO_2 with increasing atmospheric of CO_2 content. Only very small proportions of this captured CO_2 are genuinely sequestered, depending on how much reaches the seabed and how much is recycled in the microbial loop and reworked following bioturbation. All natural carbon sequestration is via burial, mainly at the seabed, where zoobenthic assemblages (consumers) live. They are an important part of the negative feedback on climate, as new and longer availability of phytoplankton is converted into increased growth (organic carbon to tissues and inorganic carbon to skeletons). The feedback value is complicated to measure because it is dynamic in space and time but also because of simultaneous positives and negatives. For example ice shelf loss leads to more open water, a) reducing albedo, thus potential to absorb more heat; b) reduces buttressing of ice sheets, thus potential for this to accelerate coastwards, c) increasing potential for gas exchange, d) generating new phytoplankton blooms, e) opening new habitat for zoobenthos and f) generating giant icebergs with ocean fertilization potential [17–20]. Even the latter components themselves each contain contrasting feedbacks on climate, for example calving of an giant iceberg such as that to break off Larsen C in 2017 may scour and recycle $4x10^4$ $tCyr^{-1}$ of benthic carbon but algal capture and seabed zoobenthic storage of new carbon contributes a net positive of 10^6 tons of carbon per year [17]. The magnitude of this negative feedback is probably similar to that of Arctic Taiga expansion [2], although this too has also complicating factors such as increased heat absorption and less than expected growth gains.

Sea-ice loss areas exceed 1,000,000 km^2 whereas ice shelf losses approximate to ~30,000 km^2 see http://nsidc.org/) so biological responses to these are the largest measured natural negative feedback on climate change. These are dwarfed as an organic carbon store by tropical forests, but these are not increasing as a result of climate change and thus not a negative feedback (their genuine sequestration potential is also low, as burial rates of carbon are very small except for water logged swamp forests). The magnitude of polar blue carbon negative feedback from sea ice losses depends on whether the carbon is calculated from primary production, secondary production, immobilized carbon or sequestered carbon. The sequestration value is considered to be as low as two orders of magnitude different along the cascade from algal production to buried sequestered benthos (**Figure 9**). Scaling up from regional samples suggests that between 2002 and 2015 the zoobenthic blue carbon negative feedback averaged ~10^7 T C in production, $4.5x10^6$ T C in immobilization or $1.6x10^6$ tons C in terms of sequestration [16] along the West Antarctic Peninsula continental shelf alone. Scaled up to the whole Antarctic continental shelf area ($4.4x10^6$ km^2) the annual zoobenthic blue carbon feedback is estimated at 30-80$x10^6$ T C $yr.^{-1}$ but including outer Subantarctic continental shelves, such as the Kerguelen Plateau doubles this [17], equivalent to 1–2% of global anthropogenic output. It is clear this feedback is dynamic, polar blue carbon storage has demonstrably increased in coincidence with climate-forced sea ice changes, at least around West Antarctica [26]. Global climate change, ozone losses and other indirect (e.g. non indigenous species invasions) or direct (e.g. harvesting) anthropogenic pressures have the potential to have major impacts on marine biodiversity [27], and thus considerably increase or decrease polar blue carbon.

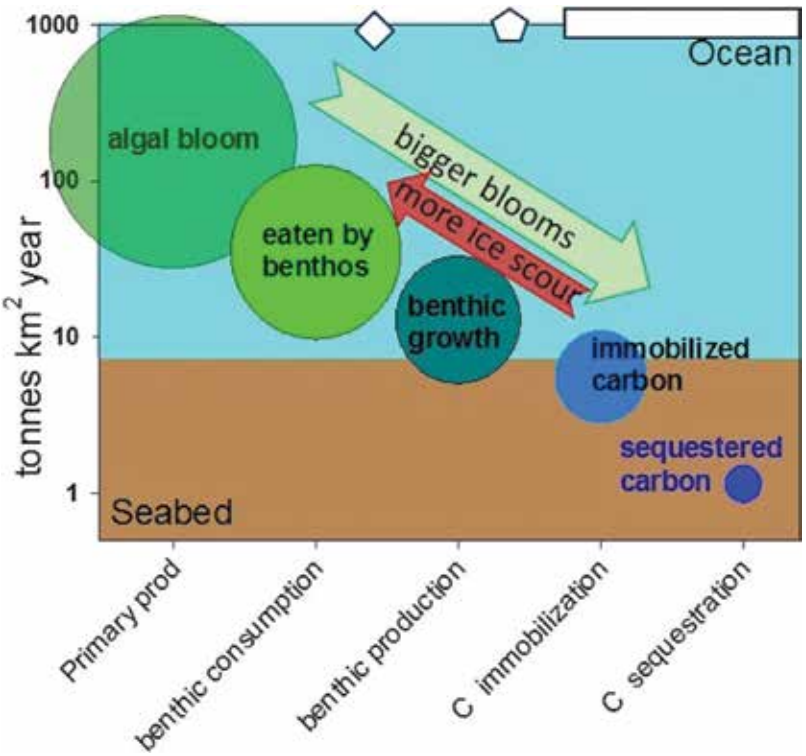

Figure 9. Cascade of blue carbon through trophic levels and states in polar waters, scaled to mean annual values. Data for the West Antarctic peninsula [16].

5. The future of polar benthic blue carbon

Carbonates already in Antarctic shelf sediment surfaces could become part of the negative feedback if calcite undersaturation is reached on the Antarctic shelves [8]. Ocean acidification is one of the bigger unknowns for the future of polar benthic carbon, in terms of the cost of calcification for organisms, the potential for dissolution whilst alive and after death [28]. Probably the biggest unknown though is how sea temperature will change. There seem to be very different sea temperature trends between the polar regions, across depths and even within seas around the Southern Ocean [29]. The strongest climate-forced trends to date have been in ice extent change. Sea ice losses, glacier retreat and ice shelf collapse are expected to be sustained, although sea ice models are still in their infancy in terms of even recreating the complexity that has already occurred. Salinity changes can be strongly linked to sea ice changes [29] and is likely to remain very important in the Arctic in terms of surface stratification and stabilization impacts. Stratospheric ozone losses have driven seasonal increases in UV and wind strength, driving knock on influences on sea ice (e.g. maintaining open water areas). The impact of all these factors on polar blue carbon to date has been explored to various levels (Sections 3 and 4) such that for some areas summary trends can be erected (**Figure 8**). Because such trends have typically relied on scaling up by area and scaling from few taxa, and rarely accounted for all environmental factors, their main purpose is essentially hypothesis testing markers. Several new independent

http://dx.doi.org/10.5772/intechopen.78237

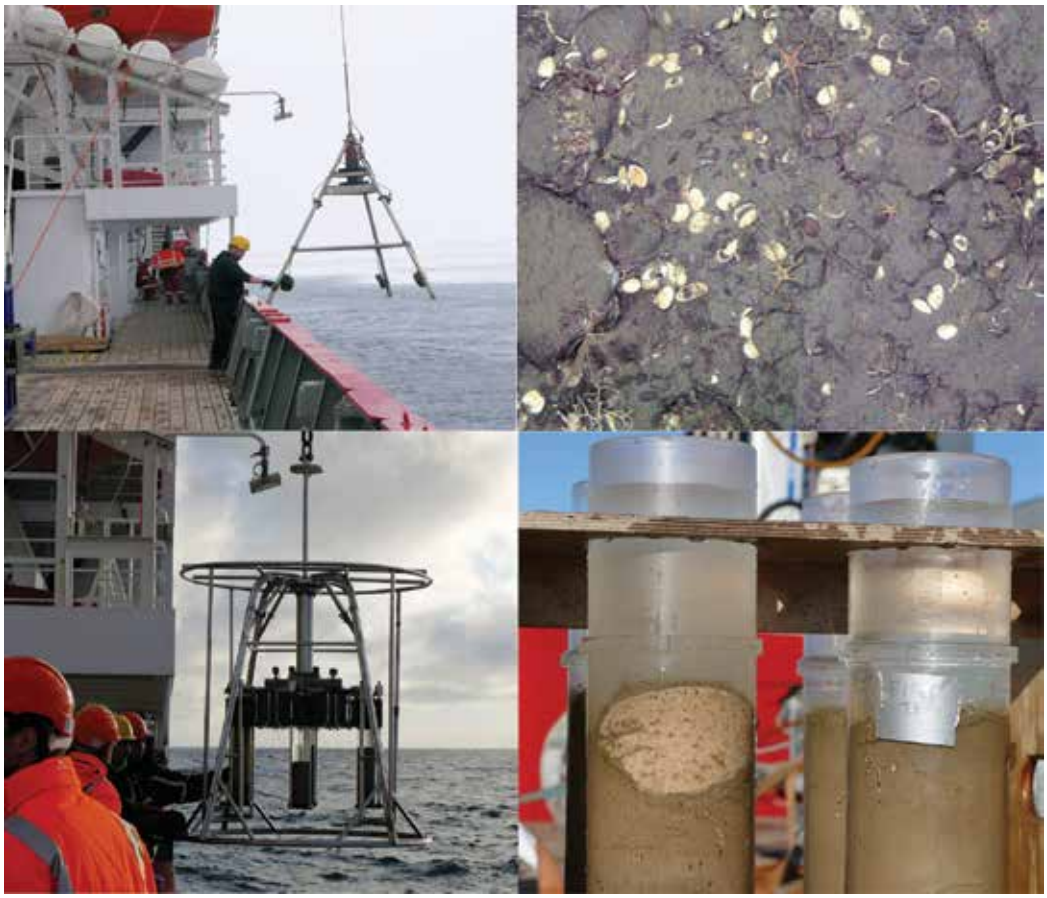

Figure 10. Apparatus used to estimate surface and sediment carbon and carbonate in polar shelf seas (here shown in the Arctic in 2017). The equipment are shelf underwater camera system (SUCS - above) and multicorer (MUC - below) and their collection products. Note the sponge bisected in one of the core tubes.

research programmes have been recently launched across polar seas to attempt to quantify and model polar carbon capture and storage, including the blue carbon component (**Figure 10**).

Current ideas on the direction of likely trends in polar blue carbon include a wide spectrum of near-future prospects [4, 9, 11, 27, 28]. Reasonable scientific scenarios have been put forward that we can expect drastic reductions in blue carbon storage under current climate projections. These are based on a (largely presumed) inability of polar biodiversity to tolerate lowered pH and increased temperature [9, 13, 27, 28]. This is partly due to the unprecedented level and pace (in recent geological time) of physical change and partly due to the limited options for migration to maintain climate envelope (stay within tolerable conditions). The moderate sea temperature rises expected over the next century could enhance carbon capture and storage [21], although scientific consensus is that more severe temperature rises are likely to reduce polar marine biodiversity performance [27]. However sustained sea ice and ice shelf losses seem likely to increase blue carbon capture and storage rates as to date, but possibly more widespread [16, 17, 26]. Processes by which this could be aided and enhanced, for example creation of artificial polar reefs, have even

been financially evaluated but are uneconomical at the current value of industrial carbon capture [30]. Patterns of blue carbon response to climate change are likely to differ strongly between the Arctic and Antarctic, because of their contrasting history and geography, human usage and disparity of current physical change. From current trends it seems most likely that moderate blue carbon increases will occur in Arctic and West Antarctic seas in the near future to be eventually replaced by more severe decreases when critically low pH and high temperatures begin to be reached. Predicting physical trends and blue carbon biological responses in East Antarctic seas is more difficult because of current variability and lack of sustained patterns. It seems intuitively likely that East Antarctic blue carbon patterns may ultimately follow those of other polar locations but with a considerable lag phase. Given the rarity of natural negative feedbacks on climate change and the importance of blue carbon as a current negative feedback, quantification and understanding of polar blue carbon change should be high as a scientific priority.

Acknowledgements

The author would like to thank the members of the projects; Antarctic Seabed Carbon Capture Change, Changing Arctic Ocean Seabed and ICEBERGS (NERC-Conicyt). The author would also like to thank the following colleagues for help with figures; Will Goodall-Copestake and Sorcha Barnes (**Figures 1**, **3**, **4**, **10**), Floyd Howard (**Figure 2**), Jo Hopkins (**Figure 6**), Jamie Oliver (**Figure 7**) and Chester Sands (**Figure 8**).

Conflict of interest

No conflicts of interest and no funding supported this work.

Author details

David Keith Alan Barnes

Address all correspondence to: dkab@bas.ac.uk

British Antarctic Survey, NERC, Cambridge, UK

References

[1] Kaiser M et al. Marine Ecology. Oxford, UK: Oxford press; 2007

[2] Housset JM, Girardin MP, Baconnet M, Carcaillet C, Bergeron Y. Unexpected warming-induced growth decline in *Thuja occidentalis* at its northern limits in North America. Journal of Biogeography. 2015;**42**:1233-1245

[3] Thomas DN. Frozen Oceans. London, UK: The Natural History Museum; 2004

[4] Barnes DKA, Tarling G. Polar oceans in a changing climate. Current Biology. 2017;**27**: R431-R510

[5] Jónasdóttir SH, Visser AW, Richardson K, Heath MR. Seasonal copepod lipid pump promotes carbon sequestration in the deep North Atlantic. Proceedings of the National Academy of Sciences of the United States of America. 2015;**112**:12122-12126

[6] Schmidt K, Schlosser C, Atkinson A, Fielding S, Venables H, Waluda C, Achterberg EP. Zooplankton gut passage mobilizes lithogenic iron for ocean productivity. Current Biology. 2016;**26**:2667-2673

[7] De Broyer C, Koubbi P. Biogeographic Atlas of the Southern Ocean. Brussels: SCAR; 2014

[8] Hauck J et al. Distribution and mineralogy of carbonate sediments on Antarctic shelves. Journal of Marine Systems. 2012;**90**:77-87

[9] McGuire AD et al. Sensitivity of the carbon cycle in the Arctic to climate change. Ecological Monographs. 2009;**79**:523-555

[10] Arntz WE, Brey T, Gallardo VA. Antarctic zoobenthos. Oceanography and Marine Biology an Annual Review. 1994;**32**:241-304

[11] Canfield DE Factors influencing organic carbon preservation in marine sediments. Chemical Geol. 1994;**114**(3-4):315-329

[12] Dieckmann GS et al. Antarctic Sea ice-a habitat for the foraminifer *Neogloboquadrina pachyderma*. Journal of Foraminiferal Research. 1991;**21**:182-189

[13] Hunt BPV et al. Pteropods in Southern Ocean ecosystems. Progress in Oceanography. 2008;**78**:193-221

[14] Ziegler AF et al. Glacial dropstones: Islands enhancing seafloor species richness of benthic megafauna in West Antarctic peninsula fjords. Marine Ecology Progress Series. 2017;**583**:1-14

[15] Barnes DKA, Sands CJ. Functional group diversity is key to Southern Ocean benthic carbon pathways. PLoS ONE. 2017;**12**(6):e0179735. https://doi.org/10.1371/journal.pone.0179735

[16] Barnes DKA. Polar zoobenthos blue carbon storage increases with sea ice losses, because across-shelf growth gains from longer algal blooms outweigh ice scour mortality in the shallows. Global Change Biology. 2017;**23**:5083-5091

[17] Barnes DKA et al. Icebergs, sea ice, blue carbon and Antarctic climate feedbacks. Philosophical Transactions of the Royal Society of London A. 2018;**376**:20170176. http://dx.doi.org/10.1098/rsta.2017.0176

[18] Peck LS et al. Negative feedback in the cold: Ice retreat produces new carbon sinks in Antarctica. Global Change Biology. 2010;**16**:2614-2623

[19] Fillinger L et al. Rapid glass sponge expansion after climate-induced Antarctic ice shelf collapse. Current Biology. 2013;**23**:1330-1334

[20] Duprat LPAM, Bigg GR, Wilton DJ. Enhanced Southern Ocean marine productivity due to fertilization by giant icebergs. Nature Geoscience. 2016;**9**:219-221

[21] Ashton GV et al. Warming by 1°C drives species and assemblage level responses in Antarctica's marine shallows. Current Biology. 2017;**27**:2698-2705

[22] Sahade R et al. Climate change and glacial retreat drive shifts in an Antarctic benthic ecosystem. Science Advances. 2015;**1**:e1500050

[23] Barnes DKA et al. Scott's collections help reveal accelerating marine life growth in Antarctica. Current Biology. 2011;**21**:147-148

[24] Atkinson A et al. Long-term decline in krill stock and increase in salps within the Southern Ocean. Nature. 2004;**432**:100-103

[25] Arrigo KR et al. Primary production in the Southern Ocean, 1997-2006. Journal of Geophysical Research 2008:113, C08004 27pp

[26] Barnes DKA. Antarctic Sea ice losses drive gains in benthic carbon drawdown. Current Biology. 2015;**25**:789-790

[27] Gutt J et al. The Southern Ocean ecosystem under multiple climate change stresses – An integrated circumpolar assessment. Global Change Biology. 2015;**21**:1434-1453

[28] McClintock JB et al. Rapid dissolution of shells of weakly calcified Antarctic benthic macroorganisms indicates high vulnerability to ocean acidification. Antarctic Science. 2009;**21**:449-456

[29] Meredith M, King J. Climate change in the ocean to the west of the Antarctic peninsula during the second half of the 20th century. Geophysical Research Letters. 2005;**32**:L19604

[30] Barnes DKA, Sands CJ. Could polar continental shelves be 'farmed' to increase carbon capture and storage? Environmental Analyses and Ecological Studies 2018;**1**:EAES.00052

Chapter 4

Carbon Dioxide Utilization and Sequestration in Kerogen Nanopores

Cudjoe Sherifa and Barati Reza

Additional information is available at the end of the chapter

http://dx.doi.org/10.5772/intechopen.78235

Abstract

Carbon dioxide (CO_2) has been injected into oil reservoirs to maximize production for decades. On the other hand, emitted CO_2 from industrial processes is captured and stored in geological formations to mitigate greenhouse gas effects. As such, greater attention is drawn to the potential of utilizing the captured CO_2 in EOR processes. A significant portion of the injected CO_2 remains trapped due to capillary forces and through dissolution in residual liquids. In organic-rich shales, the presence of isolated kerogen nanopores add to the sequestration process due to the adsorptive nature of the surface and its preference to CO_2 over methane (CH_4), in addition to the sealing capacities of these formations. This work summarizes the latest findings of the literature with the purpose of defining further areas of investigation to fully capitalize on the potential of CO_2 sequestration and utilization in kerogen nanopores.

Keywords: CCUS, enhanced oil recovery, organic-rich shales, anthropogenic CO_2, kerogen nanopores

1. Introduction

Carbon dioxide capture, utilization and storage (CCUS) technologies involve capturing carbon dioxide (CO_2) emissions to create a synergy between the high demand for fossil fuel and mitigating greenhouse gas effects at the lowest possible cost.

CCUS captures over 90% of CO_2 emissions from power plants and industrial facilities and is predicted to reduce global gas emissions by 14% in 2050. Bearing in mind that, fossil fuel-fired power plants in the United States account for 30% of U.S. total greenhouse gas (GHG) emissions, which will only continue to increase regardless [1]. The capacity of CO_2 utilization

and storage in the U.S. is approximately 30 billion metric tons, equivalent to 35 years of CO_2 emissions captured from 140 Gigawatts (GWs) of coal-fired power [2, 3].

The captured CO_2 emissions are usually injected into geologic formations such as deep saline aquifers for storage, but most recently associated with enhanced oil recovery (CO_2-EOR) in oil and gas reservoirs. Although, CO_2-EOR has been practiced for decades now, recent advances combine the recovery process with CO_2 sequestration.

CO_2-EOR involves the injection of CO_2 into an oil/gas reservoir to recover more hydrocarbons (oil and/ or gas). Mostly, the volume of the injected CO_2 differs from that of the produced fluid with CO_2, indicating trapping or storage. Hence, incorporating the storage of anthropogenic CO_2 into CO_2-EOR in already developed oil and gas reservoirs seems economically and technically feasible. Different forms of trapping mechanisms, such as hydrodynamic and capillary trapping hold the CO_2 in place to prevent movement/leakage, ubiquitous to almost all oil and gas reservoirs [2, 3].

The United States (US) leads the world in both the number of CO_2-EOR projects and in the volume of CO_2-EOR oil production due to complimentary geology (low thermal gradient and high permeability) in the Permian Basin, located in West Texas and southeastern New Mexico [4]. Approximately 11 trillion cubic feet (560 million metric tons) total volume of CO_2 is utilized in by US CO_2-EOR as compared to 100 trillion cubic feet (5090 million metric tons) per year of total US CO_2 emissions from industrial sources [1, 4–6].

Although, CO_2 storage during CO_2-EOR in conventional oil and gas reservoirs is proven effective, the potential to sequester in unconventional organic-rich shales (gas/oil) is even more promising and economical, yet there has been minimum attention given to these vast resources. Organic-rich shales are naturally suited for CO_2 storage due to the ultra-tight impermeable nature of the formation, which would curtail CO_2 leakage. Moreover, the adsorptive surface of kerogen and kerogen nanopores in shales can store substantial amounts of CO_2 in its adsorbed state [5–7]. Thus, in depleted shale gas reservoirs, injected CO_2 replaces methane (CH_4) in the kerogen micro and nanopores and adsorb to the kerogen surface for storage [7–9]. This chapter therefore investigates the potential of CO_2 sequestration in kerogen nanopores.

2. Carbon capture

Carbon capture technology started in the 1970s in North America at industrial projects before it was applied to power generation [1]. Early application of carbon capture on a commercial basis was focused on the removal of CO_2 as part of certain industrial processes in concentrated streams [1, 8]. The Department of Energy (DOE) estimates that approximately 30 million metric tons per year of pure CO_2 are currently produced at industrial facilities located within 50 miles of existing CO_2 pipeline networks [10].

Some industrial processes with large-scale carbon capture in commercial operation include coal gasification, ethanol production, fertilizer production, natural gas processing, refinery hydrogen production, and coal-fired power generation [7, 10].

- Natural sources of CO_2 are made up of underground accumulations of naturally occurring gases with 90% CO_2. As of 2015, the natural sources are projected to account for approximately 65 Mt/a of CO_2 [8].
- Natural-gas processing are also naturally occurring underground accumulations but with significant methane content. The contribution of natural-gas processing has increased from 5 Mt/a of CO_2 in 2000 to a projected 20 Mt/a of CO_2 in 2015 [8]. Some of the known challenges of natural-gas processing include: higher oxygen (O_2) content, lower CO_2 concentration, higher flue gas and high flame temperatures [1].
- Hydrocarbon conversion involves the conversion of crude oil (or hydrocarbon feedstock) into several (high-value) products to capture CO_2 as a by-product. This process is projected to increase to approximately 5 Mt/a based on known projects under construction and in final phase [8].

However, with the recent inclusion of power generation, new systems are designed to capture and concentrate CO_2 using the following processes [7]:

- Pre-combustion carbon capture

Fuel undergoes gasification instead of combustion to produce syngas made of carbon monoxide (CO) and hydrogen (H_2). Carbon monoxide (CO) is then converted to CO_2 through a later shift reaction, while a solvent separates the CO_2 from H_2. The pre-combustion carbon capture is mostly combined with an integrated gasification combined cycle (IGCC) power plant to burn the H_2 in a combustion turbine and the resulting exhaust heat, used to power a steam turbine [1, 6].

- Post-combustion carbon capture

It involves the use of chemical solvents to separate CO_2 from the resulting flue gas from fossil fuel combustion. This method is commonly used by modified power plants for carbon capture [7].

- Oxyfuel carbon capture

This process requires the combustion of fossil fuel in pure oxygen to render the CO_2-rich exhaust gas for capture [7].

In 2016, the US Energy Information Administration (EIA) reported that electricity generated from natural gas is expected to exceed that of coal for the first time [9]. This calls for more effective measures to be put in place to curtail greenhouse gas (GHG) effects.

2.1. Carbon capture benchmarks

There are about 21 commercial-scale carbon capture projects around the world with 22 more in development [7]. Below is a list of a few of the many benchmarks in carbon capture:

- As of 2017, the Archer Daniels Midland (ADM) Company captures CO_2 from Biofuels (ethanol) production, and stores in the Mt. Simon Sandstone, a deep saline formation, Decatur, IL. An estimated amount of 1.1 million tons of CO_2 is captured per year [1, 3].

- In 2017, the NRG Petra Nova Project, TX, captures 90% of CO_2 (approximately, 1.6 million tons of CO_2 per year) from a 240 MW slipstream of flue gas of existing WA Parish plant, and transported to a nearby oil field [7].
- In 2016, Abu Dhabi CCS Project Phase 1: Emirates Steel Industries, an operating iron and steel plant, used to capture CO_2 for enhanced oil recovery by the Abu Dhabi National Oil Company (ADNOC) [3, 5].
- In 2015, Shell Quest Project, AB, CA, a bitumen upgrader complex, captures about 1 million tons of CO_2 annually from hydrogen production units and injects it into a deep saline formation for sequestration [7].
- In 2013, Conestoga Energy Partners/Petro-Santander Bonanza Bioethanol plant, KS, an ethanol plant, captures and supplies approximately 100,000 tons of CO_2 per year to a Kansas EOR field [1, 5].
- In 2010, Occidental Petroleum's Century Plant (OPCP), TX, a natural gas processing facility, compresses and transports CO_2 stream for utilization in the Permian Basin, among others [3, 5].

3. Carbon dioxide utilization (CO_2: EOR)

CO_2-EOR has been successfully implemented for nearly half a century now to recover additional oil from developed conventional oil fields in the United States and around the world. It involves the injection of CO_2, either in its supercritical or gaseous state to re-pressurize a depleted reservoir pressure to cause residual oil held in the smaller pores by capillary forces to be released [9, 10]. CO_2, unlike other fluids, reaches miscibility with crude oil at lower pressures. Furthermore, it is less expensive than other miscible fluids. As such the injected CO_2 becomes soluble with the residual oil as light hydrocarbons from the oil dissolve in the CO_2 while the CO_2 density is high when oil contains a significant volume of light hydrocarbons [4, 11].

Upon discovery, an oil reservoir is initially produced by means of the pressure gradients within the reservoir that provides the energy to move reservoir fluids to the surface. This is called the primary production stage. Eventually, the reservoir pressure declines and flow to the wellbore ceases. At this moment, a range of secondary or tertiary (EOR) methods are implemented to recover additional volumes of oil. The primary stage only recovers about 5–20% of the original oil-in-place (OOIP), with considerable amount of oil left trapped in the pore spaces of the rock [9, 12].

The next stage of production is the secondary recovery, which involves the injection of a fluid, either gas or water to sustain and maintain the depleted reservoir drive, and simultaneously recover substantial amounts of the remaining OOIP. Treated produced water (waterflooding) is commonly used at this stage since it is less expensive and readily available. In most cases, the water bypasses the oil due to difference in viscosity leaving behind significant amounts of the remaining oil-in-place. Waterflooding results in approximately 50–60% of the OOIP

trapped, hence the need for CO_2-EOR in most oil reservoirs already replenished with water-flooding. Both primary and secondary recovery methods usually extract about 35% of the OOIP [4, 9, 10].

To produce more of the remaining oil-in-place, a tertiary oil recovery phase is implemented, where fluids (CO_2, nitrogen, enriched gas, polymer solutions or surfactant solutions) are injected to interact with the oil and cause substantial changes to the oil properties [12]. Carbon dioxide (CO_2) flooding is one of the most proven EOR methods, where CO_2 is injected either in its gaseous or supercritical state. The injected CO_2 is determined to reduce the interfacial tension, minimize the viscosity of the oil to make it lighter, cause the oil volume to swell, and eventually cause the oil to flow more freely within the reservoir to the producer wellbore [11].

CO_2 is mostly delivered to the field at a high pressure (>1200 psi) and density (5 lb. /gal) into injection wells within a designed pattern based on computer simulation to optimize areal sweep of the reservoir [13, 14]. Miscibility of CO_2 with the oil is important as it causes the physical forces (interfacial tension) holding the two phases apart to disappear. It occurs at a minimum pressure (MMP), where about 95% of the OOIP is recovered. Below the minimum miscibility pressure (MMP), CO_2 and oil will no longer be miscible, the oil and gas phases separate, thereby decreasing oil production rate. Significant volumes of oil are produced during CO_2-EOR. For example, the Wasson field, a Denver unit CO_2-EOR has produced more than 120 million incremental barrels of oil through 2008, with more than 2 billion barrels of OOIP and 40% of oil remaining after Waterflooding [14, 15, 19]. All types of oil reservoirs, either carbonates or sandstone could be suitable for CO_2-EOR provided the MMP can be reached [13, 14].

The operation of a CO_2-EOR project is a closed-loop system as shown in **Figure 1**, where about half of the injected CO_2 is trapped or dissolved in the reservoir and its fluids (oil and water). The produced CO_2 with oil is separated and re-injected back into the reservoir, ensuring an increase in trapped CO_2 instead of being released to the atmosphere. In addition, CO_2-EOR provides a market and revenues for the captured CO_2 from anthropogenic (industrial and power plants) sources [14, 15]. As the project matures, the volume of injected CO_2 diminishes, while recycled volumes increase. This indicates that CO_2 is being stored in the formation through a capillary trapping mechanism [10, 13, 14].

CO_2-EOR was first tested on a large-scale in the 1970s in the Permian Basin of West Texas and southeastern New Mexico. These initial projects used separated CO_2 from processed natural gas and natural sources of CO_2 instead of anthropogenic CO_2 from industrial power plants. **Figure 2** shows CO_2-EOR projects carried out around the world and in the U.S. from the 1970s to present day [9, 16]. Three developed source fields include, Sheep Mountain in south central Colorado, Bravo Dome in northeastern New Mexico, and McElmo Dome in southwestern Colorado [10]. The recent depletion of the natural source fields of CO_2 and size limitation of the pipelines for CO_2-EOR processes have paved the way for anthropogenic supplies of CO_2. In so doing, subsequent projects employ CO_2 molecules from captured emissions to supply large quantities of CO_2 for EOR processes in oil fields. Technological advancement in CO_2-EOR applications, such as 3D seismic and geomodeling reduce the rise of failures and improves the flooding efficiency [10, 13–15].

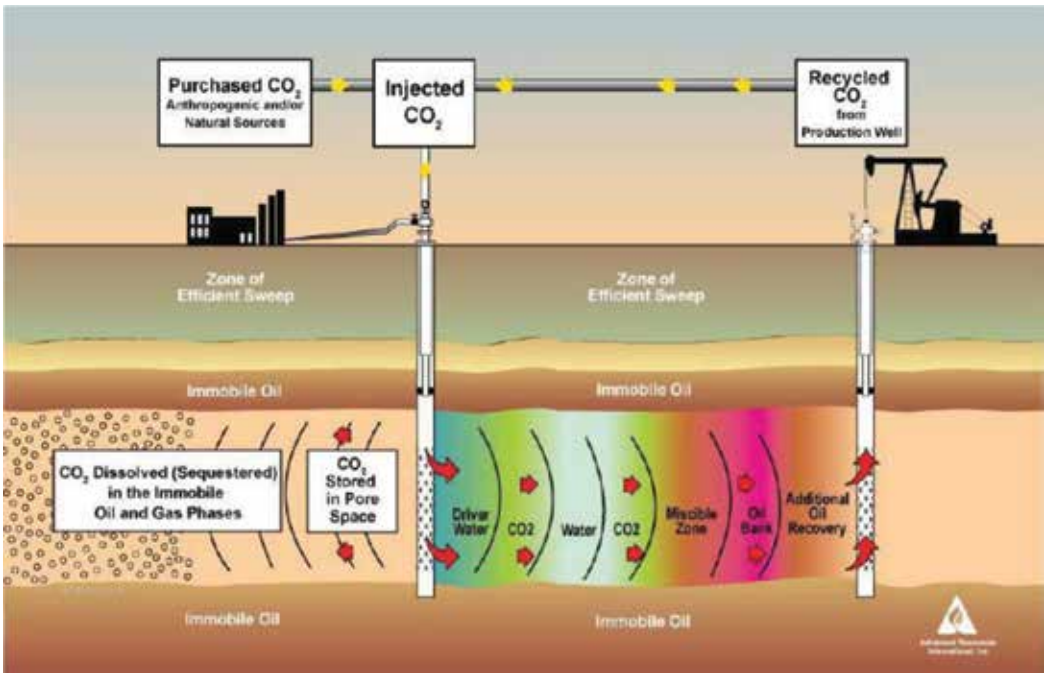

Figure 1. Schematic diagram of a closed loop CO_2-EOR [4].

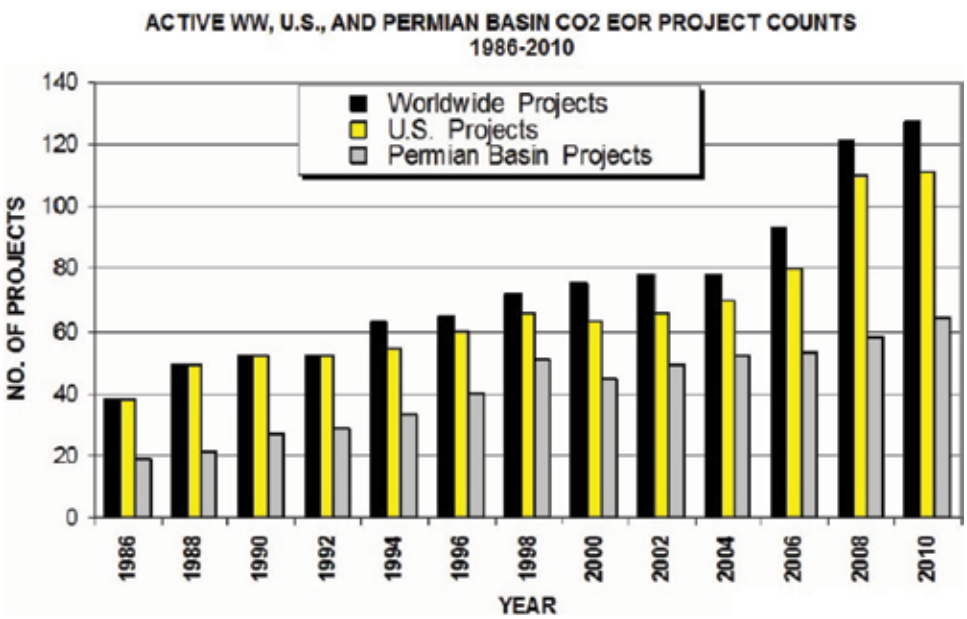

Figure 2. CO_2-EOR projects conducted worldwide and in the U.S [10].

4. Carbon dioxide sequestration

The potential of CO_2 sequestration in geologic formations is possible from the fact that certain reservoirs naturally trap and store oil and natural gas over long geological time periods until extracted [1, 4, 6, 16]. In so doing, CO_2 from power plants and industrial facilities can be trapped and stored in potential geologic formations. A large percentage of the originally injected CO_2 gets trapped in the pores of the geologic formation, while a portion of it is dissolved in the oil and also end up trapped [3, 6, 17]. These trapping processes continue as long as the CO_2 is injected. Percentage of stored CO_2 is based on total injected volumes and not on the purchased volume and is given as [10].

$$CO_{2storage}(\%) = \left(CO_{2injected} - CO_{2produced} - CO_{2losses}\right)/CO_{2purchased} \quad (1)$$

where, $CO_{2storage}$ is the CO_2 storage in metric, $CO_{2injected}$ is the total CO_2 injected, $CO_{2produced}$ is the CO_2 produced, and $CO_{2purchased}$ is the purchased CO_2 injected. CO_2 losses is estimated as the difference between total CO_2 injected and CO_2 produced. Losses may be due to leakages, infrequent power outages, among others [10].

CO_2 can be injected into conventional geological formations and stored deep underground. Most of these conventional geologic formations are at depths greater than 800 m, which eventually converts the injected CO_2 into its supercritical state. The supercritical CO_2 with a higher density than its gaseous state results in a given volume of rock capable of holding more mass of CO_2 [4, 7]. For an effective conventional geological storage, approximately 90–95% of the injected CO_2 for will be sequestered within the reservoir [4, 9, 16].

4.1. Storage mechanisms in conventional reservoirs

Trapping mechanisms encountered in CO_2-storage in conventional geologic formations include [9–11]:

• Physical trapping: hydrodynamic, stratigraphic, or structural) trapping

This involves the migration of generated hydrocarbons from organic matter (source) over long geological periods from the source rock to porous and permeable reservoir rock initially saturated with brine. The accumulated hydrocarbons are trapped below a non-permeable cap rock to prevent further migrations, and the density difference between the fluids separates the fluids into layers with gas on top, followed by oil and brine at the bottom. A similar mechanism is encountered in the case of CO_2 storage, where the less dense supercritical CO_2 plume rises due to buoyancy forces and is prevented from escaping by overlying low permeability cap rock [15]. This mechanism is considered to be relatively fast but requires characterization of the cap rock [2, 3].

• Solubility trapping

CO_2 is widely accepted to be soluble in water, as such, dissolved CO_2 can be safely stored in a geologic formation under solubility trapping. Since the CO_2- saturated brine is denser than the

unsaturated surrounding brine, density difference causes the denser brine to migrate deeper into the formation and slowly dilutes the unsaturated brine through contact. Reservoir pore pressure, temperature, and salinity of formation water are vital for solubility trapping [16]. This process occurs faster than pure diffusion, prevent CO_2 from hydrodynamically separating from other phases, and it is estimated to begin between a year and hundreds of years after CO_2 injection, also dependent on the permeability of the formation in question [2, 20].

• Mineral trapping

This process occurs over longer geological timescales than the other trapping methods, but is equally important [3]. It involves the formation of carbonic acids (H_2CO_3) as a result of CO_2 dissolution in formation brine. The resulting acid is unstable and dissociates to form groups, which react with the formation rock over long periods of time [2, 3]. In situations where, carbonate minerals are precipitated through the reaction, CO_2 is permanently trapped as a result [23].

• Capillary (residual) trapping

In a conventional sandstone oil reservoirs, brine is mostly designated as the wetting phase, while oil and gas are the non-wetting phases. In the case of carbonate rocks, oil is the wetting phase and water and gas are the non-wetting phases. In capillary trapping, the formation wetting phase surrounds the CO_2 and traps it as immobile pore scale bubbles. This process occurs over shorter time scale (right after injection) [15] compared to the other trapping mechanisms [2, 19]. In effect, the rock surface is presumed to be less water-wet in the presence of CO_2 and in the absence of oil [9].

These trapping mechanisms occur in geologic storage including [13, 14]:

• Depleted oil and gas reservoirs

Not only do these geologic formations provide a means for storing CO_2, but also offer economic opportunities as the injected CO_2 recovers additional oil from depleted oil and gas reservoirs. Moreover, additional revenue can be obtained from the cost of selling captured CO_2 to EOR operators to fund the cost of capture technology at industrial facilities and power plants [4, 14, 17]. CO_2 is injected underground and remains immobile due to some of the enumerated trapping mechanisms listed above [3, 20].

• Deep saline formations

Saline aquifers are preferred due to their large capacities and being geographically widespread. These include porous rock formations saturated with brine at greater depths with overlying shale cap rocks, which are impermeable and act as a seal to prevent CO_2 from leaking [4, 17]. The confined CO_2 also undergoes dissolution in the brine, as well as capillary trapping to render the injected CO_2 immobile. A study [2] was carried out to measure the maximum saturation and the form of capillary curve in a CO_2 – Berea sandstone system through coreflood experiments, representative of a storage location. A capillary trapping capacity of 7.8% of the rock volume for CO_2 – Berea sandstone was recorded [2]. This is to say,

if this much is recorded in an unconsolidated formation, how much more there is to expect in a consolidated formation.

- Coal beds

Coal beds are either too deep or too thin to be economically developed, as such, they could offer CO_2 storage potential due to the adsorptive nature of the pore surfaces [4, 13]. In CO_2–enhanced coalbed methane (ECBM) production, CO_2 is injected into deep coal seams to desorb methane gas to be extracted and preferentially adsorb onto the mineral surface for permanent CO_2–storage. Yet they are not thoroughly characterized and are on a small magnitude for CO_2–storage [8, 19, 21].

4.2. Storage criterion

Nonetheless, not all geologic formations will effectively store CO_2 with minimum risks of leaking due to the buoyancy of CO_2 gas. The criteria for secure storage involve some of the following parameters (**Table 1**) as reported in a successful project carried out in Canada [10].

Table 2 summarizes CO_2-EOR and CO_2 storage projects carried out in some major oil basins around the world. A total of 1297 billion barrels of CO_2 has been utilized worldwide for CO_2-EOR, while a total of 370 billion metric tons has been stored/sequestered in the process [4].

4.3. Carbon storage regulation

CO_2 storage site selection and injection are regulated by the U.S. Federal and State agencies, in addition to checking systems for CO_2 capture and storage to reduce the potential risk of stored CO_2 to humans and the environment [1, 10, 18]. Specific regulations and particular tools are commonly implemented to selected reservoirs by different companies and agencies [1, 10].

Furthermore, the Safe Drinking Water Act (SDWA) and the U.S. Environmental Protection Agency (EPA) impose safety requirements on CO_2 injection and monitoring. Whereas, the Underground Injection Control Program (UICP) considers the previous seismic history as a requirement in selecting geologic CO_2 sequestration sites to reduce the risk of small earthquakes as well as the effect of earthquakes on leakage of CO_2. **Table 3** presents a list of monitoring tools used for CO_2-EOR and CO_2 storage projects.

Adequate depth (> 1000 meters)
Strong confining seals
Minimally faulted, fractured or folded
Adequate volume and permeability for storage
No significant diagenesis

Table 1. Criteria for storage on a basin scale [10].

Region	CO_2-EOR (Billion Barrels)	CO_2 Storage capacity (Billion Metric Tons)
Asia Pacific	47	13
Central & South America	93	27
Europe	41	12
FSU	232	66
Middle East/North Africa	595	170
North America/Other	38	11
North America/U.S.	177	51
South Africa/Antarctica	74	21
TOTAL	**1297**	**370**

Table 2. CO_2-EOR and CO_2 storage in major oil basins of the world [4].

Cement integrity logs
Injection logs
Pattern and material balance techniques
Tracer injection/logging
Step rate testing
Fluid levels and reservoir pressure

Table 3. Reservoir monitoring tools used in CO_2-EOR [10].

5. CO_2 storage in unconventional shale reservoirs

As previously mentioned, conventional oil and/gas reservoirs form from the migration of petroleum and natural gas from the source (organic matter) into permeable reservoir rocks. On the other hand, unconventional shale gas/oil serve as both the source and reservoir for natural gas and liquid hydrocarbon (oil and gas condensate). These shale formations are being developed widely for oil and gas production especially in the United States (U.S) and other parts of the world. Moreover, shale formations are much more abundant and widely distributed [17] than deep un-mineable coal seams and/ or depleted oil and gas reservoirs but have not been extensively analyzed for CO_2 sequestration [19]. This is attributed to the ultra-tight nature of shales but the recent advances in horizontal drilling and hydraulic fracturing offers a new perspective into these formations [5, 19].

Shales consist of a mineral matrix (clay, pyrite, carbonate, quartz) embedded with dispersed dark kerogen (organic matter) areas as shown in **Figure 3**. Kerogen is the insoluble solid-phase nanoporous component of organic matter (decomposed plant and animal debris) in

http://dx.doi.org/10.5772/intechopen.78235

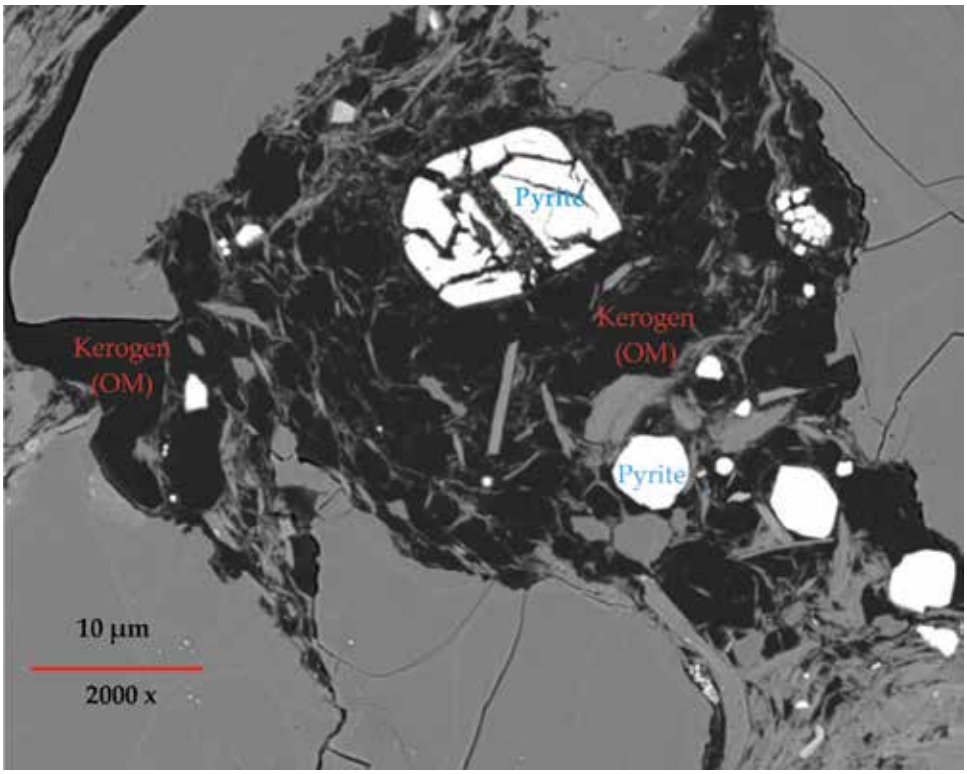

Figure 3. Backscattered electron (BSE) image of Chattanooga shale, Barber County, KS.

shale formations, which controls the gas adsorption capacity. It undergoes different stages of maturity (decomposition) at higher temperatures to produce petroleum and natural gas within the micropores (<2 nm) and mesopores (2–50 nm) [6]. The kerogen pores create a sieve for smaller CO_2 molecules, making shales more attractive for CO_2 sequestration unlike methane (CH_4) and other gas molecules [18, 30]. Thus, shales can adsorb substantial amounts of CO_2 on kerogen as well as fracture surfaces [19, 24]. The level maturity of kerogen is measured by the vitrinite reflectance (% Ro), which indicates the onset of oil (0.6–1.0 Ro%), wet gas (<0.80% Ro) and natural gas (>1.4% Ro) generations, respectively [20, 21]. Gas from shale formations are either thermogenic (generated from cracking of organic matter or the secondary cracking of oil) or biogenic (generated from microbes) [22, 26].

Because the source rock doubles as the reservoir, shales are characterized as very low permeability formations, which form strong confining seals in their own right but have surface adsorptive characteristics. As such, they require the creation of hydraulic fractures to form conduits for introducing fluids and producing them to the surface through horizontal wells. Hydraulic fracturing cracks the shale rock through injections of water, sand and chemicals at high pressure [16]. Horizontal wells with multi-stage hydraulic fractures can then be used to inject CO_2 for storage in depleted shale gas and oil reservoirs. The horizontal wells as opposed to vertical wells in conventional geologic formations add to the effectiveness of CO_2

sequestration in shales since the horizontal wells contact more of the shale formation and as a result, increase the subsurface production area of the well [19]. More so, CO_2 sequestration in shales would not require new infrastructure unlike in conventional saline aquifers [19, 20].

Most of the shale formations are located at greater depths, where the injected CO_2 is in its supercritical state, which is much preferred for both CO_2 – enhanced gas/oil recovery (EGR)/ EOR in addition to CO_2 sequestration. The injected CO_2 for EGR/EOR in organic-rich shales adsorb onto the rock surface, while concurrently releasing methane gas (CH_4) and/ or oil for natural gas and oil productions, respectively [8, 22]. Furthermore, since most of the injected CO_2 would be adsorbed to the surface of kerogen rather than exist as free gas, the problem of leakage is minimized [8]. Hence, CO_2 sequestration in shales is feasible but requires knowledge of the characteristics of different shale formations as well as gas-water-rock interactions, multiphase flow, and reservoir modeling, monitoring and verification [22, 25].

Tao and Claren [19] introduced a computational method based on historical and projected methane (CH_4) production to estimate the capacity of CO_2 sequestration in Marcellus shale in eastern United States. From the results obtained, the Marcellus shale is expected to store between 10.4 and 18.4 Gt of CO_2 (approximately 50% of total US CO_2 emissions) between now and 2030. Another point to note from Tao and Claren [19] was that injected CO_2 moves through the shale formation faster than producing CH_4 through mass transfer kinetics, which enhances CO_2 sequestration process in shales. In addition, other major shale plays like Barnett, Eagle Ford, Woodford, could provide incremental storage capacity.

Nuttal [22] performed experiments to estimate CO_2 sequestration capacity in organic-rich Devonian black shales of Eastern Kentucky to be 6.8 Gt [19]. CO_2 was found to adsorb onto clay and kerogen surfaces. A direct correlation was observed between CO_2 adsorptive capacity and the total organic carbon (TOC), where CO_2 adsorption capacity increases with increasing TOC.

Kang et *al.* [6] examined shale capacity in organic-rich shales and their added advantage of allowing linear CO_2 molecules to penetrate smaller pores otherwise inaccessible to other hydrocarbon gases. Moreover, molecular interaction of CO_2 and kerogen ensures enhanced adsorption for CO_2 sequestration in shales. Injected gas (CO_2) molecules move through the shale formation through either the organics or inorganics (or both in most cases). In the organics, CO_2 dissolves into kerogen and diffuses into the kerogen nanopores, whereas, in the inorganics, CO_2 flows through irregularly shaped pores of clays, pyrite fambroids, quartz, and carbonates. Gas permeation and history-matching pressure pulse decay experiments revealed that significant amounts of CO_2 gas reached the organics through the inorganic pores.

Busch et *al.* [5] conducted diffusive transport and gas sorption experiments on shale samples. Effective diffusion coefficients increased (implies irreversible storage of CO_2) with a corresponding decrease in the concentration of bulk CO_2 volume in the sample. The decrease in bulk CO_2 volume is attributed to the dissolution of CO_2 in formation water (brine), adsorbed to clay and kerogen surfaces or undergoes geochemical reactions.

Furthermore, reservoir models can be built and used to predict viable CO_2 storage in shale reservoirs to model diffusivity, gas-water-rock interactions, and adsorption/desorption characteristics, among others. Notably, the presence of clay bound water is known to change the

gas sorption properties in coal formations so it is likely to manifest in shales as well. These phenomena could also be well understood through experimental methods [16, 19].

With these new insights, CO_2 sequestration in shale formations looks promising, however, the underlying physics of CO_2 sequestration in kerogen nanopores, where most of the sequestration takes place is much needed. A better understanding of the fluid dynamics in kerogen nanopores and predicting effective transport properties (diffusivity, permeability, etc.) is of utmost importance to practical CO_2 sequestration applications in shales. Also, it would aid in capitalizing on the full potential of CO_2 –EGR/EOR in organic-rich shales. Therefore, the application of lattice Boltzmann method (LBM) for CO_2 sequestration in kerogen nanopores focusing on the effect of adsorption was applied.

5.1. Mechanisms of CO_2 sequestration in shales

In addition to the trapping mechanisms in conventional reservoirs, organic-rich shales have an added advantage of trapping CO_2 through adsorption in the presence of kerogen [30]. Kerogen is the insoluble component of organic matter, and measured in the lab as the total organic carbon (TOC) through pyrolysis. Thus, both hydrodynamic trapping and trapping through adsorption are dependent on the wettability of CO_2 in in shales.

Tao and Claren [19] developed a linear relationship between TOC and adsorption capacity using a number of published data sets as input into (Eqs. (2) and (3)), respectively for methane (CH_4) and carbon dioxide (CO_2).

$$[CH_4](cm^3/g) = 3.04 + 0.35(TOC(\%)) \tag{2}$$

$$[CO_2](cm^3/g) = 0.08 + 1.72(TOC(\%)) \tag{3}$$

The resulting plot showed the regression line of CO_2 adsorption capacity to be steeper than that of CH_4, implying that CO_2 is able to diffuse more readily than CH_4 into the porous kerogen due to its smaller molecular diameter [19]. Accordingly, we produced a TOC vs. gas adsorption capacity plot but with a focus on the level of TOC and its effect on gas adsorption capacity. Shale formations are in abundance and have diverse geologic settings throughout the U.S. (Appalachian basin, Williston basin, Illinois basin, Michigan basin, Permian basin, and Gulf Coast Region) for EOR and associated CO_2 storage [19, 23] but vary in kerogen content (TOC) and this variation in TOC has been found to impact the storage capacity of shales.

Figure 4 shows the TOC – gas adsorption capacity for a number of published TOC data [5, 19, 22, 23] ranging from low TOC (<1 wt. %), medium TOC (1 wt. % < TOC < 10 wt. %), high TOC (10 wt. % < TOC < 20 wt. %), and ultrahigh TOC (>20 wt. %) [24]. Highest CO_2 adsorption capacity is seen in the ultrahigh TOC region, followed by significant adsorption capacity in the high TOC region; the least adsorption capacity is observed at low TOC region. This implies that, the higher the kerogen content in shales, a significant amount of CO_2 sequestration is expected through adsorption trapping with subsequent production of significant amounts CH_4 displaced in the process. Therefore, conventional structural trapping becomes dominant

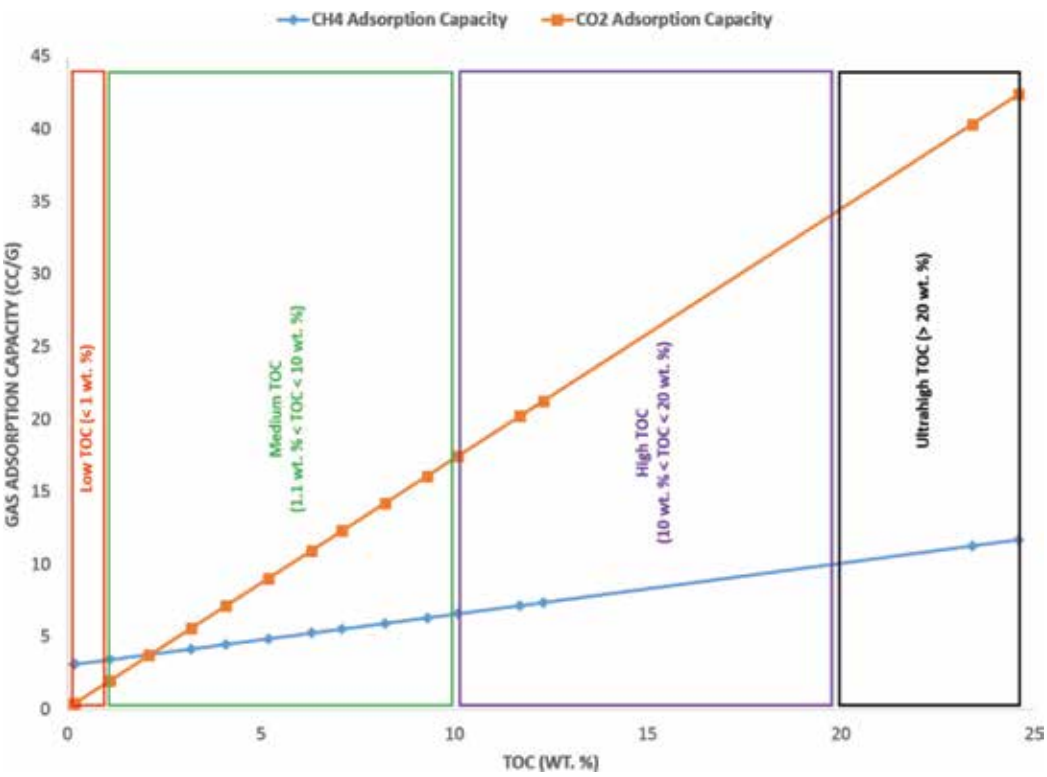

Figure 4. Gas adsorption capacity as a function of different levels of TOC.

in low TOC regions, where shale only serves as a cap rock/seal to prevent dissolved CO_2 from leaking to the surface since the mechanism of adsorption into porous kerogen (TOC) surface is close to negligible. On the other hand, within high TOC (>2 wt. %) regions, the adsorption trapping mechanism onto the kerogen surface prevails and render shale as storage medium in itself. In other words, shales with high TOC tend to be strongly CO_2-wet, whereas shales with low TOC content exhibit water-wet conditions, with medium TOC in between strongly CO_2 –wet and water-wet conditions [24]. Furthermore, the presence of interlayering clay minerals (illite) in shales also creates a large surface area for adsorption, although the weight of TOC has a much larger influence [25].

The properties of supercritical CO_2 inside small pores are of interest for subsurface carbon storage and as such require an understanding of the processes that govern the gas transport process [19, 23]. Molecular dynamics (MD) among other microscopic computational fluid dynamics as well as analytical models based on Fick's law for gas have been applied to understand the diffusion of CO_2 and CH_4 into organic pores. While, molecular dynamics simulates kerogen pore structures with the use of molecular sieves to investigate gas transport, analytical models modify continuum approaches by incorporating slip flow and diffusion. However, molecular dynamics is not feasible to simulate gas flow in porous media at large scale due to computational time and memory constraints [25, 26] and analytical models

fall short of capturing molecular pore wall effects. On the other hand, the lattice Boltzmann method (LBM), a mesoscopic numerical method is more flexible and less time consuming since a unit of gas molecules is assigned a distribution function for simulation [25, 26].

As previously outlined, the injected gas first contacts the fracture/matrix interface and then chooses to either (1) dissolve into the organic material (kerogen) and diffuse through a nanopores network or (2) enter the inorganic material and flow through a network of irregularly shaped voids [6, 18]. Therefore, the interaction of supercritical CO_2 ($scCO_2$) with porous kerogen needs to be investigated for long-term reservoir storage of CO_2 in organic-rich shales. We provide a simulation study that reveals the interaction of $scCO_2$ with porous kerogen focusing on two key features of adsorption and diffusion.

5.2. Lattice Boltzmann simulation (LBS) of CO_2 sequestration

The lattice Boltzmann method (LBM) is a numerical method for simulating fluid at the molecular scale. This method is ideal for simulating gas flow in nanoporous kerogen since the continuum flow (Darcy's law) fails due to dominating pore-wall effects at the microscale. LBM stems from the Boltzmann kinetic theory of gases, where fluids are assumed to be made up of a large number of small particles in random motion, which undergo elastic collisions to conserve mass and momentum [19, 23, 24]. However, the LBM replaces the fluid molecules with fractious particles to reduce the number of possible particles to a handful [28]. The fractious particles are then confined to the nodes of the lattice and assigned lattice velocities (e_i) at each node as shown in **Figure 4**, where the direction index $i = 0, 1, \ldots, 8$, for a D2Q9 model [29] (**Figure 5**). Following the kinetic theory, the fractious particles stream along defined lattice links and collide locally at varying lattice sites [23–25]. The streaming and collision of fluid particles by the Bhatnagar-Gross-Krook (BGK) approximation gives the lattice Boltzmann BGK equation as [19, 23–26].

$$f_i(x + e_i\,\Delta t, t + \Delta t) - f_i(x, t) = -\frac{1}{\tau}\left[f_i(x, t) - f_i^{eq}(x, t)\right] \tag{4}$$

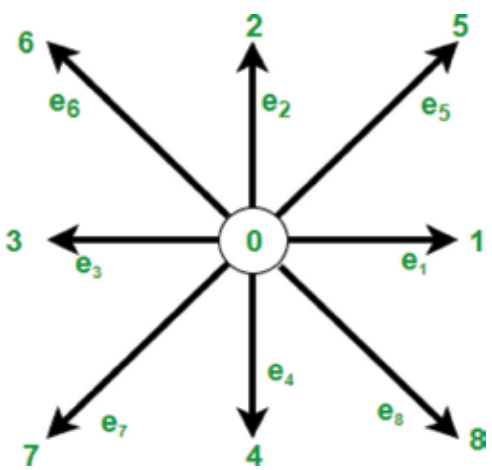

Figure 5. D2Q9 (2-D, 9-velocities) lattice nodes and velocities. Modified from [29].

where, $f_i(x, t)$ is the density distribution function, $f_i^{eq}(x, t)$ is the equilibrium distribution function, τ is the relaxation time. The left-hand side (LHS) of (Eq. (2)) represents the streaming step, while the right-hand side (RHS) constitutes the collision step.

In effect, collision of fluid particles is considered as a relaxation towards a local equilibrium, and defined for every model with varying dimensions (2-D, 3-D) and velocities (5, 9, 15, etc.).

The LBM models the distribution of and changes in the density function, from which the velocity profile is determined. Accordingly, the macroscopic fluid density and velocity are given respectively as [19, 23, 24].

$$\rho = \sum_{i=0}^{8} f_i \tag{5}$$

$$u = \frac{1}{\rho} \sum_{i=0}^{8} f_i e_i \tag{6}$$

where, ρ is the macroscopic fluid density and u is the macroscopic fluid velocity.

Several works [18, 29] have been carried out on modeling the convection problem encountered in deep saline aquifers during CO_2 sequestration with the lattice Boltzmann method (LBM). The findings include the fact that brine with a high CO_2 concentration was found to invade into the underlying unsaturated brine, causing an increase in the interfacial area between the CO_2–rich brine and CO_2 – deficient brine. In effect, this phenomenon enhanced the migration of CO_2 into the fracture and pores.

However, in organic-rich shales, most of the sequestration process takes place within the kerogen nanopores through adsorption [30, 31]. In so doing, there is the need to understand the interaction of supercritical CO_2 ($scCO_2$) with porous kerogen for long-term reservoir storage of CO_2 in organic-rich shales.

In a typical kerogen nanopore, the velocity is discontinuous at the pore wall due to the mean free path of the gas molecules exceeding the characteristic length (pore size). This phenomenon is characterized by the Knudsen number (K_n); slip flow regime falls within $0.001 < K_n < 0.1$. For chosen characteristic length 20 nm for our LBS ($K_n = 0.0243$), fluid flow falls within the slip flow regime. Slip flow boundary condition was modified for CO_2 molecules, which are predicted to not reflect at the walls but rather adsorb and desorb after some time lag [26, 27]. In effect, the velocity of the pore wall is defined to be dependent on the surface diffusion coefficient of CO_2 gas as well as Langmuir adsorption parameters based on the amount of adsorbed gas. Hence, the slip velocity at the pore-wall is given by [26, 27, 30].

$$u_{slip} = (1 - \alpha)\, u_g + \alpha u_w \tag{7}$$

where, u_{slip} is the slip velocity, u_g is the fluid velocity away from the wall, u_w is the local wall velocity dependent on the surface diffusion coefficient, and $\alpha$is the amount of adsorbed gas at the solid surface through Langmuir isotherm.

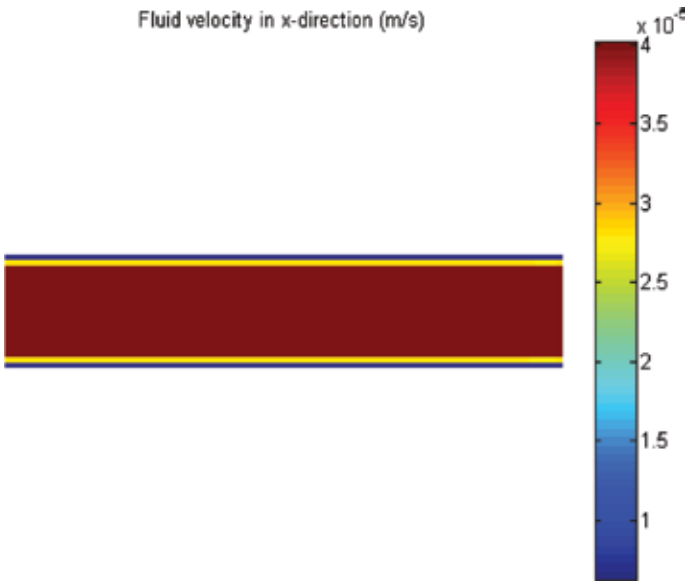

Figure 6. Composite velocity distribution of both CH_4 (center) and CO_2 (at the walls) in a 20 nm pore-slit.

Marcellus shale reservoir conditions were implemented at a high pressure of 12 MPa and temperature of 300 K. The D2Q9 LBM diffusion coefficient is known to be given in (Eq.(8)) and is directly comparable to the kinematic viscosity [28, 32].

$$D = \frac{1}{3}\left(\tau_\sigma - \frac{1}{2}\right) \tag{8}$$

where, D is the diffusion coefficient of the D2Q9 LBM and τ_σ is the relaxation time for each fluid component.

A 20-nm pore-slit is filled with both CH_4 and CO_2 at 12 MPa. Hydrodynamic velocity boundary condition is implemented at the upper and lower walls, while the pressure boundary condition is applied to the east and west ends. **Figure 6** shows the static velocity profile of both fluids in the pore-slit; CO_2 occupies the surface of the pore walls on both ends as the wetting phase, while methane occupies the center as the non-wetting phase.

Estimating the amount of adsorbed gas for CO_2 and CH_4, respectively, it was found that CO_2 adsorption capacity was much more than that of CH_4 for the same pore dimension and prevailing temperature and pressure. Furthermore, the diffusion coefficient CO_2 at $\tau = 1$ is higher than the diffusion coefficient of CH_4 at $\tau = 0.8$. The estimated magnitude of CH_4 diffusion coefficient is given in the range of 10^{-13}–10^{-10} m^2/s in carbon molecule sieves [19].

6. Conclusions

CO_2 sequestration in organic-rich shales to mitigate greenhouse gas (GHG) effects is proven to be very feasible through experimental and numerical simulations. Our literature review

and LBS suggest that organic-rich shales are capable of storing CO_2 in substantial quantities in its adsorbed state in the presence of higher TOC levels. In addition to shales being widely distributed and in abundance, the natural confining seals of the formation reduces the risk of leakage. On the other hand, CO_2-EGR/EOR can be achieved as part of the CO_2 sequestration process; CO_2-EGR/EOR produces relatively clean fuel and sustains energy demands.

However, to accurately benefit from CO_2 – sequestration in organic-rich shales, there is the need to overcome developmental challenges and understand the rock-fluid and fluid–fluid interactions in organic-rich shales for large scale pilot test and implementation.

Acknowledgements

We acknowledge the support of the Tertiary Oil Recovery Program (TORP) and Kansas Interdisciplinary Carbonates Consortium (KICC) at the University of Kansas. We would also like to thank Erin Honse (Fischer Scientific, formerly FEI) for acquisition of BSE images of our shale sample.

Conflict of interest

The authors declare no conflict of interest.

Notes

The authors declare no competing financial interest.

Appendices and nomenclature

EGR/EOR	enhanced gas recovery/enhanced oil recovery
OOIP	original oil-in-place
ECBM	enhanced coalbed methane
CO_2	carbon dioxide
$scCO_2$	supercritical CO_2
CH_4	methane
Gt	giga tons
TOC	total organic carbon/content

Ro %	vitrinite reflectance
LBM	lattice Boltzmann method
LBS	Lattice Boltzmann simulation
BGK	Bhatnagar-Gross-Krook
$f_i(x, t)$	velocity distribution function
$f_i^{eq}(x, t)$	equilibrium distribution function
τ	relaxation time
e_i	lattice velocities
ρ	macroscopic density
u	macroscopic velocity
GHG	greenhouse gas
MPa	mega Pascal
K	Kelvin
Kn	Knudsen number
nm	nanometer
u_{slip}	slip velocity
D	diffusion coefficient of D2Q9 LBM
D2Q9	2-dimensional, 9 velocity/speed model

Author details

Cudjoe Sherifa* and Barati Reza

*Address all correspondence to: reza.barati@ku.edu

University of Kansas, Lawrence, USA

References

[1] U.S. Department of Energy. Carbon Capture, Utilization, and Storage: Climate Change, Economic Competitiveness, and Energy Security; 2016

[2] Pentland CH. Measurements of Non-wetting Phase Trapping in Porous Media. London, United Kingdom: Imperial College London; 2010

[3] Bachu S. Aquifer disposal of CO_2: Hydrodynamic and mineral trapping. Energy Conversion and Management. 1994;**35**(4):269-279

[4] Kuuskraa VA, Godec ML, Dipietro P. 2 utilization from 'next generation' CO_2 enhanced oil recovery technology. Energy Procedia. 2013;**37**:6854-6866

[5] Busch A et al. Carbon dioxide storage potential of shales. International Journal of Greenhouse Gas Control. 2008;**2**(3):297-308

[6] Kang SM, Fathi E, Ambrose RJ, Akkutlu IY, Sigal RF. Carbon dioxide storage capacity of organic-rich shales. SPE Journal. December 2011:842-855

[7] Carbon Capture. Center for Climate and Energy Solutions (C2ES). [Online]. Available from: https://www.c2es.org/content/carbon-capture/. [Accessed: March 13, 2018]

[8] DiPietro P, Balash P, Wallace M. A note on sources of CO_2 supply for enhanced-oil-recovery operations. SPE Economics & Management. March 2012;**2012**:69-74

[9] (EIA) Hodge T. Natural gas expected to surpass coal in mix of fuel used for U.S. power generation in 2016. Today in Energy. [Online]. 2016. Available: https://www.eia.gov/todayinenergy/detail.php?id=25392. [Accessed: March 13, 2018]

[10] Melzer LS. Carbon dioxide enhanced oil recovery (CO_2 EOR): Factors involved in adding carbon capture, utilization and storage (CCUS) to enhanced oil recovery. Science and Engineering Ethics. February 2012:1-23

[11] U. S. D. of Energy. Carbon dioxide enhanced oil recovery. Netl. 2017:1-36

[12] Sohrabi M, Kechut NI, Riazi M, Jamiolahmady M, Ireland S, Robertson G. Safe storage of Co_2 together with improved oil recovery by Co_2-enriched water injection. Chemical Engineering Research and Design. 2011;**89**(9):1865-1872

[13] Elsharkawy AM, Poettmann FH, Christiansen RL. Measuring minimum miscibility pressure: Slim-tube or rising-bubble method? SPE/DOE Enhanced Oil Recovery Symposium. 1992;**5**:443-449

[14] Hawthorne SB, Gorecki CD, Sorensen JA, Miller DJ, Harju JA, Melzer LS. Hydrocarbon mobilization mechanisms using CO_2 in an unconventional oil play. Energy Procedia. 2014;**63**:7717-7723

[15] Chen C, Zhang D. Pore - scale simulation of density - driven convection in fractured porous media during geological CO_2 sequestration. Water Resources Research. April 2010;**46**:1-9

[16] Eshkalak MO, Aybar U, Eshkalak MO. Carbon dioxide storage and sequestration in unconventional shale reservoirs. Journal of Geosciences and Environment Protection. 2015;**3**(1):7-15

[17] Khosrokhavar R, Griffiths S, Wolf KH. Shale gas formations and their potential for carbon storage: Opportunities and outlook. Environmental Processes. 2014;**1**(4):595-611

[18] Pu H, Wang Y, Li Y. How CO_2 storage mechanisms are different in organic shale: Characterization and simulation studies. Society of Petroleum Engineers EAGE … SPE EUROPEC 2018 at the 80th EAGE Conference & Exhibition. 2016

[19] Tao Z, Clarens A. Estimating the carbon sequestration capacity of shale formations using methane production rates. Environmental Science & Technology. 2013;**47**(19):11318-11325

[20] Jarvie DM. Shale resource Systems for oil and gas: Part 1—shale-gas resource systems. Shale Reservoirs: Giant Resources for the 21st Century. AAPG Memoir. 2012:69-87

[21] Jarvie DM, Hill RJ, Ruble TE, Pollastro RM. Unconventional shale-gas systems: The Mississippian Barnett shale of north-Central Texas as one model for thermogenic shale-gas assessment. American Association of Petroleum Geologists Bulletin. 2007;**91**(4):475-499

[22] Nuttall BC. Analysis of Devonian black shales in Kentucky for potential carbon dioxide sequestration and enhanced natural gas production. Lexington, Kentucky; 2005

[23] Lopez AJ. Financial assistance funding opportunity announcement (FOA); 2018

[24] Arif M, Lebedev M, Barifcani A, Iglauer S. Influence of shale-total organic content on CO_2 geo-storage potential. Geophysical Research Letters. 2017;**44**(17):8769-8775

[25] Aljamaan H, Holmes R, Vishal V, Haghpanah R, Wilcox J, Kovscek AR. CO_2 storage and flow capacity measurements on idealized shales from dynamic breakthrough experiments. Energy and Fuels. 2017;**31**(2):1193-1207

[26] Javadpour F, Fisher D, Unsworth M. Nanoscale gas flow in shale gas sediments. Journal of Canadian Petroleum Technology. 2007;**46**(10):55-61

[27] Guo Z, Shu C. Lattice Boltzmann Method and its Applications in Engineering. Vol. 3. Singapore: World Scientif Publishing Co. Pte. Ltd; 2013

[28] Sukop MC, Thorne DT. Lattice Boltzmann Modeling. 2006;**79**(1 Pt 2)

[29] Mohamad AA. Lattice Boltzmann Method Fundamentals and Engineering Applications with Computer Codes. New York: Springer; 2011

[30] Fathi E, Akkutlu IY. Lattice Boltzmann method for simulation of shale gas transport in Kerogen. In: Proceedings of the SPE Annual Technical Conference and Exhibition. 2013;**4**(1):27-37

[31] Cudjoe S, Barati R. Lattice Boltzmann simulation of CO_2 transport in kerogen nonporous - An evaluation of CO_2 sequestration in organic-rich shales. Journal of Earth Science. 2017;**28**(5):926-932

[32] S M, Haibo Huang X-YL. Single-component multiphase Shan-Chen-type model. Multi phase Lattice Boltzmann Methods: Theory and Application. First, no. 2012. Chichester, West Sussex, UK: John Wiley & Sons, Ltd; 2015. pp. 18-64

Chapter 5

CO_2 Miscible Flooding for Enhanced Oil Recovery

Abdelaziz Nasr El-hoshoudy and Saad Desouky

Additional information is available at the end of the chapter

http://dx.doi.org/10.5772/intechopen.79082

Abstract

Carbon capture aims to mitigate the emission of CO_2 by capturing it at the point of combustion then storing it in geological reservoirs or applied through enhanced oil recovery (EOR) in a technology known as miscible flooding, so reduce CO_2 atmospheric emissions. Miscible CO_2-EOR employs supercritical CO_2 to displace oil from a depleted oil reservoir. CO_2 improve oil recovery by dissolving in, swelling, and reducing the oil viscosity. Hydrocarbon gases (natural gas and flue gas) used for miscible oil displacement in some large reservoirs. These displacements may simply amount to "pressure maintenance" in the reservoir. In such flooding techniques, the minimum miscibility pressure determined through multiple contact experiments and swelling test to determine the optimum injection conditions.

Keywords: miscible flooding, enhanced oil recovery, swelling test, minimum miscibility pressure

1. Background

CO_2 concentration in atmosphere increases due to the industrial revolution that attributed to the combustion of fossil fuels [1]. CO_2 is responsible of 64% of environmental pollution [1], so there is a dire need to mitigate its concentration to avoid global warming emissions. CO_2 miscible flooding in crude oil reservoirs is a currently successful technique to reduce its amount in the atmosphere, in addition to increasing the mobility of the oil and, consequently, increase the reservoir productivity [2]. It is preferred other than hydrocarbon gases since it does not only increase oil recovery but also causes a reduction of greenhouse gas emissions [3]. Moreover, it is a cheap technology as an ultimate long-term geologic storage solution for CO_2 owing to its economic productivity from incremental oil production offsetting the cost of carbon sequestration, and exhibit high displacement efficiency and the potential for environmental contamination

decrease through its disposal in the petroleum reservoir [1, 4]. This chapter aims to provide basic technical information concerning enhanced oil recovery by CO_2 flooding.

2. Enhanced oil recovery (EOR) processes

Owing to increased oil demand, improved oil recovery become a challenging task [3], since fossil fuels are the dominant source of the global energy supply [2] and represent about 85% of energy needs. Crude oil production occurs through three distinct phases [5–9]. The first stage is known as primary recovery, in which oil is recovered by natural reservoir energy including expansion of rock, fluid and dissolved gases, gravity drainage, and aquifer influx, or combination of these factors, which drive the hydrocarbon fluids from the reservoir to the wellbores. Primary oil recoveries range between 5 and 20% [10] of the original oil-in-place (OOIP). As reservoir pressure declines with the sustained production process, so the reservoir pressure must be built-up by injecting either water or natural gas, which drive reservoir fluid to wellbore [11]. This stage is known as secondary oil recovery, in which the recovered oil estimated to be in the range of 20–40% of the OOIP [10]. At the end of secondary recovery, a significant amount of residual oil remains in the reservoir and becomes the target for additional recovery using tertiary recovery or enhanced oil recovery (EOR) methods. EOR refers to the displacement of the remaining oil in the reservoir through injection of materials not normally present in the reservoir [10, 12–17]. Generally, EOR processes comprise the following three categories:

2.1. Thermal EOR

Injection of steam has historically been the most widely applied EOR method. Heat from steam or hot water dramatically reduces heavy oils viscosity, thus improving its flow. The process involves cyclic steam injection ("huff and puff," where steam is first injected, followed by oil production from the same well); Continuous steam injection (where steam injected into wells drives oil to separate production wells); hot water injection, and steam assisted gravity drainage (SAGD) using horizontal wells. Another set of thermal methods include, in situ combustion or fire flooding are currently implemented [18–20].

2.2. Miscible EOR

Miscible EOR employs supercritical CO_2 to displace oil from a depleted oil reservoir. CO_2 improve oil recovery by dissolving in, swelling, and reducing the viscosity of the oil. CO_2 is a cheap injection source for increasing recovery factor by the rate of 1–2$/Mscf [21]. Most CO_2 flooding processes occur in United States [22]. Hydrocarbon gases (natural gas and flue gas) in addition to compressed nitrogen used for miscible oil displacement in high deep reservoirs. These displacements may simply amount to "pressure maintenance" in the reservoir [23–25].

2.3. Chemical EOR

Chemical flooding was, up to 2000s, a less common EOR method than thermal and gas flooding, but now, huge projects are retrieved. The chemical flooding processes involve the

injection of three kinds of chemicals; alkaline, surfactant and polymer (soluble and cross-linked polymers), in addition to other chemicals such as foaming agents, acids and solvents [26] and/or combination of alkaline-surfactant-polymer flooding (ASP) [27]. In the polymer flooding method, water-soluble polymers aimed to shut-off the high-permeability areas of the reservoir and increase injected water viscosity to increase the swept areas in the reservoir [28, 29] leading to a more efficient displacement of moderately viscous oils. Addition of a surfactant to the polymer formulation may, under very specific circumstances, reduce oil–water interfacial tension (IFT) and hence remobilizing the trapped oil [30], changing surface wettability, so enhance the oil production. For some oils, alkaline may convert some naphthenic acids within the oil to surfactants that increase oil recovery. The alkaline may also play a beneficial role in reducing surfactant retention in the rock [31–34].

3. Fundamentals and mechanism of CO_2 flooding

Improvement of oil recovery occurs through different techniques, one of which is CO_2 flooding in low permeable and light-oil reservoirs [35, 36], as it can increase recovery factor from 10 to 20% [37]. Moreover, it reduces atmospheric gas emissions through CO_2 storage [38]. Gas miscible flooding implies that the displacing gas is miscible with reservoir oil either at first contact or after multiple contacts, which in turn improve the volumetric sweeping and displacement efficiencies (E_v and E_d) respectively [39, 40]. A transition zone will develop between the reservoir oil and displacing gas, where the miscibility of the injected gas depend on reservoir pressure, temperature, and oil properties [41, 42]. CO_2 miscible flooding comprises two mechanisms.

3.1. Miscible flooding

Miscible flooding depends on mobilizing the oil light components, reduction of oil viscosity, the vaporization and swelling of the oil, and the lowering of interfacial tension [41]. The injected CO_2 completely dissolve through crude oil at the minimum miscibility pressure (MMP) which determined experimentally through slim-tube tests or by mathematical correlations [3, 43, 44] and defined as, the pressure at which more than 80% of original oil-in-place (OOIP) is recovered at CO_2 breakthrough [45]. However, on an industrial scale, an oil recovery of at least 90% at 1.2 pore volume of CO_2 injected is used as a rule-of-thumb for estimating MMP [46, 47]. When the reservoir pressure is above the MMP, miscibility between CO_2 and reservoir oil is achieved through multiple-contact or dynamic miscibility, where the intermediate and higher molecular weight hydrocarbons from the reservoir oil vaporize into the CO_2 (vaporized gas-drive process) and part of the injected CO_2 dissolves into the oil (condensed gas-drive process) [48]. This mass transfer between the oil and CO_2 allows the two phases to become completely miscible without any interface and helps to develop a transition zone [49] that is miscible with oil and CO_2. CO_2 miscible flooding comprises; 1 first contact; vaporizing gas drive, and condensing gas drive [10].

A. **First contact**: in which miscible solvents mix with reservoir oil in all proportions and the mixture remains in one phase. Either through single or multiple contacts, and resulting in much improved oil recovery [50].

B. The vaporizing gas-drive process (high-pressure gas drive): achieves dynamic miscibility by in situ vaporization of the intermediate-molecular-weight hydrocarbons from the reservoir oil through injection of lean gases or CO_2 [51].

C. The condensing gas-drive process (enriched gas drive): achieves dynamic miscibility by in situ transfer of intermediate molecular weight hydrocarbons from rich solvent to lean reservoir oil through condensation process [52].

3.2. Immiscible flooding

Immiscible flooding depends on oil viscosity reduction, oil phase swelling, the extraction of lighter components, and the fluid drive [53]. When the reservoir pressure is below the MMP or the reservoir oil composition is not favorable, the CO_2 and oil will not form a single phase (i.e., immiscible). However, CO_2 will dissolve in the oil causing oil swelling, viscosity reduction and solution gas derive which in turn improve sweeping efficiency and facilitate further oil recovery [54]. Like hydrocarbon gases, CO_2 miscibility through crude oil increases with pressure and decreases with temperature [55, 56].

4. Properties of CO_2

In order to fully understand CO_2-EOR flooding, it is important to look at the properties of CO_2 and the fundamentals of the CO_2-EOR process. Under ambient conditions, CO_2 is a colorless, odorless gas and about 1.5 times heavier than air. CO_2 is (2–10 times) more soluble in oil than in the water. CO_2 increases the water viscosity and forms carbonate acid, which has a beneficial effect on shale and carbonate rocks [57]. Its properties under standard and critical conditions are summarized in **Table 1**. Above critical pressures and temperatures, CO_2 is in the supercritical state and forms a phase whose density is close to that of a liquid, even though its viscosity

Properties at standard conditions (14.7 psia, 0°C)	
Molecular weight	44.010 g/mol
Specific gravity	1.529
Density	1.95 kg/m^3
Viscosity	0.0137 mPa/s
Critical properties	
Critical pressure (P_c)	1070.6 psia
Critical temperature (T_c)	87.98°F
Critical volume (V_c)	94 cm^3/mol
Critical viscosity (μ_c)	0.0335 cp

Table 1. Properties of CO_2 under standard and critical conditions.

remains quite low (0.05–0.08 cp). This dense CO_2phase can extract hydrocarbon components from oil more easily than gaseous CO_2 [49].

5. CO_2 flooding and injection designs

Depending on the reservoir geology, fluid and rock properties, the CO_2 flooding involves the following;

5.1. Continuous CO_2 injection

This process requires continuous CO_2 injection with no other fluid. Sometimes a lighter gas, such as nitrogen, follows CO_2 injection to maximize gravity segregation.

5.2. Continuous CO_2 injection followed with water

This process is the same as the continuous CO_2 injection process except for chase water that follows the total injected CO_2 slug volume.

5.3. Conventional water-alternating-gas (WAG) followed with water

In this process, a predetermined volume of CO_2 is injected in cycles alternating with equal volumes of water. The water alternating with CO_2 injection helps overcome the gas override and reduces the CO_2 channeling consequently, improving overall CO_2 sweep efficiency.

5.4. Tapered WAG

This design is similar in concept to the conventional WAG but with a gradual reduction in the injected CO_2 volume relative to the water volume.

5.5. WAG followed with gas

This process is a conventional WAG process followed by a chase of less expensive gas (e.g., air or nitrogen) after the full CO_2 slug volume has been injected.

6. CO_2-EOR flooding projects and case studies

Several literatures stated about implementation of CO_2 and carbonated water to improve oil recovery since 1951 [45, 54, 58, 59], owing to its availability in adequate amounts from both natural and industrial sources [60]. The first field-wide application occurred in 1972 at the SACROC (Scurry Area Canyon Reef Operators Committee) unit in the Permian Basin, where the CO_2 was transported via a 200-mile-long pipeline from the Delaware-Val Verde Basin

[10]. Hashemi and Pouranfard [1] reported about the investigation of immiscible miscible CO_2 injection southwest of Iranian oil field, which has two reservoirs: Gurpi and a shallower Asmari reservoir. Main reservoir in this field is the Asmari formation with Oligocene and Miocene ages, which is divided into seven zones. Therefore, only the Asmari formation has been producing oil at commercial scale. The Asmari formation in this field consists of fractured carbonates with a low permeability matrix. The matrix has a porosity and permeability of about 0.088% and 3.4 md, respectively [1]. They concluded that the minimum miscibility pressure (MMP) was 4630 psia, The optimum injection rates for immiscible and miscible CO_2 injection scenarios were 17,000 and 30,000 Mscf/day, respectively and oil recovery factor reach 36.59% [1]. Al-Aryani and others [61] have reported on the first CO_2-EOR pilot test in the Middle East where pulsed neutron logging was used to monitor the performance of a CO_2 flood in one of the largest oil fields in Abu Dhabi, United Arab Emirates. The results of this test will be viewed with great interest based on the fact that it will have a significant impact on the application of CO_2-EOR in many oil-rich countries in the Middle East with the potential for very large additional oil recoveries. In India, a CO_2-EOR feasibility study was implemented in an oil field on the west coast, but the results are not yet publically available [62]. In China, there is ongoing research and pilot testing of CO_2-EOR and carbon sequestration in the Jilin oil field with plans to expand to other fields [63]. As of 2012, there were 15 CO_2-EOR projects outside of the United States—six in Canada, three in Brazil, five in Trinidad, and one in Turkey [64]. Of the six CO_2-EOR miscible projects in Canada, the Weyburn project is the most significant because it was the first project with the primary objective of injecting CO_2 for additional oil recovery as well as for carbon sequestration to help mitigate climate change. In recent years, there have been some serious efforts by Scottish Carbon Capture & Storage (SCCS), the Scottish Government, and other companies to investigate the possible application of CO_2-EOR in the North Sea. This interest is based on the potential for additional oil recovery from depleted oil fields using CO_2 captured from power plants and industry [10]. The objective is to gain a better understanding of the use of CO_2 in EOR operations with the goal of extending the producing life of North Sea oil fields using CO_2 captured from large emitters, such as power plants and industrial facilities, and permanently store the greenhouse gas in offshore oil reservoirs. It is estimated that there is the potential to recover 24 billion barrels of additional oil in the North Sea using the CO_2-EOR process. About 60 active miscible CO_2 projects were in operation in the United States in 1996, whereas in Canada, hydrocarbon miscible floods reach nearly ~40 active projects [35, 65]. Most CO_2-flooding projects carried out in the United States in Colorado, Louisiana, Mississippi, New Mexico, Michigan, Oklahoma, Texas, Utah, and Wyoming. During 2014, about 22 companies implemented CO_2 flooding projects; where 128 projects contributed about 126 million tons of oil [66], applied through carbonate and sandstone reservoirs with a percentage of 55 and 37% respectively, while the other 6% were implemented in tripolite reservoirs [67]. The range of porosity is from 4 to 29.5% with a permeability of 100 mD. The main operators and their productions reported in **Table 2**. The increased implementation of CO_2 flooding projects resort to its availability from natural and industrial sources in addition to its relatively low cost as a displacing agent compared to other alternatives [68]. It is observed that the outcome of these projects summarized in **Table 2**, where the recovery factor ranged from 0.15 to 36.37%. The reservoirs properties are summarized in **Table 3**.

Operator	No. of projects	Improved production ($\times 10^4$ tons)	Recovered oil (%)
Occidental	33	459.63	36.37
Kinder Morgan	3	138.34	10.94
Chevron	7	126.30	9.99
Hess	4	106.89	8.46
Denbury Resources	18	86.82	6.87
Merit Energy	7	71.12	5.63
Anadarko	6	55.79	4.41
ExxonMobil	1	45.36	3.59
Breitburn Energy	5	36.87	2.92
ConocoPhillips	2	28.42	2.25
Whiting Petroleum	1	24.51	1.94
Apache	5	23.88	1.89
XTO Energy Inc.	4	13.43	1.06
Chaparral Energy	8	9.18	0.73
Fasken	5	4.30	0.34
Core Energy	9	1.90	0.15
Others	12	31.19	2.47

Table 2. CO_2 miscible flooding operator and production dataset [66, 69, 70].

Property	Minimum	Maximum	Median	Mean
Porosity	4	29.5	12	14.25
Permeability, mD	2	700	14	44.35
API gravity	27	45	38	37
Viscosity, cp	0.4	6	1.8	1.3
Temperature, °F	83	260	108.5	133.9
Depth, ft	1150	11,950	5500	6107.3
Oil saturation (% PV)	26.3	89	46	49.6
Net thickness, ft	15	268	90	110
Minimum miscibility pressure (MMP), psia	1020	3452	1987.5	2058.4

Table 3. Properties of reservoirs subjected to CO_2 flooding.

7. Screening criteria for CO_2 flooding

Screening criteria for miscible CO_2 flooding comprise reservoir depth, pressure and temperature, minimum miscibility pressure (MMP), residual oil saturation, net pay thickness, crude oil gravity, and viscosity in addition to permeability, porosity, and reservoir heterogeneity [40]. In

Criteria	Optimum condition
Depth, ft	2500 [73]–3000 [74]
Reservoir temperature, °F	<120
Reservoir pressure, psi	>3000
Total dissolved solids (TDS)	<10,000 mg/L
Oil gravity	Medium to light oils (27–39° API)
Oil viscosity, cp	<3
Reservoir type	Carbonate reservoirs preferred than sandstone one
Minimum miscibility pressure (MMP), psi	1300–2500
Oil saturation	>20% [73]
Net pay thickness, ft	75–137
Porosity	>7%
Permeability	>10 mD

Table 4. Optimum screening criteria for CO_2 miscible flooding.

preliminary screening, according to National Petroleum Council, the optimum reservoir criteria for CO_2 miscible flooding [64, 71] are summarized in **Table 4**. Any deviation from these criteria would depend on the size of the reservoir and potential hydrocarbon recovery. For example when reservoir temperatures are greater than 120°F, additional pressure ranges from 200 to 500 psi is required to achieve miscibility. The density of CO_2 depends on the injection depth, which controls the ambient temperature and pressure and range from 0.6–0.8 g/cc [72]. The CO_2 should be injected at depth greater than 800 m, where it is in a dense phase (either liquid or supercritical) [2]. High saline reservoirs are more susceptible to CO_2 storage than low salinity reservoirs.

All reservoir lithology, including carbonate and siliciclastic are appropriate for CO_2-EOR flooding as long as they have interconnected pore space for fluid accumulation and flow. Proper reservoir characterization leads to accurate estimates of OOIP and a convenient evaluation of reservoir behavior. The OOIP calculated volumetrically, by the following equation;

$$OOIP = \frac{(7758^{*}A^{*}H^{*}\Phi^{*}Soi)}{Boi} \tag{1}$$

7758, multiplying factor, (barrels/acre-feet); A, reservoir area,(acres);h; average net reservoir thickness, (feet); Ø; average porosity of formation; S_{oi}; initial oil saturation in pore space; B_{oi}; oil formation volume factor at initial reservoir pressure (bbl/STB).

8. CO_2-miscible flooding performance and simulation

Before conducting a CO_2-flooding, its miscibility with the reservoir is determined through measurement of MMP. After that, a pilot test is conducted to check the success of the CO_2-EOR process on a small scale in the field. If all results are positive, reservoir simulation is

carried out to (a) scale-up the EOR process to an entire oil field and (b) define the optimum design of the WAG ratio and hydrocarbon pore volume injection volumes for maximum oil recovery [75]. The performance of a flooding process evaluated by exploring the slug of CO_2 and water, the performance of oil-production wells, gas-oil ratio and water cut, and the injection wells for fluid distribution among various reservoir layers, since these parameters greatly effect on the recovery factor [76].

9. Operational aspect

In order to implement a successful CO_2-miscible flooding several parameters are considered;

9.1. CO_2 source

There are three possible sources of CO_2: (1) natural hydrocarbon gas reservoirs containing CO_2 as an impurity (generally less than 25%), (2) industrial or anthropogenic sources with wide variation of CO_2 percentage in the effluent like power plants and so on [2], and (3) natural CO_2 reservoirs [49].

9.2. Surface facilities

The facility requirements for CO_2-EOR include the following items.

i. CO_2 extraction: it is extracted from the separator gas, which begins to show increasing quantities of CO_2 after its breakthrough in producing wells [77].

ii. CO_2 processing: it is purified to specification after its extraction from the separator gas and is dehydrated before compression [78].

iii. CO_2 compression: it is compressed to raise its pressure for injection [79].

9.3. Technological challenges

Technical challenges of CO_2 flooding can be summarized in the following [80].

1. Increasing CO_2 injection volumes,

2. Optimizing flood design and well placement for extracting more of the residual oil,

3. Improving the mobility ratio by increasing the viscosity of water by use of polymers, and

4. Extending miscibility by reducing the miscibility pressure through the use of liquefied petroleum gas (LPG).

10. Conclusion

The primary and secondary oil recovery produces about 20–40% of the OOIP [48]. Consequently, there is a huge amount of potentially unrecovered oil left in the reservoir, which becomes the

target for suitable EOR processes. One of the widely implemented EOR processes is CO_2-miscible flooding which recovers high amounts of crude oil and reduces environmental pollution results from gas emissions. CO_2 can be injected either as a continuous stream, water-alternating gas (WAG). Implementation of successful CO_2 miscible flooding require an accurate investigation of reservoir screening criteria comprising reservoir porosity and permeability, API gravity, oil viscosity, reservoir temperature, depth, oil saturation, and net pay thickness.

Author details

Abdelaziz Nasr El-hoshoudy* and Saad Desouky

*Address all correspondence to: azizchemist@yahoo.com

Production Department, PVT Lab, Egyptian Petroleum Research Institute, Cairo, Egypt

References

[1] Fath AH, Pouranfard A-R. Evaluation of miscible and immiscible CO_2 injection in one of the Iranian oil fields. Egyptian Journal of Petroleum. 2014;**23**(3):255-270

[2] Herzog H. Carbon Dioxide Capture and Storage. USA: Helm Hepburn, Oxford University press; 2009

[3] Karkevandi-Talkhooncheh A, Rostami A, Hemmati-Sarapardeh A, Ahmadi M, Husein MM, Dabir B. Modeling minimum miscibility pressure during pure and impure CO_2 flooding using hybrid of radial basis function neural network and evolutionary techniques. Fuel. 2018;**220**:270-282

[4] Bui M, Adjiman CS, Bardow A, Anthony EJ, Boston A, Brown S, et al. Carbon capture and storage (CCS): The way forward. Energy & Environmental Science; 2018;**11**:1062-1176

[5] El-hoshoudy A, Desouky S, Betiha M, Alsabagh A. Use of 1-vinyl imidazole based surfmers for preparation of polyacrylamide–SiO_2 nanocomposite through aza-Michael addition copolymerization reaction for rock wettability alteration. Fuel. 2016;**170**:161-175

[6] El-hoshoudy A. Quaternary ammonium based surfmer-co-acrylamide polymers for altering carbonate rock wettability during water flooding. Journal of Molecular Liquids. 2018; **250**:35-43

[7] El-hoshoudy A, Desouky S, Al-Sabagh A, Betiha M, MY E-k MS. Evaluation of solution and rheological properties for hydrophobically associated polyacrylamide copolymer as a promised enhanced oil recovery candidate. Egyptian Journal of Petroleum. 2017;**26**(3):779-785

[8] El-Hoshoudy A, Desouky S, Elkady M, Alsabagh A, Betiha M, MS. Investigation of optimum polymerization conditions for synthesis of cross-linked polyacrylamide-amphoteric

surfmer nanocomposites for polymer flooding in sandstone reservoirs. International Journal of Polymer Science. 2015;**2015**

[9] El-hoshoudy A, Desouky S, Al-sabagh A, El-kady M, Betiha M, Mahmoud S. Synthesis and characterization of polyacrylamide crosslinked copolymer for enhanced oil recovery and rock wettability alteration. International Journal of Oil, Gas and Coal Engineering. 2015;**3**(4):43-55

[10] Verma MK. Fundamentals of Carbon Dioxide-Enhanced Oil Recovery (CO_2-EOR): A Supporting Document of the Assessment Methodology for Hydrocarbon Recovery Using CO_2-EOR Associated with Carbon Sequestration. Washington, DC: US Department of the Interior, US Geological Survey; 2015

[11] El-hoshoudy A, Desouky S, Elkady M, Alsabagh A, Betiha M, Mahmoud S. Hydrophobically associated polymers for wettability alteration and enhanced oil recovery—Article review. Egyptian Journal of Petroleum. 2016;**26**:757-762

[12] Terry RE, Rogers JB, Craft BC. Applied Petroleum Reservoir Engineering. USA: Pearson Education; 2013

[13] Dusseault M. Comparing Venezuelan and Canadian heavy oil and tar sands. In: Canadian International Petroleum Conference; Petroleum Society of Canada, Calgary, Alberta, Canada, 2001

[14] Arps JJ. Estimation of Primary Oil Reserves. one Petro. 1956;**207**:182-191

[15] Dake LP. The Practice of Reservoir Engineering (Revised Edition). Amestrdam, The Netherlands: Elsevier; 2001

[16] Kovscek A. Screening criteria for CO_2 storage in oil reservoirs. Petroleum Science and Technology. 2002;**20**(7–8):841-866

[17] Archer JS, Wall CG. Petroleum Engineering: Principles and Practice. London: Springer Science & Business Media; 2012

[18] Muraza O, Galadima A. Aquathermolysis of heavy oil: A review and perspective on catalyst development. Fuel. 2015;**157**:219-231

[19] Wan T. Evaluation of the EOR Potential in Shale Oil Reservoirs by Cyclic Gas Injection. USA: Texas Tech University Libraries; 2013

[20] Babadagli T, Sahin S, Kalfa U, Celebioglu D, Karabakal U, Topguder NNS. Development of heavy oil fractured carbonate Bati Raman field: Evaluation of steam injection potential and improving ongoing CO_2 injection. SPE Annual Technical Conference and Exhibition. Society of Petroleum Engineers; 2008

[21] Manrique EJ, Muci VE, Gurfinkel ME. EOR field experiences in carbonate reservoirs in the United States. SPE Reservoir Evaluation & Engineering. 2007;**10**(06):667-686

[22] Taber J, Martin F, Seright R. EOR screening criteria revisited—Part 2: Applications and impact of oil prices. SPE Reservoir Engineering. 1997;**12**(03):199-206

[23] Plasynski S, Litynski J, McIlvried H, Srivastava R. Progress and new developments in carbon capture and storage. Critical Reviews in Plant Science. 2009;**28**(3):123-138

[24] Farajzadeh R, Andrianov A, Bruining H, Zitha PL. Comparative study of CO_2 and N_2 foams in porous media at low and high pressure−temperatures. Industrial & Engineering Chemistry Research. 2009;**48**(9):4542-4552

[25] Li S, Qiao C, Zhang C, Li Z. Determination of diffusion coefficients of supercritical CO_2 under tight oil reservoir conditions with pressure-decay method. Journal of CO_2 Utilization. 2018;**24**:430-443

[26] Schramm G. A Practical Approach to Rheology and Rheometry. Karlsruhe: Haake; 1994

[27] Abidin A, Puspasari T, Nugroho W. Polymers for enhanced oil recovery technology. Procedia Chemistry. 2012;**4**:11-16

[28] Sorbie K, Clifford P. The inclusion of molecular diffusion effects in the network modelling of hydrodynamic dispersion in porous media. Chemical Engineering Science. 1991;**46**(10): 2525-2542

[29] El-hoshoudy AN, Desouky SM. Synthesis and evaluation of acryloylated starch-g-poly (acrylamide/vinylmethacrylate/1-vinyl-2-pyrrolidone) crosslinked terpolymer functionalized by dimethylphenylvinylsilane derivative as a novel polymer-flooding agent. International Journal of Biological Macromolecules. 2018;**116**:434-442

[30] Haywood V, Yu TS, Huang NC, Lucas WJ. Phloem long-distance trafficking of GIBBERELLIC ACID-INSENSITIVE RNA regulates leaf development. The Plant Journal. 2005;**42**(1):49-68

[31] Olajire AA. Review of ASP EOR (alkaline surfactant polymer enhanced oil recovery) technology in the petroleum industry: Prospects and challenges. Energy. 2014;**77**:963-982

[32] Liu S, Miller CA, Li RF, Hirasaki G. Alkaline/surfactant/polymer processes: Wide range of conditions for good recovery. SPE Journal. 2010;**15**(02):282-293

[33] Kumar S, Panigrahi P, Saw RK, Mandal A. Interfacial interaction of cationic surfactants and its effect on wettability alteration of oil-wet carbonate rock. Energy & Fuels. 2016; **30**(4):2846-2857

[34] Chen I-C, Akbulut M. Nanoscale dynamics of heavy oil recovery using surfactant floods. Energy & Fuels. 2012;**26**(12):7176-7182

[35] Song Z, Zhu W, Wang X, Guo S. 2-D pore-scale experimental investigations of asphaltene deposition and heavy oil recovery by CO_2 flooding. Energy & Fuels. 2018;**32**(3):3194-3201

[36] Zhou X, Yuan Q, Peng X, Zeng F, Zhang L. A critical review of the CO_2 huff 'n'puff process for enhanced heavy oil recovery. Fuel. 2018;**215**:813-824

[37] Kulkarni MM. Immiscible and Miscible Gas-Oil Displacements in Porous Media. MSc Thesis. Louisiana State University and Agricultural and Mechanical College. 2003

[38] Bachu S, Adams J. Sequestration of CO_2 in geological media in response to climate change: Capacity of deep saline aquifers to sequester CO_2 in solution. Energy Conversion and Management. 2003;**44**(20):3151-3175

[39] Claridge E. Prediction of recovery in unstable miscible flooding. Society of Petroleum Engineers Journal. 1972;**12**(02):143-155

[40] Mathiassen OM. CO_2 as Injection Gas for Enhanced Oil Recovery and Estimation of the Potential on the Norwegian Continental Shelf. Trondheim, Norwegian University of Science and Technology (NTNU) Norway; 2003

[41] Thomas S. Enhanced oil recovery—An overview. Oil & Gas Science and Technology-Revue de l'IFP. 2008;**63**(1):9-19

[42] Jessen K, Kovscek AR, Orr FM Jr. Increasing CO_2 storage in oil recovery. Energy Conversion and Management. 2005;**46**(2):293-311

[43] An E-h, Desouky S. An Empirical Correlation for Estimation of Formation Volume Factor of Gas Condensate Reservoirs at Separator Conditions

[44] An E-h, Desouky S. Numerical Prediction of Oil Formation Volume Factor at Bubble Point for Black and Volatile Oil Reservoirs Using Non-Linear Regression Models

[45] Holm L, Josendal V. Mechanisms of oil displacement by carbon dioxide. Journal of Petroleum Technology. 1974;**26**(12):1427-1438

[46] Yellig W, Determination MR. Prediction of CO_2 minimum miscibility pressures (includes associated paper 8876). Journal of Petroleum Technology. 1980;**32**(01):160-168

[47] Taber JJ, Martin F, Seright R. EOR screening criteria revisited—Part 1: Introduction to screening criteria and enhanced recovery field projects. SPE Reservoir Engineering. 1997; **12**(03):189-198

[48] Merchant D. Life beyond 80—A look at conventional wag recovery beyond 80% HCPV injection in CO_2 tertiary floods. Carbon Management Technology Conference. Carbon Management Technology Conference; 2015

[49] Jarrell PM, Fox CE, Stein MH, Webb SL. Practical Aspects of CO_2 Flooding. TX: Society of Petroleum Engineers Richardson; 2002

[50] Bondor P. Applications of carbon dioxide in enhanced oil recovery. Energy Conversion and Management. 1992;**33**(5–8):579-586

[51] Stalkup FI Jr. Status of miscible displacement. Journal of Petroleum Technology. 1983; **35**(04):815-826

[52] Holm LW. Miscible displacement (1987 PEH Chapter 45). Petroleum Engineering Handbook. USA: Society of Petroleum Engineers; 1987

[53] Holm LW, Josendal VA. Effect of oil composition on miscible-type displacement by carbon dioxide. Society of Petroleum Engineers Journal. 1982;**22**(01):87-98

[54] Martin JW. Additional oil production through flooding with carbonated water. Producers Monthly. 1951;**15**(7):18-22

[55] Simon R, Graue D. Generalized correlations for predicting solubility, swelling and viscosity behavior of CO_2-crude oil systems. Journal of Petroleum Technology. 1965;**17**(01):102-106

[56] Leung LC. Numerical evaluation of the effect of simultaneous steam and carbon dioxide injection on the recovery of heavy oil. Journal of Petroleum Technology. 1983;**35**(09):1,591-1,1,9

[57] Solomon S. Carbon dioxide storage: Geological security and environmental issues–Case study on the sleipner gas field in Norway. Bellona Report. 2007. p. 128

[58] Mosavat N, Torabi F. Experimental evaluation of the performance of carbonated water injection (CWI) under various operating conditions in light oil systems. Fuel. 2014;**123**: 274-284

[59] Holm WL. Evolution of the carbon dioxide flooding processes. Journal of Petroleum Technology. 1987;**39**(11):1337-1342

[60] Ayirala S, Yousef A. A state-of-the-art review to develop injection-water-chemistry requirement guidelines for IOR/EOR projects. SPE Production & Operations. 2015;**30**(01): 26-42

[61] Aryani A, Mohamed F, Obeidi A, Brahmakulam JV, Ramamoorthy R. Pulsed neutron monitoring of the first CO_2 EOR pilot in the Middle East. In: SPE Middle East Oil and Gas Show and Conference; Society of Petroleum Engineers. 2011

[62] Srivastava RP, Vedanti N, Dimri V, Akervol I, Bergmo P, Biram R. CO_2-EOR: A feasibility study of an Indian oil field. In: 2012 SEG Annual Meeting; Society of Exploration Geophysicists. 2012

[63] Chang CW-K. Stumbling toward Capitalism: The State, Global Production Networks, and the Unexpected Emergence of China's Independent Auto Industry. Berkeley: University of California; 2011

[64] Koottungal L. Worldwide EOR survey. Oil & Gas Journal. 2012, 2012;**110**:57-69

[65] Khormali A, Sharifov AR, Torba DI. The control of asphaltene precipitation in oil wells. Petroleum Science and Technology. 2018;**36**(6):443-449

[66] Jishun Q, Haishui H, Xiaolei L. Application and enlightenment of carbon dioxide flooding in the United States of America. Petroleum Exploration and Development. 2015;**42**(2):232-240

[67] Boot-Handford ME, Abanades JC, Anthony EJ, Blunt MJ, Brandani S, Mac Dowell N, et al. Carbon capture and storage update. Energy & Environmental Science. 2014;**7**(1):130-189

[68] Goodyear SG, Koster M, Marriott K, Paterson A, Sipkema AW, Young I. Moving CO_2 EOR offshore. In: SPE Enhanced Oil Recovery Conference; Society of Petroleum Engineers. 2011

[69] Yin M. CO_2 Miscible Flooding Application and Screening Criteria. Missouri University of Science and Technology; 2015

[70] Olea RA. Carbon Dioxide Enhanced Oil Recovery Performance According to the Literature. US Geological Survey; 2017

[71] Kuuskraa V. QC updates carbon dioxide projects in OGJ's enhanced oil recovery survey. Oil & Gas Journal. 2012;**110**(7):72

[72] Sheppard M. Carbon Capture and Sequestration. Schlumberger, Paper 17; 2007

[73] Gao P, Towler BF, Pan G. Strategies for evaluation of the CO_2 miscible flooding process. In: Abu Dhabi International Petroleum Exhibition and Conference; Society of Petroleum Engineers. 2010

[74] Arshad A, Al-Majed AA, Menouar H, Muhammadain AM, Mtawaa B. Carbon dioxide (CO_2) miscible flooding in tight oil reservoirs: A case study. In: Kuwait International Petroleum Conference and Exhibition; Society of Petroleum Engineers. 2009

[75] Peterson CA, Pearson EJ, Chodur VT, Pereira C. Beaver Creek Madison CO_2 enhanced recovery project case history. In: SPE Improved Oil Recovery Symposium; Society of Petroleum Engineers; Riverton, Wyoming. 2012

[76] Perera MSA, Gamage RP, Rathnaweera TD, Ranathunga AS, Koay A, Choi X. A review of CO_2-enhanced oil recovery with a simulated sensitivity analysis. Energies. 2016;**9**(7):481

[77] Holm L. Carbon Dioxide Solvent Flooding for Increased Oil Recovery. OnePetro; 1959;**216**: 225-231

[78] Posch S, Haider M. Optimization of CO_2 compression and purification units (CO_2CPU) for CCS power plants. Fuel. 2012;**101**:254-263

[79] Benson SM, Orr FM. Carbon dioxide capture and storage. MRS Bulletin. 2008;**33**(4):303-305

[80] Papadopoulou M. Numerical Simulation Study of Low-Tension-Gas (LTG) Flooding for Enhanced Oil Recovery in Tight Formations. The University of Texas at Austin; 2017

Chapter 6

An Innovative Approach in Post Combustion Carbon Capture and Sequestration towards Reduction of Energy Penalty in Regeneration of Solvent

Vinod Krishna Sethi and Partha S. Dutta

Additional information is available at the end of the chapter

http://dx.doi.org/10.5772/intechopen.78394

Abstract

India as a fast growing economy is pursuing strategic knowledge mission for focused research in the area of climate change. Our R&D in Carbon Capture & Sequestration (CCS) will be initially focused on post combustion carbon capture on coal fired power plants. India is 3rd largest emitter of world after China and US with a share of 6.9% in global emission of CO_2, however, India's per capita GHG emission is only 1.6 MT per annum (MTPA) which is well below the world average 7.5 MTPA. National Mission on Strategic Knowledge for Climate Change aims to develop a better understanding of Climate Science impacts and challenges. The planning commission has announced the Government's interest in adding a ninth mission i.e. 'Clean Coal Technologies mission' that would include Carbon Capture & Sequestration. As regards Carbon Capture & Sequestration (CCS) on coal fired power plants in India is concerned, an innovative concept of integrating solar thermal for steam production will pave way for reducing energy penalty in regeneration of solvents from a level of over 15% to around 05%. This chapter deals with an innovative approach of CCS in which the major issues of energy penalty reduction have been taken care of through use of Solar Steam Generation, through concentrated solar plant (CSP) with 24 × 7 thermal energy storage (TES).

Keywords: carbon capture, sequestration, amine solvent, post combustion carbon capture, concentrated solar plant, MEA solvent, energy penalty, oil fired boiler, thermal energy storage (TES), halide salt

1. Introduction: current climate change policies in India and targets

India is rich in coal and is third largest coal producer in the world with estimated coal reserves of the order of 257 billion tons [1]. Coal continues to be the dominating energy source and

meets nearly 58% of total requirement of commercial energy, but accounts for over 50% of the gross emissions. Out of total annual emission of about 2100 million tons per annum (MTPA), CO_2 emitted by the coal based thermal power plants amounts to about over 1000 MTPA. With the developmental activities using fossil fuels on the anvil, the aggregate emission in the country would increase. The coal-based power plants totaling to 192 GW out of total installed capacity of 330 GW would remain main stay of India's power sector for at least 2–3 decades. India, though has lower contribution to the historical GHG accumulation, it holds a large potential for options like cost effective CCS to tackle the adverse effects of climate change [2]. Coal fired power plants in India account for more than half of the energy production in the country annually and about 52% of the total GHG emissions of the country [3, 4]. With a large number of new coal power plants, sub and supercritical, being installed, the problem of GHG emissions is likely to increase.

India has world's largest sedimentary basins. Ganga Basin and adjoining Rajasthan and Vindhya Basins offer a potential site for CO_2 storage [5].

India has made a voluntary commitment at paris agreement; COP-21, that it would decrease its carbon intensity by 30–33% by 2030 from 2005 level. To address the threat of climate change, India has further declared in UNFCC's Conference of Parties (COP21) at Paris, that it will augment 175 GW of renewable energy, out of which 100 GW would be solar PV and solar thermal. Carbon sequestration of the order of 2.5–3.0 billion tons of CO_2 through additional forest is also aimed at in the perspective five year plans and focus on adaptation in agriculture, forest, water and livelihood would be accelerated [1, 7].

The path chosen makes it imperative that the CO_2, which forms 95% of the GHG emissions be reduced. The reduction of 33% intensity as promised by India at COP-21: Paris; would translate to a decrease of CO_2 emissions from our coal plants from 0.9 kg/kWh to a level of 0.58 kg/kWh by 2030. This decrease is possible by a combination of adaptation and mitigation measures like acceleration of present pace of Low Carbon Technologies (LCT) particularly and Clean Coal Technologies (CCT) and setting up of Carbon Capture & Sequestration (CCS) plants primarily for post combustion carbon capture on our fossil fuel based sub and supercritical thermal power plants.

The Indian Power Ministry and the Department of Science & Technology have considered CO_2 capture and its sequestration through options like conversion to fuels as a far economical option than storage in sedimentary basins by [6, 7]. As per the Global Assessment Report, there is limited geological storage capacity [8], however a better potential will be found, if the concept of CO_2 storage in Basalt formations can be advanced into a matured option through focused R&D [9, 10].

Expected benefits for the environment and society at large due to the CCS implementation plan are:

- Adoption and implementation of Low Carbon Technologies will pave way for sustainable society prepared to meet the challenges of climate change.

- CO_2 sequestration is a multi-dimensional aspect involving capture of carbon from atmosphere followed by transportation, injection into favorable sites and post-injection monitoring. The favorable sites for storage of CO_2 must be reliable in the sense that CO_2 will be stored there permanently at least for 1000 years and no leakage is preferable. In this backdrop, the most suitable storage sites where CO_2 could be fixed permanently by chemical absorption and reaction respectively are depleted coal beds and saline aquifers [7].

- Carbon Capture & Sequestration would play an important role in reducing GHG emissions at the same time enabling low carbon electricity generation from Power plants. Considering a CCS integrated 500 MW unit, which emits over 3 million tons of CO_2 per annum, would be equivalent to: (a) planting over 60 million trees and maintaining them to grow for 10 years; (b) avoiding energy related emission of about 0.3 million houses [7].

R&D efforts under the aegis of various Ministries of Government of India including Department of Science & Technology, would be required to estimate the economic implications of implementing CCS in the existing coal Fired plants [11]. Nine national missions for managing climate change have been set up by the Planning Commission, which include Clean Coal Technologies and CCS as a prime mitigation measure.

It has been recommended at several forums of Ministry of Power that a better option could be carbon capture and sequestration (CCS) through the technologies of conversion of CO_2 into multipurpose fuels including biodiesel through Algae route. In a post combustion amine based CCS Plant the Energy Penalty in regeneration of solvent has been identified as a main issues in CCS deployment, as such India is taking conscious steps in the area of CCS as under following stage wise program:

- Stage-1 (1–5 years): CO_2 sequestration to selected species of Algae in ash pond in the plant area.

- Stage-2 (5–10 years): sequestration to depleted coal mines for pit-head coal based power stations.

- Stage 3A (10–15 years): sequestration to basalt rocks, saline aquifers & EOR as per site specific options.

- Stage-3B (10–15 years): for costal power stations: CO_2 hydrate formation in seabed sediments.

Innovative concept of energy penalty reduction through integration with the solar thermal could also be an option for India and other countries between tropic of cancer & capricorn viz. under International Solar Alliance launched recently with India in lead role. The CCS option towards sustainability may lead to an opportunity for course-correction in line of thinking of our Planners,

Engineers & Scientists working in the arena of Green Power technology and its development. The time appears to be ripe for implementation of CCS on an actual thermal power plant.

2. Detailed methodology of post combustion CCS on a thermal power plant: a pilot study

A pilot plant of CCS having rated capacity of curbing carbon dioxide of 500 kg/day was installed at RGPV University, Bhopal in Central India in the year 2008. The source of carbon dioxide was a baby boiler of rated capacity of producing 100 kg/h of steam. Desired amount of steam is extracted for catalytic conversion and other heating processes. Another source of flue gases is a biomass gasifier fired engine of capacity 10 kWe, which is also coupled with the system. Scrubbing of flue gas is done using solution of $NaHCO_3$, NaOH and lime for removal of SOx and Nox; and for capturing carbon dioxide from flue gas an aqueous solvent of 1–2 M monoethanolamine is used. The strip of CO_2 is sent to the three MEA solvent tanks where the MEA solvent in the three tanks absorb the CO_2 up to their saturation point. The saturated MEA containing CO_2, from the three MEA solvent tanks are sent to the saturated MEA tank. In order to remove CO_2 from the MEA saturated solvent, a striping tank is provided. The CO_2 is released from the MEA solvent in striping tank with the help of steam generated from the diesel-fired boiler. Data are recorded by combustion gas analyzer, which was customized to record data as per requirement [12]. The scheme diagram of the plant is shown at **Figure 1**. Catalytic converters/reduction units for methane, hydrogen and CO are installed for this pilot unit.

The long term "Objectives" behind setting up of a pilot plant are to provide ground for 'Feasibility study' on a large thermal units of future having CCS facility with least energy penalty. To this end, the development of Concentrated Solar Power for Steam generation for Regeneration of CO_2 captured MEA Solvent & System optimization studies are on the anvil.

The pilot plant will also provide a study and prove the viability of sequestration of CO_2 to selected species of Algae for getting optimum lipid content from the increased growth of species.

The pilot plant together with the combustion gas analyzer & data acquisition system has been used for 4000 h. Trail run for 'Uncertainty Analysis' in the experimentation. CO_2 capture level of 90–93% was achieved for the above post combustion CO_2 sources viz. a boiler and a gasifier. It was seen that H_2 formation to the extent of 21% by volume was also achieved.

The pilot plant (**Figure 2**) was utilized for variety of application during trial run of 4000 h for process stabilization such as: the study of CO_2 capture in mono ethanol amine (MEA) ranging from 1 molar to 5 molar strength; sequestration of CO_2 released from the stripper unit to variety of algae and development of lipid content for bio-diesel production. The pilot plant is also being used for development of low cost catalysts for production of fuel elements like CH_4 [13].

http://dx.doi.org/10.5772/intechopen.78394

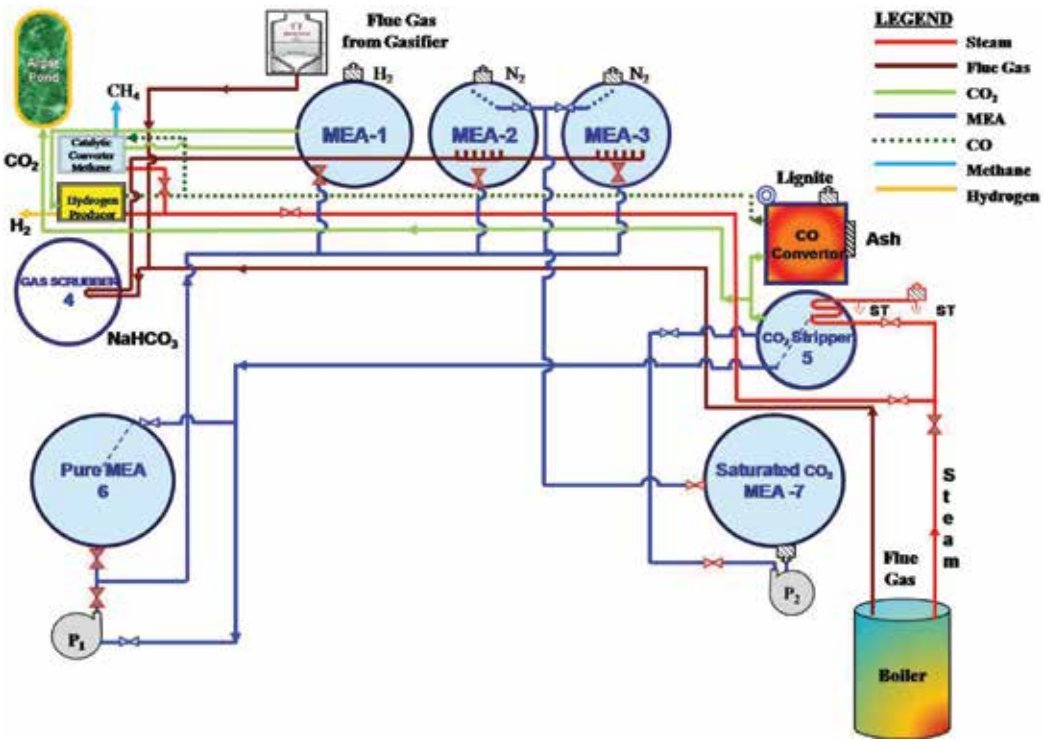

Figure 1. Scheme diagram of CO_2 capture & sequestration pilot plant.

Figure 2. CO_2 capture & sequestration plant (CO_2 & steam source—oil fired baby boiler).

A need was established soon after the 4000 h trail runs of this pilot plant to explore:

i. Optimum value of molar strength of MEA solvent for highest efficiency of capture with minimum cost penalty of regeneration.

ii. Optimum value of carbon dioxide recycling for conversion to CO to attain heat gain up to the calculated theoretical limit of 21.88%.

Simulation studies were carried out and a 1.5 molar strength was found to be optimum for CO_2 capture to the level over 90%. Further, using lignite Gasifier the carbon monoxide of the order of 20% was produced for recycling to the boiler using short-flame burners, which is close to the theoretical limit of 21.88%. The pilot plant was also used for the feasibility study of installation of CCS plant on a 500 MW thermal power plant as discussed further.

The objective of this pilot project is also to carry out feasibility study, prototype design & development of a 30% CO_2 capture & sequestration unit for installation on a 500 MW coal-fired thermal power plant as per the broad scheme given below (**Figure 3**). The project proposal also provides details of plant modification to be done by plant engineers for steam tapping from turbine extractions, as well as design and consultancy scope, etc. A full-scale plant on a 500 MW Pulverized Coal Fired Unit would require a plant of 510 tonnes/h capacity. This interdisciplinary project is expected to resolve certain frontline issues in CO_2 sequestration such as energy intensive process optimization in terms of cost of generation and development of effective catalyst for methane, hydrogen and biodiesel recovery through Algae route. This

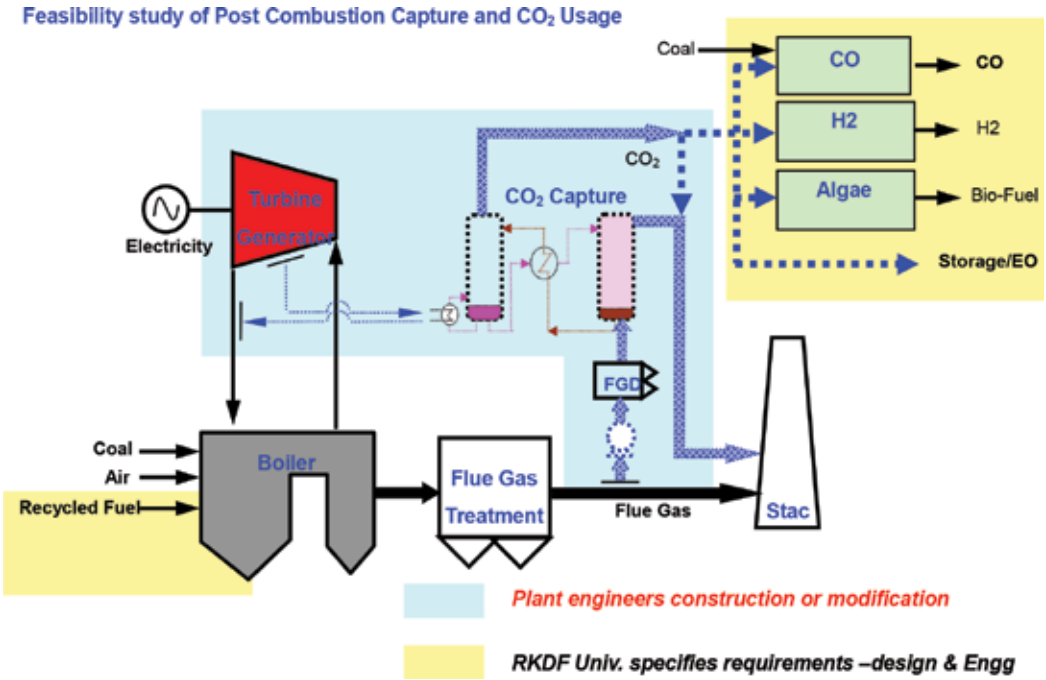

Figure 3. Conceptual diagram of a power project with CCS.

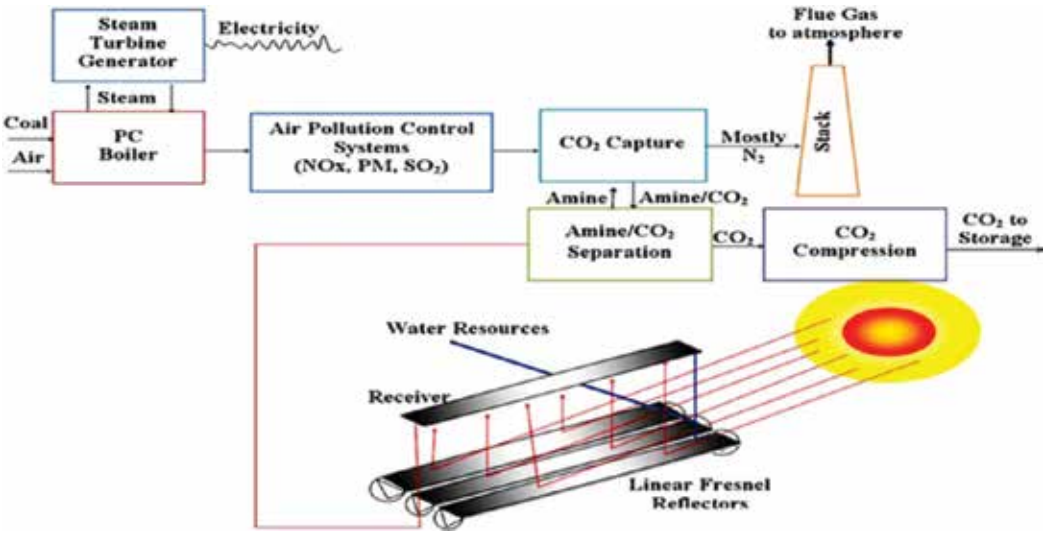

Figure 4. Scheme of implementation of CCS plant through integration with solar thermal.

scheme of retrofitting of existing 500 MW unit with CO_2 capture & recycling of CO is being discussed with power utilities like NTPC, TOSHIBA and BHEL and the broad outline of the same are given at **Figure 3**.

The methodology of implementation of CCS plant on a 500 MW unit is broadly shown in this figure. The scheme also shows steam turbine extractions for providing steam for regeneration of solvent which will cause energy penalty of the order of 15%. The same can be reduced to 4–5% level by combination of solar thermal generated steam coupled with thermal energy storage using a concentrated solar plant (CSP) as shown below in the conceptual **Figure 4**. The incorporation of solar thermal with CCS will pave way for reduction of energy penalty in regeneration of solvents [1, 7].

An amine solvent based plant with 30% CO_2 capture would mean an energy penalty of about 25% including about 15% for sequestration to mineral rocks, gas hydrates and ocean. In any case the energy penalty in our case when we are going for CO_2 conversion to multipurpose fuels the energy penalty still remains at level of 12–15% [1, 7]. The reduction to about 10% has been calculated using MATLAB simulation and shall be verified after establishment of pilot scale CO_2 capture and sequestration plant integrated with Concentrated Solar Power (CSP) for carrying out system optimization studies (**Figure 4**).

3. Solar thermal technology application in post combustion CCS on a thermal power plant

Concentrated Solar Plant (CSP) is presently a matured technology in which several thermal energy storage options are being deployed. Energy storage in form of heat offers a

potential pathway for small (local) and large (utility power plants) scale applications. Thermal storage systems provide a unique opportunity to store energy locally in the form of heat that cannot be transported over long distances. Current thermal storage systems are still in its infancy. The most common ones are large, water-heating storage tanks and molten salt-based systems at solar power plants. These systems have been designed based on the economics of water and salt, the heat capacity of water, and the latent heat of salts. Research on a large host of sensible heat storage and phase-change materials have been conducted over the past two decades. The materials parameters that are relevant for this application are: melting point, boiling point, vapor pressure, density, heat capacity, thermal conductivity, latent heat of fusion and chemical reactivity. While it is intuitive that increasing the temperature of storage could pack in more energy, barriers to the development and deployment of high energy density storage remain, including handling materials at high temperatures, associated systems costs, and operating costs. Thus sensible thermal storage systems are cost prohibitive. Phase change materials (PCM) do provide a viable economical solution for higher energy storage density. However, operation temperatures limit current PCM systems; higher temperatures cause chemical instability and reactivity with containers. Development of affordable high-density thermal storage system will only be possible by utilizing low cost earth abundant thermal storage materials in conjunction with suitable thermally insulating container materials. Current heat storage systems utilize either sensible heat storage (i.e. water in storage tanks) or latent heat storage (i.e. phase-change materials such as molten salts). The relatively low operating temperatures of these systems limit their capacity to store thermal energy; storage systems with higher temperatures would be more economical.

The technologies which hold promise for achieving temperatures in the range of 150–600°C and beyond can be categorized by the phases of matter of the materials used: liquid, gaseous, solid, as under:

- A liquid pathway is considered to look much like today's molten salt two tank tower configuration, but using a suitable high temperature and cost effective HTF/TES.
- Gaseous pathways use an inert gas flowing through a receiver to absorb the solar energy and then transfer the thermal energy to a storage system and/or the turbine working fluid.
- Solid pathways involve solid inert media which absorbs solar radiation and stores that energy as heat. When electric power is needed, the turbine working fluid is heated by the solid media.

In this CCS integrated with CSP project we examined several options of 'Solid Pathway' such as cast iron core of Mount Abu 1 MW solar plant used for steam generation, CL-CSP plant at the State technological University of MP, RGPV, in Central India in which pebbles/rock storage has been proposed for energy storage for heating air in primary cycle and steam in secondary cycle.

In this CSP to CCS integration project, we are developing an affordable high energy density (in excess of 300 kWh/m^3) thermal storage system, that can store heat at temperature around

1000°C [14, 15]. The unique aspects of this system are the selection of an alkali halide salt with high melting temperature and a corrosion resistant cheap ceramic container material. The thermal storage unit will be coupled with a high solar concentrator system (1000–10,000×). As a part of an on-going project at RKDF University in near vicinity of RGPV, funded by MNRE, the project collaborator in Solar thermal, the Rensselaer Polytechnic Institute of USA has developed flux grown crystals of high melting temperature (700–1500°C) mixed alkali halide compounds doped with metallic impurities to enhance thermal conductivity. The trade-off between material density, specific heat capacity, thermal conductivity and cost of raw material has been evaluated to develop a material system that could meet the system's specification at cost of energy storage lower than current electrochemical systems (batteries). In addition, a SiC based composite polymeric coating solution has been developed to avoid corrosion of steel containers used for the thermal storage unit [16]. These materials have been shipped to RKDF University and incorporated into the field unit (test-bed). The test-bed at RKDF comprises of a thermal storage unit, Fresnel lens based solar tracking unit to focus sunlight into the thermal storage media and a steam generation unit (for future electricity generation using a steam turbine). **Figure 5** shows the installation and initial evaluation activities of the solar thermal storage unit at RKDF University.

The expected physical outcomes of the project of CSP integration with CCS as discussed above are in terms of establishment of the pilot plant of CO_2 capture and sequestration on an actual thermal power station for future development of technology of CCS in India and countries between tropic of cancer & capricorn bestowed with high solar DNI [1, 7].

Test results have shown that the innovative halide salt used as thermal storage material stores heat to such an extent that it retains heat for over 5 days to be able to produce steam (**Figure 6**). This innovative halide salt was also tested in the pilot plant shown at **Figure 5**. The biggest challenge in this project is, however, the development of Alkali Halide Salt indigenously for which efforts are under way at RKDF University to procure some of the key components for growing crystals with high energy density, capable of retaining heat. Also efforts are underway towards indigenous development of Heliostats, Fresnel lens and low cost trackers.

Figure 5. Solar thermal storage unit at RKDF University.

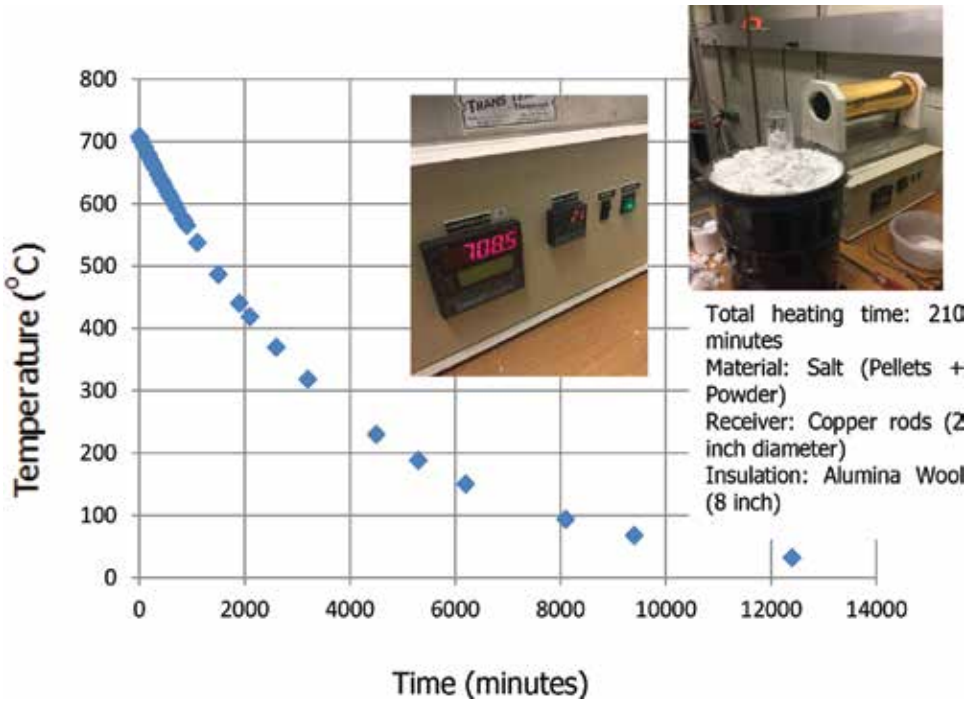

Figure 6. Thermal cooling profile testing of the halide salt at RPI, USA.

4. Conclusion & way forward

Low Carbon Technology Vision for India together with strategies, challenges & opportunities in Green Power for energy security environmental sustainability are put forward in this paper covering Carbon Capture & Sequestration as a key factor. While there is growing trend of carbon dioxide emissions by energy sector since coal continue to play role in primary energy consumption, the urgency of CCS deployment in countries where coal is the main stay is very important. A pilot plant has been developed at RGPV University, for capture of CO_2 and converting the same into useful fuel like hydrogen for fuel cell application, methane for multiple applications and bio-diesel production through algae route. MATLAB simulations have shown that the recycling of CO back to the boiler will provide heat gain up to theoretical limit of 21.88%. Further, the energy penalty in regeneration of solvent using steam produced by solar thermal plant with an innovative Halide salt as thermal energy storage material will reduce by about 10%.

Climate change has already been experienced in many parts of the world therefore state policies need to support practices that successfully keep carbon in the ground, prevent deforestation, support agricultural practice that sequesters carbon and promote sustainable land use practices that reduce emissions. Policies should push especially the more prosperous communities towards less carbon intensive lifestyles, either through taxes or incentives or both. In

addition, the path to zero-emissions must be progressive and in line with the progress of new and renewable technologies of hydro, solar and wind. The first step towards in this progressive path should be CCS.

Indigenous development of critical components of solar thermal plants for integration with CCS is nevertheless important. The following is a list of identified components that will be necessary to be developed within India at ultra-low cost by technology licensing and manufacturing technology transfer approaches by commercial entities (from abroad) to translate the existing technology for large scale adoption:

1. Large area high optical quality Fresnel lens/Heliostats/Fresnel Reflectors manufacturing with low cost.
2. High thermal storage density material development for 24 × 7 heat storage.
3. Corrosion resistance nano-coating process.
4. Ultra-low cost solar trackers.
5. Energy efficient, low maintenance cost thermal transport systems for heat exchange.

Author details

Vinod Krishna Sethi[1]* and Partha S. Dutta[2]

*Address all correspondence to: vksethi1949@gmail.com

1 RKDF University, Bhopal, India

2 Smart Lighting Engineering Research Centre RPI, NY, USA

References

[1] Sethi VK, Vyas S. An innovative approach for carbon capture & sequestration on a thermal power plant through conversion to multi-purpose fuels—A feasibility study in Indian context. Energy Procedia. 2017;**114**:1288-1296

[2] Rao Anand B, Piyush K. Cost implication of carbon capture and storage for coal power plants in India. Energy Procedia. 2014;**54**:431-438

[3] Yang A, Cui Y. Global coal risk assessment–data analysis and market research—A working paper. World Resources Institute. 2012. http://www.wri.org/publication/global-coal-risk-assessment

[4] Monthly All India Generation capacity Report. India: Central Electricity Authority, CEA; 2013. Available from: http://www.cea.nic.in/reports/monthly/executive_rep/dec13.pdf

[5] Bhandari A, Sarin N, Chadha DK. Saline aquifer: Attractive and cost effective sustainable options for carbon dioxide storage– Indian perspective. In: Souvenir & Abstract Volume, International Workshop on R&D Challenges in Carbon Capture and Storage Technology for Sustainable Energy Future. 2007. p. 26

[6] Sethi VK, Vyas S, Jain P, Gour A. A novel approach for CO_2 sequestration and conversion in to useful multipurpose fuel. Journal of Environmental Research and Development. 2011;**5**:732-736

[7] Sethi VK. Low carbon technologies (LCT) and Carbon Capture & Sequestration (CCS)—Key to green power mission for energy security and environmental sustainability, chapter 3, Carbon Utilization. Springer Nature; 2017

[8] Benson SM, Bennaceur K, Cook P. Carbon Capture and Storage in the Report, Global Energy Assessment—Towards a Sustainable Future. Cambridge UK and New York, NY, USA, and the International Institute for Applied Systems Analysis, Luxemburg, Austria. GEA: Cambridge University Press; 2012. Chapter 13. pp. 993-1068

[9] Singh AJ, Mendhe VA, Garg A. CO_2 sequestration potential of geologic formations in India. In: Proceedings of the 8th International Conference on Greenhouse Gas Control Technologies. Trondheim, Norway: Elsevier; 2006. pp. 19-22

[10] Kumar B, Charan SN, Menon R, Panicker SK. Geological CO_2 sequestration in the basalt formations of western India: A feasibility study. In: International Work Shop on R&D Challenges in Carbon Capture and Storage Technologies for Sustainable Energy Future. Hyderabad, India: NGRI; 2007

[11] Vyas S, Sethi VK, Chouhan JS, Sood A. Prospects of integrated collaborative technology of carbon dioxide capture. In: 32nd National Convention of Environmental Engineers: Challenges in Environment Management of Growing Urbanization, IEI 2016

[12] Vyas S, Chouhan JS, Sethi VK. Baseline creation for carbon dioxide capture and sequestration plant using monoethanolamine absorbent. International Journal of Current Engineering and Technology. 2016;**6**:969-972

[13] Vyas S, Sethi VK, Chouhan JS. Process flow and analysis of CCS plant installed at RGPV Bhopal. International Journal of Mechanical Engineering and Technology. 2016;**7**:387-395

[14] Dutta PS. Method and apparatus for growth of multi-component single crystals. US 7641733 (2010)

[15] Dutta PS. Apparatus for growth of single crystals including a solute feeder. US 8940095 (2015)

[16] Dutta PS. III-V ternary bulk substrate growth technology: A review. Journal of Crystal Growth. 2005;**275**:106-112

Chapter 7

Chemical Absorption by Aqueous Solution of Ammonia

Gianluca Valenti and Davide Bonalumi

Additional information is available at the end of the chapter

http://dx.doi.org/10.5772/intechopen.78545

Abstract

Carbon capture is proposed as a viable way of exploiting the fossil resources for power plants and industrial processes. The post-combustion capture by chemical absorption in amine aqueous solutions has been in use in chemical and petrochemical areas for decades. As an alternative, the absorption in aqueous ammonia has received great attention recently. The carbon capture by aqueous ammonia is based on the conventional absorption-regeneration scheme applied to the ternary system CO_2–NH_3–H_2O. It can be implemented in a chilled and a cooled process, depending upon the temperatures in the absorber and, hence, the precipitation of salts. The process simulation can be conducted in two manners: the equilibrium and the rate-based approaches. The specific heat duty is as low as 3.0, for the cooled process, and 2.2 MJ/kg_{CO2}, for the chilled one. Moreover, the index *SPECCA* is as low as 2.6, for the cooled, and 2.9 MJ/kg_{CO2}, for the chilled one. The overall energy performances from the simulations in the rate-based approach, compared against those in the equilibrium approach, result only slightly penalized. From an economic perspective, the carbon capture via chemical absorption by aqueous ammonia is a feasible retrofitting solution, yielding a cost of electricity of 82.4 €/MWh_e and of avoided CO_2 of 38.6 €/t_{CO2} for the chilled process.

Keywords: carbon capture, post-combustion capture, chemical absorption, aqueous ammonia, salt precipitation, ammonia slip

1. Introduction

The ongoing scientific debate does not focus on whether fossil fuels will have to meet a major portion of the short- and the mid-future energy demand, but rather on how they will be exploited most effectively in terms of primary energy use, environmental impact, and

end-user cost. Meanwhile, renewable sources are expected to be implemented more and more diffusely to allow independence from fossils in a later future.

Carbon capture is proposed as a viable way of effectively exploiting the conventional resources. It can be implemented in a pre-combustion, a post-combustion, or even an oxy-combustion configuration. Among them, the post-combustion option has the large benefit of being readily applicable to the already existing power plants as well as industrial processes that are fueled by coal and natural gas.

The post-combustion carbon capture can be accomplished by adsorption on solid materials or by chemical absorption in liquid solutions. The chemical absorption in amine aqueous solutions has been in use for decades in a number of chemical and petrochemical areas, such as the Oil & Gas or the urea preparation. Currently, the so-called advanced amines are under research with the goal of reducing the energy demand when applied to power plants and industrial processes. As an alternative to amines, the chemical absorption in ammonia aqueous solution has received great attention during the last decade.

This chapter covers the chemical absorption of carbon dioxide by an aqueous solution of ammonia. The next sections will present, in sequence, an overview of a number of works retrieved from the open literature, the simulation by either an equilibrium- or a rate-based approach, the environmental as well as economic assessments and, lastly, the future developments of the process itself.

2. Bibliographic review

The possibility of obtaining carbon dioxide from gas mixtures attracts the attention of inventors and investigators toward the end of the nineteenth century, as narrated by Wellford Martin and Killeffer [1]. In 1937, the two authors turn to be among the first ones to recognize the possibility of producing CO_2 from the flue gases of power plants.

In the first decades of the twentieth century, the process employing aqueous ammonia for the removal of CO_2 and H_2S is used extensively for the purification of coke-oven gas. Carbon dioxide is indeed a major component that must be removed to greatly increase the heating value of that gas. During the following years, amines, specifically alkanolamines, become preferred over ammonia for few reasons [2]. First, the use of amines leads to lower issues of pipe plugging and air polluting. Second, amines are characterized by higher effectiveness in capture H_2S, which can be used as an affordable source of elemental sulfur. Ultimately, ammonia is still an expensive substance because the industrial ammonia production is still to be established. Historically, the first alkanolamine to become commercially viable is triethanolamine (TEA) in the year 1930.

Through the last few decades, the amines that reach commercial maturity for gas purification are monoethanolamine (MEA), diethanolamine (DEA), and methyldiethanol-amine (MDEA). In particular, MEA is taken frequently as the reference process for the carbon capture in

post-combustion configuration. By contrast, the aqueous ammonia is reconsidered explicitly for carbon capture only quite recently by both research centers and industrial companies.

The following sections provide an overview of the information about the general absorption-regeneration scheme, the chemistry of solution, the thermodynamic equilibrium models, the kinetics investigations, and the aqueous ammonia process for carbon capture.

2.1. General absorption-regeneration scheme

The carbon capture by aqueous ammonia as well as aqueous amines is based on the conventional absorption-regeneration scheme, which is illustrated in **Figure 1**. In simple words, the gas to be treated flows upward through the absorber, countercurrent to the falling absorbing solution, and purified from CO_2. The generated rich solution from the bottom of the absorber is heated in a heat exchanger, recovering energy from the lean solution (see subsequent text), and enters the regenerator at a point near to its top. In the regenerator, a heat source (such as steam) releases the captured CO_2, which exits from the top of the column, while the generated lean solution from the bottom. The lean solutions flow, through the mentioned heat exchanger, to the top of the absorber closing the scheme. An exhaustive description of the absorption-regeneration scheme is provided by Kohl and Nielsen [3].

2.2. Chemistry of the solution

The carbon capture by aqueous ammonia is based on the ternary system CO_2–NH_3–H_2O, which yields an electrolyte solution. At the absorber conditions, the main reactions are [4] as follows:

$$2\,H_2O \leftrightarrows H_3O^+ + OH^- \tag{1}$$

$$CO_2 + 2\,H_2O \leftrightarrows H_3O^+ + HCO_3^- \tag{2}$$

$$HCO_3^- + H_2O \leftrightarrows CO_3^{2-} + H_3O^+ \tag{3}$$

$$NH_{3(aq)} + H_2O_{(l)} \leftrightarrows NH_4^+ + OH^- \tag{4}$$

$$NH_{3(aq)} + HCO_3^- \leftrightarrows NH_2COO^- + H_2O_{(l)} \tag{5}$$

$$NH_4^+ + HCO_3^- \leftrightarrows NH_4HCO_{3(s)} \tag{6}$$

The ternary system is explored by Burrows and Lewis as early as 1912 [5]. In a more recent work, 1982, Pawlikowski et al. [6] investigate vapor-liquid equilibria of many systems, including CO_2–NH_3–H_2O, by way of the gas-liquid chromatography for temperatures ranging from

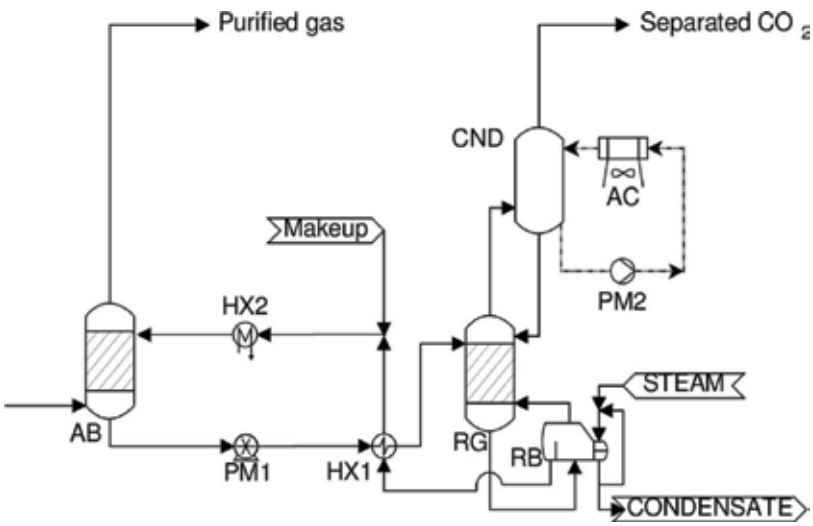

Figure 1. Process flow diagram of the absorbtion-regeneration scheme for ammonia and amines [3].

100 to 150°C. Kawazuishi and Prausnitz [7] provide measurements from previous works by other scientists with the scope of calibrating the expressions of dissociation equilibrium constants and Henry's constants for temperatures in the 100–205°C interval and for total liquid-phase concentrations to 10 molal. Göppert and Maurer [8] report vapor-liquid equilibrium data between 333.15 and 393.15 K at pressures up to about 7 MPa for water-rich mixtures and concentrations to about 16 molal for ammonia and 13 molal for carbon dioxide. In 1992, Pelkie et al. [9] use conductivity measurements to estimate the ammonium ion, $NH4^{+}$, concentration at a temperature of 25°C and over a wide span of pressures and concentrations. The vapor-liquid-solid equilibrium is considered in the work by Kurz et al. [10], which focuses on the solubility of weak electrolyte gases into the aqueous phase in the temperature range from 313 to 353 K at pressures up to 0.7 MPa. In a subsequent study, the enthalpy changes upon partial evaporation of aqueous solutions, including CO_2–NH_3–H_2O, are reported by Rumpf et al. [11] at temperatures from 313 to 393 K. Finally, speciation is measured with 13C NMR by Holmes et al. [12] at 25 and 35°C and by Mani et al. [4] at room temperature.

2.3. Thermodynamic equilibrium models

As indicated, the ternary system is an electrolyte solution. The thermodynamic model for such a complex system shall account for the electric interactions among the species, including strong and weak forces. The strong forces are described by long-range terms that represent electrostatic interactions between ions. The weak forces instead by short-range terms that represent the ion dipole interactions and the non-electrostatic interactions.

Two common equilibrium descriptions are the Electrolyte Non-Random Two Liquid (e-NRTL) model [13] and the Extended UNIQUAC model [14]. A comparison between them is proposed

by Darde et al. [15]. The most recent improvement of the Extended UNIQUAC model [16] comprises a full set of equilibrium reactions. First, speciation reactions are as follows:

$$NH_{3(aq)} + H^+ \leftrightarrows NH_4^+ \tag{7}$$

$$CO_{2(aq)} + H_2O_{(l)} \leftrightarrows HCO_3^- + H^+ \tag{8}$$

$$HCO_3^- \leftrightarrows CO_3^{2-} + H^+ \tag{9}$$

$$NH_{3(aq)} + HCO_3^- \leftrightarrows NH_2COO^- + H_2O_{(l)} \tag{10}$$

Moreover, three vapor–liquid equilibrium relations are as follows:

$$CO_{2(g)} \leftrightarrows CO_{2(aq)} \tag{11}$$

$$NH_{3(g)} \leftrightarrows NH_{3(aq)} \tag{12}$$

$$H_2O_{(g)} \leftrightarrows H_2O_{(l)} \tag{13}$$

Lastly, the four solid formations are as follows:

$$NH_4^+ + HCO_3^- \leftrightarrows NH_4HCO_{3(s)} \tag{14}$$

$$NH_4^+ + NH_2COO^- \leftrightarrows NH_2COONH_{4(s)} \tag{15}$$

$$2\,NH_4^+ + CO_3^{2-} \leftrightarrows (NH_4)_2CO_3 \cdot H_2O_{(s)} \tag{16}$$

$$2\,NH_4^+ + CO_3^{2-} + 2\,HCO_3^- \leftrightarrows (NH_4)_2CO_3 \cdot 2\,NH_4HCO_{3(s)} \tag{17}$$

Figure 2 illustrates a comparison of the experimental data by Kurz et al. [10], indicated by hollow markers, and the computed values by way of the improved extended UNIQUAC model, indicated by lines. The agreement is generally high.

2.4. Kinetics investigations

There are relatively few investigations on the kinetics for the ternary system NH_3–CO_2–H_2O. Hsu et al. [17] describe the absorption reaction kinetics of amines and ammonia solutions with carbon dioxide in flue gases. The temperature of investigation is 50°C, which is relatively high

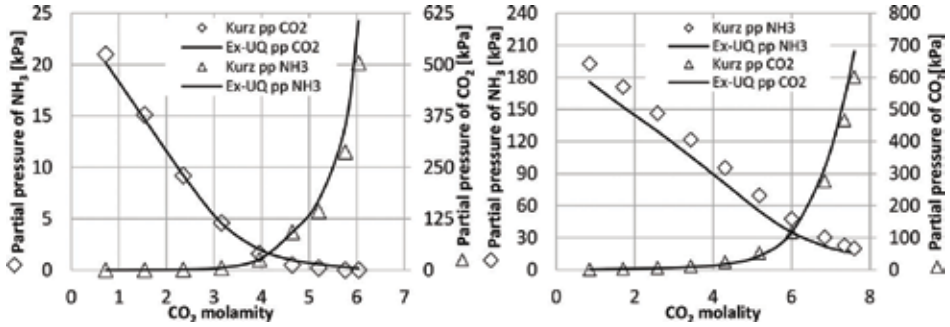

Figure 2. Comparison of the computed values via the Extended UNIQUAC model [16] (indicated by Ex-UQ) of the partial pressure of CO_2 and NH_3 against the experimental data by Kurz et al. [10]. Left: at 313 K and 6.3 molal of NH_3. Right: at 353 K and 11.8 molal of NH_3.

for the carbon capture process. Similarly, Diao et al. [18] investigate the removal efficiency of the sole ammonia solution in the 25–55°C interval and regress the parameters of the rate constant for the capture reaction in the Arrhenius form.

Among the reactions that describe the system, only a subset is expected to significantly influence the kinetics of the overall process. These kinetics-affecting reactions are as follows:

$$CO_2 + OH^- \rightarrow HCO_3^- \tag{18}$$

$$HCO_3^- \rightarrow CO_2 + OH^- \tag{19}$$

$$NH_3 + CO_2 \rightarrow NH_2COO^- + H^+ \tag{20}$$

$$NH_2COO^- + H^+ \rightarrow NH_3 + CO_2 \tag{21}$$

Among them, reactions (R18) and (R20) are considered to be the slowest. The first is studied by Pinsent et al. [19], while the second by five different works as discussed subsequently.

Reaction (R18) is investigated by Pinsent et al. [19] via the rapid thermal method in the range 0–40°C. The fitting yields the Arrhenius constant with a second order as follows:

$$\frac{-d\,CO_2}{dt} = r = k_2 * [CO_2][OH^-] \tag{1}$$

$$k_2 = A * e^{\frac{-E_A}{RT}} \text{ with } A = 4.32 * 10^{13} \frac{kmol}{(m^3 * s)} \text{ and } E_A = 13249 \frac{cal}{mol} \tag{2}$$

Moreover, Pinsent et al. [20] assess reaction (R20) by the rapid thermal method in the range of ammonia concentration between 0.027 and 0.19 mol/l. By contrast, Puxty et al. [21] study it by measuring the rate of CO_2 absorption into a falling thin film using a wetted wall column

for aqueous ammonia between 0.6 and 6 mol/L, temperature between 5 and 20°C, and the initial thin liquid film CO_2 loading between 0 and 0.8 mol_{CO2}/mol_{NH3}. Wang et al. [22] assess the kinetic of reaction (R20) by the stopped flow apparatus in the range of temperature between 15 and 45°C, ammonia concentration between 2.0 and 16 mmol/L, and the initial CO_2 between 3 and 10 mmol/L. Lastly, Jilvero et al. [23] study it by a different perspective. They implement an adsorption column in a commercial code taking the design parameters of an existing pilot plant and they tune the kinetics parameters against the experimental data.

Lillia et al. [24] conduct a comparison of these four investigations and the resulting parameters, reported in **Table 1**, for the Arrhenius equation written as follows:

$$\frac{-d\,NH_3}{dt} = r = k_2 * [NH_3][CO_2] \tag{3}$$

$$k_2 = A * e^{\frac{-E_A}{RT}} \tag{4}$$

Figure 3 visualizes the trends with respect to the (reciprocal of the) temperature and against the experimental data from the investigations. Each Arrhenius law fits the data well for each work. Apparently, though, the data themselves are not in complete agreement. The results from Pinsent et al. and Wang et al. are in mutual agreement, but in disagreement with those by Puxty et al. and Jilvero et al. Noticeably, Pinsent et al. and Wang et al. measured the data at low ammonia concentrations, while Puxty et al. and Jilvero et al. at high concentrations. In short, there is likely a dependence of the kinetic parameters on the ammonia concentration.

Subsequently, Lillia et al. [25] propose an alternative kinetics based on the two-film theory [26] as represented in **Figure 4**. Their study covers the region typical for the absorption columns: temperatures from 15 to 35°C, NH_3 concentrations from 5 to 15%, and CO_2 loadings from 0.2 to 0.6. The study yields an Arrhenius constant with a pre-exponential factor of 1.41×10^8 [mol/(m^3s)] and an activation energy of 60,680 [J/mol]. It has a linear dependence on the CO_2 concentration and a dependence on the NH_3 concentration with an exponent of 1.89.

2.5. Aqueous ammonia process for carbon capture

The concept on what was going to be referred to as the novel ammonia-scrubbing process for the carbon capture is proposed by Bai and Yeh in 1997 based on experimental data [27].

Their work highlights the remarkable potential of high removal efficiencies, over 95%, and absorption capacities, around 0.9 kg of CO_2 per kg of NH_3. Shortly after, Yeh and Bai [28] complete another experimental campaign with the scope of comparing amine and ammonia scrubbing and they confirm the potential of the second over the first solvent. Experiments are conducted at room temperature in their first work and between 10 and 40°C in the later one. In 2005, Yeh et al. [29] publish the results of three-cycle absorption-regeneration tests conducted on MEA and ammonia in a batch reactor maintained at about 25°C. They also reported an approximate estimate of energy usage that is lower than the one for MEA.

Source	Arrhenius parameters of k_2 in Eq. (4)	
	A [kmol/(m³s)]	E_A [cal/mol]
Pinsent et al. [20]	1.35×10^{11}	11,585
Puxty et al. [21]	1.66×10^{14}	14,577
Wang et al. [22]	5.01×10^{11}	12,279
Jilvero et al. [23]	6.51×10^{13}	14,362

Table 1. Arrhenius parameters of the rate of reaction (R20) from different experimental works.

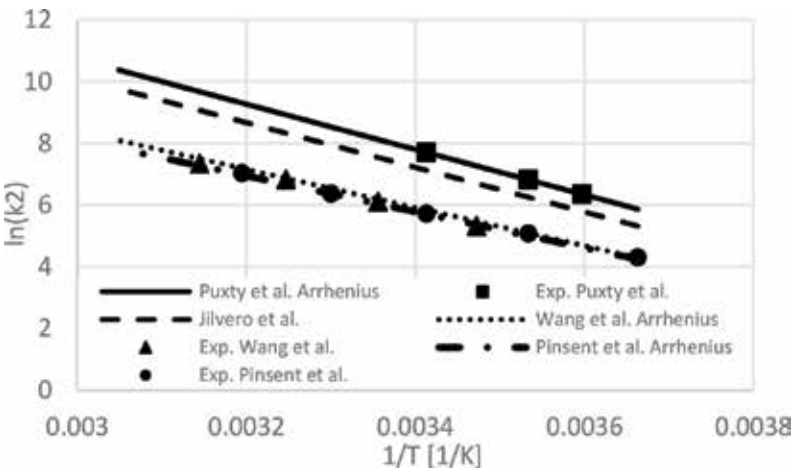

Figure 3. Comparison among values for k2 and experimental data from cited works: Puxty et al. [21], Wang et al. [22], and Pinsent et al. [20]. The dashed lines are obtained fitting the experimental data. The dashed line for Jilvero et al. [23] is the trend proposed by the authors of that work.

In 2006, EIG Inc. [30] applies for a patent on the chemical absorption of the carbon dioxide into aqueous ammonia at chilled conditions. The company Alstom is engaged in its intensive development, establishing the commercial name Chilled Ammonia Process (CAP). As summarized by Lombardo et al. [31], the chilled process is tested first at bench scale with SRI International. Later, it is verified at pilot scale with the Electric Power Research Institute and two utilities: WE energies in its Pleasant Prairie (WI, USA) and E.ON in its Karlshamm (Sweden) plant. Ultimately, the product validation is executed in the facility of the American Electric Power in Columbus (OH, USA) and in the world's largest test facility of the Technology Center of Mongstad (Norway). The process has evolved during the years and it is still under development by the company General Electric, which has acquired it recently [32].

At the same time, the process is investigated by a number of research centers. Ullah et al. [33] analyze the use of a capacitive deionization in the conventional scheme of the ammonia-based process to reduce the regeneration energy requirement, concluding that the reduction can be as much as 37.5%. Sutter et al. [34] propose instead the controlled solid bicarbonate formation to decrease the energy requirement. Precipitation, separation, and dissolution of the solid

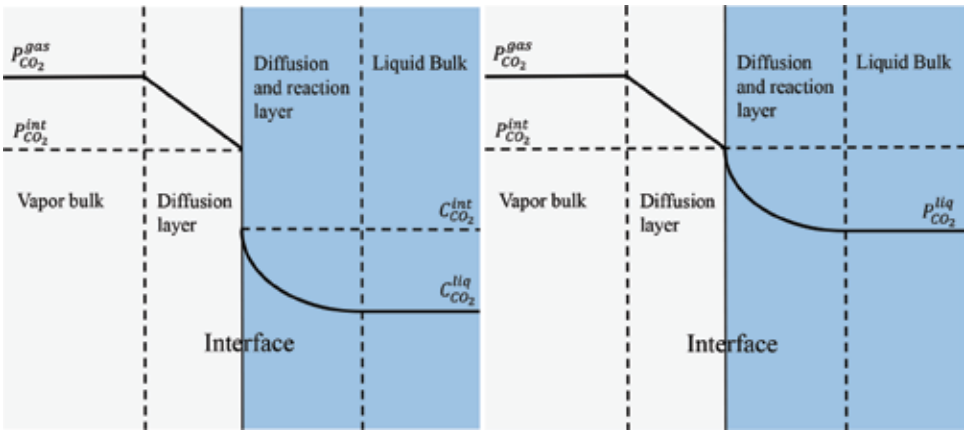

Figure 4. Representation of the two-film theory [26] applied to the ternary system CO_2–NH_3–H_2O. Left: the CO_2 partial pressure profile in the gas and the CO_2 concentration profile in the liquid phase. Right: the CO_2 partial pressure profile in both the gas and liquid phases.

phase are realized in a dedicated process section, while the packed absorption and desorption columns operate free of solids. A similar approach is proposed by Gao et al. [35], pursuing the decreasing energy consumption by the addition of alcohols to reinforce the crystallization.

Bonalumi et al. [36] suggest to operate the process at cool conditions (20–35°C) rather than chilled (5–20°C), to minimize the load on the chillers in favor of the load on air coolers. The two processes are visualized in **Figure 5**. In the cool process, one chilling load is still present

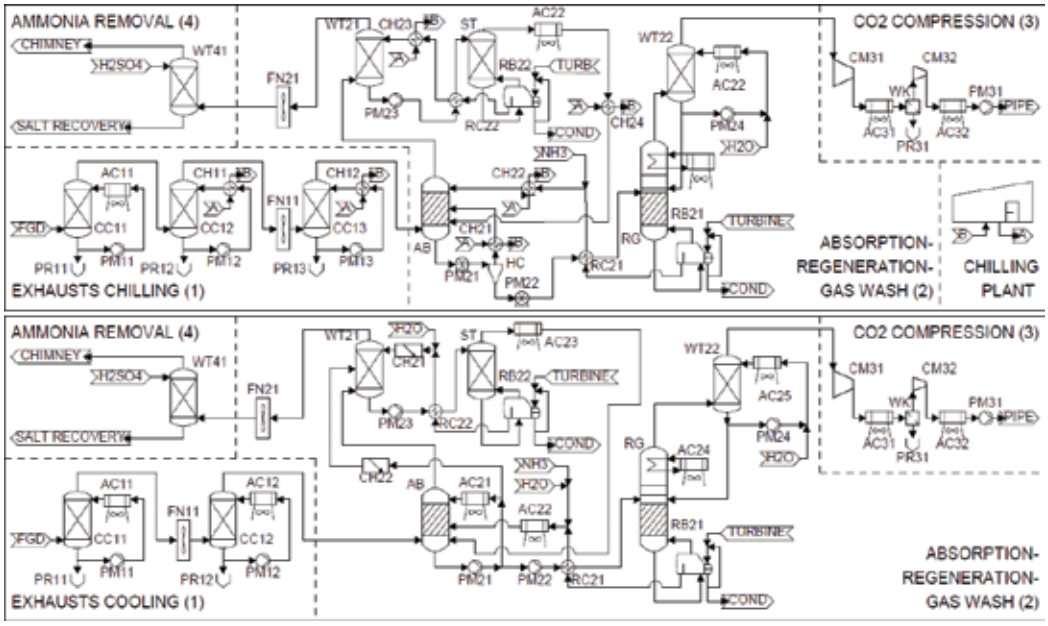

Figure 5. Process flow diagram of the chilled (top) and cooled (bottom) aqueous ammonia process.

for the water wash on top of the absorber. Water wash is required indeed to minimize the tendency of ammonia to escape from the absorber, which is called ammonia slip.

The ammonia-based capture is proposed typically for existing coal- and natural gas-fired power plants. Nonetheless, Bonalumi and Giuffrida [37] consider it for an air-blown integrated gasification combined cycle (IGCC) fired with high-sulfur coal, while Pérez-Calvo et al. [38] for cement plants, both achieving promising indications.

3. Process simulation with the equilibrium approach

In general, the computer simulation of a chemical process can be conducted in two different manners: the equilibrium- and the rate-based approaches, depending on whether the kinetics is not taken or it is taken into consideration, respectively. The results at the equilibrium represent the performance theoretically achievable, while the rate-based the realistic one.

Evaluating the integration of a power plant with the ammonia-based capture using the equilibrium approach, as both chilled and cooled processes, Bonalumi et al. [36] focus on the flue gas from a coal-fired plant, as opposed to a gas-fired. The main difference is the CO_2 concentration, which is in the neighborhood of 15%, on a volume and dry basis, for coal- and of 4% for gas-fired. The reference power plant is the one defined by the European Benchmark Task Force [39] with the scope of establishing a framework for the consistent comparison of capture technologies. The plant has a nominal net electric power output and efficiency of 754 MW_e and 45.5%. The carbon dioxide flow is 160.7 kg_{CO2}/s at a concentration of 15.2%.

In their evaluation, Bonalumi et al. [36] adopt values of the design parameters differentiated between the chilled and the cooled process, as indicated by **Table 2**. Moreover, in the chilled process, the temperature of the streams entering the absorber is 7°C, leading to a maximum temperature in the absorber of around 18°C, despite the reaction of absorption being exothermic, and promoting the salt precipitation in a wide range of concentrations of the reactants. In the cooled process, instead, the temperature of those streams is 20°C, leading to a maximum temperature in the absorber of around 27°C and preventing the solid formation.

Different indexes can be defined to assess the carbon capture performance. First, the carbon capture efficiency is defined as the ratio of the flow rates [kmol/s or kg/s] of the carbon dioxide exiting the compression island and of that entering the exhaust chilling island. As a second

Parameter	Unit	Chilled	Cooled
Ammonia initial concentration	%(mass)	20	7.5
Ammonia-to-carbon dioxide ratio	kmol/kmol	3.2	5
Recycle fraction	—	0.8	0.2
Regeneration pressure	bar	20	5
Regeneration temperature	°C	95.4	105.6

Table 2. Design parameters for the chilled and the cooled aqueous ammonia capture proposed by Bonalumi et al. [36].

common performance index, the specific heat duty [MJ_{th}/kg_{CO2}] is defined as the ratio of the reboiler heat duty [MW_{th}] and the mass flow rate [kg_{CO2}/s] of effectively captured carbon dioxide. However, this second index does not include the information on the capture efficiency (first index) nor on the temperature at which the heat duty is required (or, in equivalent terms, the loss of electric power generation from the steam turbine due to the steam bled for the regenerator).

A third index is adopted to solve this issue about the specific heat duty. Consequently, the new index allows to compare consistently plants characterized by different capture efficiencies, regeneration temperatures, and electric efficiency penalties. The Specific Primary Energy Consumption for Carbon Avoided (*SPECCA*) [MJ_{th}/kg_{CO2}] is defined as

$$SPECCA \stackrel{\text{def}}{=} \frac{HR - HR_{REF}}{E_{REF} - E} \equiv \frac{3600\left(\frac{1}{\eta_e} - \frac{1}{\eta_{e,REF}}\right)}{E_{REF} - E} \tag{5}$$

where all parameters refer to either the power plant equipped with the carbon capture or the reference plant without it: *HR* is the heat rate [MJth/MWh_e], *E* the specific CO_2 emission [kg_{CO2}/MWh_e], η_e [−] the net electric efficiency, and *REF* stays for reference.

Electric power, MW_e	Chilled	Cooled	Electric power, MW_e	Chilled	Cooled
Exhaust cooling (1)					
AC11	2.357	2.351	CH24	0.045	0.000
AC12	0.000	0.132	FN21	3.154	3.342
CH11	4.860	0.000	PM21	1.629	1.410
CH12	1.058	0.000	PM22	2.362	1.121
FN11	3.943	4.177	PM23	<0.001	0.003
PM11	0.597	0.592	PM24	0.010	0.010
PM12	0.201	0.142	Subtotal	*64.380*	*17.219*
PM13	0.102	0.000	Power island		
Subtotal	*13.148*	*7.394*	RB21	45.131	57.207
ABS-RGN-GW (2)			RB22	1.878	15.321
AC21	0.220	0.671	Subtotal	*47.009*	*72.528*
AC22	0.144	4.626	*CO_2 Compression (3)*		
AC23	0.018	1.770	AC31	0.226	0.326
AC24	0.000	0.952	AC32	0.775	0.957
AC25	0.000	0.018	CM31	6.771	15.421
CH21	36.349	2.801	CM32	6.019	14.825
CH22	20.310	0.495	PM31	1.784	0.652
CH23	0.139	0.000	Subtotal	*15.575*	*32.181*
			Total loss	**140.112**	**129.323**

Table 3. Predicted electric consumption of the capture island for the chilled and the cooled aqueous ammonia capture computed by Bonalumi et al. [36].

Parameter	Unit	Reference	MEA	Chilled	Cooled
Electric power loss	MW_e	NA	198.9	140.1	129.3
Net electric power	MW_e	754.0	562.4	613.9	624.7
Net electric efficiency	%	45.5	33.5	37.05	37.70
Specific heat duty	MJ/kg_{CO2}	NA	3.70	2.19	2.98
Specific CO_2 emission	kg_{CO2}/MWh_e	763	104	141.4	138.9
SPECCA	MJ/kg_{CO2}	NA	4.16	2.86	2.58

Table 4. Overall performances of the chilled and the cooled processes compared against a reference power plant (without carbon capture) and a plant integrated with MEA aqueous solution computed by Bonalumi et al. [36].

Regarding the results for the chilled and the cooled process, **Table 3** compares the predicted electric consumptions. The exhaust cooling and the absorption-regeneration sections are more penalizing for the chilled process due to the major consumption of the chillers. By contrast, the power island is more penalizing for the cooled process, on one side, because of a large contribution due to the higher amount of NH_3 that must be recovered by the water wash section. On the other, because of another major contribution due to the higher specific heat duty and the higher regeneration temperature that require more steam bleeding at a higher value of pressure and enthalpy from the turbine. In addition, the compression stage is more penalizing for the cooled process since the regeneration pressure is lower. Hence, from the electric consumption, the chilled process is less penalizing than the cooled one.

In its turn, **Table 4** summarizes the performances for the chilled and the cooled processes and it compares them against those of the reference power plant (without any carbon capture) and a plant integrated with carbon capture in MEA aqueous solution. From the index *SPECCA*, which is as seen the most consistent perspective for evaluating a capture technology, the cooled process is less penalizing than the chilled one, by far, than MEA.

4. Process simulation with the rate-based approach

In a recent work, Bonalumi et al. [40] adopt the rate-based approach to assess the same cooled aqueous ammonia process that they investigated earlier with the equilibrium approach [36]. **Table 5** summarizes the main results from the comparison of the performances predicted by the two approaches. The overall energy balance for the kinetic study, compared against the equilibrium study, turns to be only slightly penalized. The authors explain that this penalization originates from the larger request of energy to achieve a higher level of CO_2 purity in the lean stream from the regenerator. The differences being moderate, though, the study of an absorption capture plant with the equilibrium approach can be considered a valid method for a preliminary assessment of an ammonia-based process.

Parameter	Unit	Cooled equilibrium	Cooled rate based
Electric power loss	MW_e	129.3	136.4
Net electric power	MW_e	624.7	617.6
Net electric efficiency	%	37.70	37.27
Specific heat duty	MJ/kg_{CO2}	2.98	3.02
Specific CO_2 emission	kg_{CO2}/MWh_e	138.9	141.2
SPECCA	MJ/kg_{CO2}	2.58	2.77

Table 5. Performances of the cooled process computed with the equilibrium and the rate-based approaches by Bonalumi et al. [34, 36].

5. Economic and environmental assessments

The integration of the chilled process and an ultra supercritical power plant is analyzed by Valenti et al. [41] via a parametric analysis from the energy and the economic perspectives. The capture island is simulated with an equilibrium approach. In the parametric investigation, five parameters are varied singularly: (1) ammonia initial concentration in the aqueous solution, (2) ammonia-to-carbon dioxide ratio in the absorber, (3) regeneration pressure, (4) regeneration temperature, and (5) absorber chiller evaporation temperature. The economic analysis, with respect to a reference power plant rated at the net electric production of over 750 MW_e, shows that the capital investment of the capture island is estimated to be a relatively small portion of that of the power island. However, due to other costs and due to the performance penalties, the cost of electricity increases significantly by 37.5%, from 59.90 to 82.38 €/MWh_e; ultimately, the resulting cost of avoided CO_2 is approximately 38.64 €/t_{CO2}.

A detailed environmental life cycle analysis for an ultra supercritical power plant with and without carbon capture is proposed by Petrescu et al. [42]. Three capture islands are considered: (1) gas-liquid absorption with MDEA (monodiethanolamine), (2) gas-liquid absorption with aqueous ammonia, and (3) gas-solid absorption with calcium oxide. The environmental evaluation is performed using the "cradle-to-grave" methodology considering several upstream and downstream processes. Eleven environmental impact categories, according to the method CML 2001, are compared using GaBi software. The study highlights that carbon capture technologies decrease the global warming potential indicator, but they may increase other indicators. The amine technology achieves a good performance from the perspective of global warming, but not satisfactory from that of all others. Aqueous ammonia adsorption and calcium looping prove to be better. Some indicators, such as acidification potential, eutrophication potential, or those related to lethal concentrations (e.g., human toxicity potential, freshwater aquatic ecotoxicity potential, and marine aquatic ecotoxicity potential), are better in the case of aqueous ammonia. By contrast, some others, such as abiotic depletion fossil and abiotic depletion elements, are better in the case of calcium looping.

6. Future developments

A highly promising solvent-based CO_2 capture process, named the mixed-salt technology, is being currently developed, as reported by Jayaweera et al. [43]. This technology adds potassium carbonate to the system in order to exploit the advantages of both ammonia-based and potassium carbonate-based technologies. The simplistic representation of the CO_2 absorption and removal reaction is as follows:

$$K_2CO_3 \cdot NH_3 \cdot H_2O \cdot xCO_2 \leftrightarrows K_2CO_3 \cdot NH_3 \cdot H_2O \cdot yCO_2 \tag{6}$$

where the CO_2 loading is the numerical difference between y and x. The left and right side of the equilibrium represent the lean and rich solutions, respectively. Despite the system being characterized by the presence of several ionic species that could form a solid phase, precipitation is avoided by operating the absorber at relatively high temperatures and at concentrations below the solid-forming conditions. The expected advantages are a limited heat duty at the regenerator and a limited load for the water wash on top of the absorber.

7. Conclusions

This chapter covers the chemical absorption of carbon dioxide by an aqueous solution of ammonia for coal- and natural gas-fired power plants and industrial processes. It reports the literature review, the simulation by equilibrium- or rate-based approach, the economic as well as environmental assessments, and the future developments. Conclusions are as follows:

1. The ammonia-based technology confirms to be attractive compared to conventional amines. It can be implemented in a chilled as well as in a cooled process depending upon the temperature and, consequently, the precipitation of salts in the absorber.
2. The predicted specific heat duty, in the equilibrium approach, is 3.0 for the cooled process and 2.2 MJ/kg_{CO2} for the chilled one. Moreover, the index *SPECCA* is 2.6 for the cooled and 2.9 MJ/kg_{CO2} for the chilled. Overall, the cooled process combines the advantage of a moderate energy requirement with the absence of solid formation.
3. The predicted performances in the rate-based approach, compared against those in the equilibrium approach, result slightly penalized. The difference is due to the need of a higher level of CO_2 purity in the lean stream from the regenerator. The index *SPECCA* value changes from 2.6, as seen in the equilibrium, to 2.8 MJ/kg_{CO2}, in the rate-based approach, yielding an increase of the prediction of about 6%. Hence, the study of an absorption capture plant with an equilibrium approach is a valid methodology for a preliminary investigation and optimization process.
4. From an economic perspective, the carbon capture via chemical absorption by aqueous ammonia is a feasible retrofitting solution, yielding a predicted cost of electricity of 82.4 €/MWh_e and a cost of avoided CO_2 of 38.6 €/t_{CO2}, both for the chilled process (those for the cooled process are not reported yet in the open literature).

5. The mixed-salt technology is a promising evolution of the process to further reduce the specific heat duty and the load for the water washing on top of the absorber.

Acknowledgements

The authors gratefully acknowledge Mr. Stefano Lillia of Politecnico di Milano for his help in investigating carbon capture alternatives as well as in reviewing this chapter.

Author details

Gianluca Valenti* and Davide Bonalumi

*Address all correspondence to: gianluca.valenti@polimi.it

Politecnico di Milano, Milano, Italy

References

[1] Wellford Martin J, Killeffer DH. Carbon dioxide from power plant flue gas. Industrial and Engineering Chemistry. 1937;**29**(6):632-636

[2] Kohl AL, Nielsen RB. Chapter 4 – Removal and use of ammonia in gas purification. In: Gas Purification. Houston, Texas, USA: Gulf Professional Publishing; 1997. pp. 278-329

[3] Kohl AL, Nielsen R. Gas Purification. Houston, Texas, USA: Gulf Professional Publishing; 1997

[4] Mani F, Peruzzini M, Stoppioni P. CO_2 absorption by aqueous NH_3 solutions: Speciation of ammonium carbamate, bicarbonate and carbonate by a ^{13}C NMR study. Green Chemistry. 2006;**8**(11):995

[5] Burrows GH, Lewis GN. The equilibrium between ammonium carbonate and ammonium carbamate in aqueous solution at 25°. Journal of the American Chemical Society. 1912;**34**(8):993-995

[6] Pawlikowski EM, Newman J, Prausnitz JM. Phase equilibriums for aqueous solutions of ammonia and carbon dioxide. Industrial and Engineering Chemistry Process Design and Development. 1982;**21**(4):764-770

[7] Kawazuishi K, Prausnitz JM. Correlation of vapor-liquid equilibria for the system ammonia-carbon dioxide-water. Industrial and Engineering Chemistry Research. 1987; **26**(7):1482-1485

[8] Göppert U, Maurer G. Vapor-liquid equilibria in aqueous solutions of ammonia and carbon dioxide at temperatures between 333 and 393 K and pressures up to 7 MPa. Fluid Phase Equilibria. 1988;**41**(1-2):153-185

[9] Pelkie JE, Concannon PJ, Manley DB, Poling BE. Product distributions in the carbon dioxide-ammonia-water system from liquid conductivity measurements. Industrial and Engineering Chemistry Research. 1992;**31**(9):2209-2215

[10] Kurz F, Rumpf B, Maurer G. Vapor-liquid-solid equilibria in the system NH_3–CO_2–H_2O from around 310 to 470 K: New experimental data and modeling. Fluid Phase Equilibria. 1995;**104**:261-275

[11] Rumpf B, Weyrich F, Maurer G. Enthalpy changes upon partial evaporation of aqueous solutions containing ammonia and carbon dioxide. Industrial and Engineering Chemistry Research. 1998;**37**(8):2983-2995

[12] Holmes PE, Naaz M, Poling BE. Ion concentrations in the CO_2–NH_3–H_2O system from ^{13}C NMR spectroscopy. Industrial and Engineering Chemistry Research. 1998; **37**(8):3281-3287

[13] Chen C-C, Britt HI, Boston JF, Evans LB. Two new activity coefficient models for the vapor-liquid equilibrium of electrolyte systems, thermodynamics of aqueous systems with industrial applications. ACS Symposium Series. American Chemical Society, Washington, DC. October 29, 1980;**133**:61-89. DOI: 10.1021/bk-1980-0133.ch004

[14] Thomsen K, Rasmussen P. Modeling of vapor–liquid–solid equilibrium in gas–aqueous electrolyte systems. Chemical Engineering Science. 1999;**54**(12):1787-1802

[15] Darde V, Thomsen K, van Well WJM, Bonalumi D, Valenti G, Macchi E. Comparison of two electrolyte models for the carbon capture with aqueous ammonia. International Journal of Greenhouse Gas Control. 2012;**8**:61-72

[16] Bonalumi D, Giuffrida A. Performance Improvement of Cooled Ammonia-based CO_2 Capture in Combined Cycles with Gasification of High-sulfur Coal. Energy Procedia. 2017;**114**:6440-6447. https://doi.org/10.1016/j.egypro.2017.03.1780

[17] Hsu CH, Chu H, Cho CM. Absorption and reaction kinetics of amines and ammonia solutions with carbon dioxide in flue gas. Journal of the Air & Waste Management Association. 2003;**53**(2):246-252

[18] Diao YF, Zheng XY, He BS, Chen CH, Xu XC. Experimental study on capturing CO_2 greenhouse gas by ammonia scrubbing. Energy Conversion and Management. 2004;**45**(13-14): 2283-2296

[19] Pinsent BRW, Pearson L, Roughton FJW. The kinetics of combination of carbon dioxide with hydroxide ions. Transactions of the Faraday Society. 1956;**52**(1512):1512

[20] Pinsent BRW, Pearson L, Roughton FJW. The kinetics of combination of carbon dioxide with ammonia. Transactions of the Faraday Society. 1956;**52**(2):1594

[21] Puxty G, Rowland R, Attalla M. Comparison of the rate of CO_2 absorption into aqueous ammonia and monoethanolamine. Chemical Engineering Science. 2010;**65**(2):915-922

[22] Wang X et al. Kinetics of the reversible reaction of CO_2(aq) with ammonia in aqueous solution. The Journal of Physical Chemistry. A. 2011;**115**(24):6405-6412

[23] Jilvero H, Normann F, Andersson K, Johnsson F. The rate of CO_2 absorption in ammonia—Implications on absorber design. Industrial and Engineering Chemistry Research. 2014;**53**(16):6750-6758

[24] Lillia S, Bonalumi D, Valenti G. Rate-based approaches for the carbon capture with aqueous ammonia without salt precipitation. Energy Procedia. 2016;**101**:400-407

[25] Lillia S, Bonalumi D, Fosbøl PL, Thomsen K, Valenti G. Experimental study of the aqueous CO_2–NH_3 rate of reaction for temperatures from 15 °C to 35 °C, NH_3 concentrations from 5% to 15% and CO_2 loadings from 0.2 to 0.6. International Journal of Greenhouse Gas Control. 2018;**70**(July 2017):117-127

[26] Lewis WK, Whitman WG. Principles of gas absorption. Industrial and Engineering Chemistry. 1924;**16**(12):1215-1220

[27] Bai H, Yeh AC. Removal of CO_2 greenhouse gas by ammonia scrubbing. Industrial and Engineering Chemistry Research. 1997;**36**(6):2490-2493

[28] Yeh AC, Bai H. Comparison of ammonia and monoethanolamine solvents to reduce CO_2 greenhouse gas emissions. Science of the Total Environment. 1999;**228**(2-3):121-133

[29] Yeh JT, Resnik KP, Rygle K, Pennline HW. Semi-batch absorption and regeneration studies for CO_2 capture by aqueous ammonia. Fuel Processing Technology. 2005;**86**(14-15): 1533-1546

[30] Gal E. Ultra cleaning of combustion gases including the removal of CO_2, Patent number: WO 2006/022885 A1, 2006

[31] Lombardo G, Agarwal R, Askander J. Chilled ammonia process at Technology Center Mongstad—First results. Energy Procedia. 2014;**51**:31-39

[32] Dube SK. System for Generating Low Pressure Carbon Dioxide in a Chilled Ammonia Process. 2016. European Patent Application: EP3075431A1

[33] Ullah A, Saleem MW, Kim W-S. Performance and energy cost evaluation of an integrated NH_3-based CO_2 capture-capacitive deionization process. International Journal of Greenhouse Gas Control. 2017;**66**:85-96

[34] Sutter D, Gazzani M, Mazzotti M. A low-energy chilled ammonia process exploiting controlled solid formation for post-combustion CO_2 capture. Faraday Discussions. 2016; **192**:59-83

[35] Gao J et al. A new technique of carbon capture by ammonia with the reinforced crystallization at low carbonized ratio and initial experimental research. Fuel Processing Technology. 2015;**135**:207-211

[36] Bonalumi D, Valenti G, Lillia S, Fosbøl PL, Thomsen K. A layout for the carbon capture with aqueous ammonia without salt precipitation. Energy Procedia. 2016;**86**:134-143

[37] Bonalumi D, Giuffrida A. Investigations of an air-blown integrated gasification combined cycle fired with high-sulphur coal with post-combustion carbon capture by aqueous ammonia. Energy. 2016;**117**:439-449

[38] Pérez-Calvo J-F, Sutter D, Gazzani M, Mazzotti M. Application of a chilled ammonia-based process for CO_2 capture to cement plants. Energy Procedia. 2017;**114**:6197-6205

[39] Anantharaman R, Bolland O, Booth N, van Dorst E, Ekstrom C, Sanchez Fernandes E, Franco F, Macchi E, Manzolini G, Nikolic D, Pfeffer A, Prins M, Rezvani S, Robinson L. CArbon-free Electricity by SEWGS: Advanced materials, Reactor- and process design. D 4.9 European best practice guidelines for assessment of CO_2 capture technologies. 213206 FP7 - ENERGY.2007.5.1.1, Politecnico di Milano, Alstom UK. 2011

[40] Bonalumi D, Lillia S, Valenti G, Fosbøl PL, Thomsen K. Kinetic study of a layout for the carbon capture with aqueous ammonia without salt precipitation. Energy Procedia. 2017;**114**(November 2016):1352-1359

[41] Valenti G, Bonalumi D, Macchi E. A parametric investigation of the chilled ammonia process from energy and economic perspectives. Fuel. 2012;**101**:74-83

[42] Petrescu L, Bonalumi D, Valenti G, Cormos A-M, Cormos C-C. Life cycle assessment for supercritical pulverized coal power plants with post-combustion carbon capture and storage. Journal of Cleaner Production. 2017;**157**:10-21

[43] Jayaweera I et al. Results from process modeling of the mixed-salt technology for CO_2 capture from post-combustion-related applications. Energy Procedia. 2017;**114**:771-780

Section 2

Monitoring and Tracking of CO2 Migration

Chapter 8

Geophysical Monitoring of CO_2 Injection at Citronelle Field, Alabama

Shen-En Chen and Yangguang Liu

Additional information is available at the end of the chapter

http://dx.doi.org/10.5772/intechopen.78386

Abstract

Carbon dioxide (CO_2) injection at the Citronelle oil field in Alabama has been deployed to determine the feasibility of carbon storage and enhanced oil recovery (EOR) in the depleted oil field. Citronelle is a small size city right above the oil field, hence, to detect geohazard risks, geophysical testing method using wireless sensor, and passive seismic technique is used: the non-intrusive measurements were made at well sites along two linear arrays. The outcomes of the geophysical monitoring at the Citronelle oil field are shear-wave velocity profiles that are correlated to the static stress distribution at different injection stages. Injection history interpretation using the stress wave monitoring indicates that CO_2 injection resulted in the stressing of the strata.

Keywords: geophysical testing, Citronelle oil field, CO_2-EOR, carbon sequestration, strata stressing

1. Introduction

Carbon dioxide (CO_2) is a greenhouse gas, and the relationship between global warming and greenhouse gases has become more and more of a concern to the scientific community [1–3]. Because there is continual rise in what is already a high concentration of CO_2 in the atmosphere, it is imperative that a viable solution be implemented. Carbon capture and geologic storage is a promising method for reducing the concentration of CO_2 in the Earth's atmosphere [4–7]. The technology involves collecting CO_2 from an emission heavy source, compressing and transporting the CO_2 to a qualified site and injecting the now supercritical CO_2 at high-pressure into the reservoir. The qualified storage reservoir must satisfy stringent geological storage criteria, which may include anticline, porosity, permeability, void volume, pressure

limits, seepage characteristics, and cap rock characteristics. The reservoir should be sufficiently distanced from any potable groundwater acquifers to avoid contamination issues. Using underground depleted oil and gas reservoirs as CO_2 storage sites may have secondary advantages of enhanced oil recovery (EOR) or enhanced gas recovery (EGR) [8–10]. The additional fossil resources recovery can provide the economic incentives for CO_2 storage. Currently, there are several hundreds of oil field injection sites worldwide and in the US [11, 12].

While no CO_2 leakage has been reported at any injection sites, it is important to instate careful monitoring programs for such practices to avoid potential geohazards. Recent studies of remote sensing data indicate that some of the injection sites may have experienced surface deformation [13–15]. Effective monitoring programs should be adopted at the injection sites in order to detect changes in geological formation (geomorphology) and the presence and migration of CO_2 within the storage reservoir [16–19].

Since 2010, CO_2 has been injected for possible CO_2-EOR at a highly heterogeneous and discontinuous sandstone reservoir of the Citronelle oil field, Alabama. Citronelle oil field is a matured oil reservoir and an ideal site for CO_2-EOR and sequestration, from both reservoir engineering and geological perspectives [20, 21]. The Citronelle oil field is located about 50 km north of Mobile on the crest of the Citronelle Dome, which is a giant salt-cored anticline in the eastern

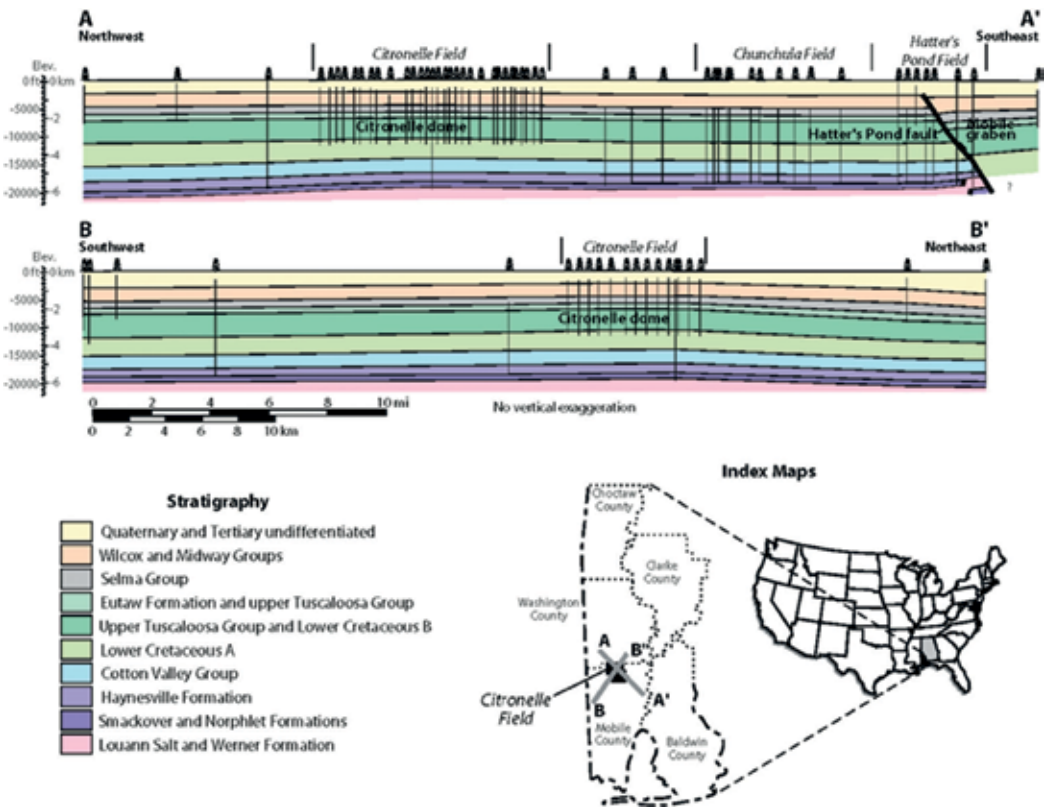

Figure 1. Structural cross sections showing Citronelle dome and location of Citronelle field.

http://dx.doi.org/10.5772/intechopen.78386

Figure 2. Typical locations of the oil wells at Citronelle, Alabama.

Mississippi Interior Salt Basin (**Figure 1**). The field covers an area of 16,400 acres directly below the city of Citronelle. In 1955, oil was first discovered by the Gulf Oil Company in the Zack Brooks Drilling Company No. 1 Donovan well. Since then, over 500 wells have been drilled and cumulative oil production has exceeded 169 million barrels at Citronelle Field.

Citronelle is a small city with a population of 3900 (2010 consensus). With most of the oil wells integrated into the cityscape, possible geohazards such as CO_2 leaks can be detrimental to the local citizens, live stocks, and the environment. Some of the wells exist within residents' backyards and farmlands (**Figure 2**). To detect risks of geohazards and monitor the injection process, geophysical testing has been performed at the site. This paper reports the outcomes of the field tests due to CO_2 injection into the Unit B-19-10 #2 well (Permit No. 3232). The goal of the geophysical testing is to establish possible relationships between shear-wave velocity profiles and the static stress distribution before, during and after the injection. Such relationships are helpful in understanding the site condition changes due to the injection activity.

2. Geophysical monitoring strategies

The intent of the carbon injection is to explore the feasibility of EOR in the tertiary production of an existing oil reservoir, as well as the potential of subsequent CO_2 sequestration. The geophysical monitoring strategy is used to assess the site geostability and potential geohazards. Site geostability for mineral extractions can be associated either with the site geological conditions pertaining to sustained production or with the large geological deformations such

as land subsidence or landslides. In the context of the current study, the association is with the latter definition. The key purpose of a geostability analysis is to determine the possibilities of significant geohazards due to formation instabilities, which may result from the CO_2-oil replacement in the Rodessa formation.

Geo-instability of an oil-producing stratum can result from the collapse of voids during the oil extraction process. The repercussions may include global subsidence, localized straining and possible microtremors to earthquakes. **Figure 3** shows a schematic of the geomaterial straining at an oil extraction well. The hypothesis is that as oil is being depleted, the surrounding geomedium may experience straining due to interfacial shear stresses resulting from the settlement and collapse of the strata. Geostability in a narrow oil field within a deep stratum, such as the Citronelle oil field, is typically not a major concern since relatively small settlement is anticipated. The geo-instability concerns in such cases can be generalized as compressibility potential assessment as well as localized stability projection.

The compression or settlement issue may involve both local elastic settlement (non-permanent deformation) and long-term creep (long-term deformation due to sustained loading). Elastic settlement is instantaneous and is a function of the weight of overburden above the layer of interest. For an oil-producing layer, elastic settlement is also a function of the system pressurization, where pressure is kept to ensure the injection fluids remain in the oil layer. Creep is difficult to assess since it is a function of time. Current geostability analysis does not include considerations of thermoelastic effects or micro-poroelastic effects for the pressurized system, for example, the Biot's equations. The rationale is that the difficulties in establishing geomaterial properties based on current geophysical measurements and assumed values only allow a grossly simplified bulk material analysis. As a result, the extensive works by Biot on poroelasticity has been greatly simplified.

Stresses in geomaterials are derived essentially from the self-weight of the overburden materials (predominantly the geo-matrix), the liquid within the voids (pore water pressure), and

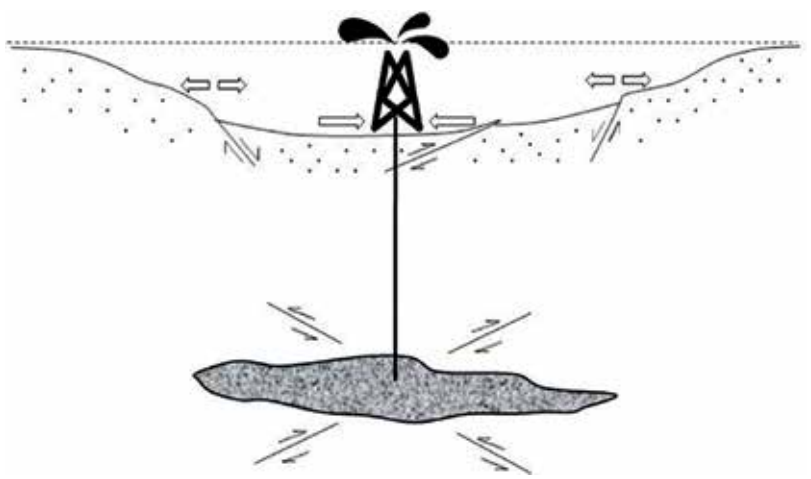

Figure 3. Poroelastic stresses due to extensive oil extraction (hollow arrows indicate surface strains and line arrows indicate interplanar shear stresses).

http://dx.doi.org/10.5772/intechopen.78386

the externally induced pressures. Hence, the total stress within the geomaterial system is equal to the summation of stress within geo-matrix and pore water pressure. The geostability study considers the effective stress, σ′, which is defined as the stress carried by geomaterial skeletons and not pore water that causes elastic deformation of the oil-producing layer:

$$\sigma^{'} = \sigma - \mu \tag{1}$$

where σ is the vertical total stress derived from unit weight of material and μ is the pore pressure. Neglecting thermal effects, the effective stress equation is further modified to include injection pressure $\sigma_{injection}$:

$$\sigma'' = \sigma' - (\sigma_{injection} - \mu) \tag{2}$$

The effective stress pressure is then used to compute the producing layer elastic deformation (non-permanent settlement) using simplified computation of rock bulk modulus (P-wave modulus), M [22]:

$$M = \rho V_p^2 \tag{3}$$

where ρ is the rock density, V_p is the P-wave velocity derived from geophysical testing conducted at Citronelle.

2.1. Geophysical testing at Citronelle field

Micro-seismicity tests have been successfully applied to address specific issues in the oil and gas industry [23, 24]. The basic principle of passive seismic monitoring is to detect small movements (regarded as microseismic events) from unknown seismic sources that can be recorded on geophones placed on site. Contrast to active geophysical testing, the passive seismic monitoring is a testing method that does not rely on a source of ground excitation. The main advantage of the passive monitoring is that it can be carried out at any time and does not require regulated field access. The disadvantage of passive sensing is the uncertainty introduced due to the lack of controlled input energy, which can result in both poor data sensitivity and poor detection accuracy.

A modified passive sensing Refractive Microtremor (ReMi) technique, Derivative of ReMi (DoReMi), as discussed below, is used at the Citronelle oil field, Alabama [25]. To improve mobility and avoid the cumbersome wiring, wireless triaxial micro-electro-mechanical system (MEMS) accelerometers have been used for the field testing. The MEMS sensors are encased in hard metal boxes and buried into the ground at sufficient depth to ensure good coupling between the sensor and the surrounding soil (at least 1 ft. (0.3 m) deep with fully compacted soil on top). The wireless sensor unit with the three directional acquisition channels can record seismic energy in three Cartesian directions (vertical and two horizontal directions). The vibration signals obtained by the wireless accelerometer are acceleration time histories, which are processed in spectral domain using p-τ transformation, or slant-stack analysis [26].

Since passive sensing assumes the signals are random in nature and the analysis is done in the spectral domain, time sequence of the sampled data is not considered. Only the vertical direction has been used in the wave motion analysis for this study.

To monitor the responses of the reservoir throughout the CO_2 injection process, two linear test arrays were conducted at the Citronelle oil field. Each test array consists of 24 measurement points, which are all located near the oil wells. The site test layout is shown in **Figure 4**. The Line 1 is generally aligning with the north to south direction, whereas, Line 2 is in general in the northeast to southwest direction. Line 1 covered approximately a distance of 30,102 ft. (9175 m) in total with approximately 1309 ft. (399 m) for sensor spacing. Line 2 is 25,603 ft. (7804 m) in total span and has a sensor spacing of 1113 ft. (339 m) between pickup points. CO_2 is injected in well No. B-19-10 #2, which is located near the intersection of the two survey lines and is in the top north end of the Citronelle oil field. The sensors were buried at each measurement point, and the recording duration for each set was set at 39.06 s. The sampling frequency was set at 512 Hz.

Background measurement was deployed prior to the start of CO_2 injection in the field. It should be noted that in order to restore the pressure in the well to the level suitable for production, water injection at the well has been conducted since 2007. CO_2 injection in well No. B-19-10 #2 started in December 2009 and at the rate of 46.5 tons/day. The CO_2 injection was stopped from December 30, 2009 to January 26, 2010, due to the triplex pump not being able to maintain the injection pressure. After a thorough problem detection process, the pumping was resumed and, as a result, the average injection rate of CO_2 was stabilized at 31.5 tons/day. The CO_2 injection history in short tons until late September 2010 is presented in **Figure 5**. Final amount of CO_2 injected in the pilot well is about 8036 short tons. The record of well head pressure at Well

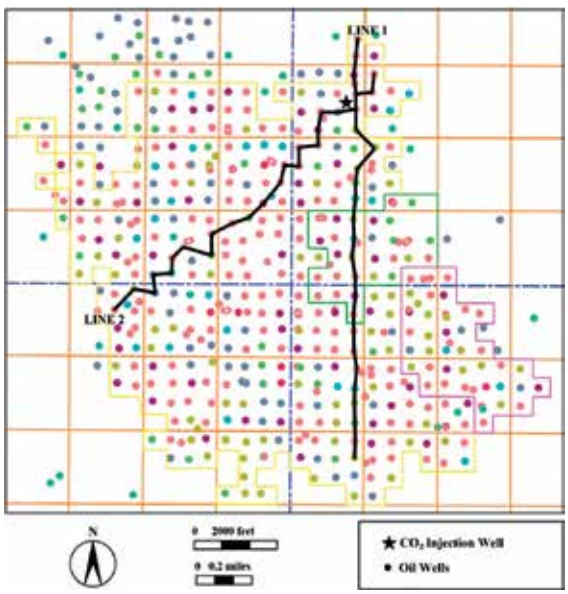

Figure 4. The testing lines at the Citronelle oil field.

http://dx.doi.org/10.5772/intechopen.78386

B-19-10 #2 from the beginning of CO_2 injection to the end of the injection is shown in **Figure 6**. The pressure has been normalized in order to compare it with the normalized stresses at the oil-bearing layer quantified based on the geophysical testing results to be presented later.

In the first month of CO_2 injection, the well head pressure changed from 2400 psig (16,547.4 kPA) to 3800 psig (26,200.1 kPA). After CO_2 injection was resumed on January 27, 2010, the range of well head is between 3800 psig (26,200.1 kPA) and 4200 psig (28,957.9 kPA). Passive tests were conducted at the Citronelle oil field in December 2009 when the start of significant CO_2 injection,

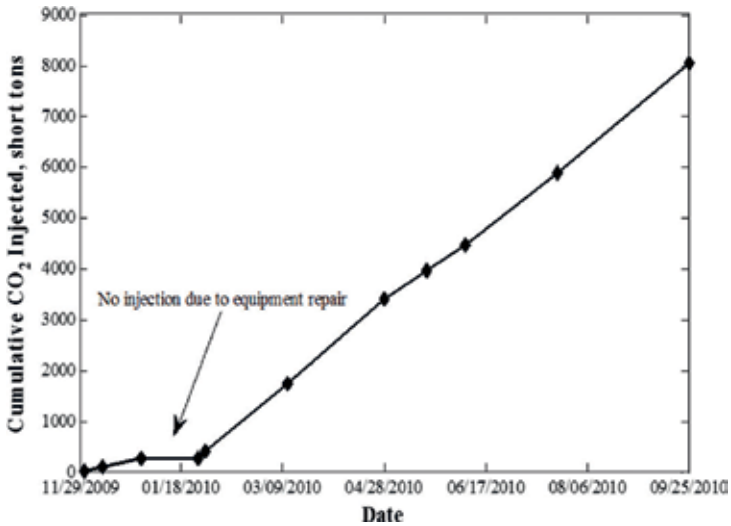

Figure 5. Record of CO_2 injection during Phase II at Well B-19-10#2.

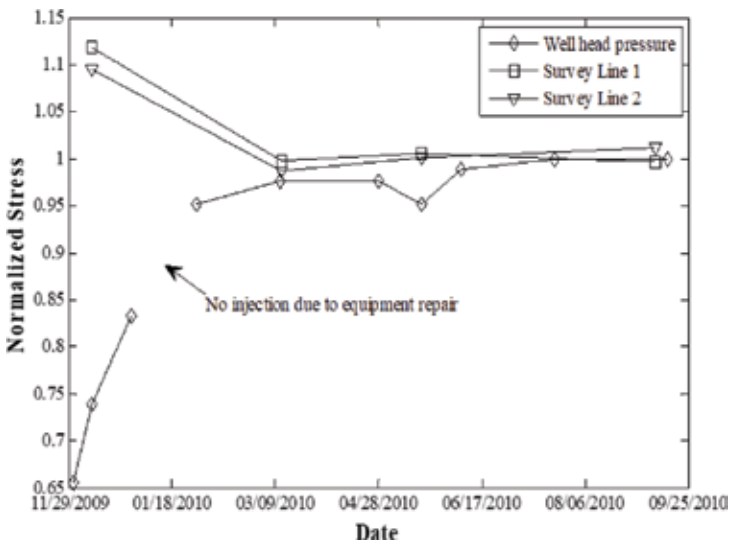

Figure 6. Normalized well head pressure at Well B-19-10#2 during CO_2 injection with geophysical test data.

and during steady CO_2 injection in March 2010, May 2010, and September 2010, respectively. Water injection was switched back immediately after CO_2 injection was completed. In addition, measurements were made after CO_2 injection in November 2010, March 2011, and May 2011, respectively. A summary of the monitoring history at the Citronelle oil field is shown in **Table 1**.

2.2. Injection history analysis

Since the monitoring process involved the three injection stages, namely, water injection (pressure building), CO_2 injection, and post-injection, it is of interest to interpret the results according to the stages. For each stage, at least three monitoring tests were performed. Hence, there are three test group data. To compare the field pressure responses at different injection stages, statistical parameters have been adopted including average shear-wave velocities and coefficient of variations.

Statistical analysis is performed first by determining the averaged shear-wave velocities at different strata for each test group along each of the test lines. The average wave velocities are defined as [27]:

$$\theta = \frac{1}{N}\sum_{i=1}^{N} x_i \tag{4}$$

where θ represents the average wave speed, x_i represents the wave speed data at the corresponding depth for each test group, and N represents the number of tests in each test group. After calculating the average shear-wave velocities, the standard deviations, α, of the corresponding data are determined as:

$$\alpha = \sqrt{\frac{1}{N}\sum_{i=1}^{N}(x_i - \theta)^2} \tag{5}$$

Test no.	Injection	Monitoring date
1	Water	8–10 October 2008
2	Water	21–22 January 2009
3	Water	15–16 June 2009
4	CO_2	9–10 December 2009
5	CO_2	11–12 March 2010
6	CO_2	18–19 May 2010
7	CO_2	8–9 September 2010
8	Water	17–18 November 2010
9	Water	16–17 March 2011
10	Water	17–18 May 2011

Table 1. Summary of monitoring history at the Citronelle oil field.

The average and standard deviation values are then used to compute the coefficient of variation (COV), C_v:

$$c_v = \frac{\alpha}{\theta} \tag{6}$$

The coefficient of variation illustrates how far a set of numbers deviates from the average value—an indication of the consistency of the layer responses as well as the repeatability of the measurements. The CO_2 injection process instigated a continuous stress building within the oil-bearing layer at the Citronelle oil field. Due to the presence of the anhydrite layer, the CO_2 remains within the oil-bearing rock and will slowly flow into the oil-bearing rock resulting in the stress built-up dissipating throughout the oil-bearing layer. As long as the anhydrite retains its integrity and that there are no break-throughs within the rock medium, the pressure at the oil-bearing layer should be consistently higher than in the strata above. Thus, the stress wave velocity at the oil-bearing layer should be higher than in the strata above. The COV and average values of the wave speed profile will be used to determine the stress state in the strata system. **Table 2** lists the C_v values from both Line 1 and Line 2 tests. **Table 2** shows that the C_v values for each layer are reduced during the injection history, indicating a stressing of the strata.

The C_v values of the wave speed at the oil-bearing layer is an indication of the stabilization of the strata pressurization process: as the oil-bearing layer pressure is building up, a larger C_v value is expected, which dropped later indicating stable pressure in the oil-bearing rock.

Layer	Before CO_2 injection		During CO_2 injection		After CO_2 injection	
	Line 1	Line 2	Line 1	Line 2	Line 1	Line 2
1	0.05	0.06	0.03	0.07	0.02	0.05
2	0.06	0.06	0.09	0.11	0.01	0.07
3	0.08	0.07	0.06	0.18	0.02	0.03
4	0.16	0.08	0.05	0.20	0.01	0.05
5	0.15	0.08	0.10	0.17	0.03	0.04
6	0.13	0.05	0.14	0.15	0.03	0.04
7	0.16	0.07	0.14	0.14	0.01	0.03
8	0.14	0.03	0.15	0.14	0.02	0.01
9	0.13	0.05	0.11	0.11	0.01	0.03
10	0.17	0.05	0.04	0.09	0.01	0.03
11	0.16	0.06	0.05	0.06	0.01	0.04
12	0.08	0.05	0.07	0.06	0.002	0.02
13	0.04	0.06	0.05	0.03	0.004	0.003
14	0.07	0.03	0.06	0.05	0.01	0.001

Table 2. Summary of C_v values for results from both Line 1 and Line 2 tests.

Table 2 shows the C_v values for each layer and each survey line. The table shows that in all cases, C_v values are less than 0.2 indicating that the strata responses are slow, and consistent and that there are no drastic events occurring during the whole injection process. The C_v values also are consistently dropping during the three stages indicating that the pressurization is gradually stabilized during the process.

Careful evaluation of **Table 2** indicates that there is a difference between the results from both survey lines: for the after CO_2 injection stage, it is seen where the C_v value is shown to be 0.01 for Line 1 and the value is 0.001 for Line 2 (Layer 14). This is an order of magnitude different. For the before CO_2 injection (initial water pumping) stage, where the C_v value is 0.07 for Line 1 and is 0.03 for Line 2. This observation may be detrimental considering the experimental resolution of the geophysical testing method, which is discussed below.

3. Geophysical response analysis and interpretations

3.1. Shear-wave speed determination

As mentioned earlier, each test line has 24 measurements points representing a total of 24 channels in data processing. To process the shear-wave velocity data, SeisOpt ReMi software was used [26]. The procedure of stress wave signal processing involves first a wave field data transformation (ReMi Vspect module was used), which converts the time domain data acquired in the field to frequency domain. An interactive Rayleigh-wave dispersion modeling was then conducted with the outcomes is 1-D shear-wave velocity models. At the end, the dispersion curves were generated [28].

Figure 7 shows the typical averaged shear-wave velocity profiles as a function of depth (measured from Line 1 and Line 2). The shear-wave velocity curve was obtained based on the averaging of the test data sets during each test stage and is shown to have a total of 14 strata. The 14th strata correspond to the measurements of shear-wave velocity to depths at around 12,500 ft. (3810 m), which is about the oil-bearing Donovan sand. As described earlier, most of the injection pressures were retained within the oil layer at around 12,500 ft. (3810 m). Hence, the test results confirmed about the pressurization of the Donovan sand and that the anhydrite layer has maintained its leak prevention integrity.

In order to compare the changes of the shear-wave velocity obtained from the geophysical tests, the data were divided into three groups: before CO_2 injection, during CO_2 injection, and after CO_2 injection. **Figures 8–10** show the shear-wave velocity curves from both Line 1 and Line 2 tests for the three stages: **Figure 8** shows the results of average shear-wave velocity versus depth curve for test 1, test 2, and test 3 (before CO_2 injection) for Line 1 and Line 2, respectively. Error bars are used to indicate the deviation of shear-wave velocity in the measurements of each group.

Both Line 1 and Line 2 show that different strata experienced different stress histories: for Line 1, the top seven layers (approximately at 6000 ft. (1829 m) depth) are shown to experience

initial increase in wave speed (during CO_2 injection) and then decreasing wave speed (after CO_2 injection); the trend reversed after 6000 ft. (1829 m) depth showing increasing wave speeds for both during and after CO_2 injections; and finally, the oil-bearing layer [around 12,000 ft. (3658 m) depth] showed slowly decreasing wave speeds. Line 2, on the other hand, showed an increase decrease trend up to 3000 ft. (914 m) depth; followed by an increasing pattern above the oil-bearing layer; and decreasing wave speeds at the oil-bearing layer. The explanation of the response history is that the oil-bearing layer experienced strata expansion due to the injection pressure and the inability of oil to escape quick enough from the oil sand; hence, the pressure is transferred to the strata above the oil-bearing layer (mostly salient saturated material), which experienced stressing (increasing wave speed). This trend reversed for the upper layer above the salient layers, which is dependent upon the balancing act of the weight of the overburden and the upward lifting of the injection pressure.

Figure 9 shows the results of average shear-wave velocity versus depth curve for test 4, test 5, test 6, and test 7 (during CO_2 injection) for Line 1 and Line 2, respectively. Wave speeds results of the last four layers shown in **Figure 9** are higher than the corresponding results shown in **Figure 8**. The increase in shear-wave velocity is associated with CO_2 injection, which caused an increase in the effective stresses in layers above the injection zone (pressurization). **Figure 10** shows the results of average shear-wave velocity versus depth curve for test 8, test 9, and test 10 (after CO_2 injection) for Line 1 and Line 2, respectively. The deviations on the graphs shown in **Figure 10** are significantly smaller when compared to **Figures 8** and **9** indicating that the strata pressurization has stabilized.

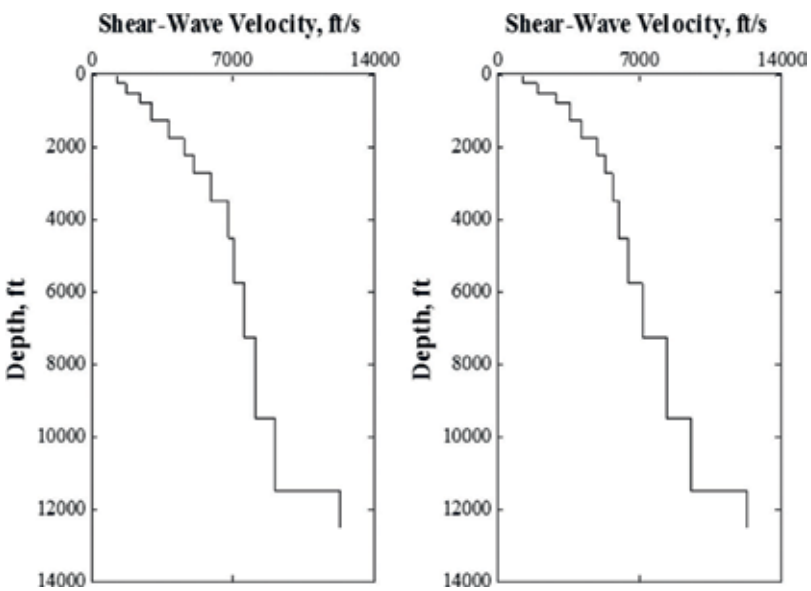

Figure 7. Average shear-wave velocity profiles versus depth from sensor survey Line 1 (left) and Line 2 (right), September 8–9, 2010.

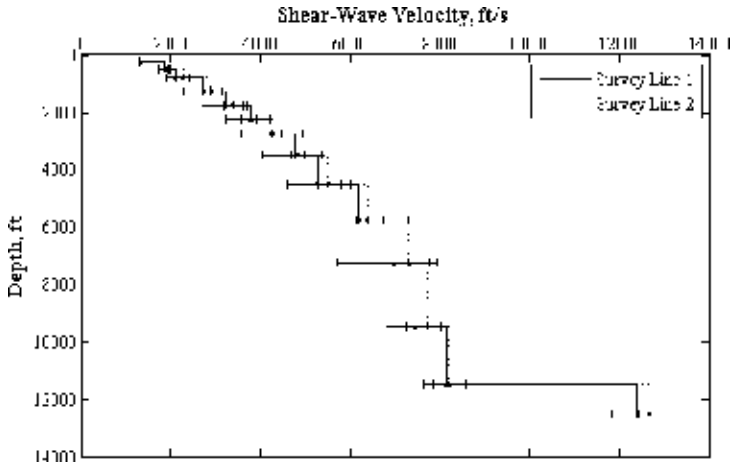

Figure 8. Average shear-wave velocity profile versus depth before CO_2 injection, average of test 1, test 2, and test 3 (Line 1 and Line 2).

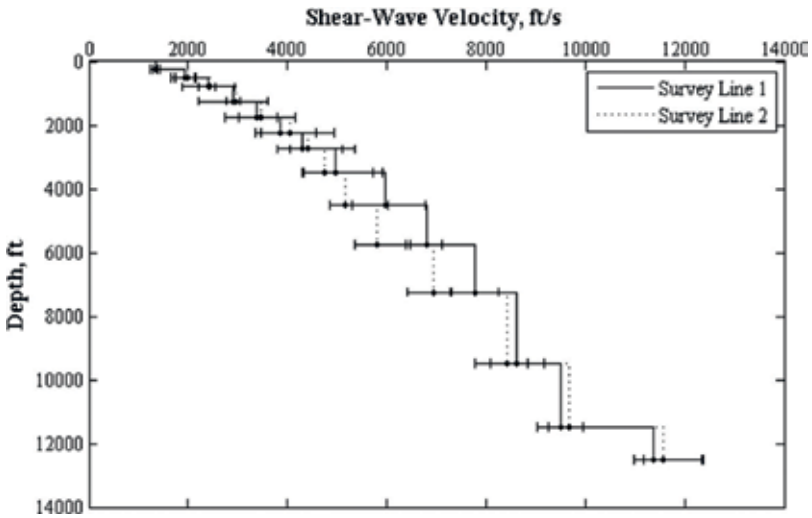

Figure 9. Average shear-wave velocity profile versus depth before CO_2 injection, average of test 4, 5, 6, and 7 (Line 1 and Line 2).

It is important to point out that the test line selection is constrained by available monitoring sites and is selected in order to help determine possible directional effects of the CO_2 migration at the oil field. Hence, the first test line would determine the likely CO_2 migration in the north-east direction, and the second test line would determine the flow in the northeast and southwest directions. When comparing the average velocity at the oil-bearing layer, the results from Line 1 indicates that the wave speed has reached 12,392 ft./s (3,777 m/s) during water injection, 11,365 ft./s (3,464 m/s) during CO_2 injection, and has dropped slightly to 11,109 ft./s (3,386 m/s) after the CO_2 injection. This indicates that there is a possibility that the supercritical CO_2 may be migrating slowly in the north-east direction.

http://dx.doi.org/10.5772/intechopen.78386

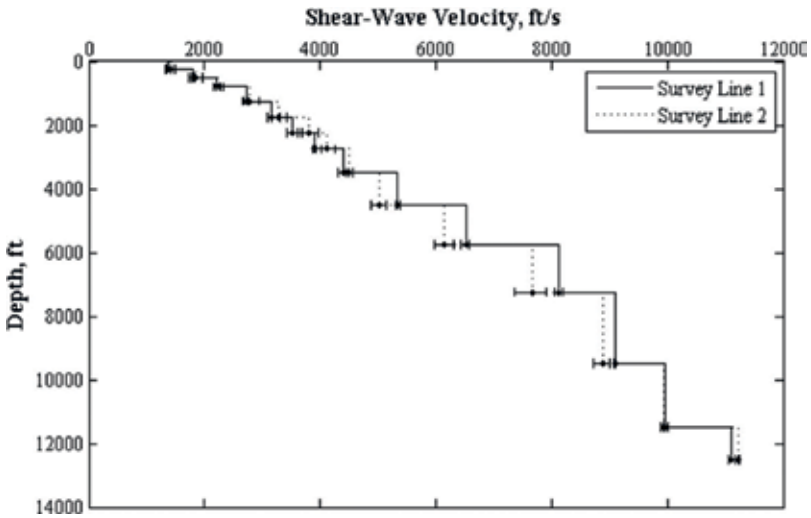

Figure 10. Average shear-wave velocity profile versus depth during CO_2 injection, average of test 8, test 9, and test 10 (Line 1 and Line 2).

On the other hand, Line 2 has wave velocity reaching 12,667 ft./s (3,861 m/s) during water injection, 11,570 ft./s (3,527 m/s) during CO_2 injection, which has dropped to 11,236 ft./s (3,425 m/s) post CO_2 injection. Again, there is a possibility of mobilization of oil/CO_2 flow—a likelihood of enhanced oil production in the months to come.

It is noticed that the strata pressure above the oil-bearing layer is slow in building up as it takes time for the pressure to dissipate into the upper strata. To study this effect, the wave speed responses above the oil-bearing layers are studied: it is shown for Line 1, the wave speed above the oil-bearing layer has increased from 8144.6 ft./s (2,482.5 m/s) initially, to 9512.9 ft./s (2,899.5 m/s) during CO_2 injection, and finally, increased to 9963.7 ft./s (3,036.9 m/s) post-injection. This indicates a slow building up of pressure. For Line 2, the wave speed immediately above the oil-bearing layer has increased from 8207.6 ft./s (2,501.7 m/s) before injection to 9664.0 ft./s (2,945.6 m/s) during CO_2 injection, and finally, to 9935.8 ft./s (3,028.4 m/s) post-injection. The interpretation of this observation is that the oil pressure is pushing against the strata above the Donovan sand and has resulted in the strata pressurization. It is concluded that the pressure build-ups are almost identical in both directions indicating uniform build-up of pressures at all directions at the Citronelle oil field.

3.2. Discussion on geophysical sensing for CO_2 injection studies

Geophysical testing has been applied to projects similar to the Citronelle field study for the purposes of determining production induced stress changes in the oil-bearing strata and site anisotropy changes. In most high-resolution seismic detections, the tests are performed with controlled excitations such as the use of explosions, seismobile vibrations, or gun shots. The results have sensitivities that can indicate possible migration of injected fluids. However, the interpretation of strata stress changes based on wave speed changes is inherently challenging, as a result of the constrained temporal and spatial resolutions. As a result, the

velocity change ratio function ($\Delta v/v$) has been suggested as a means to establish the detection of geomechanical condition changes due to oil production or fluid injection [29] and has been successfully implemented in a study to synchronized field measurements to localized microtremors [30].

To determine the stress wave speed changes, the velocity change functions are computed for before, during and after CO_2 injection:

$$\left(\frac{\Delta v}{v}\right)_i - \frac{(v_{During})_i - (v_{Before})_i}{(v_{Before})_i} \tag{7}$$

$$\left(\frac{\Delta v}{v}\right)_i = \frac{(v_{After})_i - (v_{Before})_i}{(v_{Before})_i} \tag{8}$$

$$\left(\frac{\Delta v}{v}\right)_i = \frac{(v_{after})_i - (v_{during})_i}{(v_{during})_i} \tag{9}$$

Figure 11 shows ($\Delta v/v$) for different stages of the injection process at Citronelle field indicating different strata stress plays: for both Line 1 and Line 2, it is shown that the stress waves have reduced in the injection layer (Layer 14) after CO_2 injection indicating that the CO_2 gas may have migrated at this stage. The velocity change functions for Layers 8–10 (corresponding to

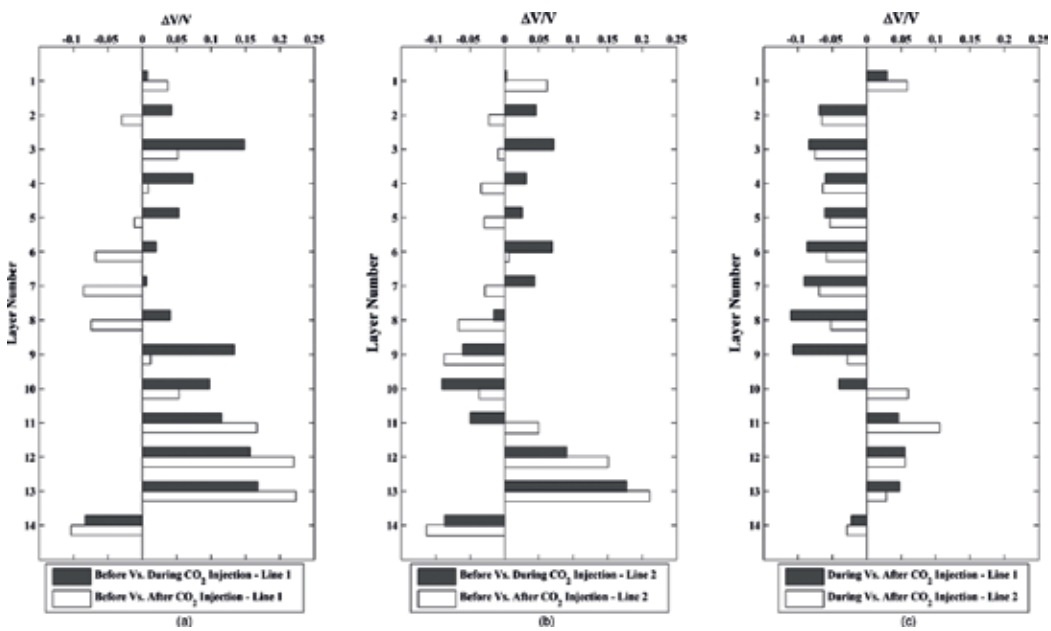

Figure 11. Velocity change functions vs. strata layers for (a) injection histories for Line 1; (b) injection histories for Line 2 and (c) injection histories for Line 1 and Line 2.

salient layer) are negative, most likely indicating a reduction in effective stress. Following Eq. (1), this may be interpreted as an increase in pore water pressure in the salient formation.

The last figure in **Figure 11** shows a comparison between Line 1 and Line 2 using Eq. (9). This figure shows that the two trends are in consistent in general and that both show the same trend of velocity increase right above the oil production strata (which shows negative velocity change functions). This further enhances the interpretation that the stress within the injection may be reduced due to migration of CO_2 plum.

A reduction of the strata pressure (shear-wave velocity) could mean a likely leak occurs within the system, which has not been identified at the Citronelle field. The shear-wave velocities at the Donovan oil-bearing layer are normalized by their average value and are plotted against the normalized well head pressure in **Figure 6**. Assuming the shear-wave velocity is a good representation of the stress level within the oil-bearing stratum, the well-fitting of the two sets of data represents that the geophysical testing method has accurately quantified the stresses within the reservoir.

4. Conclusions

Carbon sequestration through injection into a depleted oil field is an effective method to reduce atmospheric CO_2. However, proper monitoring of the CO_2 injection process is essential in order to ensure the geomechanical stability of the storage reservoir and to minimize risks of potential geohazard to the terrestrial and sub-terrestrial environments. This chapter reports the use of a passive microseismic sensing technique to monitor the CO_2 injection process at the Citronelle oil field, Alabama. The ability of the passive DoReMi technique to monitor the CO_2 sequestration process in the heterogeneous oil reservoir is demonstrated through analysis of the wave speed profiles indicating that there are strata stress build-ups during and after the injection of CO_2, which resulted in the pressurization of the Rodessa oil-bearing layers. Clear demarcation of the shear-wave velocity profile is shown for before, during, and after the CO_2 injection in the field. The detection of geomechanical deformation within the overburden of the reservoir is important for monitoring the long-term CO_2 storage—continued monitoring may provide information on possible reservoir breakthroughs and possible pathways for CO_2 leakage.

The COV value associated with the shear-wave velocity changes is suggested as a measure of the conditions at the oil field and is observed to drop in value during the CO_2 injection process, indicating that the stress state in the oil-bearing layer has reached a stable state. Thus, the COV values can be used as an indication of oil field stability during the CO_2 injection operation and have the potential for long-term monitoring of the strata stress change throughout the field operations. Further studies are needed to develop the COV value into risk index that can be used to indicate geohazard. The strata stressing is especially important to the City of Citronelle, where the oil wells (potential CO_2 leak sites) are in close vicinity to humans and livestock. Continued geophysical monitoring of the strata stress changes can help mitigate potential geohazards due to the CO_2 injection operation.

Acknowledgements

This work is supported by the US Department of Energy (USDOE), National Energy Technology Laboratory (NETL) under Cooperative Agreement No. DE-FC26-06NT43029 with the University of Alabama at Birmingham. The work is also supported by Denbury Resources, Southern Company, the Geological Survey of Alabama, the University of Alabama, the Alabama A and M University, and the University of North Carolina at Charlotte. The first author is also supported by the Doctoral Foundation of Henan Polytechnic University (B2015–78).

The authors would also like to acknowledge the technical supports and advices from Dr. Peter M. Walsh from the University of Alabama at Birmingham, Dr. Richard A. Esposito of Southern Company, Dr. Jack C. Pashin of the Geological Survey of Alabama and Mr. Gary N. Dittmar of Denbury Resources. The Technical assistance from Dr. Satish Pullammanappallil from Optim, Inc. is also greatly appreciated.

The views, opinions, findings, and conclusions reflected in this publication are the responsibility of the authors only and do not represent the official policy or position of the USDOE, NETL, or any State or other entity.

Author details

Shen-En Chen[1]* and Yangguang Liu[2]

*Address all correspondence to: schen12@uncc.edu

1 University of North Carolina at Charlotte, Charlotte, NC, USA

2 School of Resources and Environment, Collaborative Innovation Center of Coalbed Methane and Shale Gas for Central Plains Economic Region, Henan Polytechnic University, Jiaozuo, Henan Province, China

References

[1] Halmann MM, Steinberg M. Greenhouse Gas Carbon Dioxide Mitigation: Science and Technology. Boca Raton, FL: Lewis Publishers; 1999

[2] Balat M, Balat H, Acici N. Environmental issues relating to greenhouse carbon dioxide emissions in the world. Energy Exploration & Exploitation. 2003;**21**(5-6):457-473

[3] Zhong WY, Haigh JD. The greenhouse effect and carbon dioxide. Weather. 2013;**68**(4): 100-105

[4] White CM, Strazisar BR, Granite EJ, Hoffman JS, Pennline HW. Separation and capture of CO_2 from large stationary sources and sequestration in geological formations—Coalbeds

and deep saline aquifers. Journal of the Air & Waste Management Association. 2003;**53** (6):645-715

[5] Bachu S. CO_2 storage in geological media: Role, means, status and barriers to deployment. Progress in Energy and Combustion Science. 2008;**34**(2):254-273

[6] Holloway S. Underground sequestration of carbon dioxide—A viable greenhouse gas mitigation option. Energy. 2005;**30**(11-12):2318-2333

[7] Plasynski SI, Litynski JT, McIlvried HG, Srivastava RD. Progress and new developments in carbon capture and storage. Critical Reviews in Plant Sciences. 2009;**28**(3):123-138

[8] Lake LW. Enhanced Oil Recovery. Englewood Cliffs, NJ: Prentice Hall; 1989

[9] Blunt M, Fayers FJ, Orr FM. Carbon dioxide in enhanced oil recovery. Energy Conversion and Management. 1993;**34**(9-11):1197-1204

[10] Gaspar Ravagnani ATFS, Ligero EL, Suslick SB. CO_2 sequestration through enhanced oil recovery in a mature oil field. Journal of Petroleum Science and Engineering. 2009;**65** (3-4):129-138

[11] Koottungal L. Special report: 2010 worldwide EOR survey. Oil and Gas Journal. 2010;**108**(14):41-53

[12] Hosa A, Esentia M, Stewart J, Haszeldine S. Injection of CO_2 into saline formations: Benchmarking worldwide projects. Chemical Engineering Research and Design. 2011;**89** (9):1855-1864

[13] Rutqvist J, Vasco DW, Myer L. Coupled reservoir-geomechanical analysis of CO_2 injection and ground deformations at in Salah, Algeria. International Journal of Greenhouse Gas Control. 2010;**4**(2):225-230

[14] Morris JP, Hao Y, Foxall W, McNab W. In Salah CO_2 storage JIP: Hydromechanical simulations of surface uplift due to CO_2 injection at in salah. Energy Procedia. 2011;**4**:3269-3275

[15] Onuma T, Okada K, Otsubo A. Time series analysis of surface deformation related with CO_2 injection by satellite-borne SAR interferometry at in Salah, Algeria. Energy Procedia. 2011;**4**:3428-3434

[16] Chadwick RA, Arts R, Bentham M, Eiken O, Holloway S, Kirby GA, Pearce JM, Williamson JP, Zweigel P. Review of monitoring issues and technologies associated with the long-term underground storage of carbon dioxide. Geological Society, London, Special Publications. 2009;**313**(1):257-275

[17] White D. Monitoring CO_2 storage during EOR at the Weyburn-Midale Field. The Leading Edge. 2009;**28**(7):838-842

[18] Arts R, Eiken O, Chadwick A, Zweigel P, Van Der Meer L, Zinszner B. Monitoring of CO_2 injected at Sleipner using time lapse seismic data. Energy. 2004;**29**(9-10):1383-1392

[19] Giese R, Henninges J, Lüth S, Morozova D, Schmidt-Hattenberger C, Würdemann H, Zimmer M, Cosma C, Juhlin C. Monitoring at the CO_2 SINK site: A concept integrating geophysics, geochemistry and microbiology. Energy Procedia. 2009;**1**(1):2251-2259

[20] Esposito RA, Pashin JC, Walsh PM. Citronelle dome: A giant opportunity for multi-zone carbon storage and enhanced oil recovery in the Mississippi interior Salt Basin of Alabama. Environmental Geosciences. 2008;**15**(2):53-62

[21] Esposito R, Pashin J, Hills D, Walsh P. Geologic assessment and injection design for a pilot CO_2-enhanced oil recovery and sequestration demonstration in a heterogeneous oil reservoir: Citronelle field, Alabama, USA. Environmental Earth Sciences. 2010;**60** (2):431-444

[22] Hawkins K, Howe S, Hollingworth S, Conroy G, Ben-Brahim L, Tindle C, Taylor N, Joffroy G, Onaisi A. Production-induced stresses from time-lapse time shifts: A geomechanics case study from Franklin and Elgin fields. The Leading Edge. 2007:655-662

[23] Maxwell SC, Urbancic TI. The role of passive microseismic monitoring in the instrumented oil field. The Leading Edge. 2001;**20**(6):636-639

[24] Verdon JP, Kendall J-M, White DJ, Angus DA, Fisher QJ, Urbancic T. Passive seismic monitoring of carbon dioxide storage at Weyburn. The Leading Edge. 2010;**29**(2):200-206

[25] Chen S-E, Liu Y, Wang P. DoReMi—A passive geophysical monitoring technique for CO_2 injection. In: Proceedings of the SPE Eastern Regional Meeting 2011, August 17-19, 2011. Columbus, OH, USA: Society of Petroleum Engineers (SPE); 2011. pp. 254-266

[26] Optim. User's Manual: SeisOpt ReMi Version 4.0. Reno, NV: Optim, Inc; 2006

[27] Rétháti L. Probabilistic Solutions in Geotechnics. Elsevier Science; 1988

[28] Louie JN. Faster, better: Shear-wave velocity to 100 meters depth from refraction microtremor arrays. Bulletin of the Seismological Society of America. 2001;**91**(2):347-364

[29] Hatchell P, Sayers C, van den Beukel A, Molenaar M, Maron K, Kenter C, Stammeijer J, van der Valde J. Whole Earth 4D: Monitoring geomechanics, Extended Abstract. In: 73rd SEG Meeting; Dallas, USA; 2003. pp. 1330-1333

[30] Steiner B, Saenger EH, Schmalholz SM. Time reverse modeling of low-frequency microtremors: Application to hydrocarbon reservoir localization. Geophysical Research Letters. 2008;**35**(3):L03307

Chapter 9

Tracking CO_2 Migration in Storage Aquifer

Luqman Kolawole Abidoye and
Diganta Bhusan Das

Additional information is available at the end of the chapter

http://dx.doi.org/10.5772/intechopen.79296

Abstract

Monitoring technologies for CO_2 in geological carbon sequestration are based upon the physico-chemical and electromagnetic properties of the CO_2-water/brine and rock system as well as the induced events such as micro-seismicity. As CO_2 migrates in the subsurface, its interactions with elements like rock, water/brine can be used to track its presence and direction. For deep subsurface storage of CO_2, methods like electrical resistivity tomography (ERT), seismicity, capillary pressure and relative permeability as well as geochemical measurements can be reliably employed in monitoring CO_2. Other methods like membrane-sensor technique and gas accumulation chamber are mainly suitable for shallow geological sequestration. However, prior to the full-scale deployment, it is necessary to understand the principles of operations and limitations of the adopted technologies as well as obtain experimental and practical information from them. In the field application, pre-injection baseline assessment is necessary followed by critical assessments during the storage process and post-injection period. Accuracy in leakage quantification and identification of sinks are also important. Factors that can influence the results of these technologies include fluctuations of pressure, temperature, initial salinity level, initial pH level, porosity, fluid properties, porosity, tortuosity, pore size distribution, wettability, reservoir mineralogy and surface chemistry.

Keywords: CO_2, sequestration, leakage, two-phase flow, geophysical technologies membrane

1. Introduction

Climate change and the accompanying global warming are of concerns to science, engineering and political stakeholders. Particularly, the effects of climate change on the living and non-living species and the possible future impacts have led to global efforts at curtailing

the emission of greenhouse gases. The current problem of global warming emanated from anthropogenic activities, mainly from excessive use of fossil fuel for energy as well as the degradation of natural carbon sinks, especially by deforestation [1, 2]. Emissions from fossil energy source have been shown to aggravate the climate change by forming a blanket of gases which accumulate at the lower part of the atmosphere, trapping the reflected radiation from the earth, thereby raising the surface temperature [2, 3]. According to DOE [4], 90% of world's primary sources of energy still come from fossil fuel. As a result, the readiness to cut the reliance on this source of energy presents a daunting challenge. Continuous dependence of man on fossil fuel is based on the desire for an improvement in the standard of living, education, health care, and so on. These goals are directly related to energy consumption.

CO_2 concentration in the atmosphere should be reduced to the maximum of 350 ppm in order to restore the planet to the similar level obtainable in the pre-industrial revolution era (200 to ~385 ppm) [5, 6]. To mitigate the problems of climate change, efforts are being made by scientists and many technologies are under investigations and implementations to curtail the emissions of greenhouse gases into the atmosphere. To reduce human dependence on fossil fuels, energy sources from wind and sun are being considered globally. However, carbon emissions will realistically persist till the near or foreseeable future owing to the derivations of many industrial and household products from crude oil. As a result, carbon capture and storage (CCS) is a viable route to check accumulation of greenhouse gases in the atmosphere.

CCS is providing methods and procedure to deal with the CO_2 emitted from various emission sources. Advanced capture technologies have emerged from the development and discovery of novel solvents together with optimised capture procedures like pre and post-combustion capture techniques [7, 8]. CO_2 can be stored in several natural media. These storage media include ocean and saline aquifers, unminable coal seams and depleted oil reservoirs [9, 10]. Storage of CO_2 can also be made economical through its use to recover remnant oil in depleted oil reservoir [11]. Among the possible storage sites, geological carbon sequestration in saline aquifers is considered as the most viable option as it seems to have the largest carbon storage potential [12, 13]. The reasons for this include the stability and capacity of these geological media. Stable sedimentary basins are essential for dependable sequestration activities, and such basins are found in most continents [14] with estimated capacities of around 1000–100,000 gigatonnes of carbon dioxide [13]. Across the globe, **Figure 1** shows the carbon sequestration projects that are either ongoing or completed.

The current issues in the practice of geological carbon sequestration are those of safety of the process. There are concerns about the possible leakage of the CO_2 back to the atmosphere. If this occurs, humans and plants are in danger. In the case of leakage, CO_2 migrating through the subsurface may encounter potable water, with which it forms acid that can affect the plant and animal lives. In case the leakage gets into the atmosphere, at a concentration of CO_2 above 4%, its inhalation produces fatal results in humans and animals [16]. Thus, there is a need for effective monitoring of CO_2 movement and reactions at the geological sequestration site and the adjoining areas.

http://dx.doi.org/10.5772/intechopen.79296

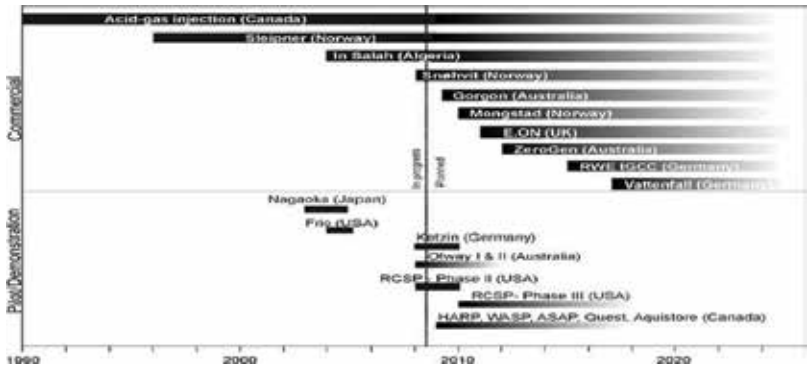

Figure 1. Carbon dioxide sequestration operations at pilot and commercial scales worldwide [15].

Many techniques for monitoring CO_2 in the Earth's surface are available. But, the effective monitoring of CO_2 in the subsurface is still posing challenges. Meanwhile, it is important that we develop effective subsurface monitoring techniques in order to avert dangers to humans, animals and plants on the Earth, animals in the ocean as well as the potable water aquifers in the subsurface that might lie along the CO_2 leakage path. For example, if CO_2 leaks from the geological sequestration site as a result of fault in the cap rock or seismic effects, subsurface monitoring measures should be efficient enough to alert the monitoring team immediately in order to possibly curtail the movement of the plume before it contaminates the subsurface potable water aquifers or before it reaches the surface. In this scenario, humans and animals can be moved away from the leakage site on time. Effective monitoring will also provide the possibility of preparing for the plume before reaching the surface by making provisions for its containment.

This chapter examines the existing monitoring techniques for the CO_2 activities in the geological carbon sequestration. The challenges inherent in these techniques are identified, and the implications of these challenges are discussed under different conditions and in different porous media.

2. CO_2 leakage and characteristics

Several mechanisms guide the leakage of CO_2 and its migration through the geological pore networks. For example, gravity override and viscous instability are phenomena that cause the CO_2 to move to the top of the injection layer bypassing large quantities of brine [14, 17, 18]. Also, if the caprock has fault line that is permeable enough for the plume, this can cause favourable pathways via which CO_2 could escape, thereby compromising the intention of the sequestration process. Also, gravity override together with viscous instability can create the vertical buoyant pressure, which the CO_2 applied on the caprock. This pressure arises mainly as a result of difference in density between the formation water and the CO_2, and the thickness of the carbon dioxide plume accumulation.

Monitoring technologies for CO_2 in geological carbon sequestration are built upon the physico-chemical and electromagnetic properties of the CO_2-water/brine and rock system or the identification of the reaction by-products and/or the coupled process effects such as micro-seismicity [19]. Monitoring can provide vital information for verification, accounting and risk assessment at storage site, and is fundamental to ensure that the effective containment of the gas has actually taken place. Monitoring also contributes to building public acceptance of the geologic storage as a viable method for mitigating greenhouse gas emissions [20]. Existing monitoring techniques include electromagnetic techniques [21], temperature signals [22] and infrared monitoring [23]. Some of these techniques have been widely demonstrated both in the laboratory and pilot applications. Electromagnetic techniques make use of the wide difference between the electrical/dielectric characteristics of CO_2 and water/brine as well as those of other geological elements to create contrasts among the phases, which can then be used to monitor the migration of the CO_2 in the aquifer or to understand the displacement of the aquifer brine by the injected CO_2. Traditionally, this electromagnetic method is often employed in the monitoring and control of two-phase flow in porous media [1, 24–26].

For the temperature signal technique, the principle employed in its use includes the fact that the dissolution of CO_2 in water is an exothermic process. As a result, the temperature of the solution is raised as CO_2 dissolves in the brine/water. Also, the change of phase of CO_2 from, for example, supercritical state to liquid or gas is accompanied by change in enthalpy. These effects are utilised in non-isothermal detection of CO_2 presence in water/brine using the temperature signal method. But the dissolution of CO_2 in water is limited. This confines the method to limited time and space because once the water/brine is equilibrated with CO_2, detecting plume migration or other activities of the CO_2 becomes difficult. Furthermore, CO_2 is known to have characteristic infrared wave absorption property. This is harnessed in the infrared monitoring technique. How well these methods can be utilised in the subsurface and large-quantity monitoring of the gas in the subsurface still poses questions.

Monitoring the region around the storage aquifers should be coupled with near-surface and surface monitoring [1]. These regions of monitoring are important because migration or leakage of CO_2 can extend to the atmospheric space. Near-surface monitoring techniques are well developed and are essential in the detection and monitoring of the gas emanating from different emission sources and even leakage from geological sequestration sites. Near-surface monitoring techniques involve the analysis of near-surface water, air and soil samples on a regular basis as CO_2 leaks can acidify the water and create conspicuous contrast between the original and current soil and air compositions [19]. Also, on the surface, gravity method [27] can be employed based on the fact that CO_2 is heavier than air and lighter than water. Thus, increase in air density and/or reduction in density of water may signify the presence of CO_2. Remote sensing of air composition [28] and surface analysis of carbon content by inelastic neutron scattering (INS) [29] are techniques also known for the surface monitoring of CO_2.

Among the monitoring methods described above, electromagnetic techniques like dielectric permittivity (ε_r), electrical resistivity (ρ) and conductivity (σ) as well as wave propagation are common in reservoir applications [1, 21, 24]. Also, tracers like SF6 are applied in the monitoring of fluid movement. To ensure safety in the case of advancing plume of CO_2, the monitoring methods should extend several hundred metres beyond the injection region. This has the potential of protecting the potable water aquifers that lie in the possible path of migrating CO_2. Apart from electrical parameters (e.g., ε, ρ and σ), capillary parameters are commonly employed in the study of two-phase flow, for example, oil and water, gas and water, and so on, and can as well be included in the monitoring techniques. This chapter is primarily concerned with the safety of the geological carbon sequestration and the techniques to ensure it. These techniques are expatiated in the following subsection.

3. CO_2 monitoring techniques

Monitoring techniques can be classified according to the different mechanisms of operations and the principles as well as the environment of applications. The following classes are popular in the literature.

With the exception of the (3) in **Table 1**, most of the techniques are mainly suitable for shallow injection layer or atmosphere. Worldwide, monitoring technologies have been in operations at many pilot sites like in Nagaoka (Japan) [30], Frio (USA) [31] and Ketzin [32]. Several other projects under the USDOE were involved in the trial of the technologies (www.fossil.energy.gov/sequestration/partnerships/index.html). Multiple monitoring technologies applied in these pilot projects were able to track the CO_2 plume in different subsurface geological environments [20].

S. No.	Classification/application environment	Techniques/parameters
1	Atmospheric CO_2	Eddy covariance
2	Soil CO_2	Soil accumulation chambers
3	Geophysical monitoring	Geoelectrical, seismic, ground penetrating radar, etc.
4	Biological stress	Multispectral image analysis of plants and microorganisms
5	Geochemical analysis	Monitoring water quality changes
6	Satellite-borne Interferometric Synthetic Aperture Radar (InSAR)	Detection of ground deformation or surface movement
7	Capillary-based parameters	Capillary pressure-saturation-relative permeability relationship

Table 1. Monitoring techniques for CO_2.

It is conventional to perform monitoring operations in three stages. The first stage is the pre-injection monitoring where background data about the CO_2 level as well as lithological parameters before injection of CO_2 can be obtained. This gives the baseline data. The injection stage monitoring follows, where ongoing changes in the soil, water and surrounding space are recorded as CO_2 is being released. Lastly, post-injection monitoring comes after the stop of the CO_2 injection.

3.1. Geophysical techniques

Geophysical monitoring techniques involve the deployment of a variety of electromagnetic and electrical surveying methods to study subsurface CO_2 activities and its interactions with the rock/soil, water/brine and other gases. These methods include geoelectrical, seismic, ground penetrating radar, gravity and electromagnetic assessment. These techniques make use of the electrical behaviours of the CO_2, water and the surrounding geological materials.

To monitor CO_2 sequestration at deep geological layer, electrical resistivity tomography (ERT) is an effective technique. Following injection of CO_2, increase will occur in the resistivity level of the bulk reservoir domain owing to the non-conductive nature of the gas. The resistivity profile may remain stagnant following steadiness in injection operation or after the stop of injection. In addition, after the stop of injection, there may occur a dip in the resistivity profile from the repeal of the contact surface of CO_2/brine and subsequent inflow of brine into the near-wellbore area [33].

From the resistivity data, saturation of CO_2 (S_{CO_2}) in the reservoir can be evaluated using inverse petrophysical relation [33] by assuming the applicability of Archie's second law:

$$S_{CO_2} = 1 - \left(\frac{\rho_o}{\rho}\right)^{1/n} \tag{1}$$

where ρ_o is the baseline resistivity and n is the saturation exponent.

ERT works effectively if properly calibrated and is well suitable to track dissolved and gaseous CO_2 [34]. Application of electrical resistivity tomography (ERT) has been demonstrated at various pilot sites (see, e.g., [33, 34]) for detecting and tracking the CO_2 and brine distribution and their migrations in the subsurface. ERT has the advantage of imaging the injection reservoir and the migration activities of the fluids. It consists of the array of borehole electrodes which can be arranged to serve as a permanent reservoir monitoring tool. It possesses the ability to map quantitative CO_2 saturation in the subsurface. ERT has been found suitable for deep geological layer survey. Example of this technique in field application is found at Ketzin pilot site, Germany. The method was used to acquire data on resistivity changes with the injection of CO_2. Also acquired was the CO_2 saturation in the storage reservoir as well as imaging of CO_2 induced resistivity change.

For near-surface measurement of CO_2 activities in shallow aquifers, direct current geoelectric can be employed [20]. As CO_2 passes through the water-filled and wetted pores, owing to dissolution and ionisation, carbonic acid is formed. This process activates the electrical characteristics of the system. The formation of acid promotes dissolution of minerals in the aqueous media which

further enhances the electrical characteristics of the system. Thus, the determination of changes in resistivity of the domain will be of immense advantage in monitoring the presence and impact of CO_2 and its subsurface movement. In pores saturated with water, migrating CO_2 can displace part of the resident water to replace its position with the gas. In this case, resistivity will increase. This phenomenon of changing electrical characteristics which occurs with the displacement and replacement of water by CO_2 was explained in the work of Abidoye and Bello [35]. They stated that for the scenario where the movement of the CO_2 into the pore led to the displacement of the resident pore water, the bulk dielectric permittivity (ε_b) of the system decreases. if the pore water was not displaced by the migrating CO_2, the presence of CO_2 in the system increases the ε_b. Direct current geoelectric is currently being used at Ressacada Farm, Brazil. The method was used to acquire resistivity changes in the course of CO_2 injection. The changes in resistivity are compared to the baseline values. At the Ressacada Farm, the resistivity value in the vicinity of the injection well increased by 50% in comparison with the baseline value. However, 8 days after the injection stopped, the resistivity change dropped to less than 14% [20].

Laboratory demonstrations and mathematical simulations of geoelectrical monitoring system were well demonstrated in the works of Abidoye and Das [36, 37], Abidoye and Bello [35], Rabiu et al. [38], Lamert et al. [39] and Dethlefsen et al. [40]. Abidoye and Das [36, 37] and Rabiu et al. [38] used unconsolidated porous media of silicate and carbonate soil samples in a sample holder of 10 cm diameter and 4 cm height. They performed simultaneous measurements of bulk relative permittivity (ε_b) and electrical conductivity (σ_b) measurements using three-pin time domain reflectometry probes (TDR probes), which was connected to the wave generator, TDR100 reflectometer (Campbell Scientific Ltd., Shepshed, UK). Using this system, the effects of pressure, temperature and salt concentration on bulk ε_b-S and σ_b-S relationships were investigated for carbonate (limestone) and silicate porous media (both unconsolidated domains) under dynamic and quasi-static supercritical CO_2 ($scCO_2$)-brine/water flow. Their results show that the ε_b in the silica sand sample decreases as the temperature rises in the $scCO_2$-water system. For the carbonate porous medium, ε_b rises only slightly with temperature. The ε_b-S curve also rises as the domain pressure increases. Furthermore, the bulk electrical conductivity (σ_b), at any particular saturation for the $scCO_2$-brine system rises as the temperature increases with a more significant increase found around full water saturation. These findings were corroborated by the work of Wraith and Or [41] where ε_b and σ_b values were found to be greater in the limestone than silica sand porous samples for similar porosity values. From their results, it can be inferred that the geoelectrical techniques are highly dependent on water saturation. Furthermore, Rabiu et al. [38] performed similar investigations with the inclusion of basalt as porous medium. Similar findings were recorded.

Field demonstrations of geoelectrical monitoring techniques were performed by Lamert et al. [39] as well as Dethlefsen et al. [40]. As in the work of Abidoye and Das [36, 37], time domain reflectometry method was used by Lamert et al. [39]. They Installed several copper electrodes at various depths up to 18.5 m below the ground level around the CO_2 injection site in order to monitor the movement of injected CO_2. They found the suitability of geoelectrical methods for monitoring injected CO_2 and geochemically altered groundwater. Similar to the conclusion of Abidoye and Das [36, 37], they also found that the site-specific conditions influence the electrical characteristics.

Apart from the abovementioned methods, other geophysical tools exist with varying capacity to monitor subsurface gas activities. For example, ground penetrating radar (GPR) is another well-established tool that can be used in subsurface CO_2 tracking. However, it has limited depth of penetration as compared to others. However, in the zone of CO_2 leakage, it can give a deeper signal penetration [42]. GPR and other technologies like magnetic resonance sounding (MRS) have depth of penetration of <60 cm [43]. Logging tools like sonic, neutron and pulsed neutron techniques also offer some effectiveness in CO_2 monitoring.

The abovementioned discussions show that myriads of geophysical monitoring techniques are in existence. But the parameters of measurements can be affected by operational conditions as well as the porous media characteristics. Monitoring strategies should, therefore, take these factors into consideration to minimise deviations of the results from the realities. This can be achieved by taking notes of site-specific characteristics that are key to effective prediction of the fate of CO_2.

3.2. Membrane-sensor system

Membrane-sensor technique only assesses the presence of subsurface CO_2 without considering its interactions with other elements of the sequestration domain. Selectively, permeable membrane having high selectivity for CO_2 can be utilised. Coupling the membrane with sensor device, the system can accumulate gas like CO_2 in its chamber which can then be quantified with signals from the sensor. Example is shown in **Figure 2** from Abidoye and Das [44]. Methods of collecting CO_2 into the gas chamber vary and depend on the convenience of the investigators. Abidoye and Das [44] demonstrated membrane-sensor technique in a laboratory experiment using a high-pressure experimental rig. The chapter shows how silicone membrane-sensor system can be employed in the monitoring of subsurface gases, especially in the leakage scenario. In their work, mass permeation, membrane resistance to gas permeation and the gas flux across the membrane are reported for two gases, namely, CO_2 and N_2. In their results, mass permeation of CO_2 through the membrane was more than 10 times higher than that of N_2, under similar conditions. It was also found to increase with the geological depths. The gas flux remains higher for CO_2 as compared to N_2. The authors established a simple criterion for distinguishing the presence of the different gases at various geological depths based on the rate at which the mass permeation of gas through the membrane occurs.

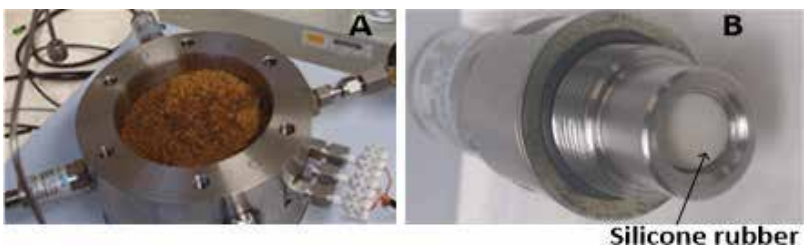

Figure 2. Photographs of (A) the sample holder showing silica sand and pressure transducer (B) the pressure transducer and the silicone rubber sheet (metal cap not shown). Sample holder size: internal diameter=10cm, sample height=4cm [44].

http://dx.doi.org/10.5772/intechopen.79296

Silicone was used by the authors due to its favourable selectivity for CO_2 permeation. Other suitable membrane can, as well, be used. Silicone membrane is a non-porous flat sheet material. Gas permeates the membrane by diffusion under the influence of the driving force, for example, the pressure difference across the membrane. This membrane-sensor method is useful in the early detection of CO_2 migration or leakage from geological reservoirs. Early detection at depth will allow for more time to prepare and plan for the CO_2 plume before its arrival in shallow groundwater or the earth's surface [45]. In application, alarm system can be triggered to signify the presence of CO_2, if the mass permeation rate follows the power law model provided in Eq. (2). This equation can be used to program the membrane-sensor system.

$$y = 1\,0^{-8}\,x^{1.0652} \tag{2}$$

where y is the rate of mass permeation into the membrane-sensor chamber in kg/h and x is the geological depth in metre (m). The equation conforms to the profile of CO_2 permeation curve through silicone membrane. Other gases will very likely deviate from the pattern.

The abovementioned analysis shows that the CO_2 has unique mass permeation rate that is different from that of N_2 and conceivably other gases found in the porous media. With the relation of the mass permeation rate to geological depth, using Eq. (2), the authors showed that the membrane-sensor system can be used to monitor gas leakage under different geological conditions. Thus, at any depth, the system can be applied to give unique indication of gas present. Membrane coupled with miniaturised sensor can be installed at depth to perform the monitoring operations.

Field applications of similar monitoring method were performed by Zimmer et al. [45]. They demonstrated the applicability of silicone rubber as a membrane in the detection of gases present in the underground and boreholes. Investigations by Zimmer et al. [45] were connected to the geological carbon sequestration project (CO2SINK) in Ketzin, Germany. They successfully demonstrated the detection of the CO_2 front at observation wells, located at different distances to the injection well, using the gas membrane sensor that includes the silicone rubber. However, the analyses of the gases through the device rely on the mass spectrometer located on the ground surface.

3.3. Gas accumulation chamber

Measuring subsurface gas and monitoring its movement can be used for the delineation of fault zones and for the characterisation of migration process dynamics [20]. According to Chiodini et al. [46], such measurements have been used for environmental research in geothermal and volcanic areas to determine CO_2 flux rates. Oliva et al. [20] used the technique of gas accumulation chamber to measure CO_2 emissions, soil temperature and moisture on PVC collars arranged in a square grid with 1 m spacing centred on the injection well. They performed the measurements before CO_2 injection, during the whole injection period and 7 days after the injection stopped. Field application of this method was demonstrated at the Ressacada Farm, Brazil, where parameter like CO_2 flux rate was collected. The authors were able to establish relationship between resistivity changes in injection aquifer to the CO_2 flux rates in the same area.

3.4. Geochemical measurement technique

Geochemical monitoring techniques for subsurface CO_2 activities are aimed at acquiring information about interactions and reactions of CO_2 with rock, soil, water and other gases in the subsurface. Products of such interactions and reactions are often the main targets in the monitoring and measurements. Following dissolution of CO_2 in the aquifer water, carbonic acid is produced, which makes the solution acidic and lowers the pH. Furthermore, increase in acid level may lead to the dissolution of rock minerals, thus, raising the concentration of major and trace minerals in the solution. Dethlefsen et al. [40] stated that the most significant geochemical processes, which occur during the CO_2 contamination of potable water are the changes in the pH and the resultant changes in the electrical conductivity (σ) of the fluid–fluid-porous media system (i.e., CO_2-water-porous media system). Popular mineral dissolution that occurs includes carbonates, sulphides, iron oxy-hydroxide minerals and surface reactions such as adsorption/desorption and ion exchange [20].

Geochemical monitoring techniques involve the use of chemical parameters and their appropriate sensors to detect the interactions of CO_2, water, soil/rock and the subsurface gases. Oliva et al. [20] performed geochemical monitoring of CO_2 activities in shallow well by sampling multilevel wells installed in the vicinity of the injection well. From such observatory wells, groundwater samples can be collected before, during and after the injection periods at intermittent schedules. Measurements of temperature, pH, electrical conductivity, oxidation–reduction, salinity and dissolved oxygen can be performed in-situ. Indicator parameters like alkalinity, acidity, ferrous iron (Fe^{2+}) and anions bromide (Br^-), chloride (Cl^-), nitrate (NO_3^-), nitrite (NO_2^-) phosphate (PO_4^{3-}), sulphate (SO_4^{2-}) and acetate (CH_3COO^-) can be obtained from such measurements.

Geochemical activities of CO_2 can vary based on the chemical characteristics of the domain rock/soil. That was why Abidoye and Das [37] performed geochemical monitoring of CO_2 activities in silicate and carbonate porous minerals, to investigate the characteristics of the water-saturated porous media contaminated by CO_2, in the laboratory. They used pH measurements, silicone rubber membrane in the monitoring of CO_2 diffusion in the porous media and the geoelectrical measurement techniques for the determination of the bulk dielectric constant (ε_b) and the bulk electrical conductivity (σ_b) of the CO_2-water-porous media system.

Their results showed three stages in the profile of pH change with time as CO_2 dissolved and diffused in water-saturated silica sand. The initial stage was characterised by quick fall in the pH value from the start of the experiment. This behaviour was connected with quick dissolution of CO_2 and the formation of carbonic acid along with bicarbonate. At the second stage, there was a short rise in pH value. This was explained to be owing to the reverse reaction, which resulted into the formation of aqueous and gaseous CO_2 and water. At the last stage, static equilibrium has been attained in the system which was marked by constant pH value, which remained unchanged till the end of the experiment. During these stages, the bulk electrical conductivity (σ_b) changed in accordance with the fluctuation of the pH values. Since ionic species are formed during the dissolution, σ_b increased accordingly. According to the authors, the rise in σ_b coincided with the initial stage of the change in the pH of the system. The σ_b was higher in limestone than silica sand, and it increased with depth or domain

pressure. Furthermore, the authors provided a mathematical relationship showing that σ_b is dependent on the pH and its initial value, σ_{bi}. This is shown in Eq. (3):

$$\sigma_{br} = 3.87\,\sigma_{bi}^{0.42}\,pH_r^{-0.4} \tag{3}$$

The equation has a regression value of 0.997 and SSE of 0.0023. σ_b is the bulk electrical conductivity in S/m. σ_{bi} is the value of the σ_b in the domain before the injection of CO_2. σ_{br} is the ratio of the steady state to the initial values of the σ_b (i.e., value of σ_b, when the pH is at the steady state, divided by the value of σ_b, before the injection of CO_2). pH_r is the ratio of the steady-state value to the initial value of the pH.

3.5. Capillarity-based monitoring technique

Capillary pressure (P^c) and relative permeability (K_r) for wetting (water) and non-wetting phases (CO_2) are parameters of key importance in modelling the two-phase flow processes encountered during transport of immiscible phases in the underground [47] and they constitute critical parameters used to history match and design field-scale injection projects using reservoir simulators [48]. On two-phase flow, several publications exist concerning capillary pressure-saturation relationship (P^c-S) [49–55] while several others are based on the K_r-S relationship [56–59].

In the context of geological carbon sequestration, flow of supercritical CO_2-water ($scCO_2$-water) can be considered as a two-phase system. Characterisation of such flow can be performed with capillary pressure–saturation-relative permeability relationships (P^c-S-K_r) [1]. This is because CO_2 is only slightly soluble in brine. The solubility occurs briefly, and afterwards CO_2 continues as separate phase in the porous medium.

Injected CO_2 moves through permeable pore networks of the storage reservoir. This movement determines its distribution and stability within reservoirs used for carbon sequestration (Tokunaga and Wan 2013), and this process is dependent on capillary interactions with the displaced brine [60, 61]. Multiphase flow models are powerful tools to understand and predict the capillary activity and trapping of supercritical-CO_2 ($scCO_2$) in deep saline geologic formations. The constitutive relationship between capillary pressure (P^c) and saturation (S_w) is the essential input parameter into these multiphase models. Reliable predictions of CO_2 storage require understanding the capillary behaviour of supercritical CO_2 [62].

However, capillary pressure measurements are influenced by the sand and fluid properties. During injection, the distribution of CO_2 and brine in the pore space varies with distances from the well, and is controlled by the drainage P^c-S_w relation of the reservoir. After the stop of CO_2 injection or relaxation of injection pressure, the displaced brine attempts to reoccupy original position by displacing some of the CO_2. This is referred to as imbibition and is also described by reverse cycle of P^c-S_w curve. The incomplete rewetting or incomplete displacement of the CO_2 by the imbibing brine will lead to major storage mechanism- capillary trapping, which relies on the path- and history-dependent saturation characteristics to control distributions of multiphase fluid flow in pore spaces [63–65].

Routine measurements of P^c-S_w relationship include by porous plate, mercury injection or centrifuge methods. Plug et al. [26] measured drainage and imbibition relations in quartz sand packs of different grain sizes using CO_2 and water with the porous plate technique. They determined the drainage and imbibition cycles of the P^c-S_w relationship and were able to determine residual trapped CO_2 saturation (S_{nwr,CO_2}). The parameter, S_{nwr,CO_2}, is key to determining the success of the storage process because it indicates the amount of the CO_2 that is permanently immobilised. Tokunaga et al. [62] also used drainage and imbibition processes to determine P^c-S_w relationship on quartz sand for $scCO_2$-brine at pressures of 8.5 and 12.0 MPa (45°C). They also determined S_{nwr,CO_2}. Their results show that $scCO_2$ will easily enter silica-rich reservoirs and be stored through capillary trapping at fairly high S_{nwr,CO_2}.

In relation to field applications of P^c-S_w technique, the work of Pini et al. [66] report P^c-S_w relationship for consolidated media, namely, the Berea and Arqov sandstone samples. Discussing the relation in reference to temperature, the curves for the Berea sandstone showed that capillary pressure decreases as temperature reduces, and this behaviour was attributed to an increase in CO_2 dissolution as the temperature decreases reducing the interfacial tension. Thus, P^c-S_w relationship curve can be influenced by subsurface conditions, reservoir characteristics and fluid properties. Complex dependence of P^c-S_w behaviour on fluid properties, porosity, pore geometry and tortuosity, pore size distribution, wettability, reservoir mineralogy, geochemistry, and surface chemistry make the relationship difficult to predict [65].

Field applications of these techniques involve coring of rock samples from the injection reservoir. On these samples, core-flooding operations are performed often in the laboratory. Capillary pressure, relative permeability and residual gas saturations are often the targeted parameters for measurement. The techniques have been used to assess safety and performances of geological carbon sequestration in the UK and Australia [66] and at Ketzin pilot site in Germany [67].

4. Conclusion

Myriads of techniques are currently in existence to detect and monitor CO_2 interactions with water/brine, rock/soil and other gases as well as its migration through complex pore networks. These techniques utilise the physico-chemical and electromagnetic properties of the CO_2-water/brine and rock/soil system as well as the induced events such as micro-seismicity. However, prior to the full-scale deployment of the monitoring technologies, it is necessary to understand the principles of operations and limitations of the adopted technologies as well as obtain experimental and practical information from them. Some of them are suitable for deep geological layer while many are appropriate at the shallow aquifers.

Among the monitoring technologies, geophysical tools have gained more grounds in monitoring pilot sequestration projects across the globe. Techniques like seismic method, electrical resistivity tomography (ERT) offered good promise, especially at deeper levels in the scale of hundred metres to kilometres, while the likes of direct current geoelectric and ground penetration radar (GPR) are only good for monitoring at near-surface or shallow storage

reservoirs. However, in order to effectively assess the potential effects of CO_2 leakage for any of the methods, a pre-injection baseline is critical followed by critical assessments during the storage process and post-injection period.

Among the challenges in the majority of the field applications are the accuracy in leakage quantification and the myriads of factors that can influence the outputs of the measurement techniques, making them non-unique. Accuracy in leakage quantification is often due to the offset in background natural variability and the detection limits of the techniques currently available. Factors that can influence the results of these technologies include pressure, temperature, initial salinity level, initial pH level, porosity, fluid properties, porosity, pore geometry and tortuosity, pore size distribution, wettability, reservoir mineralogy, geochemistry and surface chemistry.

Finally, it is encouraging that important instruments and tools for laboratory and shallow aquifer monitoring techniques are readily available and may be affordable by intended users. However, the cost of the deployment of full-scale monitoring technique for deep geological layer sequestration remains a challenge. Thus, focus should be on bringing down the cost by encouraging price competition among potential manufactures while governments should also make necessary fund available.

Author details

Luqman Kolawole Abidoye[1]* and Diganta Bhusan Das[2]

*Address all correspondence to: abidoye.luqman@uniosun.edu.ng

1 Civil Engineering Department, Osun State University, Osogbo, Nigeria

2 Chemical Engineering Department, Loughborough University, Loughborough, Leicestershire, United Kingdom

References

[1] Abidoye LK, Das DB, Khudaida K. Geological carbon sequestration in the context of two-phase flow in porous media: A review. Journal of Critical Reviews in Environmental Science and Technology. 2015;**45**(11):1105-1147

[2] Karl TR, Melillo JM, Peterson TC. Global Climate Change Impacts in the United States. New York: Cambridge University Press; 2009

[3] Solomon S, Qin D, Manning M, Chen Z, Marquis M, Averyt KB, Tignor M, Miller HL, editors. Climate Change 2007: The Physical Science Basis. Contribution of Working Group I to the Fourth Assessment Report of the Intergovernmental Panel on Climate Change. Cambridge: Cambridge University Press; 2007

[4] DOE. Fossil fuels. 2010. http://www.energy.gov/energysources/fossilfuels.htm. [Accessed: 11/14/2010]

[5] Hansen J, Sato M, Kharecha P, Beerling D, Berner R, Masson-Delmotte V, Pagani M, Raymo M, Royer DL, Zachos JC. Target atmospheric CO_2: Where should humanity aim? arXiv preprint arXiv:0804.1126; 2008

[6] Houghton JT, Ding YDJG, Griggs DJ, Noguer M, van der Linden PJ, Dai X, Maskell K, Johnson CA. Climate Change 2001: The Scientific Basis. Cambridge: Cambridge University Press; 2001

[7] Abu-Khader MM. Recent progress in CO_2 capture/sequestration: A review. Energy Sources, Part A: Recovery, Utilization, and Environmental Effects. 2006;**28**(14):1261-1279

[8] Stephens JC. Growing interest in carbon capture and storage (CCS) for climate change mitigation. Sustainability: Science Practice and Policy. 2006;**2**(2):4-13

[9] Siemons N, Bruining H, Castelijns H, Wolf KH. Pressure dependence of the contact angle in a CO_2–H_2O–coal system. Journal of Colloid and Interface Science. 2006;**297**(2):755-761

[10] White DJ, Burrowes G, Davis T, Hajnal Z, Hirsche K, Hutcheon I, Majer E, Rostron B, Whittaker S. Greenhouse gas sequestration in abandoned oil reservoirs: The international energy agency Weyburn pilot project. GSA Today. 2004;**14**(7):4-11

[11] Farajzadeh R. Enhanced Transport Phenomena in CO_2 Sequestration and CO_2 EOR [PhD Thesis]. The Netherlands: Technical University Delft; 2009

[12] Fujii T, Satomi N, Yoshiyuki S, Hiroshi I, Toshiyuki H. Sorption characteristics of CO_2 on rocks and minerals in storing CO_2 processes. Natural Resources. 2010;**1**(1):1-10

[13] Zahid U, Lim Y, Jung J, Han C. CO_2 geological storage: A review on present and future prospects. Korean Journal of Chemical Engineering. 2011;**28**(3):674-685

[14] Metz B, Davidson O, de Coninck H, Loos M, Meyer L. IPCC Special Report on Carbon Dioxide Capture and Storage. Intergovernmental Panel on Climate Change. Working Group III. Geneva, Switzerland: Cambridge University Press; 2005

[15] Michael K, Golab A, Shulakova V, Ennis-King J, Allinson G, Sharma S, Aiken T. Geological storage of CO_2 in saline aquifers. A review of the experience from existing storage operations. International Journal of Greenhouse Gas Control. 2010;**4**(4):659-667

[16] Bartosik R, Cardoso L, Rodríguez J. Early detection of spoiled grain stored in hermetic plastic bags (silo-bags) using CO_2 monitoring. In: Proceeding of 8th International Conference on Controlled Atmosphere and Fumigation in Stored Products. 2008. pp. 550-554

[17] Gasda SE. Numerical Models for Evaluating CO_2 Storage in Deep, Saline Aquifers: Leaky Wells and Large-Scale Geological Features. Princeton, NJ, USA: Princeton University; 2008

[18] Saripalli KP, McGrail BP, White MD. Modeling the sequestration of CO_2 in deep geological formations. In: First National Conference on Carbon Sequestration. 2001. pp. 1-19

[19] Espinoza DN, Kim SH, Santamarina JC. CO_2 geological storage—Geotechnical implications. KSCE Journal of Civil Engineering. 2011;**15**(4):707-719

[20] Oliva A, Moreira ACDCA, Chang HK, do Rosário FF, Musse APS, Melo CL, Bressan LW, Ketzer JMM, Contant MJ, Lazzarin HSC, Cavelhão G. A comparison of three methods for monitoring CO_2 migration in soil and shallow subsurface in the Ressacada pilot site, southern Brazil. Energy Procedia. 2014;**63**:3992-4002

[21] Nakatsuka Y, Xue Z, Garcia H, Matsuoka T. Experimental study on CO_2 monitoring and quantification of stored CO_2 in saline formations using resistivity measurements. International Journal of Greenhouse Gas Control. 2010;**4**(2):209-216

[22] Bielinski A, Kopp A, Schütt H, Class H. Monitoring of CO_2 plumes during storage in geological formations using temperature signals: Numerical investigation. International Journal of Greenhouse Gas Control. 2008;**2**(3):319-328

[23] Charpentier F, Bureau B, Troles J, Boussard-Plédel C, Michel-Le Pierrès K, Smektala F, Adam JL. Infrared monitoring of underground CO_2 storage using chalcogenide glass fibers. Optical Materials. 2009;**31**(3):496-500

[24] Abidoye LK, Das DB. Scale-dependent dynamic capillary pressure effect for two-phase flow in porous media. Advances in Water Resources. 2014;**74**:212-230. DOI: 10.1016/j.advwatres.2014.09.009

[25] Mahmood A, Warsi MF, Ashiq MN, Sher M. Improvements in electrical and dielectric properties of substituted multiferroic $LaMnO_3$ based nanostructures synthesized by co-precipitation method. Materials Research Bulletin. 2012;**47**(12):4197-4202

[26] Plug W-J, Slob E, Bruining J, Moreno Tirado LM. Simultaneous measurement of hysteresis in capillary pressure and electric permittivity for multiphase flow through porous media. Geophysics. 2007;**72**(3):A41-A45

[27] Alnes H, Eiken O, Stenvold T. Monitoring gas production and CO_2 injection at the Sleipner field using time-lapse gravimetry. Geophysics. 2008;**73**(6):WA155-WA161

[28] Leuning R, Etheridge D, Luhar A, Dunse B. Atmospheric monitoring and verification technologies for CO_2 geosequestration. International Journal of Greenhouse Gas Control. 2008;**2**(3):401-414

[29] Wielopolski L, Mitra S. Near-surface soil carbon detection for monitoring CO_2 seepage from a geological reservoir. Environmental Earth Sciences. 2010;**60**(2):307-312

[30] Kikuta K, Hongo S, Tanase D, Ohsumi T. Field test of CO_2 injection in Nagaoka, Japan. In: Proceedings of the 7th International Conference On Greenhouse Gas Control Technologies. 2004. pp. 1367-1372

[31] Hovorka SD, Meckel TA, Tervino RH. Monitoring a large-volume injection at Cranfield, Mississippi—Project design and recommendations. International Journal of Greenhouse Gas Control. 2013;**18**:345-360

[32] Förster A, Norden B, Zinck-Jørgensen K, Frykman P, Kulenkampff J, Spangenberg E, Erzinger J, Zimmer M, Kopp J, Borm G, Juhlin C, Cosma CG, Hurter S. Baseline characterization of the CO2SINK geological storagesite at Ketzin, Germany. Environmental Geosciences. 2006;**13**:145-161

[33] Schmidt-Hattenberger C, Bergmann P, Labitzke T, Wagner F. CO_2 migration monitoring by means of electrical resistivity tomography (ERT)—Review on five years of operation of a permanent ERT system at the Ketzin pilot site. Energy Procedia. 2014;**63**(2014):4366-4373

[34] Yang X, Lassen RN, Jensen KH, Looms MC. Monitoring CO_2 migration in a shallow sand aquifer using 3D crosshole electrical resistivity tomography. International Journal of Greenhouse Gas Control. 2015;**42**:534-544. DOI: 10.1016/j.ijggc.2015.09.005

[35] Abidoye LK, Bello AA. Simple dielectric mixing model in the monitoring of CO_2 leakage from geological storage aquifer. Geophysical Journal International. 2017;**208**:1787-1795. DOI: 10.1093/gji/ggw495

[36] Abidoye LK, Das DB. Geoelectrical characterization of carbonate and silicate porous media in the presence of supercritical CO_2-water flow. Geophysical Journal International. 2015;**203**(1):79-91. DOI: 10.1093/gji/ggv283

[37] Abidoye LK, Das DB. pH, geoelectrical and membrane flux parameters for the monitoring of water-saturated silicate and carbonate porous media contaminated by CO_2. Chemical Engineering Journal. 2015;**262**:1208-1217

[38] Rabiu KO, Abidoye LK, Das DB. Geo-electrical characterization for CO_2 sequestration in porous media. Environmental Processes. 2017;**4**:303-317. DOI: 10.1007/s40710-017-0222-2

[39] Lamert H, Geistlinger H, Werban U, Schütze C, Peter A, Hornbruch G, Schulz A, Pohlert M, Kalia S, Beyer M, Großmann J, Dahmke A, Dietrich P. Feasibility of geoelectrical monitoring and multiphase modeling for process understanding of gaseous CO_2 injection into a shallow aquifer. Environmental Earth Sciences. 2012;**67**(2):447-462

[40] Dethlefsen F, Köber R, Schäfer D, Al Hagrey SA, Hornbruch G, Ebert M, Beyer M, Großmann J, Dahmke A. Monitoring approaches for detecting and evaluating CO_2 and formation water leakages into near-surface aquifers. Energy Procedia. 2013;**37**:4886-4893

[41] Wraith JM, Or D. Temperature effects on soil bulk dielectric permittivity measured by time domain reflectometry: Experimental evidence and hypothesis development. Water Resources Research. 1999;**35**(2):361-369

[42] Arts RJ, Baradello L, Girard JF, Kirby G, Lombardi S, Williamson P, Zaja A. Results of geophysical monitoring over a "leaking" natural analogue site in Italy. Energy Procedia. 2009;**1**(1):2269-2276

[43] International Energy Agency. World Energy Outlook. 2011. https://www.iea.org/newsroom/news/2011/november/world-energy-outlook-2011.html

[44] Abidoye LK, Das DB. Permeability, selectivity and distinguishing criterion of silicone membrane for supercritical CO_2 and N_2 in the porous media. Journal Porous Media. 2018. Article accepted (JPM-25108)

[45] Zimmer M, Erzinger J, Kujawa C. The gas membrane sensor (GMS): A new method for gas measurements in deep boreholes applied at the CO2SINK site. International Journal of Greenhouse Gas Control. 2011;**5**(4):995-1001

[46] Chiodini G, Cioni R, Guidi M, Marini L, Raco B. Soil CO_2 flux measurements in volcanic and geothermal areas. Applied Geochemistry. 1988;**13**:543-552

[47] Aggelopoulos CA, Tsakiroglou CD. The effect of micro-heterogeneity and capillary number on capillary pressure and relative permeability curves of soils. Geoderma. 2008;**148**(1):25-34

[48] Doughty C. Modeling geologic storage of carbon dioxide: Comparison of non-hysteretic and hysteretic characteristic curves. Energy Conversion and Management. 2007;**48**(6):1768-1781

[49] Bottero S, Hassanizadeh SM, Kleingeld PJ. From local measurements to an upscaled capillary pressure–saturation curve. Transport in Porous Media. 2011;**88**(2):271-291

[50] Bottero S, Hassanizadeh SM, Kleingeld PJ, Heimovaara TJ. Nonequilibrium capillarity effects in two-phase flow through porous media at different scales. Water Resources Research. 2011;**47**(10):W10505

[51] Das DB, Gauldie R, Mirzaei M. Dynamic effects for two-phase flow in porous media: Fluid property effects. AIChE. 2007;**53**(10):2505-2520

[52] Goel G, O'Carroll DM. Experimental investigation of nonequilibrium capillarity effects: Fluid viscosity effects. Water Resources Research. 2011;**47**(9):W09507

[53] Hassanizadeh SM, Gray WG. Thermodynamic basis of capillary pressure in porous media. Water Resources Research. 1993;**29**(10):3389-3405

[54] Mirzaei M, Das DB. Dynamic effects in capillary pressure–saturations relationships for two-phase flow in 3D porous media: Implications of micro-heterogeneities. Chemical Engineering Science. 2007;**62**(7):1927-1947

[55] Nordbotten JM, Celia MA, Dahle HK, Hassanizadeh SM. On the definition of macroscale pressure for multiphase flow in porous media. Water Resources Research. 2008;**44**(6):1-8

[56] Anderson W. Wettability literature survey. Part 5: The effects of wettability on relative permeability. Journal of Petroleum Technology. 1987;**39**(11):1453-1468

[57] Bennion B, Bachu S. Drainage and imbibition relative permeability relationships for supercritical CO_2/brine and H_2S/brine systems in intergranular sandstone, carbonate, shale, and anhydrite rocks. SPE Reservoir Evaluation & Engineering. 2008;**11**(3):487-496

[58] Lenormand R, Delaplace P, Schmitz P. Can we really measure the relative permeabilities using the micropore membrane method? Journal of Petroleum Science and Engineering. 1998;**19**(1-2):93-102

[59] Water M, Abaci S, Whittaker N. Relative permeability measurements for two phase flow in unconsolidated sands. Mine Water and the Environment. 2006;**26**(2):12-26

[60] Benson SM, Cole DR. CO_2 sequestration in deep sedimentary formations. Elements. 2008;**4**(5):325-331

[61] IPCC. Carbon Dioxide Capture and Storage. In: Metz B, Davidson O, de Coninck H, Loos M, Meyer L, editors. UK: Cambridge University Press; 2005. pp. 431

[62] Tokunaga TK, Wan J, Jung J-W, Kim TW, Kim Y, Dong W. Capillary pressure and saturation relations for supercritical CO_2 and brine in sand: High-pressure pc(Sw) controller/meter measurements and capillary scaling predictions. Water Resources Research. 2013;**49**:4566-4579. DOI: 10.1002/wrcr.20316

[63] Haines WB. Studies in the physical properties of soil: V. The hysteresis effect in capillary properties, and the modes of moisture distribution associated therewith. The Journal of Agricultural Science. 1930;**20**:97-116

[64] Raeesi B, Morrow NR, Mason G. Capillary pressure hysteresis behavior of three sandstones measured with a multistep outflow–inflow apparatus. Vadose Zone Journal. 2014;**13**(3)

[65] Wang S, Tokunaga TK. Capillary pressure–saturation relations for supercritical CO_2 and brine in limestone/dolomite sands: Implications for geologic carbon sequestration in carbonate reservoirs. Environmental Science & Technology. 2015;**49**(12):7208-7217

[66] Pini R, Krevor SCM, Benson SM. Capillary pressure and heterogeneity for the CO_2/water system in sandstone rocks at reservoir conditions. Advances in Water Resources. 2012;**38**:48-59

[67] Class H, Mahl L, Ahmed W, Norden B, Kuhn M, Kempka T. Matching pressure measurements and observed CO_2 arrival times with static and dynamic modelling at the Ketzin storage site. Energy Procedia. 2015;**76**(2015):623-632

Chapter 10

Interfacial Tension and Contact Angle Data Relevant to Carbon Sequestration

Prem Bikkina and Imran Shaik

Additional information is available at the end of the chapter

http://dx.doi.org/10.5772/intechopen.79414

Abstract

Interfacial tension (IFT) between "native reservoir fluid" and "injected CO_2" and the contact angle (CA) among the reservoir rock, native reservoir fluid, and injected CO_2 are major factors that dictate the relative permeability and capillary pressure characteristics which in turn control the fluid flow and distribution characteristics in the reservoir and cap rocks. This chapter is a comprehensive review on the state-of-the-art of the experimentally measured and theoretically predicted IFT and CA data of water/brine-CO_2-quartz/calcite/mica systems that are relevant to CO_2 sequestration. Experimental techniques used to generate the IFT and CA data and details of molecular simulations used to predict the data are discussed. Respective comparisons of the IFT and CA data reported by various research groups are also made. Possible reasons for disagreements in the published literature are discussed, and suggestions are made for future research in this area to address the potential technical issues in order to obtain reproducible data.

Keywords: CO_2 sequestration, contact angle, interfacial tension, wettability, quartz, calcite, mica

1. Introduction

CO_2 (or carbon) sequestration is a process of injecting CO_2, that is typically captured at point sources such as coal gasification plants, and oil & gas production and refining facilities, into subsurface formations that have sufficient storage volume and stratigraphic confinement for it to be stored indefinitely to reduce its atmospheric concentration levels in order to mitigate the adverse effects of global warming [1–5]. Saline aquifers, depleted oil & gas reservoirs, and unminable coal seams are commonly considered host sites (shown in **Figure 1**) with

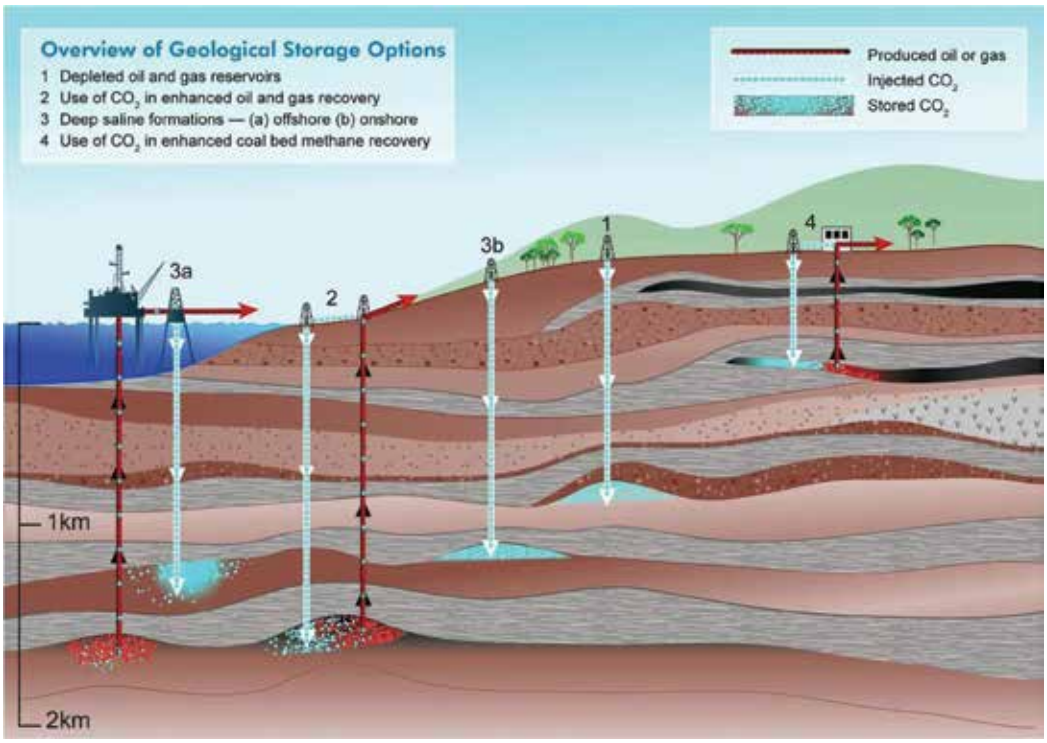

Figure 1. CO_2 sequestration methods (Source: SRCCS Figure TS-7, IPCC).

their respective advantages and disadvantages [6]. For example, saline aquifers are present in widespread areas so the CO_2 transportation cost is minimum but their storage and safety potentials are not well characterized, whereas depleted oil & gas reservoirs are well characterized but are scarcely present and hence the transportation cost from source to storage site is higher. CO_2 injection into oil & gas reservoirs and unminable coal seams may potentially recover enhanced oil and coalbed methane, respectively [6].

An ideal carbon sequestration site would consist of a reservoir rock with high porosity and permeability and a caprock with adequate sealing integrity. High porosity and permeability of the reservoir rock are important to have sufficient storage volume and efficient injection process, respectively. The low permeability caprock would facilitate the structural and stratigraphic confinement, which is a primary storage mechanism in the early years of the storage process, of the injected CO_2 [7].

Structural/stratigraphic trapping, residual/capillary trapping, solubility trapping, and mineral trapping are different types of trapping mechanisms for the injected CO_2. These trapping mechanisms are effective at various time scales during and after the injection process as shown in **Figure 2**. Structural/stratigraphic trapping is very critical during and in the first few years after the injection process. The injected CO_2 is normally lighter than brine or oil in the host site; hence, the buoyant force leads CO_2 towards caprock where it is stratigraphically

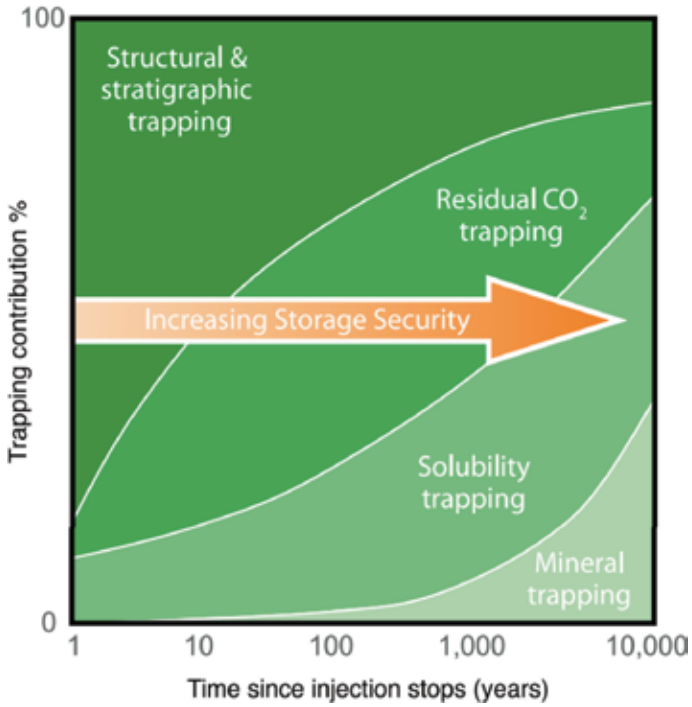

Figure 2. Post-injection contributions of CO_2 trapping mechanisms (Source: Figure 5.9 from IPCC 2005).

confined. During the injection process, CO_2 displaces the native reservoir fluid(s) (water and/or oil) and the displacement is usually a drainage process since CO_2 is usually the non-wetting phase (NWP). During injection, CO_2 moves forward and/or upward in the porous media, under the influence of positive capillary pressure (i.e., pressure in NWP–pressure in WP) and gravitational force, displacing the WP until irreducible wetting phase saturation ($S_{WP,r}$). After the injection is stopped (or pressure in NWP is reduced), WP moves back (imbibition) until the capillary pressure becomes zero. During the imbibition, WP displaces a fraction of the CO_2 while trapping the remaining fraction of the CO_2 as immobile disconnected ganglia [8]. This capillary immobilization of the CO_2 is termed as capillary or residual trapping. Later, portions of the immobile and mobile CO_2 dissolve in the native reservoir fluid(s), and the process is called solubility trapping [4]. The dissolved CO_2 reacts with minerals in the reservoir rock and forms solid carbonate minerals and is called as mineral trapping [4]. The percent trapping contributions of the four trapping mechanisms after the injection period are schematically shown in **Figure 2**.

The four trapping mechanisms, especially stratigraphic and residual trapping, are dependent on IFT and CA of the rocks and fluids involved [9]. The stratigraphic trapping depends upon the caprock's capillary entry pressure for CO_2. The capillary entry pressure is a function of the pore size, IFT between the native fluid (usually brine) in the caprock and injected CO_2, and relative wetting preference (CA) of the fluids to the caprock. The CA is the angle between the two tangent lines drawn at a point on three-phase contact line, one along fluid-fluid interface

and the other drawn along solid-fluid interface, as shown in **Figure 4(a)**, and is normally measured into the denser fluid phase. If the CA is higher than 90°, the rock has more preference to CO_2 compared to the native fluid, and hence it can easily imbibe into the caprock and leak through it. An ideal caprock for stratigraphic trapping would have strong wetting preference to native fluid (i.e. a CA value close to 0°).

Akbarabadi and Piri conducted 30 unsteady- and steady-state drainage and imbibition coreflooding tests in a medical CT scanner for CO_2-brine (10 wt.% NaI, 5 wt.% NaCl, and 0.5 wt.% $CaCl_2$) system in three different types of sandstone rock samples with 14.3–21.2% and 50–612 mD ranges of porosities and permeabilities [9]. They reported that at a given initial brine saturation (S_{wi}), less $scCO_2$ (11 MPa, 55°C) was trapped compared to gaseous CO_2 (3.46 MPa, 20°C) and the observed difference was attributed to brine being relatively less wetting to the rock in the presence of $scCO_2$. However, it should be noted that the above saturations were volume fractions and in terms of actual mass of the fluids trapped, $scCO_2$ is nearly 4 times higher than the gaseous CO_2. They also reported that about 49–83% of the initial CO_2 was capillary trapped during secondary brine imbibition. The influence of wettability on residual trapping of CO_2 was investigated by Rahman et al. [10]. They conducted microcomputed tomography (microCT) core-flooding experiments using 5 mm diameter and 10 mm length water-wet and oil-wet (originally water-wet sample was treated with 99.9 mol% purity Dodecyltriethoxysilane) Bentheimer sandstone samples having 22% porosity and 1800 mD permeability and CO_2-brine (7 wt.% NaI doped) fluid systems at 10 MPa and 318 K. The reported air-water CAs on the water-wet and oil-wet porous core samples were 0 and 130°, respectively. From the experimental findings, they concluded that lesser residual trapping occurs in oil-wet reservoirs (17.7% of initial CO_2) compared to water-wet reservoirs (29.4% of initial CO_2). The range of %capillary trapped CO_2 reported by Akbarabadi and Piri is much higher compared to the range reported by Rahman et al. [9, 10]. The difference in the %capillary trapped CO_2 ranges may be due to the differences in porosities and applied capillary pressures, as both the properties are known to affect the residual NWP saturation [8]. It should also be noted that the pore volumes of the core samples used by Akbarabadi and Piri [9] and Rahman et al. [10] were 24.1–36.3 cc and 0.044 cc, respectively.

Tokunaga et al. and Wang and Tokunaga conducted drainage and imbibition capillary pressure measurements for CO_2-brine (1 M NaCl) system in unconsolidated quartz [11] and limestone [12] sandpacks at 45°C and 8.5 and 12 MPa. The reported porosities of the sandpacks were ~38%. Based on the capillary pressure curves, they concluded that higher capillary trapping is possible for $scCO_2$ at higher pressures. The measured $S_{NWP,r}$ in both fresh and 1.5 months aged sandstone packs were 8% at 8.5 MPa, whereas the saturations for limestone sand were 11 and 25%. At 12 MPa, the measured $S_{NWP,r}$ in 3 months aged and 4.5 months aged sandstone packs were 20 and 32% and in fresh, 1.5 months aged, and 4 months aged limestone sand were 29, 25, and 44%, respectively. It should be noted that the above $S_{NWP,r}$ were measured at zero capillary pressure. By using capillary scaling criteria, they inferred that long-term (in the order of months) exposure of $scCO_2$ alters the wettabilities of the sands towards less brine-wet state.

For a safe and efficient sequestration process, an accurate representation of IFT and CA that strongly influence the relative permeability and capillary pressure is essential [13]. Further,

both IFT and CA data trends with pressure, temperature, and native and injected fluids compositions are of paramount importance during and post-injection periods [14]. Quartz/silica, calcite, and mica are dominant mineral species both in the reservoir and caprock systems; so, in this chapter, we review the current understanding on the effects of relevant process parameters on IFT and CA, the agreements and disagreements in the published data (both from the experimental and molecular simulation works), and potential reasons for the disagreements.

2. Measurement techniques

Sections 2.1 and 2.2 discuss key details of measurement techniques used for the IFT and CA data, respectively.

2.1. Interfacial tension

Drop shape analysis techniques (e.g., ADSA and ADSA-NA) that are suitable for direct measurement of IFT at high pressure and temperature conditions were used for most of the reported CO_2-water/brine IFT data [13, 15–28]. In general, the drop shape analysis methods involve: (1) formation of aqueous phase droplet in continuous CO_2 phase as shown in **Figure 3(a)** or CO_2 bubble/droplet in continuous aqueous phase as shown in **Figure 3(b)**, via a needle inside a pressure cell; (2) capturing the droplet image; (3) inputting the phase densities; and (4) obtaining IFT by matching the drop profile to the solutions of the Laplace equation [18, 25]. Capillary rise method was also used for the IFT data [29].

The following are the critical factors suggested to obtain reproducible IFT and/or CA data by: mutual saturation of the fluids and using saturated fluid densities [15]; placing thermocouple close to droplet phase [19]; avoiding contamination caused either due to low purity fluids and/or dissolution/rusting of wetted parts in fluids due to chemical incompatibility [30];

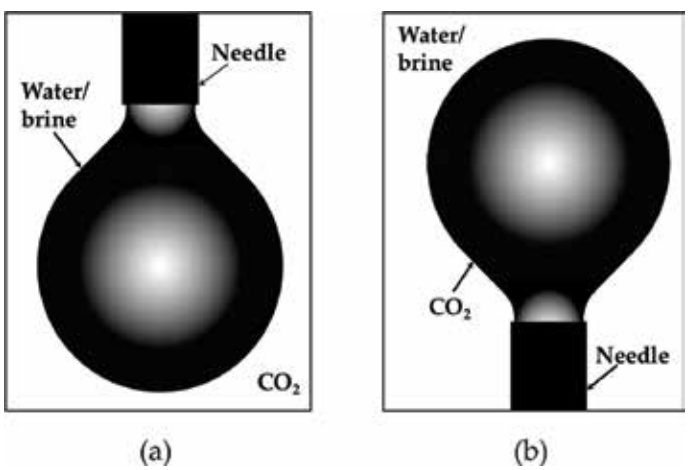

Figure 3. (a) Aqueous fluid droplet in CO_2 and (b) CO_2 bubble/droplet in aqueous fluid.

preventing droplet evaporation due to leakage of fluids and/or using unsaturated fluids [31]; and using same type of substrates with similar surface chemistry and morphology [32, 33].

2.2. Contact angle

Wettability of an inert solid surface is its relative affinity towards a fluid in the presence of another immiscible or sparingly soluble fluid. CA measurement is a widely used and accepted method for quantifying wettability of a surface. Direct and indirect measurement methods have been used for the published CA data [12, 16, 23, 31–38]. Direct methods include static

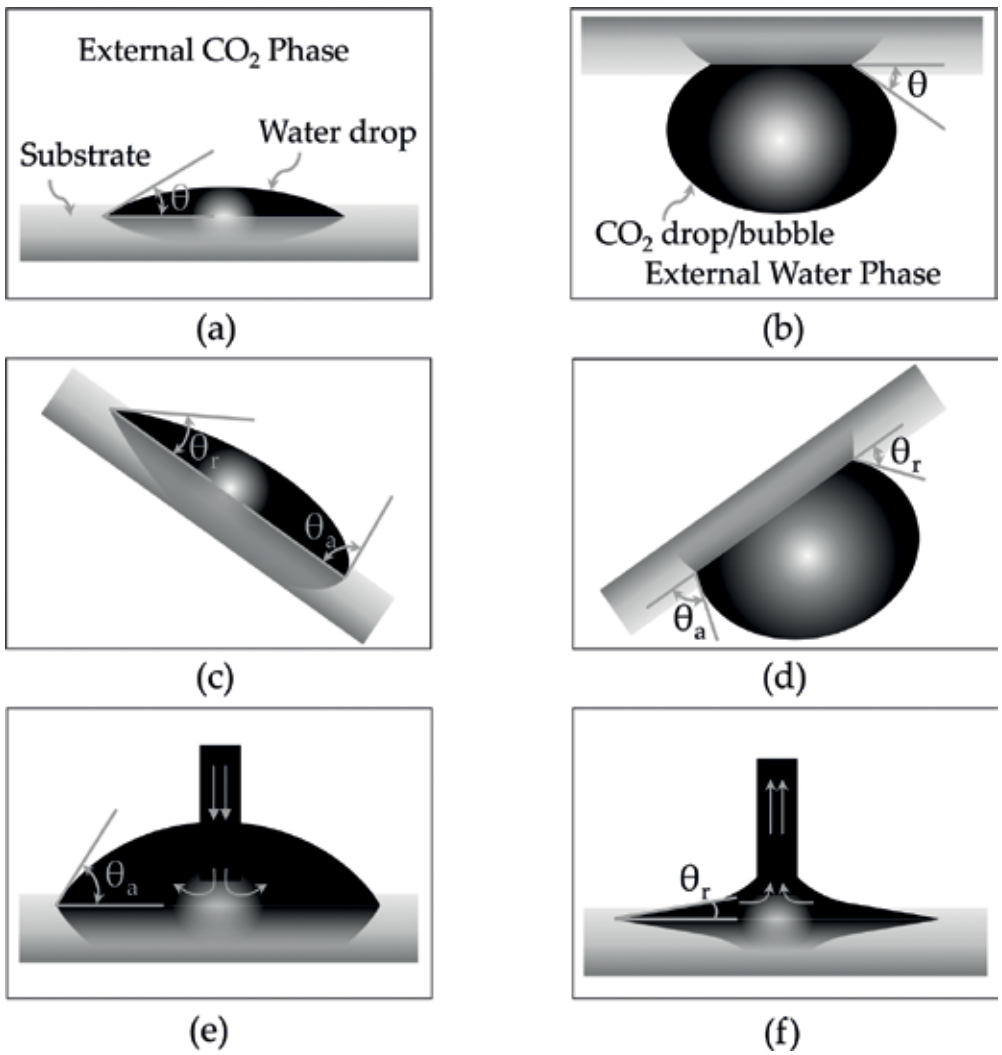

Figure 4. (a) Sessile aqueous fluid droplet on substrate in CO_2; (b) captive CO_2 bubble/droplet on substrate in aqueous fluid; (c) sessile aqueous fluid droplet on inclined substrate in CO_2; (d) captive CO_2 bubble/droplet on inclined substrate in aqueous fluid; (e) advancing aqueous fluid droplet on substrate in CO_2; and (f) receding aqueous fluid droplet on substrate in CO_2. Notation: θ—static CA; θ_a—aqueous fluid advancing CA; and θ_r—aqueous fluid receding CA.

(sessile-drop and captive-bubble) and dynamic (advancing and receding) CA measurements. Both the static and dynamic CAs were conducted using aqueous fluid as the droplet phase (called as sessile drop method, shown in **Figure 4(a)**) or the CO_2 phase as the bubble/droplet phase (captive bubble method, shown in **Figure 4(b)**).

For static CA measurement, the droplet phase is slowly released through a needle and deposited on the substrate immersed in external phase. In the case of advancing CA (w.r.t. droplet phase) measurement, either the droplet phase volume is slowly increased so that the three-phase contact line advances to an area where it was previously occupied by the external phase as shown in **Figure 4(e)** or the substrate is slowly titled so that the droplet phase advances on it due to gravitational or buoyant force. In the tilting base method, both the advancing and receding CAs can be measured simultaneously as shown in **Figure 4(c)** and **(d)**. Similarly, in the case of receding CA measurement, the droplet phase volume is slowly decreased so that the three-phase contact line recedes as shown in **Figure 4(f)**. CO_2 advancing (water/brine receding) CA is relevant for CO_2 injection into the reservoir and also to determine the capillary entry pressure of the caprock and thus to estimate the capacity of the host site to hold the injected CO_2. CO_2 receding (water/brine advancing) CA is required to estimate the amount of CO_2 that can be capillary trapped in the host site [39].

With the recent advancements in CT and microCT technologies, some researchers performed in-situ pore-scale CA measurements [37]. The procedure involves: (1) loading the core sample in an X-ray transparent coreholder; (2) scanning dry and wet core samples at various fluid saturations; (3) identifying rock and fluid phases in the collected tomographs; and (4) measurement of CA values either manually or using an automated algorithm.

CA data can be indirectly estimated from relative permeability or capillary pressure curves. Based on endpoint relative permeability of CO_2 in a core-flooding experiment where CO_2 displaces aqueous phase, relative wetting preferences of the fluids for the rock can be inferred. Typically, the endpoint relative permeability value less than 0.2 represents a strongly CO_2-wet porous media, whereas a value from 0.7 to 1 represents a strongly CO_2 non-wetting porous media. An endpoint relative permeability value close to 0.5 indicates an intermediate wetting state [36]. Advancing and receding CAs can also be estimated through capillary scaling of the drainage and imbibition capillary pressure curves [11, 12].

3. Fluids and substrate preparation methods

Sections 3.1 and 3.2 discuss the fluids and substrate preparation methods and their potential impact on the IFT and CA data.

3.1. Fluids

Various compositions of aqueous-rich phase and CO_2-rich phase fluids, ranging from pure water and CO_2 to brines containing different types of salts and salinities, and CO_2 streams with impurities such as H_2S, SO_2, N_2, and Ar have been used for both the published IFT and

CA data. The details of the compositions of the fluid phases, ranges of pressure and temperature, whether the fluids had been mutually saturated before the IFT and CA measurements, whether the saturated fluid phase densities were used for the IFT measurement, and how the phase densities were obtained are provided in **Table 1**.

3.2. Substrates

Quartz is one of the polymorphs of silica (SiO_2). The other polymorphs include tridymite, cristobalite, coesite, stishovite, etc. There are two types of quartz based on the geometrical positions of the atoms: α-quartz and β-quartz [51]. The published CA data were collected on α-quartz as it is related to typical pressure and temperature ranges of CO_2 sequestration. Calcite and aragonite are the two polymorphous groups of carbonate minerals. Calcite ($CaCO_3$) is a mineral in calcite group. Generally, these minerals are impure, but majority of the CA data were collected on Iceland Spar calcite crystals which are pure $CaCO_3$ [33, 34, 52]. Mica group is a subdivision of phyllosilicates. Muscovite ($KAl_3Si_3O_{10}(OH)_2$), also known as common mica or potash mica, is the most common form of mica. Phlogopite ($KMg_3(AlSi_3O_{10}(OH,F)_2$), called as Mg-Mica, is another form of mica. Mica is usually soft and has perfect basal cleavage [53]. Both muscovite [27, 35, 40, 54, 55] and phlogopite [34] micas have been used for CA data related to carbon sequestration.

In a short communication, Iglauer et al. attempted to identify possible reasons for the observed scatter in the reported CA data of quartz/glass-CO_2-water/brine systems [30]. Different cleaning procedures such as acetone washing followed by DI water rinsing, piranha solution (5:1 v/v H_2SO_4 and H_2O_2) cleaning (etching), and air plasma cleaning were evaluated. Approximately 0° CAs on the surfaces cleaned using piranha solution and air plasma were reported. It was also reported that the CA of piranha solution cleaned substrate increased to about 25° when a clean paper towel was used to wipe the substrate and to 70° when the substrate was kept in the laboratory atmosphere for several weeks. Even though both the piranha solution and plasma cleaning could give near 0° CA, plasma cleaning was suggested based on its relative merits in terms of health and environmental hazards. However, there is a significant scatter in the CA data of plasma cleaned quartz/silica surfaces. For example, water advancing CAs reported for Ar plasma and 20% O_2–80% Ar plasma cleaned quartz surfaces were 40 and 16°, respectively [56]. The publication also reported advancing and receding CAs of about 39 and 23° for piranha solution cleaned quartz surface. Another study reported an air-water CA of about 45° on silica that had been cleaned using reactive ion etching oxygen plasma [57].

As Iglauer et al. [30] pointed out, surface contamination is one of the critical factors that affects wettability of a substrate; however, severe surface cleaning methods such as plasma or piranha etching could also alter the surface chemistry and/or morphology both of which are known to modify the wettability of a substrate [58, 59]. Quartz/silica surface cleaning has been done using degreasing chemicals such as acetone, methanol, and trichloroethylene and strong oxidizing agents such as hot nitric acid, hydrogen peroxide, and hydrofluoric acid that may remove surface layer [56].

Author (Year)	Aqueous-rich phase	CO_2-rich phase	P (MPa)	T (K)	Pre-equilibrated?	Densities for IFT	Cleaning chemicals
Chun et al. (1995) [29]	DIW	CO_2	0.1–18.6	278–344	No	Water: NM, CO_2: Pure	NM
Chiquet et al. (2007) [18]	0–0.34 M NaCl	CO_2	5–48	308–383	Yes	DM	C: NM
Chiquet et al. (2007) [55]	0.01–1 M NaCl	CO_2	1–11	NM	No	NA	S: TND
Bachu et al. (2008) [20]	0–5.72 M NaCl	CO_2	2–27	293–398	Yes	DM	NM
Shah et al. (2008) [21]	Water	CO_2:H_2S, 70:30 mol%	0.45–15.6	313–393	Yes	Water: PRSW, CO_2: PRSW	NM
Chalbaud et al. (2009) [13]	0–2.75 M NaCl	CO_2	4.5–25.5	300–373	Yes	Brine: SWRC, CO_2: Pure	C: DIW
Espinoza et al. (2010) [23]	0–3.42 m NaCl	CO_2	0.1–20	296.5 ± 1.5	No	Brine: PGM, CO_2: DS	NM
Georgiadis et al. (2010) [24]	DIW	CO_2	1–60	298–374	No	NIST	C: HITC
Aggelopoulos et al. (2011) [22]	0.045–1.5 M NaCl: $CaCl_2$, 50:50 mol%	CO_2	5–25	300–373	Yes	Brine: SWRC, CO_2: Pure	C: EDC
Bikkina et al. (2011) [15]	DIW	CO_2	1.48–20.76	298–333	Yes	Water: HB, CO_2: MS	C: ADC
Bikkina (2011) [31]	DIW	CO_2	1.48–20.76	298–323	Yes	NA	C: AD, Quartz: AD, Calcite: DIW
Broseta et al. (2012) [40]	0.08–6 M NaCl	CO_2	0.5–15.5	282–413	Yes	NA	NM
Jung et al. (2012) [41]	0–5 M NaCl	CO_2	0.1–25	318	Yes	NA	C: DIW, S: Ethanol
Shariat et al. (2012) [25]	DIW	CO_2	6.89–124.1	323–478	No	BM	NM
Farokhpoor et al. (2013) [35]	0–0.8 M NaCl	CO_2	0.1–40	309–339	No	NA	S: DDN C: WMC
Saraji et al. (2013) [16]	DIW	CO_2	3.45–11.72	308–333	Yes	DM	S: IHND

Author (Year)	Aqueous-rich phase	CO_2-rich phase	P (MPa)	T (K)	Pre-equilibrated?	Densities for IFT	Cleaning chemicals
Iglauer et al. (2014) [30]	0–0.342 M NaCl & 1 M $NaHCO_3$	CO_2	0.1–13.89	296–323	No	NA	Piranha solution or air plasma
Saraji et al. (2014) [42]	0.2–5 M NaCl	CO_2 + SO_2 (0–6 wt%)	13.89–27.68	323–373	Yes	DM	S: IHND
Al-Yaseri et al. (2015) [26]	0.084 M NaCl	CO_2 + N_2 (0–50 mol%)	13	333	No	GS	S: Acetone and air plasma
Arif et al. (2016) [27]	0–5.13 M NaCl	CO_2	0.1–20	308–343	No	NM	S: Air plasma for 45 min
Kravanja et al. (2018) [28]	0.3 M Brine*	CO_2 + Ar (0–100 vol%)	0.1–40	313–363	Yes	DM	NM

DIW: DI water; C: cell; S: substrate; NM: not mentioned; NA: not applicable; DM: Anton Paar DMA density meter; PRSW: Peng and Robinson [43] and Søreide and Whitson [44]; SWRC: Søreide and Whitson [44] and Rowe and Chou [45]; PGM: Perry and Green [46] and McCutcheon et al. [47]; DS: Duan and Sun [48]; NIST: National Institute of Standards and Technology Chemistry Webbook; BM: Blue M Model CSP-400A; HB: Hebach et al. [49]; MS: modified Spycher et al. [50]; GS: from Georgiadis et al. [24]; TND: tensioactive solution, 10% nitric acid solution and DI water; HITC: hexane, isopropanol, and/or toluene, CO_2 flush; KID: KOH-isopropanol solution and DI water; CNE: cyclohexane, nitrogen, and ethanol; EDC: ethanol, DI water, and CO_2; ADC: acetone, DI water, and CO_2; DA: DI water and acetone; DDN: DI water, Deconex, and 6% nitric acid solution; WMC: water, methanol, and dry CO_2; IHND: IPA, H_2SO_4 with 10% Nochromix, DI water [43–50].*(10.88 g/L KCl, 6.68 g/L $NaHCO_3$, 3.14 g/L NaCl, and 2.38 g/L K_2CO_3).

Table 1. Details of fluids, process conditions, and cleaning chemicals used for published IFT and CA data.

Iglauer et al. concluded that a clean quartz/silica surface should have a 0° air-water CA; however, since the wettability of quartz/silica is primarily determined by surface silanol (Si-OH) group density that could vary from a sample to sample, the CA does not necessarily be 0° [30, 60, 61]. For example, as reported in [58], even a freshly prepared silica surface has an air-water CA of about 45°. The publication also mentions that cleaning methods such as acid washing would hydroxylate the surface and correspondingly reduce the CA (or make it hydrophilic). Suni et al. mentioned that plasma treatment induces a highly disordered surface structure and significantly increases the surface silanol group density [59]. Lamb and Furlong reported that when the surface silanols on a quartz substrate are changed to siloxane (Si-O-Si) bridges, the substrate becomes less water-wet with an advancing CA of 44° and a receding CA of 39° [60].

Quartz, calcite, and mica substrates used for published CA data have many orders of magnitude difference in their surface roughness values. For example, quartz and calcite substrates with surface roughness values ranging from 0.5 to 1300 nm [16, 32, 34, 38] and 7.5 to 250 nm [33, 34], respectively, were used for the CA measurements. CA values are known to be affected by the surface roughness values and cleaning methods [32, 33, 56, 62]. The trends of the effect of surface roughness on CAs measured on quartz and calcite substrates are discussed in CA data comparison section.

4. Theoretical studies on IFT and contact angle data

Molecular dynamics simulations for the prediction of IFT and CA data were performed by various research groups for systems pertaining to CO_2 sequestration [19, 63–70]. The simulation procedure consists of choosing potential models for molecules, intermolecular interaction models for short-range and/or long-range interactions, initial and boundary conditions, and the ensemble (NVE, NVT, NPT, etc.), followed by simulation until equilibration criteria is satisfied. After simulation, the results (IFT/CA data) are analyzed and compared with experimental values. The models evaluated were CO_2—DZ, EPM2, flexible EPM2, PPL and TraPPE; Water—SPC, SPC/E, TIP4P2005, F3C, and flexible F3C; and NaCl brine—SD and DRVH [19, 63, 64, 66, 68].

The predictions on the effect of temperature and pressure on IFT for CO_2-water system were found to be in good agreement with experimental data for the models used by Nielsen et al. (PPL-TIP4P2005 and renormalized PPL-SPC/E) and Liu et al. (TraPPE-TIP4P2005 (and SD model for NaCl) below 250°C except at 150°C and EPM2-SPC at 150°C), whereas EPM2-TIP4P2005 model combination used by Iglauer et al. and Liu et al. resulted in overprediction of IFT [64–66]. EPM-SPC/E model combination used by Kvamme et al. and Nielsen et al. underpredicted IFT data in the low-pressure region (<4 MPa) and overpredicted in the high-pressure region (>10 MPa) [19, 65]. Nielsen et al. [65] observed the similar trend for DZ-SPC/E model combination, and they also observed that PPL-SPC/E model combination underpredicted IFT throughout 0–40 MPa. In agreement with experimental data [20, 22, 41, 42], IFT was found to increase with salinity by Zhao et al., Iglauer et al., and Liu et al. [63, 64, 66].

Various research groups performed CA predictions for water/brine–CO_2–quartz/silica systems using molecular dynamics simulations [64, 67, 69, 70]. Iglauer et al. and McCaughan et al. considered fully coordinated quartz (i.e., siloxane bridges (Si-O-Si) and no silanol groups) surface structure and they only used short-range force field parameters Si-O (bonded) and O-O (non-bonded) retrieved from Beest and Kramer [64, 67, 71] in their simulations. Iglauer et al. [64] reported an abrupt increase in CA (0–80°) for water-CO_2-quartz system at 300 K in the low-pressure region (0–6.7 MPa) and a nearly constant CA above 6.7 MPa. Simulations performed by McCaughan et al. [67] for 1 M $CaCl_2$ brine-CO_2-quartz system at 300 K yielded similar CA values with pressure showing negligible effect of the divalent ions. At 350 K, significantly smaller CA values near both sides of the phase changing pressure were reported by Iglauer et al. [64] and the CA values at pressures above 17 MPa were found to be identical for 300 and 350 K. They also reported no significant effect of salinity (1 and 4 m NaCl) on CA at 300 K and ~4 MPa.

Liu et al., McCaughan et al., and Chen et al. considered hydroxylated quartz surfaces with different silanol group densities ranging from 1.6 to 9.4 OH/nm^2 for CA measurements [67, 69, 70]. Liu et al. [70] modeled a pristine silica plane having silicon atoms on the surface as hydrophobic surface and its partially hydroxylated variant with a silanol density of 1.6 OH/nm^2 as hydrophilic surface. They reported that CA on the hydrophilic surface increased from ~60 to ~90° when the CO_2 density increased from 0 to 1 g/cc. In the case of hydrophobic surface, water droplet with a CA of 115° at

0.2 g/cc CO_2 density lost its contact from the surface upon further increase in CO_2 density. At 300 K and 10 MPa, McCaughan et al. [67] reported that the CA reduced with increasing silanol group density (42° at 1.7 OH/nm^2 to 35° at 3.7–4.5 OH/nm^2). Chen et al. [69] performed molecular simulations, on fully hydroxylated silica surface with 9.4 OH/nm^2 silanol group density, using force field parameters for Si-O, O-H, O-Si-O, Si-O-Si, and Si-O-H groups to predict CAs for brine-CO_2-quartz systems. 0–3 M NaCl and $CaCl_2$ brines were used in the study. The predicted static CAs (e.g., 22.6° for water) agreed well with their experimental results (20–21°). Their results indicate that CA slightly increases (about 7–13°) with ionic strength (0–3 M), and the trend is similar for both monovalent and divalent ions. They also reported that CA dependence on pressure and temperature is insignificant within the conditions tested (7 and 9.6 MPa at 318 K and 10.9 MPa at 333 K).

Tenney and Cygan performed molecular dynamics simulations for brine-CO_2-clay system at 330 K and 20 MPa and reported CO_2 CAs for hydrophilic gibbsite and hydrophobic siloxane surfaces in the presence of water, NaCl, and $CaCl_2$ brine solutions. The reported CO_2 CAs were 169° in water and 180° in both brines on the hydrophilic surface, whereas on the hydrophobic surface, the reported CO_2 CAs were 145° in water, 141° in 0.78 M NaCl brine, and 145° in 0.26 M $CaCl_2$ brine [68].

5. Interfacial tension data comparison

There have been a significant number of experimental and simulation studies on the IFT data of CO_2-water/brine systems at typical reservoir pressure and temperature conditions. In general, a fair agreement in the trends and values can be observed in the data reported by various research groups [15, 20, 28, 29, 72]. **Figure 5** shows reproducibility of the effect of pressure on IFT data for CO_2-water system at 298 K.

As shown in **Figure 5**, IFT sharply decreased with pressure when the CO_2 is gas and it becomes nearly constant when the CO_2 is liquid. It should be noted that Hebach et al., Bachu and Bennion, Bikkina et al., and Kravanja et al. used pendant drop method, whereas Chun et al. used capillary rise method [15, 20, 28, 29, 72]. The lowest IFT reported by Chun et al. [29] near the phase changing pressure was explained by Hebach et al. [72] as a potential consequence of the placement of thermocouple away from the droplet.

Similarly, IFT vs. pressure trends were also observed at above critical temperature of CO_2-rich phase, as shown in **Figure 6** [15]. Majority of the reported experimental and molecular simulations IFT data for CO_2-water system show an increase in IFT with temperature when the CO_2-rich phase is gas and the temperature is above the critical temperature and when CO_2 is gaseous phase [15–17, 20, 24, 29, 64, 72]. The increase in IFT with temperature is higher near the phase changing pressure from gaseous to supercritical CO_2. At very low pressures (of about 2.5 to 3.5 MPa), the IFT vs. temperature isotherm crossover was reported by Hough et al. [17], Chun et al. [29], and Hebach et al. [72], but Hebach et al. [72] hypothesized that the observed crossover of the isotherms could be due to the use of pure component phase densities instead of saturated phase densities for CO_2 and water. Bikkina et al. [15] used saturated phase densities for their IFT data and did not observe the crossover point to a pressure as low

http://dx.doi.org/10.5772/intechopen.79414

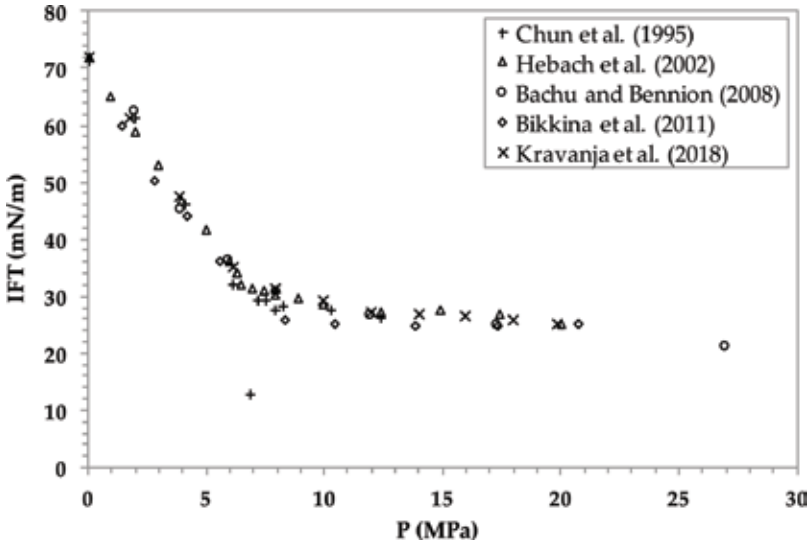

Figure 5. Comparison of published IFT data for CO_2-water system at 298 K [15].

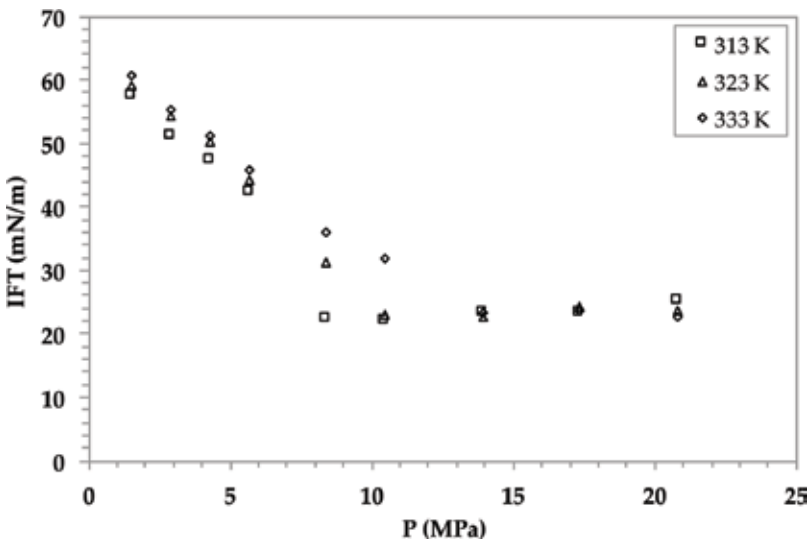

Figure 6. IFT isotherms for the CO_2-water system at various pressures [15].

as 1.48 MPa, as shown in **Figure 6**. For pressures above ~13 MPa and temperatures above the critical temperature (i.e., supercritical state), no or insignificant effect of temperature on IFT was reported [15, 17, 29, 64, 65, 72]. Whereas, a decrease in IFT with temperature between 212 and 400°F and pressure up to 18,000 psia was reported by Shariat et al. [25]. It should be noted that the experimental temperatures used for Shariat et al. [25] data are much higher than others.

As shown in **Figure 7**, an invariant IFT vs. "aqueous and CO_2 phase density difference ($\Delta\varrho$)" irrespective of the pressure and temperature until a $\Delta\varrho$ of about 600 kg/m^3 and then a steep increase in IFT with $\Delta\varrho$ was reported by Bikkina et al. [15]. Similar trends were reported by Chalbaud et al. for CO_2-NaCl brine system [13].

There has been a common agreement on the effect of salinity on IFT data (from experimental measurements and molecular simulations) of CO_2-brine systems [13, 15, 20, 22, 42, 63–65]. At a given pressure and temperature condition, IFT was observed to increase with salinity. Aggelopoulos et al. [22] reported that the increase in IFT, at a given molality of aqueous phase, is more than double for $CaCl_2$ solution compared to that of NaCl solution reported by Chalbaud et al. [13], and this increase was attributed to the presence of divalent cations in the case of $CaCl_2$ solution.

The influence of H_2S, SO_2, N_2, and Ar contamination in CO_2 stream on IFT were investigated by Shah et al., Saraji et al., Al-Yaseri et al., and Kravanja et al., respectively [21, 26, 28, 42]. Shah et al. [21] conducted water-H_2S IFT measurements up to 15 MPa and at 120°C and water-(30, 70 mol% H_2S:CO_2) IFT measurements up to 15 MPa and at 77°C. Upon combined analyzation of their IFT data along with Chiquet et al. [18] water-CO_2 IFT data, they concluded a strong decrease of IFT with increase in H_2S content in CO_2. A significant linear decrease in IFT (i.e. from 29 mN/m in the case of pure CO_2 to 18 mN/m in the presence of 6 wt% SO_2) was reported by Saraji et al. [42]. The presence of weakly bounded surface complex between SO_2 and water molecules at the supercritical fluid/liquid interface was suggested as the probable reason for the decrease in IFT. Pressure, temperature, and salinity conditions used in their experiments were 3000 psig, 60°C, and 1 M brine, respectively.

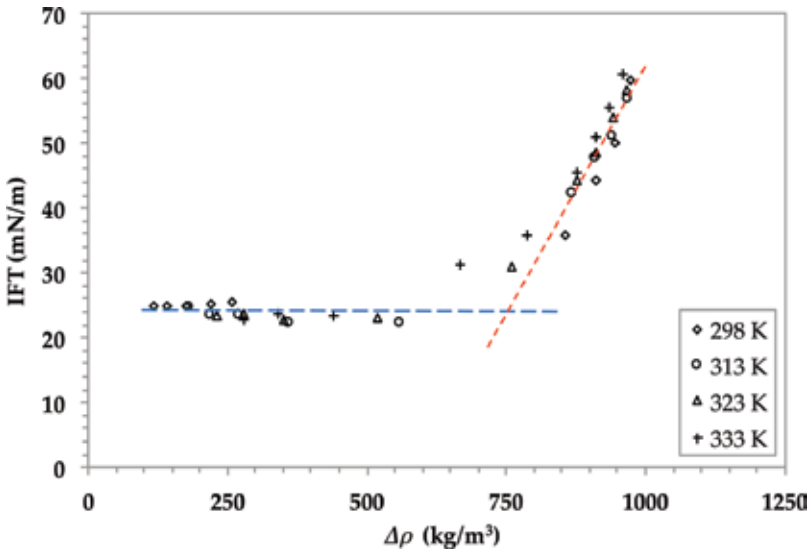

Figure 7. Effect of phase density difference on IFT for the CO_2-water system at various temperatures [15].

Effect of N_2 contamination on IFT was studied by Al-Yaseri et al. [26]. About 5000 ppm NaCl brine and 50:50 mol% CO_2-N_2 mixture were used as aqueous and gas phases, and the IFT measurements were conducted at 13 MPa and 333 K. It was found that 50 mol% N_2 has negligible effect on IFT (CO_2-brine IFT of 38.7 ± 3.9 mN/m and 50:50 mol% CO_2/N_2 mixture-brine IFT of 40.6 ± 3 mN/m) within experimental uncertainty. Kravanja et al. [28] measured IFT between CO_2 stream containing Ar impurity and 23.26 g/L salinity brine and found that the presence of 5 and 10 vol.% Ar impurity in CO_2 stream has negligible effect on IFT within the temperature and pressure ranges of 40–90°C and 7.5–40 MPa.

6. Contact angle data comparison

There is a significant scatter in the reported CA (wettability) data [30, 54]. The reported CA data include static [23, 30, 31, 41] and dynamic [16, 27, 30, 32, 33, 35, 38, 42, 55] CAs. The data also include measurements of water/brine droplet on substrate in CO_2 [23, 26, 27, 30, 31, 33, 38, 41] and CO_2 bubble/droplet on substrate immersed in aqueous phase [34, 35, 41, 42, 54, 55]. One of the major reasons for the apparent spread in CA data is in fact due to the comparison of the data collected at significantly different process parameters. For example, the CA data collected on quartz substrates having orders of magnitude, different surface roughness values, and at different temperatures and salinities were compared [38]. Similar inappropriate comparisons were also made for calcite [33] and mica substrates [27]. It should also be noted that even static and dynamic CAs have been compared [27, 33].

It is possible that the so-called smooth and pure substrates used for some of the published data may have surface chemical and physical heterogeneity which could cause significant CA hysteresis (i.e., the difference between advancing and receding CAs). In general, static CA falls somewhere between the advancing and receding CAs [73]. Hence, it is inappropriate to compare static and dynamic CAs. Some researchers reported surface roughness data of their substrates [16, 27, 32–34, 38, 41, 42, 74]. The reported quartz surface roughness data range from 0.5 to 1300 nm (5 orders of magnitude). In the case of mica, Wang et al. [34] used phlogopite mica with 250 nm surface roughness and Arif et al. [27] used muscovite mica with a roughness value of 12 nm.

Al-Yaseri et al. thoroughly investigated the influence of surface roughness on advancing and receding CA trends of quartz-CO_2-water system using the substrates of different surface roughness (RMS) values: 56, 210, 560, and 1300 nm [32]. They found that as the roughness increases from 56 to 1300 nm, advancing and receding CAs at 296 K and 10 MPa decrease by ~6.5 and ~2°, respectively, whereas at 323 K, the CAs decrease by ~14 and ~14°, respectively. The effect of surface roughness on advancing and receding CA trends of calcite-CO_2-water system was studied by Arif et al. using calcite substrates of surface roughness (RMS) values: 7.5, 30, and 140 nm [33]. They noted that as the roughness increases from 7.5 to 140 nm, both the advancing and receding CAs at 323 K and 15 MPa decrease by ~10°. There have not been any systematic experimental studies reported on the influence of surface roughness on CA of mica-CO_2-water system.

Al-Yaseri et al. and Arif et al. measured advancing and receding CAs on quartz and calcite substrates placed on 12° and 15° (w.r.t horizontal) tilted bases, respectively. About a 6 μl water droplet that was not pre-saturated with CO_2 was dispensed on to the titled substrate and the advancing and receding CAs were measured on droplet images extracted from the recorded video [32, 33].

Al-Yaseri et al. [32], Arif et al. [27], and Arif et al. [33] also investigated the effect of pressure, temperature, and salinity on advancing and receding CAs of quartz-CO_2-water, mica-CO_2-water, and calcite-CO_2-water systems, respectively. The pressure, temperature, and salinity ranges studied for quartz, mica, and calcite substrates were: 0.1–20 MPa, 296–343 K, and 0–35 wt% (NaCl, $CaCl_2$, and $MgCl_2$); 0.1–20 MPa, 308–343 K, and 0–30 wt% NaCl; and 0.1–20 MPa, 308–343 K, and 0–20 wt% NaCl, respectively. For both quartz and calcite substrates, advancing and receding CAs increased with pressure, but the effect of temperature was different for the substrates. Both the advancing and receding CAs increased with temperature in the case of quartz, but the opposite trend was reported for calcite. In the case of quartz, both the advancing and receding CAs increased with salinity and the increase was higher for $MgCl_2$, followed by $CaCl_2$ and NaCl. Whereas in the case of calcite, salinity has negligible effect on both the advancing and receding CAs up to 5 wt% NaCl and the CAs increased with salinities above 5 wt% NaCl. The effect of pressure and temperature on advancing and receding CA trends of mica was similar to that of calcite. The effect of salinity on mica CA was similar to that of quartz.

Broseta et al. conducted water/brine advancing and receding CA measurements on quartz, calcite, and mica substrates [40]. For quartz, insignificant change in receding CAs with pressure (0.5–14 MPa) and salinity (0.08–6 M NaCl) was observed, whereas increase in the advancing CAs with the pressure and salinity was reported. For calcite, the receding and advancing CAs increased by 8 and 15°, respectively, with pressure (0.5–14 MPa) at 0.08 M and 308 K. In case of mica, the change in receding CAs with pressure was less than 10°, but a significant increase (up to ~40°) in advancing CAs with pressure was observed when there was CO_2 adhesion to mica. However, when there was no CO_2 adhesion, the increase in advancing CAs with pressure was only about 10°. Wan et al. also observed CO_2 adhesion on mica and similar levels of hysteresis in CA; however, they did not observe any clear CA trends with pressure and salinity [54].

Espinoza and Santamarina [23] and Bikkina [31] measured static CAs by placing a single aqueous fluid droplet on substrate (quartz/calcite) at a given temperature and pressure and successively injected CO_2 into the measurement cell to increase the system pressure. For quartz substrate at 298 K (below critical temperature of CO_2, $T_{c,CO2}$), they did not observe any significant effect of pressure on CA, both in gaseous and liquid regions; however, the values reported by Espinoza and Santamarina [23] and Bikkina [31] were ~20 and ~45°, respectively. At 313 and 323 K (i.e., above $T_{c,CO2}$), Bikkina [31] observed about 5° increase in CA in gaseous region compared to 298 K and the CA gradually decreased in supercritical region. The surface roughness values of the substrates used were not reported in both the above studies. Bikkina [31] used equilibrated fluids and the droplet was placed on the substrate at 1.48 MPa, whereas Espinoza and Santamarina [23] used non-equilibrated fluids and the

droplet was placed at 0.1 MPa. Bikkina [31] reported a significant shift in CA towards less water-wet state upon repeated exposure of the substrates to liquid or $scCO_2$. Desorption of physisorbed water and subsequent capping of the silanols (on quartz surface) by CO_2 were proposed as the possible mechanism for the observed CA shift, and hence the CA measurement systems with CO_2 as droplet phase may not observe this phenomenon due to insufficient CO_2 volume [75]. Kim et al. (2012) observed a dewetting phenomenon in brine-filled silica micromodels upon exposure to $scCO_2$. The tested pressure, temperature, and salinities were 8.5 MPa, 318 K, and 0.01–5 M NaCl. The pore-scale CAs were observed to increase from near 0 to 80° upon exposure to $scCO_2$, and the highest CA increase was observed in the case of 5 M brine [76].

For calcite substrate, at ~298 K, both Espinoza and Santamarina [23] and Bikkina [31] reported a sudden dip (~6°) in the CA at the phase changing pressure. The CA values reported by Bikkina [31] were 45–48° in CO_2 gaseous region and 42–40° in the CO_2 liquid region. The corresponding values reported by Espinoza and Santamarina [23] were 35 and 30°, respectively. Andrew et al. performed pore-scale CA measurements for CO_2-brine-carbonate (99.1% calcite and 0.9% quartz) system at 10 MPa and 323 K, after secondary imbibition. The observed CA values were in the range of 35 and 55° [37].

Wang et al. [34] reported CAs of dissolving CO_2 bubble/droplets as water/brine advancing CAs, so it appears that the CAs are neither static nor dynamic. It should be noted that the dissolution occurred irrespective of using pre-equilibrated fluids. If there exists evaporation/dissolution of the droplet, the corresponding CA can increase, decrease, or stay constant depending upon the relative molecular forces among the three phases involved and the triple line movement [77–79]. Farokhpoor et al. [35] reported that water/brine receding CAs on quartz and calcite and no significant effect of pressure on the CAs were observed. They reported increase in CAs with temperature and salinity for quartz substrate, but a decrease in CA with salinity for calcite substrate.

Three significantly different CA trends with pressure have been reported for quartz/silica: (1) no or insignificant change in CA [23, 31, 35, 69]; (2) sudden increase in CA near the phase changing pressure [40–42]; and (3) asymptotic increase in CA with increase in pressure [32, 64]. Al-Yaseri et al. found a remarkable linear correlation between CA and density of gas for quartz-brine (4.48 M = 20 wt% NaCl +1 wt% KCl) system [80]. The correlation is applicable for a wide range of gases. Temperature was found to change the slope of the correlation.

Saraji et al. [42] studied the influence of SO_2 contamination in CO_2-rich phase on advancing and receding CAs (using drop addition and withdrawal method) on quartz at 3000 psig, 60°C, and 1 M NaCl. They observed insignificant difference in the CAs with 1 and 6 wt% SO_2 compared to those measured for pure CO_2 at the same pressure, temperature, and salinity. Effect of N_2 contamination on water advancing CA on quartz was studied by Al-Yaseri et al. [26] using drop addition method. About 5000 ppm NaCl brine and 50:50 mol% CO_2:N_2 mixture were used as aqueous and gas phases, and the CA measurements were conducted at 13 MPa and 333 K. They reported 47 ± 3.4°, 33.9 ± 6°, and 40.6 ± 3.9° water advancing CAs for CO_2-brine, 50:50 mol% CO_2:N_2 mixture-brine, and N_2-brine systems, respectively.

7. Recommendations for future work

We believe that the potential reasons for the scatter in the CA data are due to the differences in: substrate types used (e.g., muscovite mica and phlogopite mica, quartz and silica), their preparation methods, and surface roughness values and patterns; fluid types (i.e. purities of droplet and external phase fluids and whether the fluids had been mutually saturated in the presence of substrate material); chemical compatibility of the materials used in the experimental facilities with the cleaning and process chemicals; types of CA data reported (e.g., static or dynamic CAs, sessile or captive, one droplet/bubble for a given pressure range or new droplet/bubble at each pressure). Repeatability in the data is necessary but not sufficient. Reproducibility is what is important. So, comparisons should only be made among the data collected using same system of solid and fluids, purities and preparation methods, measurement techniques, and especially type of CA data. We suggest microCT-based in-situ CA measurement with automated three-phase contact line detection for simultaneously obtaining several hundreds of thousands of CA values, as performed by AlRatrout et al. [81]. The method may also provide relative permeability and capillary pressure data for indirect estimation of wettability. One disadvantage of the suggested method is the requirement of doping the fluids. We also suggest in-situ surface chemical analysis as performed by Tripps and Combs [75] during the CA measurement in order to know any surface chemical alterations responsible for CA changes.

8. Conclusions

A detailed overview on the published IFT and CA (experimental and molecular simulation) data relevant to CO_2 sequestration is presented. Overall, the IFT trends reported by various research groups are found to be in good agreement, but there exists significant scatter in the reported CA data. Potential reasons for the disagreements in CA data are discussed, and recommendations are made for future research to obtain reproducible CA data.

Acknowledgements

The authors convey their sincere gratitude to Intergovernmental Panel on Climate Change (IPCC), Geneva, Switzerland, for kindly providing the permission to use Figure TS.7; Figure 5.9 from IPCC 2005: IPCC Special Report on Carbon Dioxide Capture and Storage, prepared by Working Group III of the IPCC (Metz, B., O. Davidson, H.C. de Coninck, M. Loos, and L. A. Meyer (eds.)). Cambridge University Press, Cambridge, United Kingdom and New York, NY, USA. The authors would like to convey their sincere appreciation to ACS publishers for kindly granting the permission to use Figures 8(a), 10, and 12 from [15].

Conflict of interest

The authors declare no competing financial interest.

Notes/Thanks/Other declarations

The lead author, Dr. Prem Bikkina, would like to express his sincere appreciation for Drs. Jiamin Wan and Tetsu Tokunaga (Lawrence Berkeley National Laboratory, USA), Dr. Stefan Iglauer (Edith Cowan University, Australia), and Dr. Daniel Broseta (Université De Pau Et Des Pays De L'adour, France) for their participation in the scientific discussions with him on the topics related to this chapter.

Author details

Prem Bikkina* and Imran Shaik

*Address all correspondence to: prem.bikkina@okstate.edu

Oklahoma State University, Stillwater, USA

References

[1] Bachu S. Sequestration of CO_2 in geological media: Criteria and approach for site selection in response to climate change. Energy Conversion and Management. 2000;**41**(9):953-970

[2] Oldenburg CM, Pruess K, Benson SM. Process modeling of CO_2 injection into natural gas reservoirs for carbon sequestration and enhanced gas recovery. Energy & Fuels. 2001;**15**(2):293-298

[3] Shaw J, Bachu S. Screening, evaluation, and ranking of oil reservoirs suitable for CO_2-flood EOR and carbon dioxide sequestration. Journal of Canadian Petroleum Technology. 2002;**41**(9):51-61

[4] Bachu S, Adams JJ. Sequestration of CO_2 in geological media in response to climate change: Capacity of deep saline aquifers to sequester CO_2 in solution. Energy Conversion and Management. 2003;**44**(20):3151-3175

[5] Benson SM, Cole DR. CO_2 sequestration in deep sedimentary formations. Elements. 2008;**4**(5):325-331

[6] Haefeli S, Bosi M, Philibert C. Carbon Dioxide Capture and Storage Issues—Accounting and Baselines Under the United Nations Framework Convention on Climate Change (UNFCCC). Paris, France: International Energy Agency; 2004. Available from: http://www/.iea.org/papers/2004/css.pdf

[7] Holloway S. Underground sequestration of carbon dioxide—A viable greenhouse gas mitigation option. Energy. 2005;**30**(11-12):2318-2333

[8] Holtz MH. Optimizing Permanent CO_2 Sequestration in Brine Aquifers: Example from the Upper Frio, Gulf of Mexico. Carbon dioxide sequestration in geological media—State of the science. AAPG Studies in Geology. 2009;**59**:429-437

[9] Akbarabadi M, Piri M. Relative permeability hysteresis and capillary trapping characteristics of supercritical CO_2/brine systems: An experimental study at reservoir conditions. Advances in Water Resources. 2013;**52**:190-206

[10] Rahman T et al. Residual trapping of supercritical CO_2 in oil-wet sandstone. Journal of Colloid and Interface Science. 2016;**469**:63-68

[11] Tokunaga TK et al. Capillary pressure and saturation relations for supercritical CO_2 and brine in sand: High-pressure Pc (Sw) controller/meter measurements and capillary scaling predictions. Water Resources Research. 2013;**49**(8):4566-4579

[12] Wang S, Tokunaga TK. Capillary pressure–saturation relations for supercritical CO_2 and brine in limestone/dolomite sands: Implications for geologic carbon sequestration in carbonate reservoirs. Environmental Science & Technology. 2015;**49**(12):7208-7217

[13] Chalbaud C et al. Interfacial tension measurements and wettability evaluation for geological CO_2 storage. Advances in Water Resources. 2009;**32**(1):98-109

[14] Li Z et al. CO_2 sequestration in depleted oil and gas reservoirs—Caprock characterization and storage capacity. Energy Conversion and Management. 2006;**47**(11-12):1372-1382

[15] Bikkina PK, Shoham O, Uppaluri R. Equilibrated interfacial tension data of the CO_2–water system at high pressures and moderate temperatures. Journal of Chemical & Engineering Data. 2011;**56**(10):3725-3733

[16] Saraji S et al. Wettability of supercritical carbon dioxide/water/quartz systems: Simultaneous measurement of contact angle and interfacial tension at reservoir conditions. Langmuir. 2013;**29**(23):6856-6866

[17] Hough E, Heuer G, Walker J. An improved pendant drop, interfacial tension apparatus and data for carbon dioxide and water. Transactions of the American Institute of Mining and Metallurgical Engineers. 1959;**216**:469-480

[18] Chiquet P et al. CO_2/water interfacial tensions under pressure and temperature conditions of CO_2 geological storage. Energy Conversion and Management. 2007;**48**(3):736-744

[19] Kvamme B et al. Measurements and modelling of interfacial tension for water + carbon dioxide systems at elevated pressures. Computational Materials Science. 2007;**38**(3):506-513

[20] Bachu S, Bennion DB. Interfacial tension between CO_2, freshwater, and brine in the range of pressure from (2 to 27) MPa, temperature from (20 to 125) °C, and water salinity from (0 to 334 000) mg L^{-1}. Journal of Chemical & Engineering Data. 2008;**54**(3):765-775

[21] Shah V et al. Water/acid gas interfacial tensions and their impact on acid gas geological storage. International Journal of Greenhouse Gas Control. 2008;**2**(4):594-604

[22] Aggelopoulos C, Robin M, Vizika O. Interfacial tension between CO_2 and brine (NaCl + $CaCl_2$) at elevated pressures and temperatures: The additive effect of different salts. Advances in Water Resources. 2011;**34**(4):505-511

[23] Espinoza DN, Santamarina JC. Water-CO_2-mineral systems: Interfacial tension, contact angle, and diffusion—Implications to CO_2 geological storage. Water Resources Research. 2010;**46**(7)

[24] Georgiadis A et al. Interfacial tension measurements of the (H_2O+CO_2) system at elevated pressures and temperatures. Journal of Chemical & Engineering Data. 2010;**55**(10): 4168-4175

[25] Shariat A et al. Laboratory measurements of CO_2-H_2O interfacial tension at HP/HT conditions: Implications for CO_2 sequestration in deep aquifers. In: Carbon Management Technology Conference. 2012

[26] Al-Yaseri A et al. N_2 + CO_2 + NaCl brine interfacial tensions and contact angles on quartz at CO_2 storage site conditions in the Gippsland basin, Victoria/Australia. Journal of Petroleum Science and Engineering. 2015;**129**:58-62

[27] Arif M et al. Impact of pressure and temperature on CO_2–brine–mica contact angles and CO_2–brine interfacial tension: Implications for carbon geo-sequestration. Journal of Colloid and Interface Science. 2016;**462**:208-215

[28] Kravanja G, Knez Ž, Hrnčič MK. The effect of argon contamination on interfacial tension, diffusion coefficients and storage capacity in carbon sequestration processes. International Journal of Greenhouse Gas Control. 2018;**71**:142-154

[29] Chun B-S, Wilkinson GT. Interfacial tension in high-pressure carbon dioxide mixtures. Industrial & Engineering Chemistry Research. 1995;**34**(12):4371-4377

[30] Iglauer S et al. Contamination of silica surfaces: Impact on water–CO_2–quartz and glass contact angle measurements. International Journal of Greenhouse Gas Control. 2014;**22**: 325-328

[31] Bikkina PK. Contact angle measurements of CO_2–water–quartz/calcite systems in the perspective of carbon sequestration. International Journal of Greenhouse Gas Control. 2011;**5**(5):1259-1271

[32] Al-Yaseri AZ et al. Receding and advancing (CO_2 + brine + quartz) contact angles as a function of pressure, temperature, surface roughness, salt type and salinity. The Journal of Chemical Thermodynamics. 2016;**93**:416-423

[33] Arif M et al. CO_2 storage in carbonates: Wettability of calcite. International Journal of Greenhouse Gas Control. 2017;**62**:113-121

[34] Wang S, Edwards IM, Clarens AF. Wettability phenomena at the CO_2–brine–mineral interface: implications for geologic carbon sequestration. Environmental Science & Technology. 2012;**47**(1):234-241

[35] Farokhpoor R et al. Wettability behaviour of CO_2 at storage conditions. International Journal of Greenhouse Gas Control. 2013;**12**:18-25

[36] Levine JS et al. Relative permeability experiments of carbon dioxide displacing brine and their implications for carbon sequestration. Environmental Science & Technology. 2013;**48**(1):811-818

[37] Andrew M, Bijeljic B, Blunt MJ. Pore-scale contact angle measurements at reservoir conditions using X-ray microtomography. Advances in Water Resources. 2014;**68**:24-31

[38] Sarmadivaleh M, Al-Yaseri AZ, Iglauer S. Influence of temperature and pressure on quartz–water–CO_2 contact angle and CO_2–water interfacial tension. Journal of Colloid and Interface Science. 2015;**441**:59-64

[39] Peters EJ. Advanced Petrophysics: Dispersion, Interfacial Phenomena. Vol. 2. Austin, TX: Live Oak Book Company; 2012

[40] Broseta D, Tonnet N, Shah V. Are rocks still water-wet in the presence of dense CO_2 or H_2S? Geofluids. 2012;**12**(4):280-294

[41] Jung J-W, Wan J. Supercritical CO_2 and ionic strength effects on wettability of silica surfaces: Equilibrium contact angle measurements. Energy & Fuels. 2012;**26**(9):6053-6059

[42] Saraji S, Piri M, Goual L. The effects of SO_2 contamination, brine salinity, pressure, and temperature on dynamic contact angles and interfacial tension of supercritical CO_2/brine/quartz systems. International Journal of Greenhouse Gas Control. 2014;**28**:147-155

[43] Peng D-Y, Robinson DB. A new two-constant equation of state. Industrial and Engineering Chemistry Fundamentals. 1976;**15**(1):59-64

[44] Søreide I, Whitson CH. Peng-Robinson predictions for hydrocarbons, CO_2, N_2, and H_2S with pure water and NaCl brine. Fluid Phase Equilibria. 1992;**77**:217-240

[45] Rowe AM Jr, Chou JC. Pressure-volume-temperature-concentration relation of aqueous sodium chloride solutions. Journal of Chemical and Engineering Data. 1970;**15**(1):61-66

[46] Perry RH, Green DW. Perry's Chemical Engineering Handbook. 7th ed. New York: McGraw-Hill; 1997

[47] McCutcheon SC, Martin JL, Barnwell TO Jr. Water quality. In: Handbook of Hydrology. Vol. 11. 1993. p. 73

[48] Duan Z, Sun R. An improved model calculating CO_2 solubility in pure water and aqueous NaCl solutions from 273 to 533 K and from 0 to 2000 bar. Chemical Geology. 2003;**193**(3-4):257-271

[49] Hebach A, Oberhof A, Dahmen N. Density of water + carbon dioxide at elevated pressures: measurements and correlation. Journal of Chemical & Engineering Data. 2004;**49**(4): 950-953

[50] Spycher N, Pruess K, Ennis-King J. CO_2-H_2O mixtures in the geological sequestration of CO_2. I. Assessment and calculation of mutual solubilities from 12 to 100 C and up to 600 bar. Geochimica et Cosmochimica Acta. 2003;**67**(16):3015-3031

[51] Lecture Notes—Silica Polymorphs. [Cited: June 3, 2018]. Available from: http://www.science.smith.edu/geosciences/min_jb/SilicaPolymorphs.pdf

[52] Carbonates. [Cited: June 3, 2018]. Available from: http://www.minerals.net/mineral_glossary/carbonates.aspx

[53] Mica group. [Cited: June 3, 2018]. Available from: http://www.minerals.net/mineral_glossary/mica_group.aspx

[54] Wan J, Kim Y, Tokunaga TK. Contact angle measurement ambiguity in supercritical CO_2–water–mineral systems: Mica as an example. International Journal of Greenhouse Gas Control. 2014;**31**:128-137

[55] Chiquet P, Broseta D, Thibeau S. Wettability alteration of caprock minerals by carbon dioxide. Geofluids. 2007;**7**(2):112-122

[56] Eske LD, Galipeau DW. Characterization of SiO_2 surface treatments using AFM, contact angles and a novel dewpoint technique. Colloids and Surfaces A: Physicochemical and Engineering Aspects. 1999;**154**(1-2):33-51

[57] Alam AU. Surface Analysis of Materials for Direct Wafer Bonding. 2014

[58] Horn R, Smith D, Haller W. Surface forces and viscosity of water measured between silica sheets. Chemical Physics Letters. 1989;**162**(4-5):404-408

[59] Suni T et al. Effects of plasma activation on hydrophilic bonding of Si and SiO_2. Journal of the Electrochemical Society. 2002;**149**(6):G348-G351

[60] Lamb RN, Furlong DN. Controlled wettability of quartz surfaces. Journal of the Chemical Society, Faraday Transactions 1: Physical Chemistry in Condensed Phases. 1982;**78**(1):61-73

[61] Bolis V et al. Hydrophilic and hydrophobic sites on dehydrated crystalline and amorphous silicas. Journal of the Chemical Society, Faraday Transactions. 1991;**87**(3):497-505

[62] Sneh O, George SM. Thermal stability of hydroxyl groups on a well-defined silica surface. The Journal of Physical Chemistry. 1995;**99**(13):4639-4647

[63] Zhao L et al. Molecular dynamics investigation of the various atomic force contributions to the interfacial tension at the supercritical CO_2–water interface. The Journal of Physical Chemistry B. 2011;**115**(19):6076-6087

[64] Iglauer S, Mathew M, Bresme F. Molecular dynamics computations of brine–CO_2 interfacial tensions and brine–CO_2–quartz contact angles and their effects on structural and residual trapping mechanisms in carbon geo-sequestration. Journal of Colloid and Interface Science. 2012;**386**(1):405-414

[65] Nielsen LC, Bourg IC, Sposito G. Predicting CO_2–water interfacial tension under pressure and temperature conditions of geologic CO_2 storage. Geochimica et Cosmochimica Acta. 2012;**81**:28-38

[66] Liu Y et al. Simulations of vapor–liquid phase equilibrium and interfacial tension in the CO_2–H_2O–NaCl system. AICHE Journal. 2013;**59**(9):3514-3522

[67] McCaughan J, Iglauer S, Bresme F. Molecular dynamics simulation of water/CO_2-quartz interfacial properties: Application to subsurface gas injection. Energy Procedia. 2013;**37**:5387-5402

[68] Tenney CM, Cygan RT. Molecular simulation of carbon dioxide, brine, and clay mineral interactions and determination of contact angles. Environmental Science & Technology. 2014;**48**(3):2035-2042

[69] Chen C et al. Water contact angles on quartz surfaces under supercritical CO_2 sequestration conditions: Experimental and molecular dynamics simulation studies. International Journal of Greenhouse Gas Control. 2015;**42**:655-665

[70] Liu S, Yang X, Qin Y. Molecular dynamics simulation of wetting behavior at CO_2/water/solid interfaces. Chinese Science Bulletin. 2010;**55**(21):2252-2257

[71] Van Beest B, Kramer GJ, Van Santen R. Force fields for silicas and aluminophosphates based on ab initio calculations. Physical Review Letters. 1990;**64**(16):1955

[72] Hebach A et al. Interfacial tension at elevated pressures measurements and correlations in the water + carbon dioxide system. Journal of Chemical & Engineering Data. 2002;**47**(6):1540-1546

[73] Marmur A et al. Contact angles and wettability: Towards common and accurate terminology. Surface Innovations. 2017;**5**(1):3-8

[74] Jafari M, Jung J. Variation of contact angles in Brine/CO_2/Mica system considering short-term geological CO_2 sequestration condition. Geofluids. 2018;**2018**

[75] Tripp C, Combes J. Chemical modification of metal oxide surfaces in supercritical CO_2: The interaction of supercritical CO_2 with the adsorbed water layer and the surface hydroxyl groups of a silica surface. Langmuir. 1998;**14**(26):7348-7352

[76] Kim Y et al. Dewetting of silica surfaces upon reactions with supercritical CO_2 and brine: Pore-scale studies in micromodels. Environmental Science & Technology. 2012;**46**(7):4228-4235

[77] Shi L et al. Wetting and evaporation behaviors of water–ethanol sessile drops on PTFE surfaces. Surface and Interface Analysis. 2009;**41**(12-13):951-955

[78] Anantharaju N, Panchagnula M, Neti S. Evaporating drops on patterned surfaces: Transition from pinned to moving triple line. Journal of Colloid and Interface Science. 2009;**337**(1):176-182

[79] Bikkina PK. Reply to the comments on "Contact angle measurements of CO_2–water–quartz/calcite systems in the perspective of carbon sequestration". International Journal of Greenhouse Gas Control. 2012;**7**:263-264

[80] Al-Yaseri AZ et al. Dependence of quartz wettability on fluid density. Geophysical Research Letters. 2016;**43**(8):3771-3776

[81] AlRatrout A et al. Automatic measurement of contact angle in pore-space images. Advances in Water Resources. 2017;**109**:158-169

Edited by Ramesh K. Agarwal

This book is divided in two sections. Several chapters in the first section provide a state-of-the-art review of various carbon sinks for CO_2 sequestration such as soil and oceans. Other chapters discuss the carbon sequestration achieved by storage in kerogen nanopores, CO_2 miscible flooding and generation of energy efficient solvents for postcombustion CO_2 capture. The chapters in the second section focus on monitoring and tracking of CO_2 migration in various types of storage sites, as well as important physical parameters relevant to sequestration. Both researchers and students should find the material useful in their work.

Published in London, UK

IntechOpen

ISBN 978-1-83881-716-9